Western Australian School of Mines: Minerals, Energy & Chemical Engineering

Microwave Plasma Dry Reforming of Methane Technology for Syngas Production and Liquified Petroleum Gas (LPG)

Nabil Majd Alawi

This thesis is presented for the Degree of

Doctor of philosophy

of

Curtin University

February 2020

Declaration

To the best of my knowledge and belief, this thesis contains no materials previously published by any other person except where due acknowledgment has been made.

This thesis contains no material which has been accepted for the award of any other degree or diploma in any university.

Signature:

Date: **05/02/2020**

Abstract

This research provides a comprehensive study of the dry reforming of methane (DRM), which converts two main greenhouses gases (CH_4 and CO_2) to syngas (H_2 and CO) and Liquified Petroleum Gas (LPG) by using a microwave plasma reactor system at atmospheric pressure. The work was performed in two stages.

In the *first stage*, the Box–Behnken design (BBD) method was used to determine the optimum experimental conditions on the plasma stability and the syngas, LPG productions. This stage was divided into two parts. First part, the interactive microwave power (MWP), CO_2/CH_4 ratio (R), and total flow rate (TFR) at the same time were studied. The synergistic effects and optimisation of all parameters on the CO_2, CH_4 conversions, H_2, CO selectivities and yields, and H_2/CO ratio have been investigated at different conditions of MWP, R, and TFR. The BBD method based on the response surface methodology (RSM) was utilised to optimise the plasma values of the three key factors of MWP, R, and TFR based on the impact on conversions of CO_2 and CH_4 and produced syngas production (H_2 and CO) selectivities, yields, and H_2/CO ratio. With the desirability value of 0.93, the optimum values of 700 W (MWP), 2/1 (R), and 2.1 L min^{-1} (TFR) were identified with CO_2 and CH_4 conversions of 44.82% and 79.35%, respectively; H_2 and CO selectivities and yields of 50.12% and 39.77% and 58.42% and 32.89%, respectively; and H_2/CO ratio of 0.86. Regression analysis indicates the good fitting between experimental and theoretical calculations. The results indicated that both MWP and TFR have a major significant effect on the reactant conversions, followed by R. Meanwhile, the value of R has a significant impact on the H_2, CO yields followed MWP and TFR. In contrast, the synergistic effect between MWP-R was significant on the H_2 selectivity, while the MWP-TFR and R-TFR were less significant on the CO_2 and CH_4 conversions, CO selectivity, H_2 and CO yields, and H_2/CO ratio, respectively. Second part, the effects of the CH_4, CO_2, and N_2 flow rates and their interactions on the conversions of CH_4 and CO_2, selectivities and yields of H_2 and CO, and H_2/CO ratio are also investigated and discussed. It was found that the most important factor influencing the CO_2 and CH_4 conversions, selectivities and yields of H_2 and CO, and ratio of H_2/CO was the CO_2 feed gas flow rate. The maximum desirable H_2/CO ratio was 0.92, and this was achieved at CH_4, CO_2, and N_2 gas feed flow rates of 0.2, 0.4, and 1.5 L min^{-1}, respectively.

In the *second stage*, the microwave plasma method was used via three parts. First, nitrogen-plasma DRM was investigated for a wide range of N_2 flow rates (0.3–1.5 L min^{-1}), MWP (700–1200 W), R (2–5), TFR (0.45–2.1 L min^{-1}), and reaction time (20–480 min) to find the effects of these parameters on the plasma stability and the syngas, LPG productions based on the CO_2 and CH_4 conversions, H_2 and CO yields, and syngas H_2/CO ratio. The MWP significantly affects the CH_4 and CO_2 conversions, selectivity, and yield of CO. In contrast, the MWP has a negative effect on the selectivity and yield of H_2 and the ratio of H_2/CO. The study also found that the conversion of CH_4 and the selectivity of CO increased rapidly with increased R, while the conversion of CO_2, selectivity of H_2, yield of H_2 and CO, and ratio of H_2/CO exhibited opposite behaviours. The TFR slightly affects the conversions of CH_4 and CO_2, the selectivities and yields of H_2 and CO. Meanwhile, the H_2/CO ratio sharply increased with increased TFR. DRM performances in the nitrogen-plasma atmosphere were stable for up to 8 h. The highest conversions of CH_4 and CO_2, the yield of H_2, CO, and H_2/CO ratio of 79.35%, 44.82%, 39.77%, 32.89%, and 0.86, respectively, were achieved.

Then, the performance of microwave-assisted DRM at atmospheric pressure (in terms of CH_4 and CO_2 conversions, H_2 and CO selectivities and yields, and H_2/CO ratio) was studied as functions of Ar gas flow rate (0.3–1.5 L min^{-1}), MWP (700–1200 W), R (2–5), TFR (0.45–2.1 L min^{-1}), and reaction time (20–480 min), respectively. DRM performances in the Ar gas atmosphere were stable for up to 8 h. The results of N_2-plasma DRM and Ar-plasma DRM were compared at the same experimental conditions. However, using DRM in Ar gave higher selectivities, yields, and a higher syngas ratio relative to using DRM in N_2. Maximum CH_4 and CO_2 conversions, H_2 and CO selectivities and yields, and H_2 were obtained at Ar of 1.5 L min^{-1}.

Finally, the combined dry and steam reforming of methane (DRM and SRM), abbreviated as CSDRM, was experimentally studied to determine the effects of the process parameters such as steam concentration (5.5–42.5 vol. %), MWP (700–1200 W), TFR (0.02–0.125 mole min^{-1}), and reaction time (20–480 min), respectively, at fixed CH_4, CO_2, and N_2 feed flow rates of 0.008, 0.016, 0.062 moles min^{-1}, respectively, on the plasma stability and syngas production. To minimise the carbon formation and plasma instability, the concentration of CH_4 and CO_2 in N_2-plasma was maintained at a low level in this study. The long-term test results show that at the steam

concentration of 0.45 vol. %, MWP of 700 W, and TFR of 0.125, the carbon formation was not detectable. The CSDRM performance was continuously stable for up to 8 h. This reaction condition offers an opportunity to study the effect of adding water on the feed on the syngas ratio H_2/CO. The test results show that a higher CH_4 conversion (82.74%), H_2 selectivity (98.79%), and yield (81.73%) were achieved compared with those of the DRM at the same operating conditions. With the steam addition, the desired H_2/CO ratio for the Fischer–Tropsch synthesis process can be obtained.

Publications

The following publications have resulted from this research.

Published journal papers:

1- Alawi, N. M., Barifcani, A., & Abid, H. R. (2018). Optimisation of CH_4 and CO_2 conversion and selectivity of H_2 and CO for the dry reforming of methane by a microwave plasma technique using a Box–Behnken design. *Asia‑Pacific Journal of Chemical Engineering*, *13*(6), e2254.
Doi: https://doi.org/10.1002/apj.2254.

2- Alawi, N. M., Pham, G. H., Barifcani, A., Nguyen, M. H., & Liu, S. (2019, July). Syngas formation by dry and steam reforming of methane using microwave plasma technology. In *IOP Conference Series: Materials Science and Engineering* (Vol. 579, No. 1, p. 012022). IOP Publishing.
Doi:10.1088/1757-899X/579/1/012022.

3- Alawi, N. M., Sunarso, J., Pham, G. H., Barifcani, A., Nguyen, M. H., & Liu, S. (2020). Comparative study on the performance of microwave-assisted plasma DRM in nitrogen and argon atmospheres at a low microwave power. *Journal of Industrial and Engineering Chemistry*, 85 (2020) 118–129.
Doi: 10.1016/j.jiec.2020.01.032.

4- Alawi, N. M., Nguyen, M. H., Barifcani, A., & Liu, S. (2019). Synergistic effects and optimization of syngas production and plasma stability of microwave plasma dry reforming of methane. *Asia‑Pacific Journal of Chemical Engineering*. (Under reviewing).

5- Alawi, N. M., Nguyen, M. H., Barifcani, A., & Liu, S. (2019). Modelling and optimization of different parameters on the syngas production by plasma dry reforming of methane using a response surface methodology. *Asia‑Pacific Journal of Chemical Engineering*. (Under reviewing).

Published conference papers:

1- Alawi, N. M., Pham, G. H., Barifcani, A. (2018, 27-28 August). *Microwave Plasma Dry Reforming of Methane at High CO_2/CH_4 Feed Ratio*. Paper presented at the International Conference on Chemical Engineering and Nanoparticle Synthesis. Paris, France.

2- Alawi, N. M. & Barifcani, A. (2017, 10-12 December). *Optimization of microwave plasma dry reforming of methane using the response surface methodology*. Paper presented at the One Curtin International Postgraduate Conference, Miri, Sarawak, Malaysia.

3- Alawi, N. M. & Barifcani, A. (2018, 26-28 November). *A comparative study of the experimental investigation and response surface optimization of dry reforming of methane*. Paper presented at the One Curtin International Postgraduate Conference, Miri, Sarawak, Malaysia.

4- Alawi, N. M., Pham, G. H., Barifcani, A., Nguyen, M. H., & Liu, S. (2019, 10-11 April). *Effect of steam addition on the syngas formation from microwave plasma dry reforming of methane*. Paper presented at the 1st International Conference on Petroleum Technology and Petrochemicals. University of Technology, Baghdad, Iraq.

Acknowledgments

First of all, I must thank Allah and his guardians for giving me the patience and the ability to complete this work. Then, I would like to express my deep thanks to Professor Shaomin Liu for his perfect supervision and guidance during my PhD study. He has always been helpful, friendly, and ready to support me through his patience, advice, and encouragement.

I would also like to express my gratitude to Dr Ahmed Barifcani, my co-supervisor, for his invaluable suggestions, motivation, stimulating discussions, and perpetual direction throughout my study time in our regular meetings. His guidance and support have been invaluable on both personal and academic levels.

I would like to extend my sincere gratitude and profound respect to previously main supervisor and recently associate supervisor, Dr Gia Hung Pham, for his patience, advice, support, and encouragement during my study. I am greatly indebted to him for his timely advice, hearty concern for my research, and the intensive, regular meetings to guide me throughout my time as his student.

I would also like to extend my appreciation to the University of Technology/ Ministry of Higher Education & Scientific Research in Iraq for sponsoring me and giving me this great opportunity to study for my PhD degree at such a well-known university the Curtin University.

I would like to convey my gratitude to professor Vishnu Pareek for being the chairperson of my thesis committee. I sincerely thank the Department of Chemical Engineering at Curtin University for providing a pleasant research environment. Also,

I am thankful to Dr. Hussein Rasool Abid in the Chemical Engineering Department at Curtin University for his bits of help in different situations during my study. I would like thank Dr. Jaka Sunarso in the Chemical Engineering Department at Swinburne University of Technology, Malaysia for his help in my study. My thanks are owed to

Table of Contents

Chapter 9: Conclusions and Recommendations for Future Work

List of Figures

List of Tables

List of Acronyms, Abbreviations, and Notations

The following is a list of acronyms, abbreviations, and notations used in this thesis.

NG	Natural Gas
CH_4	Methane Gas, L min^{-1}
CO_2	Carbon Dioxide Gas, L min^{-1}
N_2	Nitrogen Gas, L min^{-1}
H_2	Hydrogen Gas, L min^{-1}
CO	Carbon Monoxide, L min^{-1}
H_2/CO	Hydrogen/ Carbon Monoxide ratio
H_2, CO	Synthesis Gas
C	Carbon
O_2	Oxygen
SRM	Steam Reforming of Methane
POM	Partial Oxidation of Methane
DRM	Dry Reforming of Methane
CSDRM	Combined SRM and DRM
ΔH	Change in enthalpy
GD	Glow Discharge
CD	Corona Discharge
SD	Silent Discharge
DBD	Dielectric Barrier Discharge
RFD	Radiofrequency Discharge
MWD	Microwave Discharge
DC	Pulsed Direct Current
AC	Alternating Current
AD	Arc Discharge
PTD	Plasma Torch Discharge
MWP	Microwave Power
SC	Steam Concentration
RT	Residence Time
R	CO_2/CH_4 ratio
TFR	Total Feed Rate
BBD	Box-Behnken Design
CCD	Central Composite Design
RSM	Response Surface Methodology
DoE	Design of Experimental
Ar	Argon Gas, L min^{-1}
SC	Steam Concentration, Vol. %
FTS	Fischer-Tropsch Synthesis
GTL	Gas-to-Liquid
LPG	Liquified Petroleum Gas
O/C	Atomic Ratio
RWGS	Revers Water Gas Shift
T_o	Gas Temperature

T_i	Ion Temperature
T_r	Rotational Temperature
T_v	Vibrational Temperature
T_e	Electron Temperature
CCPs	Capacitively Coupled Plasmas
ICPs	Inductively Coupled Plasma
P	Power Absorbed
D	Depth of Microwave Penetration
MIP	Microwave-Induced Plasma
CMP	Capacitively Coupled Microwave Plasma
MPT	Microwave Plasma Touches
MCFR	Microwave Continuous Flow Reactor
SWSP	Surface Wave Sustained Plasma
TIA	Torch with Axial Gas Injection
MPT	Microwave Plasma Torch
Ar	Argon Gas
NO	Nitrogen Oxide
HCN	Cyanide
VSWR	Voltage Standing Wave Ratio
MFC	Mass Flow Controller
GC	Chromatography
MSD	Mass Selective Detector
TCD	Thermal Conductivity detector
H_2O	Water
x_i	Coded value of the actual value
X_i, X_o	Actual value of the factor at the center point
ΔX_i	Step change value
Y	Response
β	Coefficient
β_0	Constant coefficient
β_i	Coefficient for linear
x_i	Initial input parameters
β_{ii}	Quadratic coefficient
β_{ij}	Coefficient for interactions
ANOVA	Analysis of Variance
R^2	Coefficient of determination
2D	Two Dimension
3D	Three Dimension
DF	Desirability Function
ST	Standard error
SS	Squares Sum
DF	Degree of Freedom
x_i	Individual parameter
x_ix_j	Interaction of two parameters
xi^2	Quadratic term coefficient
RT	Reaction Time
eV	Electronvolt

1

Chapter 1: Introduction

1.1 Background and Motive

Recent scientific studies have shown that human activities have caused global warming and subsequent climate change because of the increasing demand for energy. The higher usage of fossil fuels such as coal, oil, natural gas (Hamzehlouia, Jaffer, & Chaouki, 2018; Khoja, Tahir, & Amin, 2017) produces methane (CH_4) and carbon dioxide (CO_2), which are considered major sources of greenhouse gases, as shown in Figure 1.1 and they have a negative impact on the life of organisms from an environmental and health perspective. In the past few decades, these negative effects have caused problems and disasters on Earth-like melting of ice at the poles and floodings in low-lying countries such as the Netherlands.
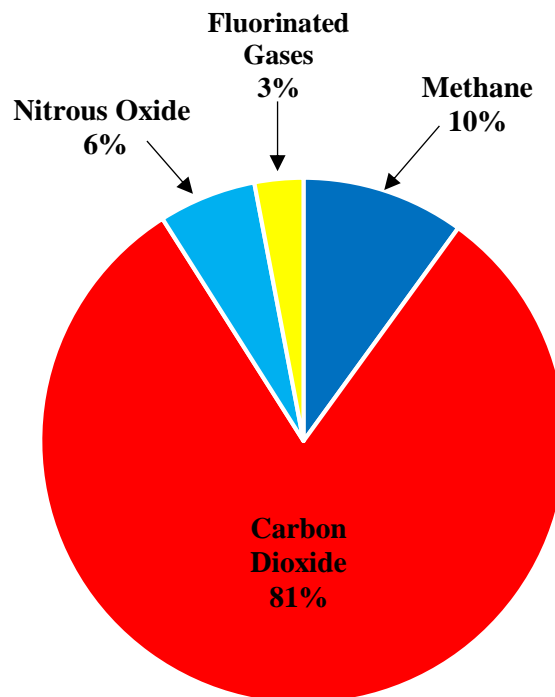
Figure 1. 1 Major sources of greenhouse gas emissions

Consequently, it has become imperative to depend on modern and economical technologies using greenhouse gases as alternative sources for energy generation, chemicals, electricity, heat, and fuels (Xin Tu & Whitehead, 2014). Greenhouse gases

are undesirable products of energy and chemicals produced from fossil fuel-based resources and can be used more productively in their concentrated forms as a feedstock for the production of syngas (Ashcroft, Cheetham, Green, & Vernon, 1991; Bradford & Vannice, 1999; W. Chen, Zhao, Xue, Chen, & Lu, 2013; Dalin Li, Nakagawa, & Tomishige, 2011; Yu et al., 2015). Syngas is a mixture of carbon monoxide (CO) and hydrogen (H_2) that can be directly utilised as fuel for combustion with oxygen (O_2) or as a fuel in molten carbonate and solid oxide fuel cells as well as a raw materials for the production of chemicals such as ammonia, ethanol, methanol, alcohol acetic acid, dimethyl ether, methyl formate, diesel, and gasoline, as shown in Figure 1.2 (Abdullah, Ghani, & Vo, 2017; Allah & Whitehead, 2015; L. Li et al., 2018; Pena, Griboval-Constant, Lecocq, Diehl, & Khodakov, 2013; Tanios et al., 2017; Yabe, Mitarai, Oshima, Ogo, & Sekine, 2017; X. Zhang et al., 2015).
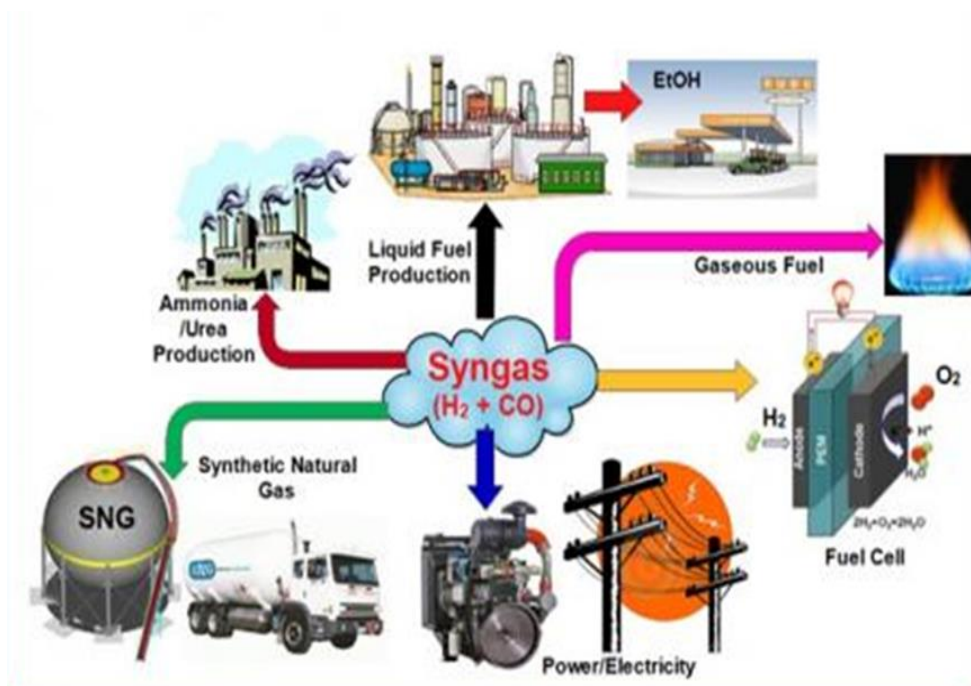
Figure 1. 2 General Mechanism of Syngas Applications

Three different chemical pathways have been established to convert CH_4 to syngas, i.e., (1) steam reforming of CH_4 (SRM, Equation (1-1)), (2) partial oxidation of CH_4 (POM, Equation (1-2)), and (3) dry reforming of CH_4 (DRM, Equation (1-3)).

$$CH_4 + H_2O \rightarrow CO + 3H_2 \qquad \Delta H^\circ{}_{298\,k} = 206\ kJ/mol \qquad\qquad (1\text{-}1)$$

$$CH_4 + \frac{1}{2}O_2 \rightarrow CO + 2H_2 \qquad \Delta H^\circ{}_{298\,k} = \text{-}36\ kJ/mol \qquad\qquad (1\text{-}2)$$

$$CH_4 + CO_2 \rightarrow 2CO + 2H_2 \qquad \Delta H^\circ{}_{298\,k} = 247\ kJ/mol \qquad\qquad (1\text{-}3)$$
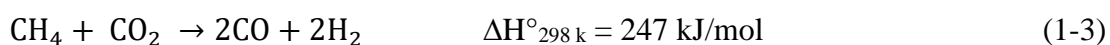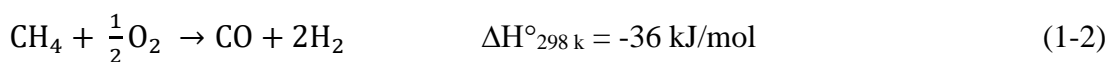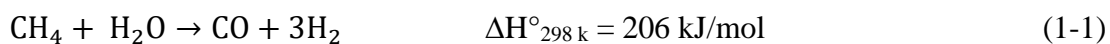
SRM is presently one of the most widely used pathways to obtain syngas (and H_2) from CH_4 because it generates syngas with the highest H_2 to CO ratio of 3 among the three pathways (Rowshanzamir & Eikani, 2009). SRM, however, is a highly endothermic reaction (ΔH (298 K) = 206 kJ mol^{-1}) that requires a temperature above 700 °C to activate and self-sustain (Z. Wang, Ashok, Pu, & Kawi, 2017), which translates to high capital and energy investments requirement. POM, on the other hand, is a mildly exothermic reaction (ΔH (298 K) = -36 kJ mol^{-1}) (Centi, Quadrelli, & Perathoner, 2013). Although the H_2 to CO ratio of POM is approximately 2, which is ideal for syngas conversion to liquid fuels and methanol *via* Fischer–Tropsch (F–T) process, pure O_2 is required for POM because the downstream process cannot endure the presence of the excessive amount of nitrogen (N_2). Such a pure O_2 requirement leads to high investment and energy costs (Z. Wang et al., 2017). DRM is unique in the sense that it combines two greenhouse gases, CH_4, and CO_2 to produce syngas with the lowest H_2/CO ratio of 1 (Shapoval & Marotta, 2015; Tanios et al., 2017; Tao et al., 2011; Yu et al., 2015). Despite the fact that DRM is an extremely endothermic reaction (ΔH (298 K) = 247 kJ mol^{-1}), the interest to DRM comes mainly from three aspects, i.e. (1) Reduction in the net emission of CH_4 and CO_2 if the energy for DRM is supplied by a non-hydrocarbon source, (2) Lower operating cost compared to SRM and POM, and (3) Increased selectivity towards long-chain hydrocarbons during the subsequent F–T process enabled by a low H_2 to CO ratio (Pakhare & Spivey, 2014).

Plasma-induced DRM has recently emerged as an attractive alternative to conventional DRM because it can enhance the reaction performance and suppress the carbon deposition issues with respect to conventional DRM (Shapoval et al., 2014; Snoeckx, Zeng, Tu, & Bogaerts, 2015; Tao et al., 2011). Although there are two different plasma technologies, i.e. non-thermal (cold) plasma and thermal (hot) plasma, upon which the reaction can take place, the former is generally preferred over the latter because of the significantly lower energy consumption in the former case (Bo, Yan, Li, Chi, & Cen,

2008; Eliasson & Kogelschatz, 1991; Goossens, 2012). A non-thermal plasma reaction can be induced *via* glow discharge (GD), corona discharge (CD), silent discharge (SD), dielectric barrier discharge (DBD), radiofrequency discharge (RFD), or microwave discharge (MWD) (Aw, Crnivec, Djinovic, & Pintar, 2014; Bo et al., 2008; Tao et al., 2011). By using microwave irradiation, plasma reaction can be performed in a homogeneous, controlled, and rapid manner (Aziznia, Bozorgzadeh, Seyed-Matin, Baghalha, & Mohamadalizadeh, 2012; Nüchter, Ondruschka, Bonrath, & Gum, 2004). Such features essentially enable reproducibility and scale-up of the reaction (Kustov & Sinev, 2010).

In the presence of microwave irradiation, dissociative collisions of molecules occur. These collisions lead to the formation of reactive atoms, ionised gases, free electrons, and free positive and negative ions, activating the plasma-induced reaction (Eliasson & Kogelschatz, 1991; Ghorbanzadeh, Norouzi, & Mohammadi, 2005; Heijkers et al., 2015; Menéndez et al., 2010; Shapoval & Marotta, 2015; Tao et al., 2011; Thornton, 1983; Xiao et al., 2015). Numerous workers have reported the performance of plasma-induced DRM in terms of CH_4 and CO_2 conversions, H_2 and CO selectivities, yields, and the molar ratio of H_2/CO at atmosphere(s) (Choi, Chun, Ma, & Hong, 2016; S. M. Chun, Hong, & Choi, 2017; Cleiren, Heijkers, Ramakers, & Bogaerts, 2017; Czylkowski, Hrycak, Jasiński, Dors, & Mizeraczyk, 2016; Jamróz, Kordylewski, & Wnukowski, 2018; Javier, Moreno, Stankiewicz, & Stefanidis, 2016, 2017; Khoja et al., 2017; Pakhare & Spivey, 2014; Serrano-Lotina & Daza, 2014; Snoeckx et al., 2015; Uhm, Kwak, & Hong, 2016; Wnukowski & Jamróz, 2018; Zherlitsyn, Shiyan, & Demchenko, 2016). These studies have revealed discrepancies. Some of them have shown positive effects, while others have reported negative effects in the effects of microwave-assisted DRM, aside from the microwave power (MWP), rection time (RT), CO_2/CH_4 ratio (R), total flow rate (TFR), reactor type, and design. Thus far, however, there have been few discussions about the effects of MWP, R, and TFR on plasma stability and syngas production. Therefore, this present study is aimed to deeply study this issue.

Identifying the optimum performance of the plasma process using standard experiments is time-consuming and costly because of the need for multiple experiments at different test conditions (Ayodele, Khan, Nooruddin, & Cheng, 2017). To reduce the difficulty in determining the optimum performance of the plasma

process, previous studies have used the chemical model (Abbasi et al., 2017; Abedini et al., 2017; Challiwala, Ghouri, Sengupta, El-Halwagi, & Elbashir, 2017; De Bie, van Dijk, & Bogaerts, 2015; Hafizi, Rahimpour, & Hassanajili, 2016; Mei, He, Liu, Yan, & Tu, 2016; Montgomery, 2017; Ramachandran, Balasubramanian, & Ananthapadmanabhan, 2011; Senseni, Fattahi, Rezaei, & Meshkani, 2016; Sidik et al., 2016; L. Wu, Yick, Ng, & Yip, 2012). The results show that the chemical model is useful in determining the optimum value for output responses. This model requires a significantly lower number of experiments compared to using a traditional method (Mei et al., 2016). Moreover, the Box–Behnken design (BBD) method was used to find the optimising conditions based on the experimental results. The response surface methodology (RSM) based on a three-parameter and three-level BBD has been developed to determine the effects of independent process parameters. The use of the design of an experimental (DoE) method to optimise the plasma chemical reactions in the DRM microwave plasma is still limited.

In contrast, one of the other important parameters that strongly affect the performance and stability of reaction performance is the type and the flow rate of the additive gas (N_2, Ar, He, or H_2) used in the reaction (Indarto, Choi, Lee, & Song, 2006; Motasemi & Afzal, 2013). Previous studies have primarily concentrated on using additive gases such as N_2 (Chung & Chang, 2016; Hwang, Song, & Cha, 2010; Indarto et al., 2006; X. S. Li, Zhu, Shi, Xu, & Zhu, 2011; Long, Shang, Tao, Yin, & Dai, 2008; Sun et al., 2012; Tao, Qi, Yin, & Dai, 2008; Yan Xu et al., 2013; B. Zhu et al., 2012) and Ar (Allah & Whitehead, 2015; Daihong Li et al., 2009; Marafee, Liu, Xu, Mallinson, & Lobban, 1997; Moshrefi, Rashidi, Bozorgzadeh, & Haghighi, 2013; Ravari, Fazeli, Bozorgzadeh, & Sadeghzadeh Ahari, 2017; Seyed-Matin et al., 2010; Shapoval et al., 2014; Tao et al., 2009; Q. Wang, Yan, Jin, & Cheng, 2009b; B. Yan, Wang, Jin, & Cheng, 2010; Zhou, Xue, Kogelschatz, & Eliasson, 1998) as inert gases to generate the plasma flame by CH_4 reforming. The main processes in non-thermal plasmas operating in N_2 and Ar gases are dissociative collisions of molecules, resulting in the generation of reactive atoms, formation ionised gas with free electrons, and free positive and negative ions (Lieberman & Lichtenberg, 2005). These studies found a good outcome with the use of Ar or N_2 as an inert gas. However, the comparison between the efficiency of N_2 and Ar in the production of syngas under the same test conditions is limited.

Recent years, some research results on CH$_4$ reforming by CO$_2$ and water by using microwave plasma have been reported in the literature (Czylkowski et al., 2016; L. Li et al., 2016). From these studies, the results show that adding steam into DRM is effective and leads to increased conversion of CH$_4$, selectivity, and yield of H$_2$. To address these gaps, this research determines the optimum conditions of the MWP, R, TFR and also the flow feed flow rates for CO$_2$, CH$_4$, and N$_2$ by using the BBD method with RSM to achieve high plasma stability and syngas production. In addition, this work examines the effects of the MWP, R, and TFR on the stability of plasma and the production of syngas by using N$_2$ and Ar in the long term. Furthermore, this research also investigates the effect of adding water to the plasma stability under the same DRM experimental conditions. Figure 1.3 shows the aims of the present work.
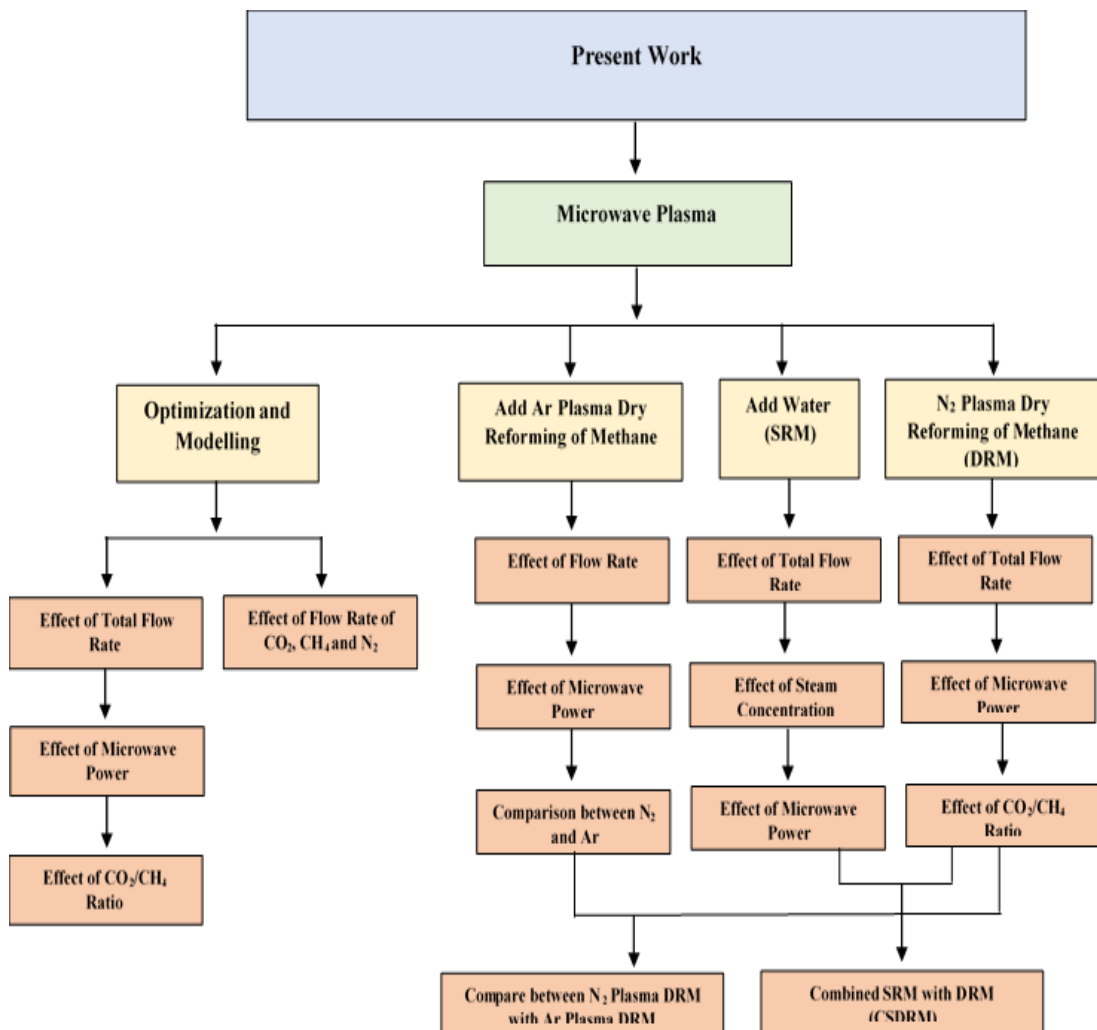
Figure 1. 3 Block diagram of the present work

1.2 Objectives

Based on the background mentioned previously, the primary objectives are as follows:

1- To predict the optimisation of MWP, R, and TFR and their interactions on the CH_4 and CO_2 conversions, selectivities and yields of H_2 and CO, and H_2/CO ratio to determine the optimum conditions in terms of the plasma stability and the syngas production.

2- To predict the optimisation of the effects of the feed gas flow rate (CO_2, CH_4, and N_2) and their interactions on the CH_4 and CO_2 conversions, selectivities and yields of H_2, and CO ratio to find which gas is most significant in terms of the plasma stability and the syngas production.

3- To investigate the effects of DRM on the plasma stability and the syngas production at atmosphere pressure.

4- To investigate the effects of N_2 and Ar as inert gases on the plasma stability and the syngas production at atmospheric pressure and under the same experimental conditions for N_2 and Ar.

5- To investigate the effect adding steam on the stability of plasma and the performance of process at low MWP and low feed flow rates and compare them with DRM at the same experimental conditions.

1.3 Significances

The findings of this research help to develop our understanding of the microwave plasma technique by addressing some important points:

1- This research provides an alternative method for using CO_2 and CH_4, which could yield economic and environmental benefits.

2- The current study contributes to the extant literature by providing more detailed investigations regarding the CO_2 and CH_4 utilisation in the syngas production and different clean fuels; in particular, previous studies have reported contradictory results.

3- This study investigates the effects of MWP, R, and TFR on the plasma stability and the syngas production using BBD. Also, this study provides a fitting model for predicting the CH_4 and CO_2 conversions, selectivities and yields of H_2 and CO, and ratio of H_2/CO.

4- This study optimises of feed flow rate for DRM using a BBD, and it provides a fitting model for predicting the CH_4 and CO_2 conversions, selectivities and yields of H_2 and CO, and ratio of H_2/CO.

5- The results of optimization could help to control on the stability of the plasma flame and the syngas production under various test conditions. The findings could help to develop the current databases for future studies when addressing the same type of microwave reactor. The experimental results of this research provide an initial indication of the effects of additive gases such as N_2 and Ar in the plasma stability and syngas production.

6- This research studies the effects of hybrid DRM with SRM on plasma stability and syngas production under different parameters such as MWP, R, steam concentration (SC), and TFR.

1.4 Thesis Organisation

To establish the research objectives, this thesis is divided into nine chapters, including the current chapter, and the contents of each chapter are briefly outlined as shown in Figure 1.4) as follows:

Chapter 1: This chapter includes briefly the historical review for syngas production, and the applications are presented. In addition, the chapter explains the general concept of plasma technology and its applications. The objective, as well as the summary of this thesis, are also presented in this chapter.

Chapter 2: This chapter presents a review of previous studies that have been reported in the DRM using a microwave plasma technique. A critical review of the results of earlier work is presented to explain the analyses conducted in this research. It also discusses the combined DRM and SRM in the plasma process. The numerical and theoretical studies used to predict the optimum MWP, R, TFR, feed flow rate for CH_4, CO_2 and N_2 are presented as well. Moreover, plasma chemistry, classifications, and

applications are presented. The microwave plasma process and the factors affecting plasma stability are also addressed. Furthermore, the effects of additive gases in plasma DRM are discussed. In addition, the effect of adding steam (SRM) in plasma DRM is also discussed.

Chapter 3: This chapter provides an overview of the research methodology employed to achieve the research objectives, and detailed descriptions of the experimental setup and analytical instruments are deeply presented.

Chapter 4: This chapter studies the optimisation of the DRM process using BBD. The effects of MWP, R, and TFR on the plasma stability and the syngas production were studied.

Chapter 5: This chapter presents the optimisation of the DRM process using BBD. The effects of feed flow rate (CH_4, CO_2, and N_2) on the plasma stability and the syngas production were investigated.

Chapter 6: This chapter is specified for the study of DRM using an N_2 plasma microwave technique at atmospheric pressure. The effects of the N_2 flow rate, MWP, R, TFR, and RT were studied.

Chapter 7: This chapter includes the study effects of additive gases and different parameters on plasma stability and syngas production. The effects of Ar flow rate, MWP, R, TFR, and RT were studied, and this chapter compares N_2-plasma and Ar-plasma at the same experimental conditions.

Chapter 8: This chapter presents the effect of adding the steam on the syngas formation from microwave plasma DRM. The effects of the process parameters such as SC, MWP, and TFR on the plasma stability and the syngas production were also investigated. Moreover, combining SRM with DRM at the same conditions was also studied.

Chapter 9: This chapter concludes all the results from different sections and discusses the recommendations for future work.

```
┌─────────────────────────────────────────────────────────────────┐
│   Thesis Outline: Study of Dry Reforming of Methane Using Microwave Plasma Technique │
└─────────────────────────────────────────────────────────────────┘
```

Chapter 1
Introduction

1.1 Background and Motive 1.2 Objectives 1.3 Significances 1.4 Thesis Organisation

Chapter 2
Literature Review

2.1 Introduction 2.2 Carbon dioxide and Methane Chemistry 2.3 CO_2 and CH_4 utilization 2.4 Plasma Chemistry 2.5 Microwave Discharges in Plasma Chemistry 2.6 The Role of Additive Gas in Plasma Dry Reforming of Methane

Chapter 3
Experimental Procedure

3.1 Introduction 3.2 Experimental Set up 3.2.1 Power Supplier 3.2.2 Microwave Power Head (Generator) 3.2.3 Quartz Reactor 3.2.4 Feeding Gases and Mass Flow Rate Controller 3.2.5 Water Addition Line 3.2.6 Feed and Product Sampling 3.2.7 Chemical Analysis 3.3 Design of Experiments (DoE)

Chapter 4
Operation and Optimization of the Microwave Power, CO_2/CH_4 Ratio and Total Feed Flow Rate by a Microwave Plasma Technique Using a Box-Behnken Design

4.1 Introduction 4.2 Result and Discussion 4.3 Optimization and validation of models 4.4 Investigating the performance of a typical experiment 4.5 Summary

Chapter 5
Optimization and modelling of the Dry Reforming of Methane by a Microwave Plasma Technique Using a Box-Behnken Design

5.1 Introduction 5.2 Approximate Model Function 5.3 Result and Discussion 5.4 Summary

Chapter 6
Stability of Plasma Zone of Dry Reforming of Methane by using Nitrogen

6.1 Introduction 6.2 Results and Discussions 6.3 Summary

Chapter 7
Comparative study on the performance of microwave-assisted plasma dry reforming of methane in nitrogen and argon atmospheres at a low microwave power irradiation

7.1 Introduction 7.2 Results and Discussions 7.3 Comparison between the N_2-Plasma and the Ar-Plasma DRM 7.4 Summary

Chapter 8
Syngas formation by steam reforming of methane using microwave plasma technology

8.1 Introduction 8.2 Results and Discussions 8.3 Microwave Plasma Steam Combined with Dry Reforming of Methane 8.4 Summary

Chapter 9
Conclusions and Recommendations
9.1 Introduction 9.2 Conclusions 9.3 Recommendations and future work

Figure 1. 4 Diagrammatic representation of the thesis' organization

2

Chapter 2: Literature Review

2.1 Introduction

In recent decades, there has been increasing concern regarding serious issues connected to climate change because of its effect on the environment. One of these main issues is the large-scale release of greenhouse gases emission to the atmosphere (Budiman, Song, Chang, Shin, & Choi, 2012; Ismail & Ani, 2015; M.-w. Li, Xu, Tian, Chen, & Fu, 2004). Recently, natural gas (CH_4) has become one of the top sources of energy available throughout the world because it is largely used in industry to produce H_2 or syngas (H_2, CO) (Jasiński, Dors, & Mizeraczyk, 2009). There are three major methods used to convert CH_4 into syngas, and these are SRM (Akbari-Emadabadi, Rahimpour, Hafizi, & Keshavarz, 2017; Nawfal et al., 2015), POM (Figen & Baykara, 2018; Peymani, Alavi, & Rezaei, 2016) and DRM (Itkulova, Zakumbaeva, Nurmakanov, Mukazhanova, & Yermaganbetova, 2014; L. Li et al., 2017; Oyama, Hacarlioglu, Gu, & Lee, 2012; Usman, Daud, & Abbas, 2015). Through such means, the microwave-assisted DRM has become the best solution to solve the environmental and economic problems and produce clean fuels (Naeem, Al-Fatesh, Khan, Abasaeed, & Fakeeha, 2013khoncheh, 2015 #366). DRM refers to the chemical reaction of CH_4 and CO_2 to form H_2 and CO (Johnsen, Ryu, Grace, & Lim, 2006; Y. Li, Wang, Zhang, & Mi, 2008). Syngas is an important intermediate for the downstream production of a wide range of chemicals and synthetic fuels (Markewitz et al., 2012). Because the relatively low H_2 to CO ratio, this process is attractive for the Fischer–Tropsch synthesis (FTS) process of the gas-to-liquid (GTL) technologies (Ahmadpour & Taghizadeh, 2015; Akande, Aboudheir, Idem, & Dalai, 2006; Al-Sobhi & Elkamel, 2015; Freitas & Guirardello, 2014; Hu, 2010).

2.2 Carbon dioxide and Methane Chemistry

CO_2 and CH_4 are the famously known gases that have a significant effect on our life and the future of the Earth. CO_2 is distinguished as a colourless, odourless gas heavier than air and has a permanent quadrupole moment of $-8.58 \pm 0.35 \times 10^{-40}$ C m^2 (Pradier & Pradier, 2014). CO_2 is found at low concentrations in our atmosphere; therefore, it is considered not harmful. In the case of CO_2 reaching a high concentration in the

atmosphere, it could displace O_2 in the air and can affect respiratory function and then cause excitation followed by depression of the central nervous system (J. Paul & Pradier, 1994b). The boiling point of CO_2 is -78.5 °C (-109.3 °F; 194.7 K), while the melting point is -56.6 °C (-69.8 °F; 216.6 K). CO_2 could be generated from petroleum and natural gas by burning fossil fuels, principally oil and coal. Second, natural gas is used in transportation, heating, the generation of electrical power, and in the production of cement (Caldeira & Wickett, 2005). Human activities have negatively affected the concentration of CO_2 in the atmosphere.

Consequently, increasing the CO_2 concentration in the atmosphere more than the standard limits has caused global warming problems. These problems are because of the photo characteristic of CO_2 which can damage the transparency of the atmosphere and absorb infrared light which is usually reflected from the Earth's surface or passes through the atmospheric layers to space when the concentration of CO_2 is in the allowable range. CO_2 is inert at standard conditions; however, it can be dangerous and react with many materials if the temperature reaches more than 195 °C.(Karamé, Shaya, & Srour, 2018; J. Paul & Pradier, 1994a). Therefore, CO_2 is considered the major cause of climate change because of its greenhouse properties and continuous accumulation in the atmosphere (Caldeira & Wickett, 2005; Pradier & Pradier, 2014). CO_2 can be commercially used in industries from food processing, the manufacturing of many products, and to firefighting, but its use as feedstock in the production of syngas is considered one of the most important uses from an environmental perspective (Pettinau, Mureddu, & Ferrara, 2017).

In contrast, CH_4 is the simplest member of the paraffin series of hydrocarbons. Its chemical formula is CH_4, meaning it has one carbon atom bonded to four hydrogen atoms (Sellers, Spiteri, & Perrone, 2009). CH_4 is a colourless, odourless, flammable, and nontoxic gas, and it is lighter than air. CH_4 occurs abundantly in nature and as a side product of certain human activities such as the following emissions: burning of coal and natural gas for electricity generation in power stations, combustion of biomass, and decomposition of organic matter in landfills (Crabtree, 1995). CH_4 is one of the raw materials used in the production of ethanol, methyl chloride, methylene chloride and is also used to produce ammonia and acetylene. In general, CH_4 is very stable, but it is combustible in the presence of air. More specifically, CH_4 becomes very dangerous and could cause an explosion if the CH_4 content is between 5 to 15 %

volume (Whitman, Bowen, & Boone, 2006). The boiling point of CH_4 is -162.0 °C (-259.6 °F), and the melting point is -182.5 °C (-296.5 °F). It burns readily in air, forming CO_2 and water vapour; the flame is pale, slightly luminous, and very hot. In addition, the CH_4 is considered the second most devastating greenhouse gas after CO_2 (Caballero & Pérez, 2013). Recently, CH_4 is widely used for fuel in homes, commercial establishments, and factories because of its abundance, low cost, ease of handling, and cleanliness. CH_4 is considered one of the important sources of H_2 production and some organic matters (Khalil, 2013). Besides, other valuable chemicals derived from CH_4 include methanol, chloroform, carbon tetrachloride, and nitro CH_4 (Kirschke et al., 2013). The incomplete combustion of CH_4 yields carbon black, which is widely used as a reinforcing agent in rubber used for automobile tyres (Olah et al., 2015).

The main difference between CO_2 and other greenhouse gases, particularly CH_4, is the large heat of formation of CO_2. It is thermodynamically favourable to convert CH_4 to valuable products, but the conversion of CO_2 needs an energy-rich co-feed (J. Paul & Pradier, 1994a). The simplest method to convert CO_2 into an energetic product is its deoxygenation to produce CO, a reaction that can be performed either by a thermal or by a radiative route. Such a non-catalysed process is very energy demanding. The produced CO can be burnt with air to give energy and CO_2 (Aresta, Dibenedetto, & Angelini, 2013). However, unlike CO_2, which has a quadrupole moment and can be captured both physically and chemically in a variety of solvents and porous solids, CH_4 is completely nonpolar and interacts very weakly with most materials (J. Kim et al., 2013).

2.3 CO_2 and CH_4 utilization

In recent years, the idea of taking advantage of greenhouse gases has grown because of many reasons such as the elimination of the risk of the emission of these gases directly into the atmosphere and as well as the increased fuel price in the world markets. The utilisation of greenhouse gases is not only considered environmentally viable only but also economically viable (Alper & Orhan, 2017). The following are some of the possible chemical routes in fixing CO_2 and CH_4.

2.3.1 Gas-to-Liquid Process

Before the 21st century, natural gases were transported by pipelines, trucks, trains, or ships, and it was uneconomical, non-environmental, and much more expensive than transporting liquid petroleum. Therefore, there is an urgent and necessary need to find a technique that can solve these problems. The GTL technique has become the best solution for these problems by converting natural gas or other gaseous hydrocarbons into longer-chain hydrocarbons, such as gasoline or diesel fuel (Maqbool, Park, & Lee, 2014).

The GTL is a refinery process, which consists of three main units: syngas production, Fischer-Tropsch synthesis (FTS), and upgrading of FT products (Aasberg-Petersen, Christensen, Nielsen, & Dybkjær, 2003), as shown in Figure 2.1. The first step in the FTS-GTL process is converting natural gas, which is mostly CH_4, to a mixture of H_2, CO_2, and CO. This mixture is called syngas (Salehi & Save, 2013; Wilhelm, Simbeck, Karp, & Dickenson, 2001; Yagi et al., 2005). The basic routes to syngas production from natural gas are SRM, catalytic or non-catalytic POM, and DRM (Rafiee & Hillestad, 2012). The next step in the GTL method is the F–T reaction, which combines H_2 with CO to form different liquid hydrocarbons. These liquid products are then further processed into the final step that uses different refining technologies for developing liquid fuels (Shamkhali, Omidkhah, Towfighi, & Jafari Nasr, 2012), as presented in Figure 2.1.

GTL process has many commercial, industrial, and environmental advantages, such as the production of clean energy sources (liquid fuels) (Fleisch, Sills, & Briscoe, 2002). Liquid fuels have many economic features such as they are much easier to transport from remote locations relative to the natural gases (Kresnyak, Price, & Wagner, 2018; Patience & Boffito, 2016). In addition, the yields of light and middle products are high (Behroozsarand & Zamaniyan, 2017).
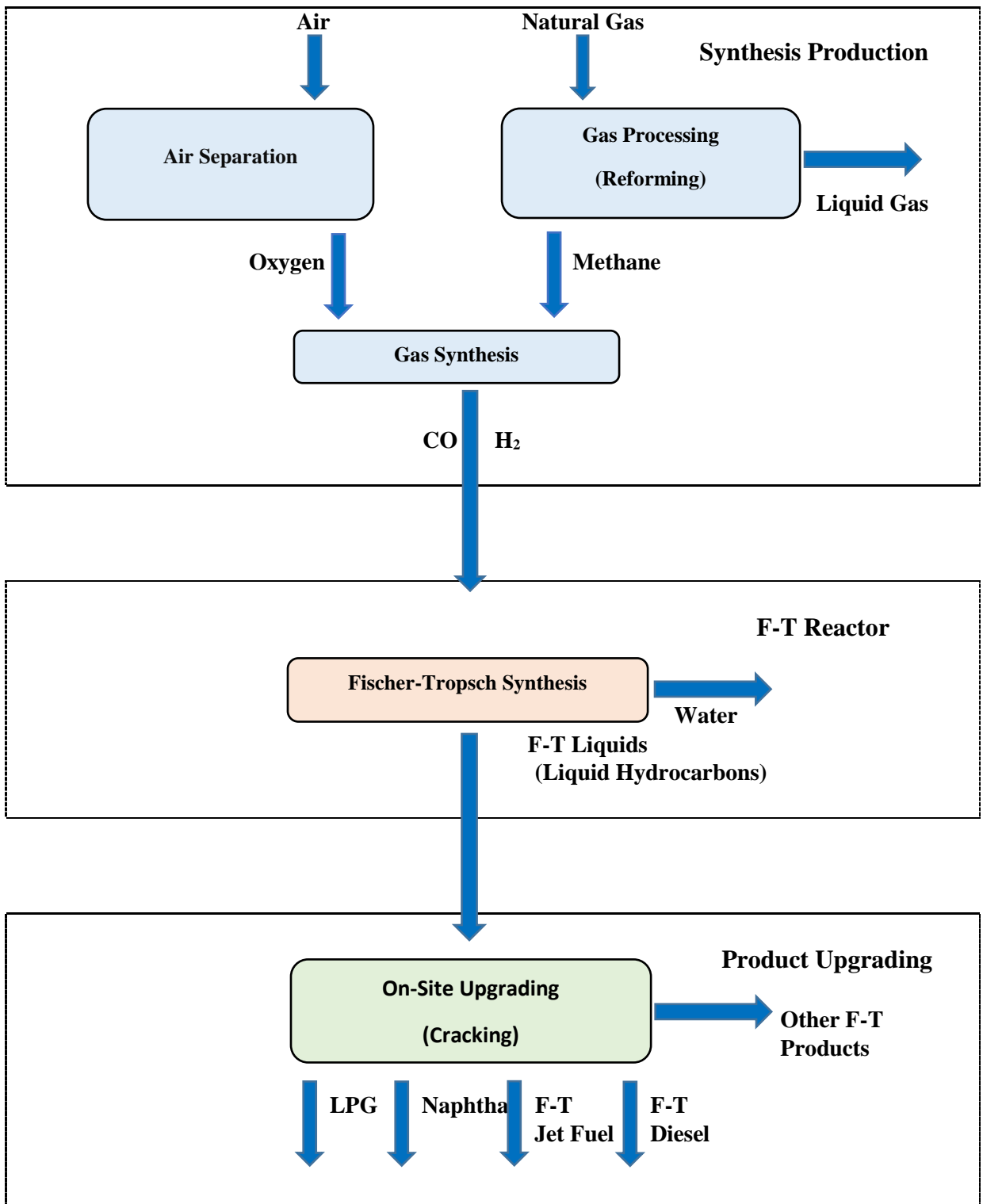
Figure 2. 1 Gas To Liquid (GTL) Block Flow Diagram

2.3.2 DRM Process and its comparison with others

Greenhouse gases such as CH_4 and CO_2 are undesirable products of energy and chemicals production from fossil fuel-based resources, and these gases can be used more productively in their concentrated forms as a feedstock for the production of syngas (Ashcroft et al., 1991; Bradford & Vannice, 1999; W. Chen et al., 2013; D. Li et al., 2011; Xin Tu & Whitehead, 2014; Yu et al., 2015). DRM is an attractive process from an environmental perspective because it involves the conversion of two greenhouse gases (Equation 1-3, Chapter 1) that can be renewably generated as syngas (Xin Tu & Whitehead, 2014). Syngas is produced mainly from different hydrocarbon materials, such as natural gas, refinery gases, liquified petroleum gas (LPG), naphtha, heavy residues, and solid fossil fuels such as petroleum, biomass, coal, pet coke, and biogas (L. Li et al., 2018). Generally, natural gas is one of the most commonly used sources because includes CH_4, thus is abundant in nature, has low cost, and is the cleanest energy source compared with other sources (Spath & Dayton, 2003; Wilhelm et al., 2001).

As shown in Figure 2.2, syngas plays an important role in chemical engineering because it is an intermediate for synthesising of a variety of important and essential chemical feedstock and environmentally clean and liquid fuels such as ammonia, methanol, ethanol, acetic acid, methyl format, dimethyl ether, synthetic gasoline, and diesel via the Fischer–Tropsch process (Abdullah et al., 2017; Ghouri et al., 2016; Kasht, Hussain, Ghouri, Blank, & Elbashir, 2015; Pakhare & Spivey, 2014; Ross, Van Keulen, Hegarty, & Seshan, 1996; Rostrup-Nielsen, 2000; Usman et al., 2015; W. Wang, Wang, Ma, & Gong, 2011).
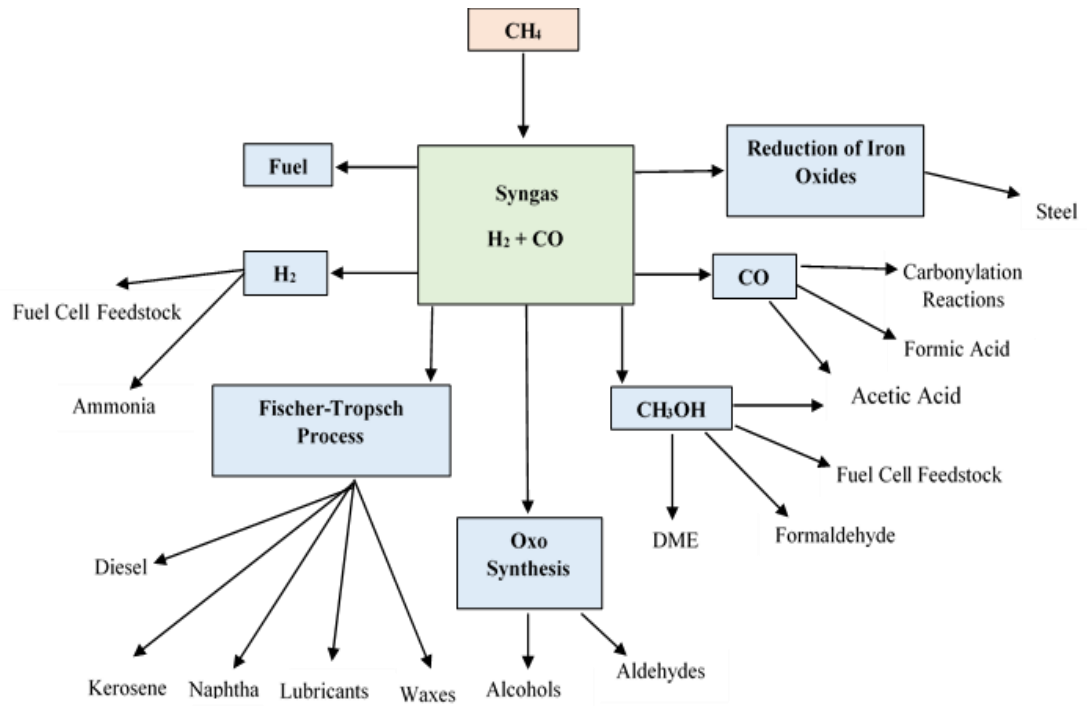
Figure 2. 2 Schematic diagram showing the main applications of syngas

Recently, numerous scientific approaches have been implemented to convert the CH_4 into syngas as presented in Chapter 1, such as SRM (Equation 1-1, Chapter 1) (Pacheco et al., 2015), POM (Equation 1-2, Chapter 1) (Centi et al., 2013), DRM (Equation 1-3, Chapter 1) (L. Li et al., 2017), and Table 2.1 summarises the advantages and disadvantages of the three main reforming technologies used to produce syngas. Table 2.1 shows that DRM and SRM technologies have high H_2 yields because they do not use air as an oxidant. However, these methods require high operating conditions of temperature and pressure to complete the reaction because they are endothermic reactions (Abdullah et al., 2017).

Table 2. 1 Advantages and disadvantages for four types of Reforming of Methane

Type of Reforming	Advantages	Disadvantages	References
SRM	H_2/CO ratio of 3 Highest H_2 yield Mostly extensive Oxygen not required	Endothermic reaction Requires high temperature and pressure Highest air emissions High energy cost	(Gangadharan, Kanchi, & Lou, 2012; Samuel, 2003)
POM	Exothermic reaction H_2/CO ratio of 2 Quick dynamic response Less careful thermal management Feedstock desulfurization not required	Only works on certain fuels (sensitive to natural gas qualities) Requires to an air separation plant (oxygen plant) Very high process operating temperature Lowest H_2 yield	(Iwarere, Rohani, Ramjugernath, & Fulcheri, 2015)
DRM	H_2/CO ratio is almost one CO_2 conversion 100% Highest H_2 yield CO_2 converts instead of releasing into the atmosphere Low raw material cost	Endothermic reaction Requires high temperature and pressure High energy cost	(Centi et al., 2013; Fakeeha, Ibrahim, Naeem, & Al–Fatesh, 2014; Serrano-Lotina & Daza, 2014)

The most important technology for high syngas production is SRM. It is a produced gas mixture with a high H_2/CO ratio (Akbari-Emadabadi et al., 2017). This technology is an endothermic reaction (Equation 1.1) that needs a high temperature (higher than 700 °C) to activate the reforming reaction, as shown in Table 2.1 (Nawfal et al., 2015). The POM method is considered an exothermic reaction (Equation 1-2), and it has an advantage of quick dynamic response with less thermal management, as presented in Table 2.1. (Iwarere et al., 2015). However, this method only works with certain fuels (sensitive to natural gas qualities) and requires an air separation plant (Álvarez Galván et al., 2018). In addition, this method has the lowest H_2 yield because it uses air as an oxidant (Holladay, Hu, King, & Wang, 2009). As shown in Table 2.1, DRM is an endothermic reaction (Equation 1-3) that requires operating temperatures over 640 °C and at atmospheric pressure to achieve high equilibrium conversions of CO_2 and CH_4 (Choi et al., 2016). At temperaturic pressure between 560 and 700 °C, carbon formation is thermodynamically favoured by both decompositions of CH_4 and the Boudouard reaction (2-1 and 2-3, respectively). To reduce carbon formation, DRM is

usually performed at temperatures greater than 750 °C, where carbon formation is less thermodynamically favourable (S. M. Chun et al., 2017).

The severity of carbon deposition is more pronounced in dry reforming of CH_4 than for SRM or POM because of the low O/C atomic ratio in the feed gas, which is made worse with higher CO_2 content (Kraus et al., 2002). Increasing the operating pressure above atmospheric pressure may be preferable in the industry to minimise reactor dimensions and improve reaction rates; however, this also increases the rate of carbon deposition. The DRM main reaction (Equation 1-3), is followed by three side reactions (see Table 2.2): CH_4 decomposition (Equation 2-1), reverse water gas shift (RWGS) reaction (Equation 2-2), Boudouard reaction (Equation 2-3), and carbon gasification reaction (Equation 2-4).

Table 2. 2 The DRM reactions

Reaction Designation	Reaction	ΔH°_{298K} kJ mol^{-1}	Reaction Priority	Equation Number
Methane Decomposition (Methane Cracking)	$CH_4 \rightleftarrows C + 2H_2$	+74.9	Side Reaction	2-1
Revers Water Gas Shift (RWGS)	$CO_2 + H_2 \rightleftarrows CO + H_2O$	+41.2	Side Reaction	2-2
Boudouard (CO Disproportionation)	$2CO \rightleftarrows CO_2 + C$	-172.4	Side Reaction	2-3
Carbon Gasification	$C + H_2O \rightleftarrows CO + H_2$	-131.3	Side Reaction	2-4

2.3.3 Combined SRM and DRM

Based on advantages introduced in the previous sections, the combined SRM and DRM, abbreviated as CSDRM (Equation 2-5), also known as bi-reforming of CH_4, has recently appeared as a promising technique because it is capable of generating a suitable syngas for the F–T process by using the greenhouse gases and water (Noureldin, Elbashir, & El-Halwagi, 2013; Olah et al., 2015).

$$3CH_4 + CO_2 + 2H_2O \rightarrow 8H_2 + 4CO \qquad \Delta H = +712 \text{ kJ/mol} \qquad (2\text{-}5)$$

The CSDRM can produce syngas with flexible H_2/CO ratios of 2.0 (Choudhary & Mondal, 2006; A. R. Kim et al., 2015; Pour & Mousavi, 2015). The H_2/CO ratio of syngas produced via the CSDRM can be controlled by changing the composition of the feed gas (H_2O, CO_2, and CH_4) (Czylkowski et al., 2016; L. Li et al., 2016).

CSDRM is a complex process because many side reactions can occur simultaneously, as illustrated in Table 2.2.

The combined SRM and DRM has many advantages such as a high conversion of CH_4, good selectivity, yield of H_2, and this combination can produce a suitable H_2/CO syngas ratio (Holladay et al., 2009; Roh et al., 2007). Another important advantage in this method is a reduction in the amount of soot produced (Pour & Mousavi, 2015). CSDRM has been used in industry for several years (Choudhary & Mondal, 2006; Choudhary & Rajput, 1996; Hegarty, O'Connor, & Ross, 1998; Noronha et al., 2003). A further advantage of this process is the continuation of CO_2 release from SRM because of the RWGS reaction (Olah et al., 2015), as shown in Equation 2-5.

Recently, some research results on CH_4 reforming by CO_2 and water using microwave plasma are reported in the literature (Czylkowski et al., 2016; L. Li et al., 2016). From these studies, the results show that adding steam into the DRM is effective and increases the conversion of CH_4, selectivity and yield of H_2, and H_2/CO ratio of syngas production. Unfortunately, some knowledge gaps about the combined effect of steam concentration and microwave power on the process performance and product quality have remained unknown. Therefore, another main aim of the present work is studying the combined influence of the process parameters (input MWP, SC, and TFR) on the syngas ratio (H_2/CO) under microwave irradiation at atmospheric pressure.

2.4 Plasma Chemistry
2.4.1 Introduction

Plasma is considered a technology that can be utilized to improve the chemical reactions performance (Leonov & Yarantsev, 2006). Generally, plasma contains a mixture of free electrons; negative and positive ions; atoms; molecules; radicals; photons, and some neutral species (Alexander Fridman, 2008). The plasma state can exist for a wide range of pressures, as shown in Figure 2.3; it has been classified based on their electron temperature and electron density.
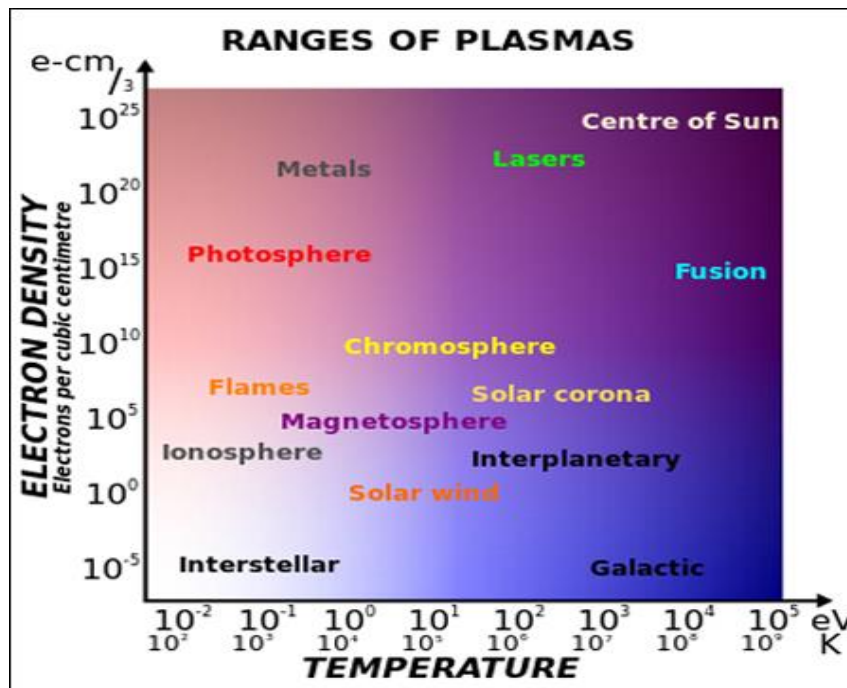
Figure 2. 3 Range of Plasma (taken from (Peratt, 1997))

The scientific study of plasma generation began in 1808 with Sir Humphry Davy's development of the steady-state DC arc discharge. However, it was Davy's protégée, Michael Faraday, who significantly moved this science forward with his development of the high voltage DC electrical discharge tube in the 1830s. Faraday first introduced the idea of ions as carriers of electricity, and he distinguished between the cathode and anode and also the notions of cations and anions (Foest, Schmidt, & Becker, 2006). The first person identified plasma was Sir William Crookes using a Crookes tube in 1879, and who called it ''the radiant matter,'' (J Reece Roth, 2001). After over a century of research, the term "plasma" was originated in 1920 by Lewi Tonks, and Irving Langmuir adopted (Langmuir, 1928; Tonks & Langmuir, 1929).

Plasmas are mostly known as electrical discharges that can often be seen in both the natural world and anthropogenic worlds such as lightning, the northern lights, and fluorescent lamps. Generally, plasma is an ionized gas, which means the conversion of natural atoms or molecules into electrons and positive ions. In this case, the electrons are free and not connected to the atom or molecule (Alexander Fridman, 2008). The free electrons move very fast, and they gain enough kinetic energy from the electric field. The energy is transferring by the collisions of electron neutral (Schutze et al., 1998). When shedding an electric field, the electron ejects away from

the nucleus, resulting in more positive and negative charges called ions. Positive ions are major players in the plasma chemical processes (Meichsner, Schmidt, Schneider, & Wagner, 2012).

In this case, the electrons are first getting energy from the electric fields, because of their low mass and high mobility (Hazeltine, 2018). Then, electrons transmit the energy to all other plasma components, providing energy for ionization, excitation, dissociation, and other plasma chemical processes (Schunk & Nagy, 2009). Inelastic collisions lead to transferring the electron kinetic energy into internal energy of neutral species and lead to the breakdown of gas. These internal energies give rise to free radicals, ions, and free electrons that are very reactive and can easily induce chemical reactions. Table 2.3 presents the different inelastic collision processes (Eliasson & Kogelschatz, 1991).

Table 2. 3 Main inelastic collision processes

Electron/Molecular		
Reaction	**Inelastic Collisions**	**Equation Number**
Excitation	$e^- + A_2 \rightarrow A_2^* + e^-$	2-6
Dissociation	$e^- + A_2 \rightarrow 2A + e^-$	2-7
Attachment	$e^- + A_2 \rightarrow A_2^-$	2-8
Dissociative Attachment	$e^- + A_2 \rightarrow A^- + A$	2-9
Ionization	$e^- + A_2 \rightarrow A_2^+ + 2e^-$	2-10
Dissociative Ionization	$e^- + A_2 \rightarrow A^+ + A + e^-$	2-11
Recombination	$e^- + A_2^+ \rightarrow A_2$	2-12
Detachment	$e^- + A_2^- \rightarrow A_2 + 2e^-$	2-13
Atomic/Molecular Reactions		
Reaction	**Inelastic Collisions**	**Equation Number**
Penning Dissociation	$M + A_2 \rightarrow 2A + M$	2-14
Penning Ionization	$M^* + A_2 \rightarrow A_2^+ + M + e^-$	2-15
Charge Transfer	$A^\pm + B \rightarrow B^\pm + A$	2-16
Ion Recombination	$A^- + B^+ \rightarrow AB$	2-17
Neutral Recombination	$A + B + M \rightarrow AB + M$	2-18
Decomposition		
Reaction	**Inelastic Collisions**	**Equation Number**
Electric	$e^- + ab \rightarrow A + B + e^-$	2-19
Atomic	$A^* + B_2 \rightarrow AB + B$	2-20
Synthesis		
Reaction	**Inelastic Collisions**	**Equation Number**
Electric	$e^- + A \rightarrow A^* + e^-, A^* + B \rightarrow AB$	2-21
Atomic	$A + B \rightarrow AB$	2-22

A and B means represent atoms and M stands for a temporary collision partner

The physics definition for the plasma is an ionized gas with an equal the density of positive and negative charges (Conrads & Schmidt, 2000; Sturrock, 1994). According to the definition, the plasma is categorized by a variety of parameters including pressure, temperature, and density of electrons (Safa, Ghomi, & Niknam, 2014). Plasma flame can be generated from a gas by the application of electric field energy, electric field beams, and radiation or by adiabatic gas compression (Gousset, Panafieu, Touzeau, & Vialle, 1987). The molecules become more energetic with increasing temperature and leading to the matter will passage in the four cases of solid, liquid, gas and finally plasma, which clarifies the meaning of the title "4th state of matter" (Liston, 1989; Moustakas, Fatta, Malamis, Haralambous, & Loizidou, 2005). Although plasma is closely related to the gas phase, it differs in several using, as shown in Table 2.4.

Table 2. 4 Difference between the plasma and the gas

Gas	Plasma
Electrical conductivity in the gas is very low	Electrical conductivity in the plasma is very high
Gas molecules do not work independently	Electrons, ions, protons, and neutrons in the plasma work independently
The velocity of the gas particles regularly is distributed in all directions	The velocity of the plasma particles is not systematically distributed in all directions
Gas reactions occur as a result of collisions of two particles, while the gas reaction occurs from collisions of three particles is rare.	Plasma reactions occur as a result of the collision of particles of gases entering with each other.

The principles of plasma generation are summarized in Figure 2.4 (Meichsner et al., 2012). Additionally, many of the sources of the particles for different chemical reactions (also forming new components that change the properties of materials) are generated inside the reactor (Mabrouk, Lemont, & Baronnet, 2012). As a rule, there are some gases that can be utilized to generate the plasma flame such as argon, hydrogen, helium, nitrogen, oxygen, air, steam, CO, and CO_2 (Xiao et al., 2015).
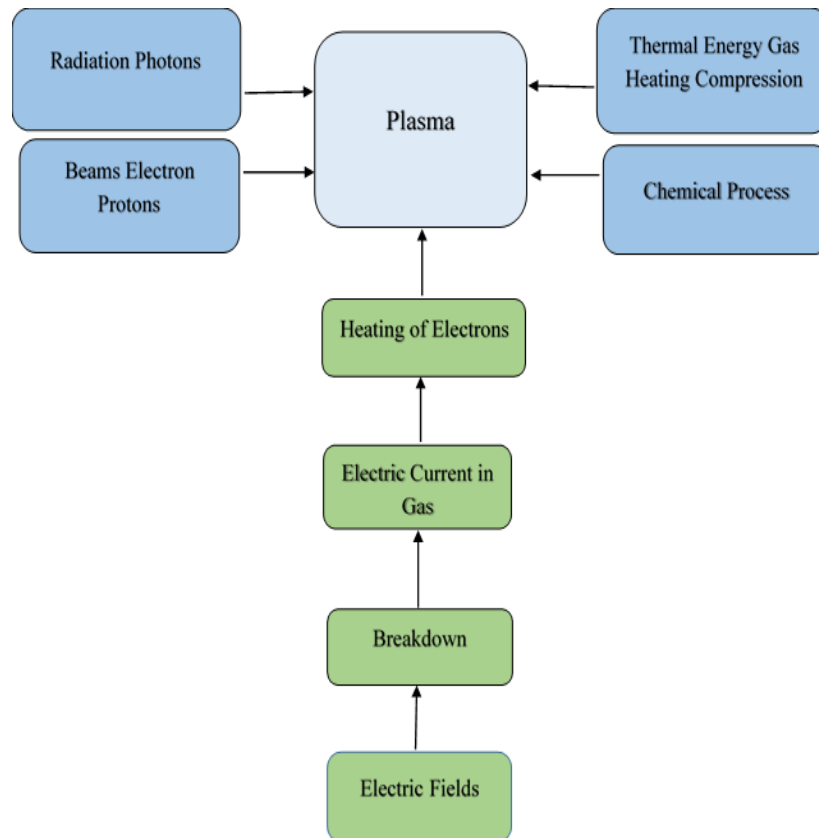
Figure 2. 4 Principles of plasma generation

Plasma is also present in the upper region of the Earth's atmosphere (at altitudes > 100 km) (Alexander Fridman, 2008) where interactions with cosmic radiation lead to the dissociation of atmospheric gas molecules. This produces a region of ions and freely moving electrons, known as the ionosphere. The plasma process is considered a suitable method to produce a gas-phase reaction which is used to convert methane (CH_4) and carbon dioxide (CO_2) into syngas (H_2 and CO) (Long et al., 2008; Snoeckx et al., 2015).

The stability of plasma is an important consideration in the study of plasma chemistry. Many parameters that effect on the plasma stability and performance such as feed gas flow rate, R, reactor design, residence time, and discharge power, as shown in Figure 2.5 (Mei et al., 2016; Snoeckx et al., 2015).
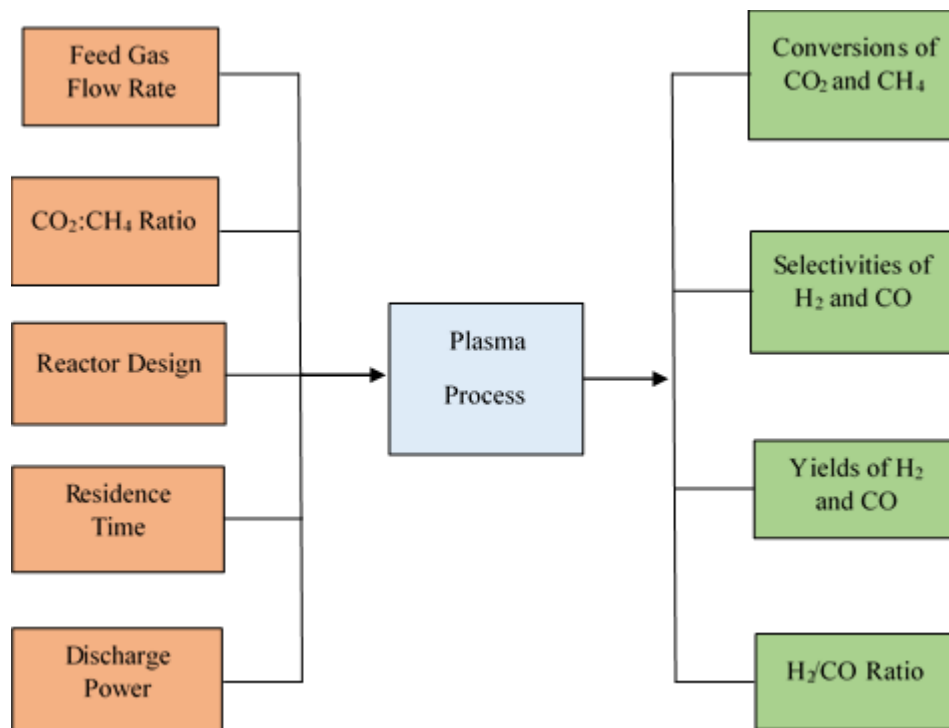
Figure 2. 5 Parameters Affecting on Plasma Process

Firstly, the effect of the feed gas flow rate is considered an important variable on the plasma stability and the performance of the process, such as conversions, selectivities, yields, and syngas ratio. Cleiren et al. (2017) reported that the feed flow rate affects the conversion, selectivity, yield, and syngas (H_2/CO) ratio. They also found that increasing the CH_4 flow rate leads to a decrease in the conversions of CO_2 and CH_4, selectivities, and yields of H_2 and CO. While, the syngas ratio increased with increasing the flow rate of CH_4. The reason for this could be related to the residence time of the gases in the microwave discharge zone. In other words, the increasing the gas feed flow rate leads to the shorter treatment time of gases inside the reactor (Cleiren et al., 2017; Pakhare & Spivey, 2014; Serrano-Lotina & Daza, 2014).

Secondly, The R has a significant effect on the stability of plasma and the conversion, selectivity, yield, and H_2 to CO molar ratio. (Khoja et al., 2017; Pakhare & Spivey, 2014) have pointed out that the R affects the plasma stability and performance of the process. They noticed that the CH_4 conversion, as well as the CO selectivity increase with increasing CO_2 flow rate, while CO_2 conversion, H_2 selectivity, H_2 and CO yields, and H_2/CO ratio all decreased. Increasing R results in a higher collision probability between carbon dioxide and energetic electrons, so an increase in CO_2 conversion to

CO and atomic O, followed by an increase in methane conversion due to the reaction between CH_4 and atomic O is observed (Q. Wang, Yan, Jin, & Cheng, 2009a; A. Wu et al., 2014). They also, (Adris, Elnashaie, & Hughes, 1991) concluded that the reactor design affects the plasma stability and process performance. Moreover, Ashcroft et al. (1991) reported that the CO_2 and CH_4 conversions, H_2 and CO selectivities and yields and H_2/CO ratio decrease with increasing residence time.

Finally, the discharge power had been found to be another significant variable affecting the stability of plasma and the performance of the reactor system. (Aziznia et al., 2012; Jiang et al., 2002; J.-Q. Zhang, Zhang, Yang, & Liu, 2003) reported that the discharge power affects the plasma stability and process performance. They found that the conversions of CO_2, CH_4, and N_2, CO selectivity and H_2, CO yields increase, during H_2 selectivity and H_2/CO ratio decrease with increasing power. The increase in power could lead to enhancement in the electric field, electron density and gas temperature (S. M. Chun et al., 2017; A. Ozkan et al., 2015; X Tu & Whitehead, 2012).

2.4.2 Types of Plasma

Generally, plasma can be classified into two main streams are based on temperature, including high-temperature plasma (such as thermonuclear fusion plasmas or thermal arc torches) and the other is low-temperature, as shown in Table 2.5.

Table 2. 5 Classifications of Plasma

Low-Temperature Plasma		High-Temperature Plasma
Thermal Plasma	**Non-Thermal Plasma**	
$T_0 \approx T_i \approx T_r \approx T_v \approx T_e \leq 2 \times 10^4\,K$	$T_0 \approx T_i \approx T_r < T_v << T_e \leq 10^5\,K$	$T_0 \approx T_i \approx T_r \approx T_v \approx T_e \geq 10^7\,K$

Note. T_o: gas temperature; T_i: ion temperature; T_r: rotational temperature; T_v: vibrational temperature and T_e: electron temperature (Hippler, Pfau, Schmidt, & Schoenbach, 2001)

The low temperature is sub-divided into thermal (hot or fusion plasma) and non-thermal (cold or gas discharge), which are also known as equilibrium and non-equilibrium plasmas, respectively, as shown in Figure 2.6. More details about the thermal and non-thermal plasma will be presented in section 2.4.2.1 and 2.4.2.2.
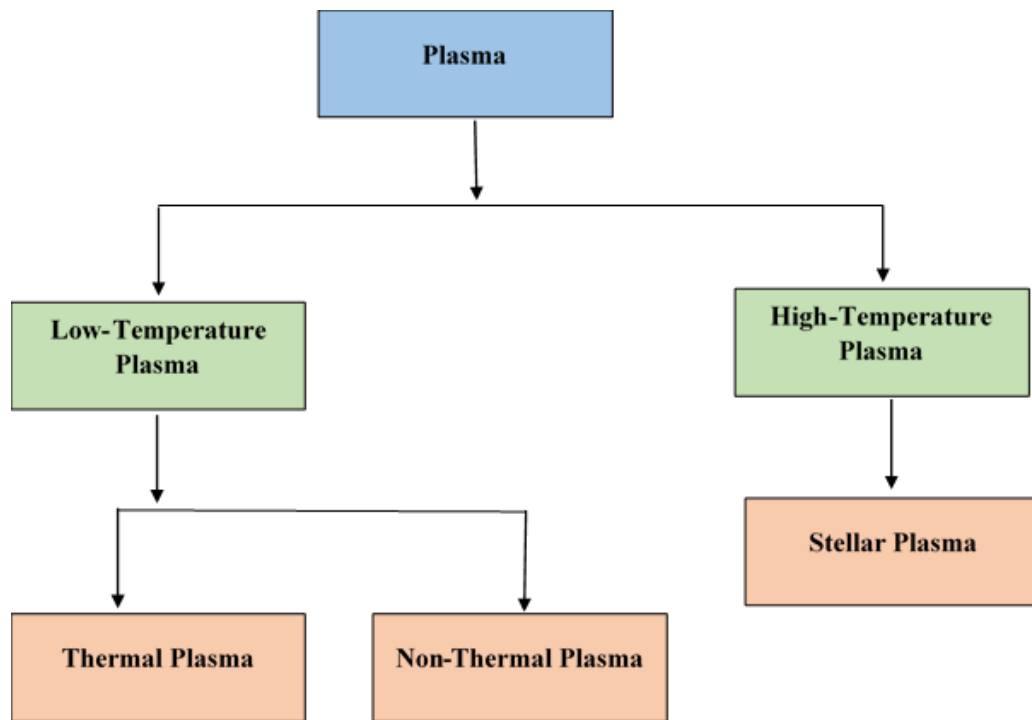
Figure 2. 6 Plasma Classicitication based on Temperature

2.4.2.1 Thermal Plasma

Thermal plasma occurs in cases where the energy of particles in the gas and the energy of the electrons are in thermal equilibrium. A thermal plasma consists of ions, electrons, heavy particles, and neutral species that are at the same temperature, and the collisions between electrons and gas molecules frequently occur because of the transfer of power from the electric field to electrons (Foest et al., 2006; Petitpas et al., 2007). Thermal plasma is generally any plasma in thermodynamic equilibrium mainly because the gas temperature T_o is similar to the ion temperature T_i, rotational temperature T_r, vibrational temperature T_v, and electron temperature T_e, as shown in Table 2.5 (Boulos, Fauchais, & Pfender, 2013).

The thermal plasmas are characterised by the consumption of high power, and they can operate in the atmosphere. Furthermore, electrons are not in equilibrium within their ensemble. The main reason for this is the non-equilibrium thermodynamic behaviour between direct and reverse processes. For example, collisions of fast electrons are responsible for gas excitation and the production of electron-ion in plasma volume; consequently, radiation breakout to the wall, electron, and radiation

are lost in plasma. That is why the collision rate in gas discharge is generally very low, and high-energy electrons are constrained for the inelastic collision to bring a large volume of low-energy electrons to an equilibrium with high-energy electrons (Godyak, 2006).

There are many main limitations of using thermal plasmas for plasma chemical applications, including high-energy consumption, high chemical reaction temperature during energy consumption, and the required special cooling systems for the treatment of high temperatures. In thermal plasma processing, chemical reactions proceed through the dissociation of the reagents in the plasma followed by recombination of atoms and radicals in cooler parts of the flow. Therefore, thermal plasmas cannot be chemically selective (Monette, Bartnikas, Czeremuszkin, Latreche, & Wertheimer, 1999). Several different types of thermal plasma can be classified based on the kind of applied electric field used to generate the plasma flame, including continuous or pulsed direct current (DC), alternating current (AC), arc discharge, and plasma torch discharge (Aw et al., 2014; Jamróz et al., 2018).

2.4.2.2 Non-Thermal Plasma

Non-thermal plasma discharge is not in thermodynamic equilibrium either because the ion temperature is different from the gas temperature T_o or the electron temperature T_e, as shown in Table 2.5 (Yap, Tatibouët, & Batiot-Dupeyrat, 2018). The thermal plasma typically is characterised by low temperature (near room temperature), low electrical input power low pressure (1 atmosphere), and low energy consumption (Paulmier & Fulcheri, 2005). Therefore, the non-thermal plasma is better than thermal plasma for chemical reaction, efficiency, and selectivity. In addition, thermal plasma usually has an equilibrium temperature between the electrons and ions that can be several thousand degrees kelvin or higher (Petitpas et al., 2007).

During low-pressure gas discharge, the collision rate between electrons and gas molecules is not frequent enough for non-thermal equilibrium to exist between the energy of the electrons and the gas molecules (Pearlman, Demydovych, Rabinovich, & Shenoy, 2018). High-energy electrons produced in non-thermal plasma lead to the formation of active chemical species and radicals. Consequently, the high-energy particles are mostly composed of electrons, while the energy of the gas molecules is at

room temperature (Goossens, 2012). Recently, non-thermal plasma methods are very hot topics because of the high removal efficiency, energy yields, and good economy (Urashima & Chang, 2000).

The most commonly used non-thermal plasma for the dry reforming of CH_4 are DBD, CD, GD, gliding arc discharge (GAD), MWD, spark discharge (SD), and radiofrequency discharge (RFD) (Chung & Chang, 2016). First, the DBD is a non-thermal plasma, which is a non-uniform plasma discharge, which can be operated at atmospheric pressure (Meichsner et al., 2012; Mustafa, Fu, Liu, et al., 2018). The DBD reactor consists of two electrodes with one or more dielectric barriers positioned in the discharge gap, as shown in Figure 2.7 (Tao et al., 2011). It is driven by a sinusoidal AC voltage in the frequency range from 50 Hz to 500 kHz (A.-J. Zhang, Zhu, Guo, Xu, & Shi, 2010). There are numerous studies performed for a variety of applications, including environmental, fuel conversion applications, CO_2 dissociation, H_2S decomposition, biological, medical, and industrial applications (Bo et al., 2008; Mustafa, Fu, Lu, et al., 2018; Tao et al., 2011).
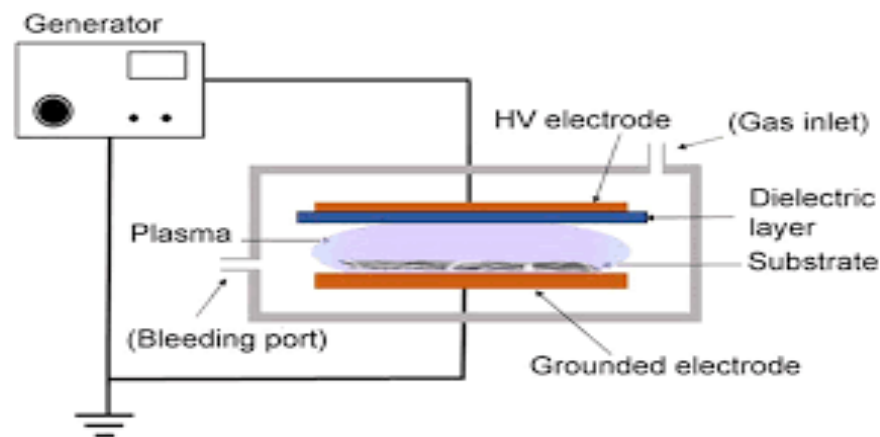
Figure 2. 7 Schematic of the DBD Plasma

Then, the corona (CD) is an example of non-thermal plasma and can occur at or near atmospheric pressure in regions of non-uniform electric fields (Meichsner et al., 2012; Palaskar & Desai, 2016). A CD can be formed by applying either continuous or pulsed DC voltage between two electrodes, as shown in Figure 2.8 (Chang, Lawless, & Yamamoto, 1991). CD is divided into two main types based on the current, positive, and negative corona (Riba, Morosini, & Capelli, 2018). In both types, the high current

flow could lead to the formation of a single spark discharge that bridges the discharge gap (X. Chen et al., 2017). Moreover, the CD has several commercial and industrial applications such as ozone generators, photocopiers, particle precipitators, air ionisers, photons production, N_2 lasers, removing particulate matter from air streams, and sanitising pool water (K. Yan et al., 1998).
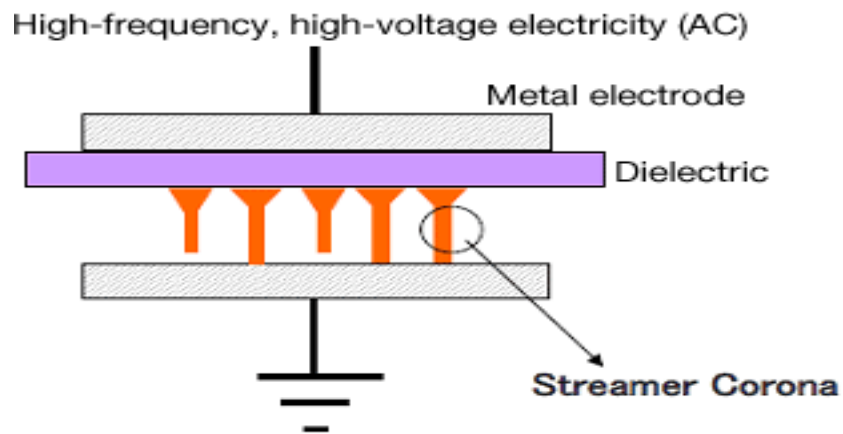
Figure 2. 8 Schematic of the CD Plasma

Next, the GD is another non-thermal plasma type generated by the application of DC or low-frequency (<100 kHz) electric field to the gap between two metal electrodes, as shown in Figure 2.9 (Bogaerts, Neyts, Gijbels, & van der Mullen, 2002; Meichsner et al., 2012). GD is characterised by high-voltage, low current, and low-pressure discharge (less than 10 mbar), and because of its low-pressure characteristics, the glow discharge is not suitable for chemical synthesis (A Fridman, Chirokov, & Gutsol, 2005). In addition, GD is characterised by a cathode layer and the anode layer (Klemensø et al., 2011). Moreover, GD has a distinct self-sustained continuous DC discharge with a cold cathode that emits electrons as a result of secondary emission (van Dijk, 2017).
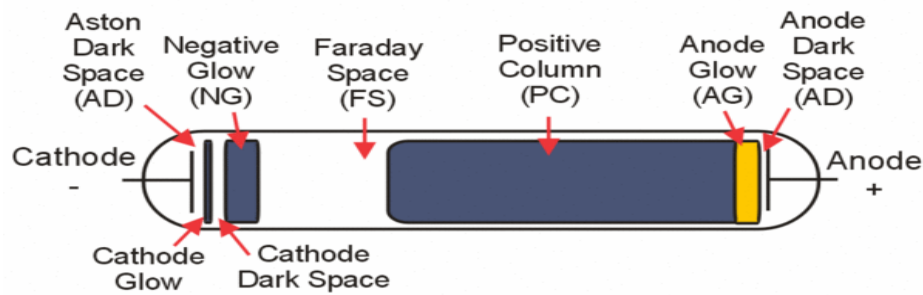
Figure 2. 9 Schematic of the GD Plasma

The radiofrequency discharge (RFD) is an electromagnetic field that can exist in both thermal and non-thermal regimes (again, pressure-dependent) (Bruggeman, Iza, & Brandenburg, 2017; Chabert & Braithwaite, 2011; A Fridman et al., 2005). In general, RFD plasma has two main types, capacitively coupled plasmas and inductively coupled plasma (Bo et al., 2013; Bogaerts & Alves, 2017). RFD can be applied between two planar electrodes usually spaced a few centimetres apart, as shown in Figure 2.10 (Pärnaste, Bäcklund, & Walenius, 2018). Moreover, RFD can be used to generate weakly ionised plasma at low pressures (1–103 Pa), high frequencies (1–100 MHz), and wavelengths (3–300 m) (Meichsner et al., 2012; Nizio, 2016). The RFD is more expensive compared than the other discharges because it requires a power supply in addition to generating the plasma (Lieberman & Lichtenberg, 2005; Patil, Wang, Hessel, & Lang, 2015). RFD has many environmental and industrial applications such as fuel conversions, CO_2 dissociation, and H_2S decomposition (Bonizzoni & Vassallo, 2002). However, the RFD shares many similar properties with the MWD (Nikolic et al., 2012).
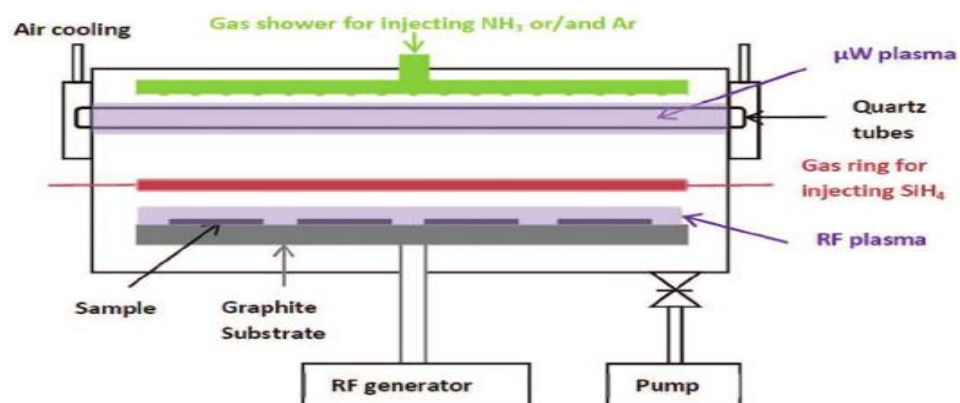
Figure 2. 10 Schematic of the RFD Plasma

Finally, the MWD can exist as both thermal (at atmospheric pressure) and non-thermal discharges (low pressure), as shown in Figure 2.11 (Conrads & Schmidt, 2000). MWD is also classified as a high-frequency discharge (same as RFD), and both MWD and RFD generate plasma through electromagnetic waves, causing oscillations and collisions of particles (Boenig, 1988). The collisions yield new electrons to sustain the plasma, in contrast to DBD and CD, where electrons can be released by the electrodes on bombardment by heavy particles (i.e., secondary electrons).
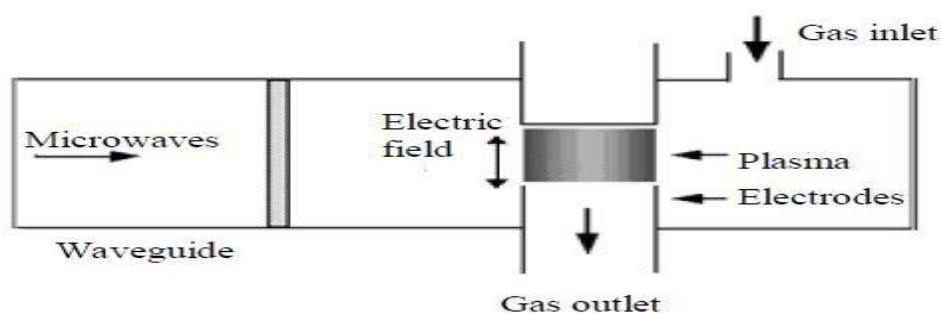
Figure 2. 11 Schematic of the MWD Plasma

2.4.3 Plasma Chemical Applications

Plasma chemistry is considered one of the most important technologies currently discovered. The investigations have begun into the use of plasma chemical for a wide range of applications as a potential replacement for more traditional methods of chemical synthesis. Table 2.6 summaries some of the important applications showing various stages of development (Hippler et al., 2001).

Table 2. 6 Applications of Plasma Chemical

Applications	Processes	Products
Surface Modification	**Etching**	Structuring/Materials Fabrication Processes (micro-electronics, micro-optical components, micro-mechanics, semi-conductors)
		Cleaning (assembly lines, vehicle exhaust)
		Metallic Components for cars and aircrafts
		Fuel Ignition
		Aerospace Engineering
	Functionalization	Hydrophilic and hydrophobic coatings for textiles
		Anti-reflective coatings for lenses
		Graftability
		Adhesability
		Printability
	Interstitial modification	Diffusion (bonding)
		Implantation (hardening)
		Metal cutting
		Cubic boron nitride films for cutting tools
		Polymeric and Catalytic thin-films
	Deposition Change of Properties	Mechanical (tribology)
		Chemical (corrosion protection), O_3 generation
		Electrical (integrated circuits)
		Plasma Display Panels (Large-area flat-screen televisions)
		Optical (antireflecting coating)
	Architecture	Crystallographic (lateral diamonds)
		Morphologic (scaffolds for cells)
		Electromagnetic radiation
		Luminescent lamps/ Fluorescent
Volume-related transformation	**Energy conversion** Electrical Energy to EM radiation	High-pressure metal vapor lamps
		Gas lasers
		Microwave generation
		Excimer radiation sources (excimer-based UV)
		Improvement of the efficiency of solar cells
		Flue gas cleaning of fuel-burning power plants
		Improve the thermal isolation of windows (self-cleaning)
		Nuclear energy
		Fusion of DT
	Plasma chemistry transforming into specific compounds	Production of precursors
		Production of excimers
		Production of synthesis gas

		Synthesis of acetylene production (C_2H_2)
		Odors
	clean-up of gases	Destruction of odorous molecules
		Destruction of volatile organic compounds (VOCs) from diesel exhausts and flue gases
Carrier functions	**Electrical current**	Circuit breakers
		Spark gap switches
	Heat	CO_2 laser discharges for cutting and welding arcs
		Plasma spray
		Thermoelectric drivers
Particle sources	**Electrons**	-
	Ions	-
	Neutrals	-
	Radicals	-
Biomedical Techniques	**Tissue engineering**	-
	Blood coagulation	-
	Deactivation of micro-organisms	-
	Sterilization of instruments and surfaces	-
Environmental	**Annihilation of toxic wastes**	-
	Remediation of air and water pollution	-

2.4.4 Design of Experimental (DoE)

The effects of these parameters do not independently affect each other; therefore, their interactions must be considered. To reduce the difficulty in determining the optimum performance of the plasma process, previous studies have used the chemical model (Abbasi et al., 2017; Abedini et al., 2017; Challiwala et al., 2017; De Bie et al., 2015; Hafizi et al., 2016; Mei et al., 2016; Montgomery, 2017; Ramachandran et al., 2011; Senseni et al., 2016; Sidik et al., 2016; L. Wu et al., 2012). The results show that the chemical model is useful in determining the optimum value for output responses. This model requires a significantly lower number of experiments compared to using a traditional method (Mei et al., 2016).

The DoE can be classified into two main types BBD and Taguchi methods (De Bie et al., 2015). The ability to use more than one input factor is a significant advantage of DoE. The most used methodology in DoE is the RSM (Senseni et al., 2016). This

facility assumes various input variables and output responses to be connected. In this method, the impact of single variables and their interactions on each response is more easily understood by 3D and contour interpretations (Hafizi et al., 2016). Two design methods, in response to the surface methodology, have been used to determine the optimisation of the plasma process via the central composite design (CCD) and BBD (Abedini et al., 2017).

Fewer experiments are necessary when using the BBD method, making this the preferred choice over the CCD method (Montgomery, 2017). During the 1950s, Box and collaborators developed the RSM (L. Wu et al., 2012). RSM is one of the most useful experimental design methodologies for building the relationship between the multiple input parameters and output responses, enabling us to get a better understanding of the effects of individual factors and their interactions on the responses by three-dimensional and contour interpretations (Challiwala et al., 2017).

However, the identification of the influences of significant factors and determination of the optimum operating conditions for syngas production by plasma microwave technology still needs more research. In this study, three parameters-three levels of a BBD (DBD) are applied to investigate the impacts of the significant parameters including MWP, R, TFR, CH_4, CO_2, and N_2 flow rates on plasma stability and syngas production by the DRM microwave plasma method.

2.5 Microwave Discharges in Plasma Chemistry
2.5.1 Introduction

Microwave has recently emerged as an effective tool in various technological and scientific fields. In this technique, there is a prerequisite for the best use, which is a comprehensive understanding of the fundamentals of microwave matter interactions (Motshekga, Pillai, Ray, Jalama, & Krause, 2012; Venkatesh & Raghavan, 2004). Microwaves heating is usually only known as dielectric heating, and it is commonly using in-house cooking, diamond synthesis, and IC manufacturing (Thostenson & Chou, 1999). Microwave technology was discovered in the 1940s as a new technique, and it was developed for use in radar applications during World War II (Jones, Lelyveld, Mavrofidis, Kingman, & Miles, 2002; Scott, 1993).

Microwaves comprise the shortest wavelength region of the radio spectrum and part of the electromagnetic spectrum (Sievenpiper, Zhang, Broas, Alexopolous, & Yablonovitch, 1999) that move at the speed of light with wavelengths ranging between 100 cm and 100 mm (Kustov & Sinev, 2010), and their waves are located between radio waves and infrared radiation in the electromagnetic spectrum (Will, Scholz, & Ondruschka, 2004), as shown in Table 2.7 (Motasemi & Ani, 2012).

Table 2. 7 The region of the Electromagnetic spectrum

Waves	Frequency (HZ)	Wavelength (m)
Long Wave Radio	3×10^5	10^3
AM Broadband Radio	3×10^6	10^2
Short Wave Radio	3×10^7	10^2 - 10
VHF TV	3×10^7 - 3×10^8	10 - 1
FM Broadband Radio	3×10^7 - 3×10^8	10 - 1
Microwaves	3×10^8 - 3×10^{11}	$1 - 10^{-3}$
Far Infrared	3×10^{11} - 3×10^{13}	10^{-3} - 10^{-5}
Infrared	3×10^{13} - 3×10^{14}	10^{-5} - 10^{-6}
Visible Light	3×10^{14}	10^{-6}

Generally, the word microwave means "very short wave" and consists of two fields, namely electric and magnetic, as shown in Figure 2.12 (Kappe, Stadler, & Dallinger, 2012). The electric field is generated from the repulsion of the two electrons from each other, and the magnetic field is produced by moving the charge as a result of moving other charges (Ozbek & Akman, 2016).
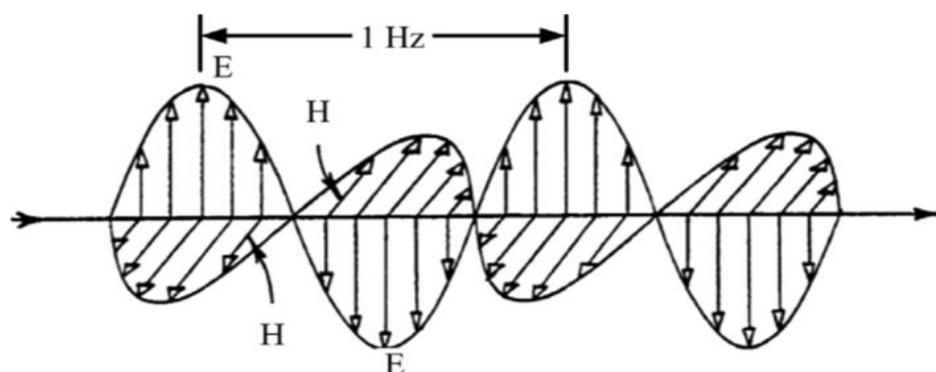
Figure 2. 12 Microwaves in two field Electric (E) and magnetic(H)

Microwaves have corresponding frequencies between 300 MHz and 300 GHz (Clark, Folz, & West, 2000); and the frequency is allocated to cellular phones, radar, and satellite communications (Meredith, 1998). Most microwave reactors for chemical synthesis operate at 2.45 GHz frequency (Datta, 2001), which corresponds to a wavelength of 12.25 cm, and they can operate over a wide pressure range (from 10^{-5} mbar^{-1} bar) (Nüchter et al., 2004). There are two main important parameters for microwave processing, power absorbed (P) and microwave penetration depth (D) (Clark et al., 2000). Microwaves contain many properties that distinguish them from other discharges, as shown in Figure 2.13.
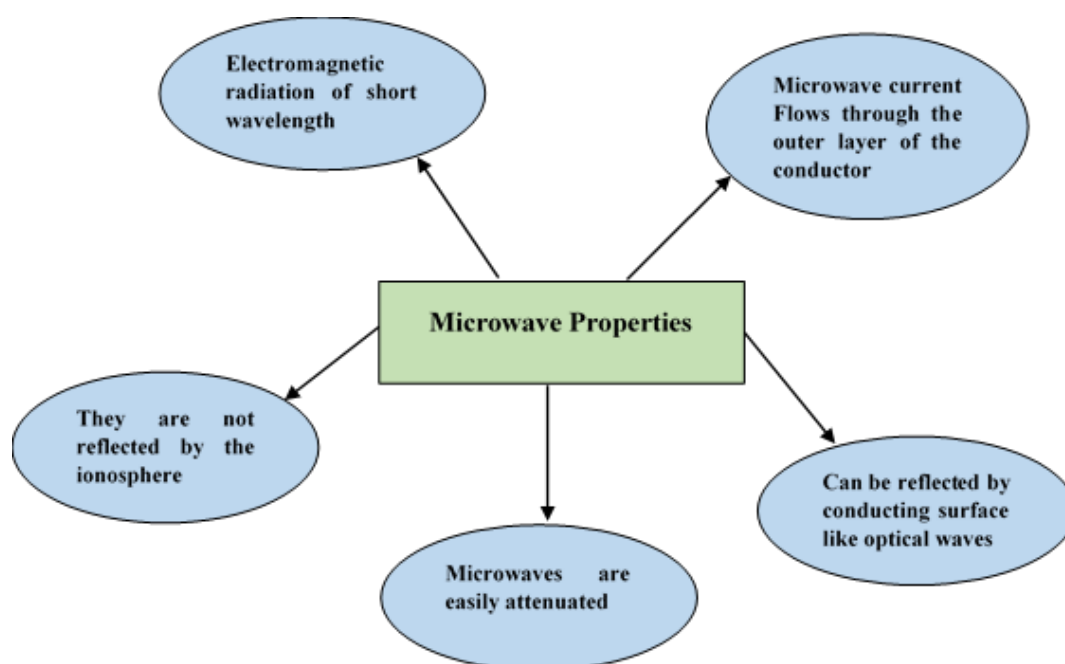
Figure 2. 13 Microwave properties

Microwave technology has many advantages that will make it necessary in the industry nowadays (Cha-um, Rattanadecho, & Pakdee, 2009; Jones et al., 2002; T. Wang & Liu, 2000). One of the most important advantages is that the energy transfer is rapid, volumetric, and uniform and is achieved by heating by radiation with microwaves (Aparna, Basak, & Balakrishnan, 2007; Aziznia et al., 2012; Nüchter et al., 2004). The energy of microwaves is delivered directly to materials by molecular interactions with the electromagnetic field (Mishra & Sharma, 2016). Microwaves are characterised by faster reaction rates, less energy, clean power, being quiet, shorter residence times, good conversions, better selectivities, and higher yields (Kustov & Sinev, 2010).

Microwaves are one of the best methods to transfer energy because of the energy introduced via radiation instead of heat transfer and convection (Ismail & Ani, 2015). In addition, the physical and mechanical properties are improved through the use of microwaves such as smooth operators, electrodeless reactors, high plasma density, high electron mean energy, and high-energy efficiency (Heijkers et al., 2015; Menéndez et al., 2010; Y.-F. Wang, Tsai, Chang, & Kuo, 2010). Moreover, microwave technology is environmentally friendly because it reduces hazardous and harmful emissions and yields the synthesis of new materials (Clark & Sutton, 1996).

Based on these useful advantages, microwave technology has many applications in various technical and scientific fields such as food processing, cooking, drying, pasteurisation, sterilisation, thawing, tempering, baking and preservation of food materials (Gupta & Leong, 2008; Metaxas & Meredith, 1983; I. A. Ozkan, Akbudak, & Akbudak, 2007; Song et al., 2016), plasma processing, microwave heating, activated carbon regeneration (Hesas, Daud, Sahu, & Arami-Niya, 2013), communication of radar, telemetry of space (Araszkiewicz, Koziol, Lupinska, & Lupinski, 2007; Scott, 1993; Zhao et al., 2010), pollution control, wastewater clean-up, medical waste treatment, and many other physical and chemical fields recently developed (Chandrasekaran, Ramanathan, & Basak, 2012; Lidström, Tierney, Watheyb, & Westmana, 2001; Siores & Do Rego, 1995).

Microwave heating is different from conventional thermal heating in many ways. Conventional heating (traditional heating) is a transfer of the heat from the material surface to the core by conduction, convection, and radiation. However, microwave heating is a conversion of the energy from the core to the surface of the material by the electromagnetic field, as shown in Figure 2.14 (Motasemi & Ani, 2012). Furthermore, the microwave method is much better than the conventional method because it has low pressure and temperature operation (Xiao et al., 2015).
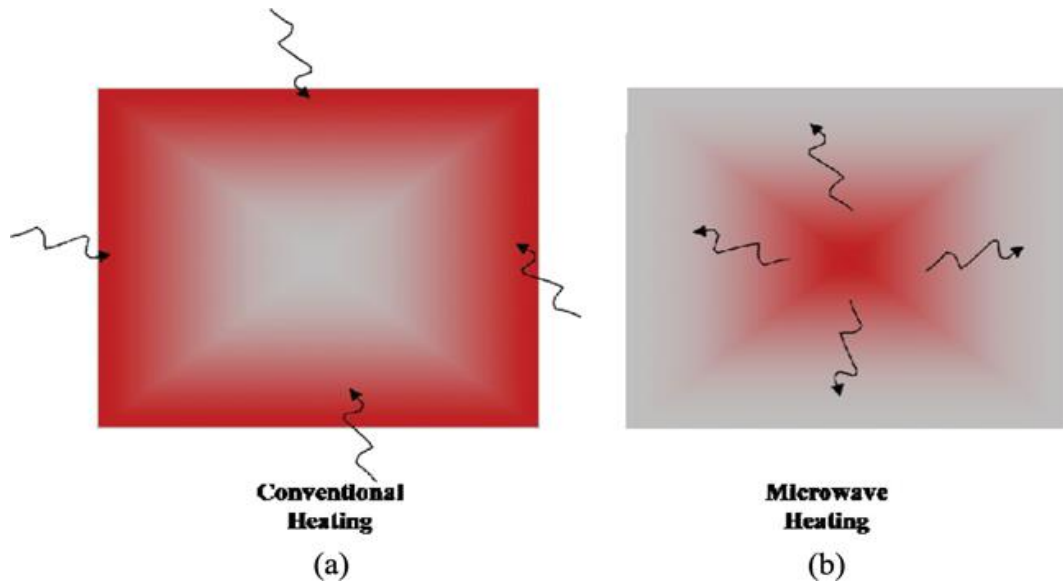
Figure 2. 14 Heating Mechanisms of heat generation in (a) conventional heating and (b) microwave heating (Singh, Gupta, Jain, & Sharma, 2015)

In addition, there are many differences between microwave and conventional heating regarding energy transfer, thermal efficiency, and physical properties. Table 2.8 summarises the comparison between microwave and conventional heating (C. Yin, 2012).

Table 2. 8 Comparison between Microwave and Conventional Heating

Microwave Heating	Conventional Thermal Heating
Conversion of heat by the electromagnetic field	Transfer of heat by conduction, convection, and radiation
Uniform and rapid heating	Non-uniform and slow heating
Volumetric heating	Superficial heating
Heat Conversion is rapidly and efficiently	Heat Transfer is slowly and inefficient
Unlimited by material thermal conductivity	Limited by material thermal conductivity
Material-selective heating	None material-selective heating
High safety and automation control	Not safe
Conversion dependent on material's properties	Transfer not dependent on material's properties
Heating is accurate and controlled	Heating is inaccurate and uncontrollable
Dependent on material's properties	Less dependent

Microwave technology has been developed and used as a source for atomic spectroscopy since the early 1970s (Suib & Zerger, 1993). Then, the microwaves

became famous and spread vigorously at the end of the 1970s and 1980s because of the evolution of life and openness of the commercial market (Wan, 1993). In the early 1980s, interestingly, the laboratories of research on microwave radiations as an energy source were increased because of the rapid development of industries (Wan, 1993). During the period from 1981 to 1999, the microwave field was gradually increased because microwaves were used to assistant in the heterogeneous gas-phase reactions (Will et al., 2004). In the past 20 years, the number of research published articles in this area has steadily increased. As indicated in Figure 2.15.
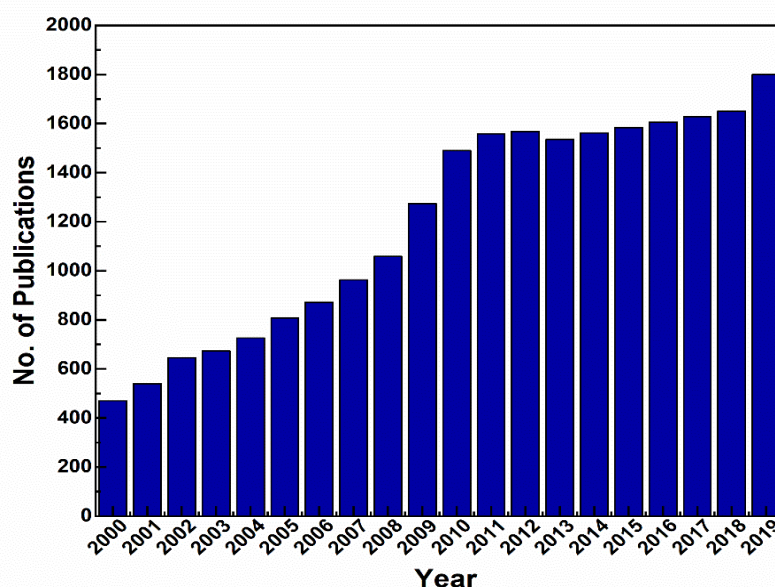
Figure 2. 15 Evolution of the Publications of Microwave Processes 2000-2019 SCIFINDER®

As a result, the microwave field has occupied a prominent place in modern kitchens. The microwave has become more available to a greater number of people because it is cheap, easy to use, and time-saving (Czylkowski et al., 2016; Thostenson & Chou, 1999). Also, Figure 2.15 shows that the increase has become more prominent from 2010 to 2016 and is still rising (see Figure 2.15). The reason for this increase is that the majority of scientists and researchers have increased attention for microwaves technology to academic and industrial fields for excellent thermal characteristics (M. J. Williams et al., 2016).

2.5.2 Microwave Plasma Technique

Microwave plasma technology has been discovered and used since the 1970s and has gradually increased because of the need for a new technique to reduce the time, effort, and cost (Croslyn, Smith, & Winefordner, 1997). The principle of microwave plasma work is to prepare a large electrical field to excite and ionise the gases under certain pressure and temperature, thus generating more electrons. Increasing the electrical field leads to an increased rate of inelastic collision between electrons and atoms while generating more ions and electrons. In addition, the significant electrical resistivity generated across the system causes high temperature and electrons density (Ruj & Ghosh, 2014; Thostenson & Chou, 1999). The microwave plasma technique is widely used in reforming reaction or H_2 production because of its lower energy consumption as well as its ease of maintenance (Zherlitsyn et al., 2016). Figure 2.16 shows that the number of articles published in the microwave plasma field is increasing with time.
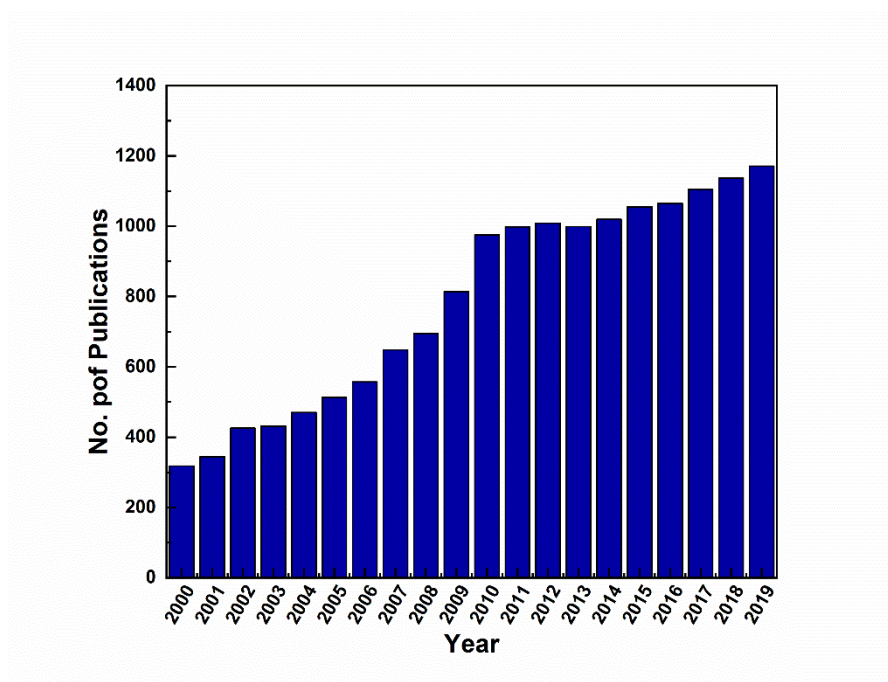
Figure 2. 16 Evolution of the Publications of Microwave Plasma 1979-2019 SCIFINDER[®]

Microwave plasma is classified into three main types, microwave-induced plasma (MIP), capacitively coupled microwave plasma (CMP), and microwave plasma touches (MPT). Table 2.9 shows the advantages and disadvantages of each type and

shows that each type has a unique feature. First, MIP has been studied in the last decade because of the great applications of atmospheric microwave plasma, which is generated by transmitting microwaves from the generator through a coaxial cable to a resonant cavity (Rosenkranz & Bettmer, 2000). MIP has many benefits from strong gas ionisation because of an efficient microwave coupling with the gas (J. Yin, Zhao, Zhan, & Duan, 2017). MIP also generates a considerable amount of thermal energy that can be used to heat large volumes of gas (Tendero, Tixier, Tristant, Desmaison, & Leprince, 2006). In addition, MIP is created and maintained by using an electromagnetic energy source with frequencies in the range of 300 MHz–10 GHz (Jena, Gupta, Pippara, & Pal, 2019). MIP has high power densities, making them excellent atomisation sources for metals and non-metals, and they also operate easily at low power, as shown in Table 2.9 (Culp & Ng, 1995).

In most cases, MPT has low flow rates and forward power, ease of turn ability, no contamination from electrode material, and reduced sensitivity to the introduction of liquid aerosols (Yang, Zhang, Yu, & Jin, 2000). The plasma in MIP does not contact the tip of the electrode (absence of electrodes); therefore, this plasma does not suffer from contamination from the electrode material (Javanbakht, Fathollahi, Divsar, Ganjali, & Norouzi, 2013). MIP sources have different types such as the microwave continuous flow reactor (John R Roth, 1995; Woskov et al., 1996), surface wave sustained plasma (Moisan, Hubert, Margot, Sauvé, & Zakrzewski, 1992), torch with axial gas injection (TIA) (Jonkers et al., 1996; Moisan, Sauve, Zakrzewski, & Hubert, 1994), MPT (Prokisch et al., 1999), and microwave cavity plasma, as shown in Table 2.9 (Beenakker, 1976; Okamoto, 1996). However, MIP does not accommodate liquid sample introduction well and sometimes is even extinguished. Moreover, optimisation of the plasma with frequency is not easy.

Secondly, CMP is formed by transmitting microwaves from the magnetron through a rectangular waveguide to an electrode (Jankowski & Reszke, 2010). CMP offers several advantages such as easily accommodating gases, liquid sample introduction, and operation at high powers (Croslyn et al., 1997). In addition, CMP has demonstrated promising results in the direct analysis of solid samples (Winefordner, Wagner, & Smith, 1996). While CMP tends to be slightly less precise and suffers from a higher than MIP, as shown in Table 2.9. Lastly, MPT works differently from other microwave plasmas because Ar, N_2, and He gases plasma can be generated at a very

low flow rate and forward power (D. Zhu et al., 2017). Apparently, in most cases, MPT has many more benefits than other microwave plasma technologies including operation at atmospheric pressure, low flow rates, forward power, and ease of turnability (Chhawchharia, Sahoo, Balamurugan, Sukchai, & Yanine, 2018), no contamination from electrode material, and reduced sensitivity to the introduction of liquid aerosols (Croslyn et al., 1997). However, the plasma has not contacted the tip of the electrode and therefore does not suffer from contamination from the electrode material (Jin, Zhu, Border, & Hieftje, 1991).

Table 2. 9 Advantage and Disadvantage of Microwave Plasma Types

Type	Transfer Energy	Advantages	Disadvantages	Refs.
Microwave-Induced Plasma (MIP)	Coaxial Cables	High power density Works quickly	Does not accommodate liquid samples Plasma optimization is not easy	(Culp & Ng, 1995; Uden, 1995)
Capacitively Coupled Microwave Plasma (CMP)	Waveguide	Accommodating both gaseous and liquid samples Direct analysis of solid samples	Operation is at high powers Less precise and suffers	(Winefordner et al., 1996)
Microwave Plasma Torch (MPT)	Antenna	Operation at atmospheric pressure Ease of tenability No contamination from the electrode material Reduced sensitivity to the introduction of liquid aerosols	Low flow rates and forward power	(Jin et al., 1991)

2.5.3 Application of Microwave

According to the aforementioned microwave advantages, microwave technology is widely used in various applications for different aspects such as microwave heating (N. H. Williams, 1967), industrial (Bogaerts et al., 2002; Hammer, 1999; S. Kim, Sekiguchi, & Doba, 2013), biomechanical, radar, and communication (Zhao et al.,

2010); see Figure 2.17. Microwave energy has yielded general and commercial applications in a few areas, including food processing and vulcanisation of rubber (H.-L. Chen, Li, Liang, Sun, & Li, 2017) that involve relatively high-volume, continuous processing (Horikoshi, Schiffmann, Fukushima, & Serpone, 2018). In addition to the previously mentioned applications, more work has been performed to investigate the use of microwaves for the processing of a wide range of materials in the manufacturing industry (Falk & Issels, 2001), including ceramics, polymers, composites (ceramic and polymer matrix), powders, and minerals (Singh et al., 2015). In addition, microwave technologies have been investigated in a broad range of plasma processes such as surface modification (Grill, 1994; Lieberman & Lichtenberg, 1994), chemical vapour infiltration (Porter, D'Angio, Binner, Cinibulk, & Mogilevsky, 2017), powder processing (Roy, Agrawal, Cheng, & Gedevanishvili, 1999), chemical synthesis and processing (Iravani, Korbekandi, Mirmohammadi, & Zolfaghari, 2014) and waste remediation (Sivagami, Padmanabhan, Joy, & Nambi, 2019).

Recently, microwave technologies have been used for the heating of atmospheric pressure plasmas for gasification because such plasmas present considerable interest in a wide range of environmental applications: air pollution control (Abolentsev, Korobtsev, & Medvedev, 1995; Rani et al., 2008), wastewater cleaning (Malik, Ghaffar, & Malik, 2001), biomedical (such as bio-decontamination) (Yasuda, 1990), sterilisation (Laroussi et al., 1999) industrial applications (Bogaerts et al., 2002; Hammer, 1999), material and surface treatment (Grill, 1994; Lieberman & Lichtenberg, 1994), electromagnetic wave shielding (J Reece Roth, 2003), carbon beneficiation and nano-tube growth (Jašek et al., 2006; Zajíčková et al., 2005), and element analysis (Green et al., 2001). Despite the considerable efforts that have been expended in microwave process development, there has been little industrial application to date, with most of the effort still in the laboratory stage.
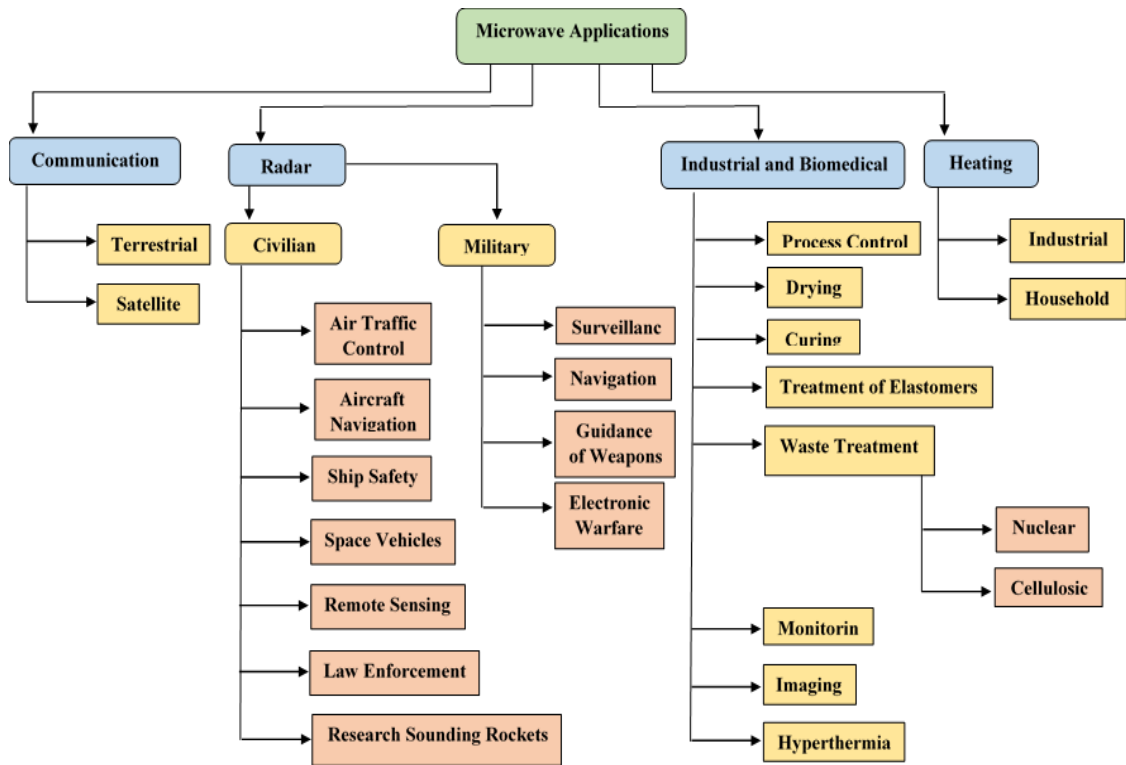
Figure 2. 17 Microwave Applications

2.5.4 Microwave-Assisted Plasma DRM

Microwave plasma technique is one of the most important microwave applications in the industrial field and is well suited for enhancing chemical reactions because of its characteristics of low cost, ease of control, and wide temperature and pressure ranges (Chandrasekaran, Ramanathan, & Basak, 2013). Lately, microwave plasma technology has been developed for the conversion of CO_2 and CH_4 to produce syngas (Tao et al., 2011), and the plasma must be coupled as a load in the power circuit. This coupling is accomplished via waveguides where a quartz tube is inserted into the waveguide (Espiau & Chang, 2009). The plasma is ignited and confined to the quartz tube (Ferreira & Moisan, 2013). This technique uses the microwave magnetic field and additive gases such as N_2 and Ar gases and a stable generation plasma (Ozbek & Akman, 2016). The main processes in non-thermal plasmas operating in N_2 and Ar gases are dissociative collisions of molecules, resulting in the generation of reactive atoms, formation of ionised gas with free electrons, and free positive and negative ions (Lieberman & Lichtenberg, 2005).

2.6 The Role of Additive Gas in Plasma microwave-assisted DRM
2.6.1 Introduction

In microwave-assisted DRM, in addition to the MWP, R, TFR, reactor type and design, one of the other important parameters that strongly affect the performance and stability of reaction performance is the type and the flow rate of the additive gas that is used in the reaction (Indarto et al., 2006; Motasemi & Afzal, 2013). High reactant conversions can be obtained for dry reforming of CH_4 with the use of carrier gas to dilute CH_4 and CO_2 (Taghvaei, Jahanmiri, Rahimpour, Shirazi, & Hooshmand, 2013). Not all inert carrier gases can be considered inert in the plasma state because of the presence of high densities of electrons and excited gas molecules (Mei, Zhu, He, Yan, & Tu, 2014). Gases such as He and Ar have low breakdown voltages in comparison with CH_4 and CO_2 and can have a significant effect on the reaction chemistry because of increased ionisation in the plasma discharge (Ramakers, Michielsen, Aerts, Meynen, & Bogaerts, 2015). However, inert gases are expensive and would require separation from the reaction products (Ramakers et al., 2015). For these reasons, dry reforming of CH_4 in plasma with the use of a diluent gas is not considered industrially relevant. This thesis also focuses on using N_2 and Ar as additive gas in dry reforming of CH_4 using microwave plasma.

Additive gases are the important parameters affecting the stability of plasma and the production of syngas. There are many parameters that affect the plasma flames such as the type and flow rate of carrier gas (such as N_2, Ar, He, H_2, and O_2), microwave output power, reactor design, type of reactor, and residence time (Motasemi & Afzal, 2013). The main processes in non-thermal plasmas operation in N_2 and Ar gases are dissociative collisions of molecules, resulting in the generation of the reactive atoms, formation of ionised gas with free electrons, and free positive and negative ions (Lieberman & Lichtenberg, 2005).

In recent years, several studies have focused on using additive gases such as N_2 (Chung & Chang, 2016; Hwang et al., 2010; Indarto et al., 2006; X. S. Li et al., 2011; Long et al., 2008; Sun et al., 2012; Tao et al., 2008; Yan Xu et al., 2013; B. Zhu et al., 2012) and Ar (Allah & Whitehead, 2015; Daihong Li et al., 2009; Marafee et al., 1997;

Moshrefi et al., 2013; Ravari et al., 2017; Seyed-Matin et al., 2010; Shapoval et al., 2014; Tao et al., 2009; Q. Wang et al., 2009b; B. Yan et al., 2010; Zhou et al., 1998) as inert gases to generate the plasma flame by CH_4 reforming. However, to the best of the authors' knowledge, no report has been published using N_2 and Ar as inert gases to generate plasma flame in the production of syngas under the same test conditions for N_2 and Ar. This work also compares the findings of adding the N_2 and Ar gases in terms of CH_4 and CO_2 conversions, H_2 and CO selectivities, H_2 and CO yields, and H_2/CO ratio.

2.6.2 Nitrogen-Plasma

N_2 is diatomic gas; therefore, it is usually used to generate a high-energy plasma flame through the dissociation and ionisation process (Chung & Chang, 2016; Hwang et al., 2010; Indarto et al., 2006; X. S. Li et al., 2011; Long et al., 2008; Sun et al., 2012; Tao et al., 2008; Yan Xu et al., 2013; B. Zhu et al., 2012). N_2 is considered as an inert gas and has a triple strongest bond (N≡N) structure formation with the three unpaired electrons of each atom (Motasemi & Afzal, 2013) (Lieberman & Lichtenberg, 2005). The electrons and protons energy sources initiate a complex set of chemical reactions that primarily lead to CH_4, CO_2, and N_2 dissociation (Országh, Danko, Ribar, & Matejčík, 2012). Free nitrogen atoms easily react (at atmospheric pressure and high temperature) with most elements to form nitrides, and even when two free nitrogen atoms collide, producing an exciting N_2 molecule, they may release so much energy on collision with even such stable molecules such as CO_2 and CH_4 to cause homolytic fission into radicals such as CO and O or C and $2H_2$ (Országh et al., 2012).

Atomic nitrogen is prepared by passing an electric discharge through nitrogen gas, and then the plasma flame is generated (Indarto et al., 2006). Triple bonds have short bond lengths and high dissociation energies and are thus very strong (Országh et al., 2012). The conversion of N_2 could be attributed to the high temperature inside the plasma reactor and because of the high energy from the microwave. There is another method to generate the plasma from N_2 by using eclectic-induced reactions. The plasma-induced by electron beam has much higher energy than the energy needed for ionisation and dissociation (Conrads & Schmidt, 2000; Meger et al., 1999; Pei, Zhang,

Chen, & Lu, 2013; Schmidt, Föste, Michel, & Šapkin, 1982). N_2 gas is dissociated because of the applied high energy, as shown in Equation 2-23, which produces the plasma flame. Moreover, the produced N atoms may adhere to the wall of the quartz tube and lead to the recombination of nitrogen atoms again, as shown in Equation 2-24 (Volynets, Lopaev, & Popov, 2016). This mechanism leads to the reproduction of N_2 gas and reduces the conversion rate in the product.

$$N_2 + e^- \rightarrow N^* + N^* + e^- \tag{2-23}$$

$$N^* + N^* + wall + e^- \rightarrow N_2 + e^- \tag{2-24}$$

The temperature inside the plasma reactor is usually above 1600 °C, which is enough to break down the triple bonds of N_2. Then, some of the N_2 may contribute to the production of ammonia as a side reaction (Indarto et al., 2006; Wnukowski & Jamróz, 2018).

$$N_2 + 3H_2 + e^- \rightarrow 2NH_3 + e^- \tag{2-25}$$

In addition, some of the N_2 amounts can contribute to producing cyanide and nitrogen oxides as a side reaction (HCN, CN, and NO) (Indarto et al., 2006).

$$N_2 + e^- \rightarrow 2N^* + e^- \tag{2-26}$$

$$N_2 + CO_2 \rightarrow CN + NO_2 + e^- \tag{2-27}$$

$$N_2 + CO + e^- \rightarrow CN + NO + e^- \tag{2-28}$$

$$CN + O_2 + e^- \rightarrow HCN + H^* + e^- \tag{2-29}$$

$$CN^* + H_2 + e^- \rightarrow HCN + H^* + e^- \tag{2-30}$$

In addition to the by-products, there is the possibility that N_2 has reacted with the CO_2, H_2, CO, and O_2 to form various oxides of nitrogen such as NO, NO_2, NO_3, N_2O, N_2O_3, N_2O_4, N_2O_5, N_2O, and $N(NO_2)_3$ (Greenwood & Earnshaw, 2012).

$$N_2 + O_2 + e^- \rightarrow 2NO + e^-$$ (2-31)

2.6.3 Argon-Plasma

Ar is a non-reactive gas and has a very heavy ion, but it ionises to form a plasma by microwave radiation (H. Zhang et al., 2013). Despite being chemically inert under normal conditions, Ar was employed as the plasma gas because it forms plasma easily in the discharge's devices, has a simple and well-defined atomic spectrum, and is readily available in high purity. Ar needs high temperatures (more than 7000 °C) and high pressure (more than 7 atm) to react with side products and then form other chemicals (William, Lide, & Bruno, 2011). Therefore, Ar-plasma at atmospheric pressure does not react with elements such as CH_4 and CO_2 to form any side products (Meija & Possolo, 2017).

Recombination of electrons with ions is a process of fundamental importance in the control of physical and chemical changes in plasmas and can be readily studied in a discharge plasma (Desai, 1969). In the plasma reactions, electrons resulting from these reactions and the Ar atoms that gain them replace lost electrons and attain the stability of atoms inside the reactor according to the Equation 2-32 (Desai, 1969).

$$Ar + e \rightarrow Ar^* + e$$ (2-32)

The CH_4 molecules get energy from the excited Ar atoms instead of electrons:

$$CH_4 + Ar^* \rightarrow CH_3 + H + Ar$$ (2-33)

3

Chapter 3: Research Methodology and
Analytical Techniques

3.1 Introduction

This chapter introduces details of the experimental work comprising the experimental design and regression analysis procedures used for microwave plasma technology. The experimental setup of microwave plasma reactors, microwave radiation leak tests, experimental conditions, calculation methods, and experimental design and regression analysis via JMP procedure are described. The details of each part in the experimental work and the calculations of CH_4, CO_2 conversions, the selectivities and yields of H_2, CO, and H_2/CO ratio are also discussed in this chapter. The JMP statistical discovery software was utilised to investigate the effect of the interaction among many parameters with each other on plasma stability and syngas production, and the organisation of this section is depicted in Figure 3.1.
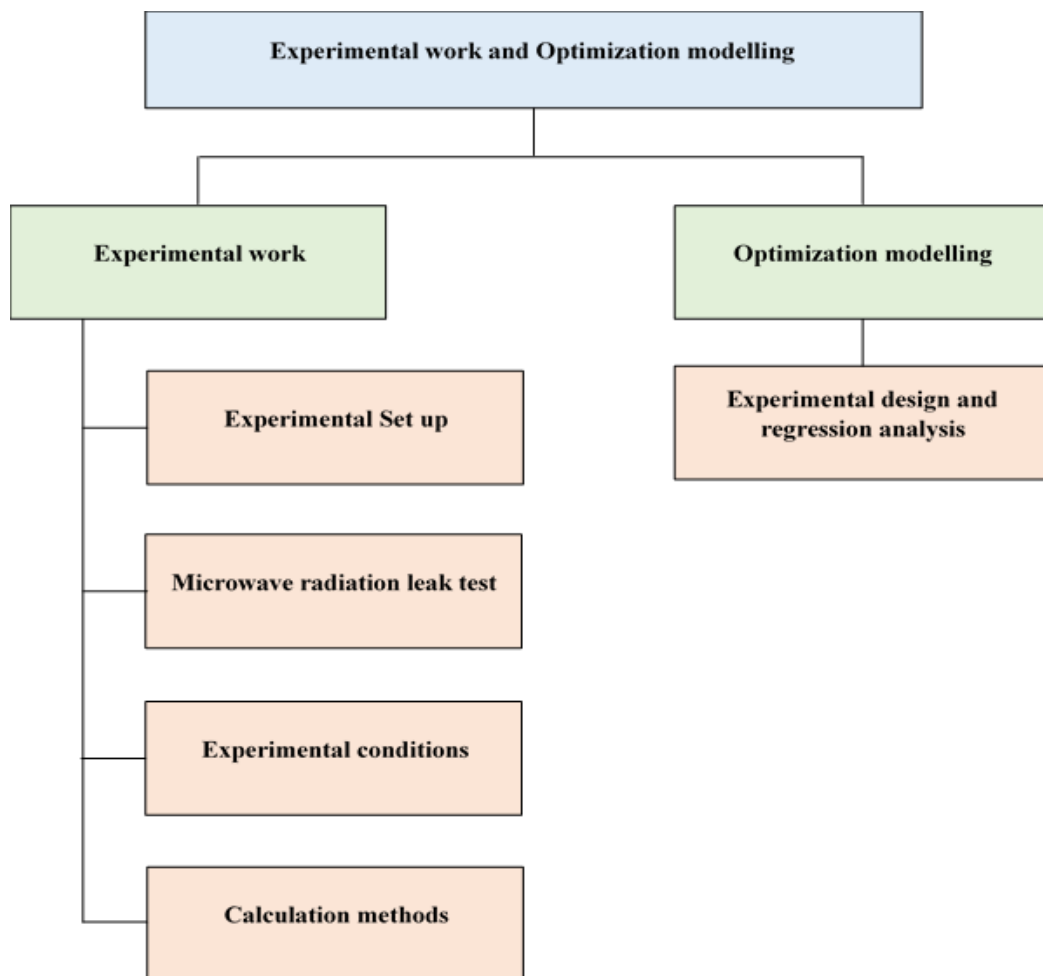
Figure 3. 1 Structure of experimental work and optimization modelling

3.2 Experimental Work

A commercial microwave reactor system (Alter, SM 1150T, Canada) was used in the present study. The experimental work consisted of the experimental setup, microwave radiation leak test, experimental conditions, and calculation methods. This section explains the details of each part of the microwave plasma system, and each measurement was repeated three times to avoid possible variances.

3.2.1 Experimental Set-up

The schematic diagram of the experimental setup for syngas production microwave-assisted plasma DRM, which fundamentally consists of 16 parts, is shown in Figure 3.2. The details about each part are described in the following sections.
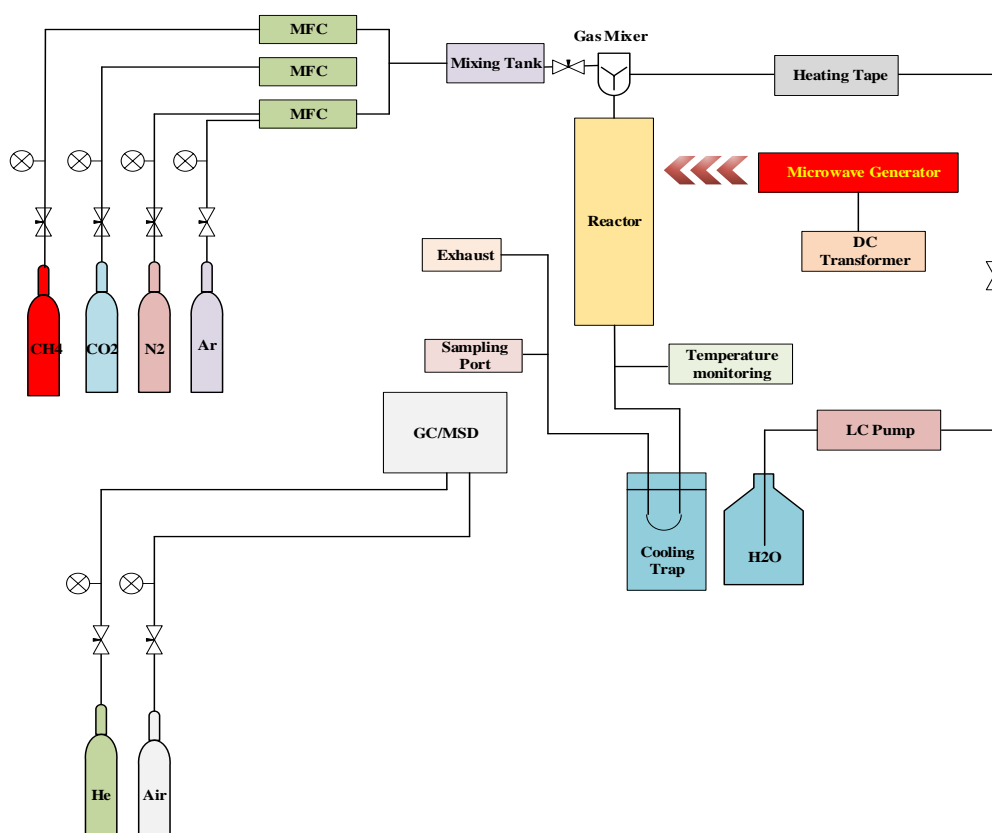
Figure 3. 2 Microwave Plasma Setup

3.2.1.1 Power Supplier

The power supplier (Hanlec) is one of the most important parts of the microwave plasma reactor because it is used as a transformer to convert the electric power to an electrical load (DC) to operate the microwave generator, as shown in Figure 3.3.

Figure 3. 3 Power supplier (hanlec)

3.2.1.2 Microwave Power Head (Generator)

The microwave generator system consisted of a separate rack-mountable power supply and remote magnetron head modules; these user-friendly systems were easily installed and operated with a minimal amount of setup, as shown in Figure 3.4 (a–d). Local controls provide complete functionality conveniently near the work area as well as remotely via the fully functional analogue and digital (serial) remote control interfaces. Included with each system was a complete set of interconnecting cabling between the two modules for safe and convenient setup and operation.

The power supply module (Alter, SM 1150T, Canada) is a compact, air-cooled, switch-mode power supply designed to drive most nominal 3 kW with a frequency of 2.45 GHz (Figure 3.4a). The power supply module combines state-of-the-art inverter (switch-mode) technology with microprocessor controls to provide high performance in a compact and lightweight package. An embedded microprocessor allows multi-functional user programmability. In addition, the power supply was operated by the DC transformer from various currents.

The forward and reverse power monitor indicates actual delivered microwave power, while the reverse power monitor indicates power reflected from the load, as shown in Figure 3.4b. The power output can be adjusted continuously from 10 up to 100% using an external analogue signal or panel controls.

The magnetron head module (GA4313) was used to convert DC power into microwave energy, as shown in Figure 3.4 (c and d). The magnetron head has been constructed in aluminium or stainless steel, and it is connected with the power supply via a cable assembly (Figure 3.4 c). The magnetron head can accommodate other water-cooled systems via multiple distributors to reduce the high temperature, as shown in Figure 3.4d.

(a)
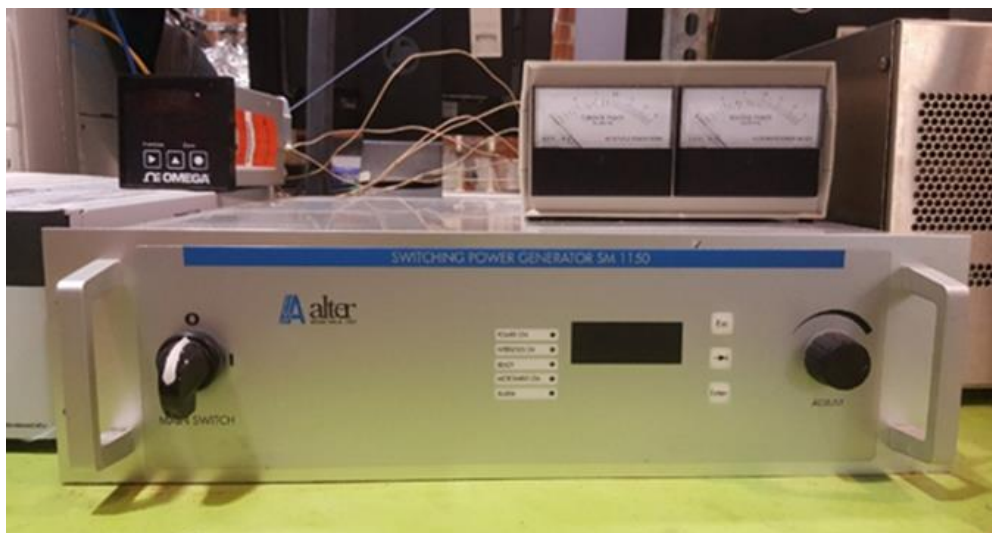
(b)

(c)   (d)
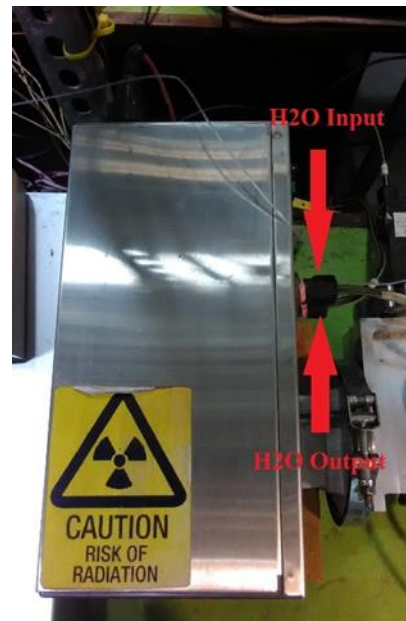
Figure 3. 4 Microwave Power Head (a) magnetron power supply module; (b) forward and reverse power monitor; (c) magnetron head and (d) magnetron head water-cooled system

3.2.1.3 3-Port Circulator

The model GA1112 is a waveguide 3-port circulator designed for high power industrial heating applications requiring high reliability and rugged construction, as shown in Figure 3.5 (a and b). These circulators are most often used with dummy loads in an

isolator configuration for magnetron protection, but they are also useful for other purposes in conjunction with devices such as phase shifters and variable attenuators, as shown in Figure 3.5 (a and b). The switch 3-port circulator was designed to drive with a nominal frequency of 2.45 GHz and continuous maximum power of 3 kW (forward and reverse power). Reverse power is diverted to and absorbed by the dummy load (Figure 3.5 a). The 3-port circulator (GA1112) is a dip brazed aluminium waveguide with brass water line connections to reduce the high temperature, as shown in Figure 3.5b.

(a) (b)
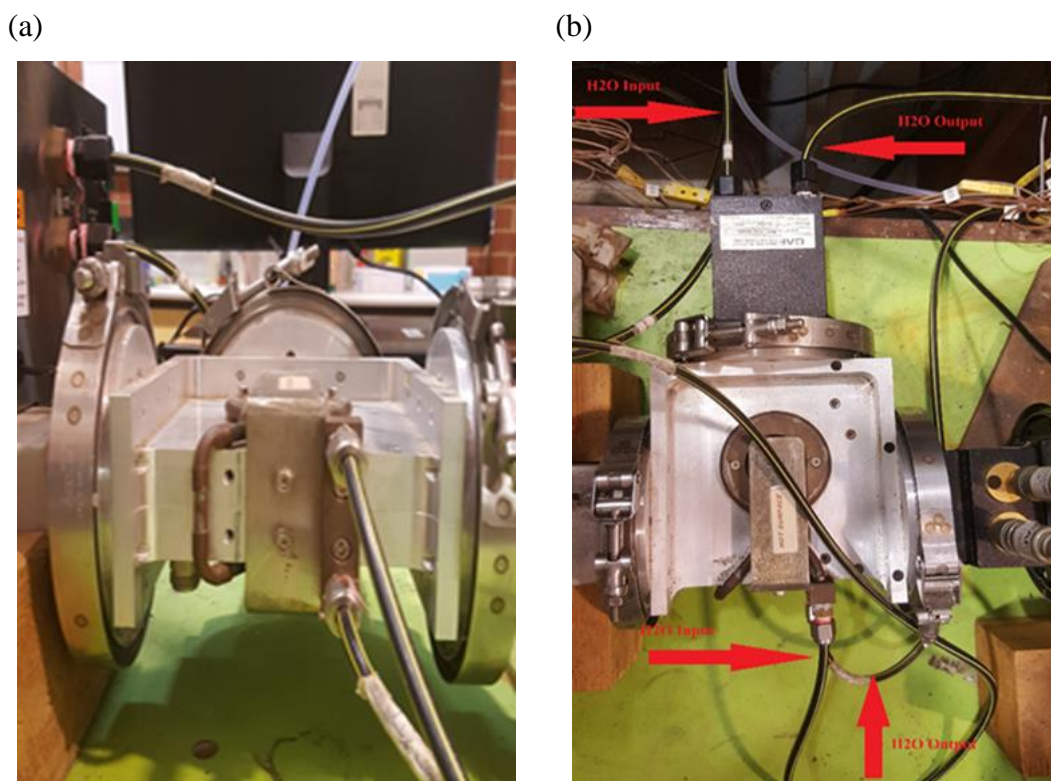
Figure 3. 5 Port circulator (a) 3-port circulator and dummy load and (b) copper water lines system

3.2.1.4 Dual directional coupler

The dual directional coupler (GA3104) is part of the WaveProbe^{TM} family of waveguide couplers that offer high-performance microwave power monitoring in a small package, as shown in Figure 3.6. The WaveProbe^{TM} secret to accurate and reliable waveguide power measurement is in the design of the prob itself. Utilizing a

common loop-type design, the probe terminates in a proprietary RF resistor configuration that provides excellent directivity and a stable coupling factor (Figure 3.6). The switch dual directional coupler is designed to drive frequency 2.45 GHz +/- 0.05 GHz and input power 6 kW continuously. The dual directional coupler (GA3104) was made of an aluminium waveguide and finished with a clear chemical film (Alodine); black paint, as shown in Figure 3.6.
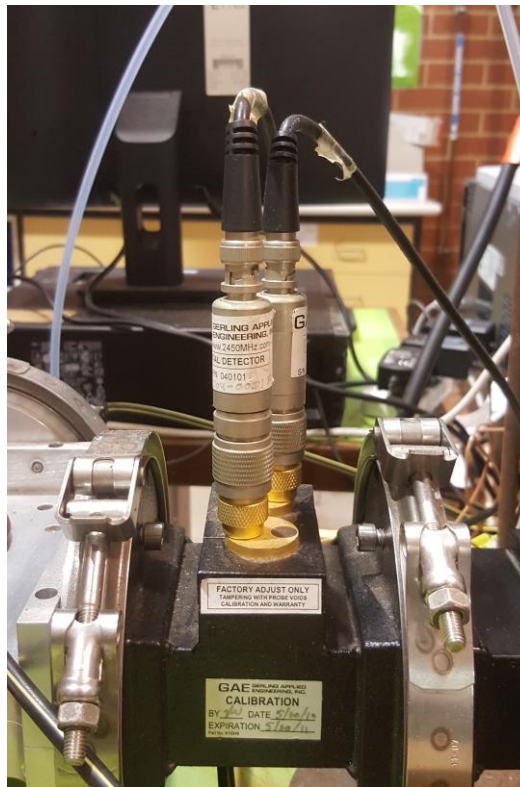
Figure 3. 6 Dual directional coupler

3.2.1.5 Precision high power E-H tuner

GAE's family of precision high power E-H tuners are Model GA1018 designed for load impedance matching in high power microwave heating systems, as shown in Figure 3.7. These E-H tuners are particularly useful under conditions of combined high power and high voltage standing wave ratio in which conventional stub tuners are more likely to cause voltage breakdown and arcing. The plunger is adjusted by a precision screw assembly that allows ultra-fine tuning and minimises backlash. A multi-turn dial with digital readout enables precise, repeatable positioning (Figure 3.7).

The simple yet rugged design of E-H tuners makes them ideal for a variety of laboratory, production, and OEM applications. The switch precision high power E-H tuner is designed to drive at a frequency of 2.45 GHz +/- 0.05 GHz and an input power of 3 kW. The high precision power E-H tuner (GA1018) is a dip brazed aluminium waveguide and is finished with a chemical conversion coating on a waveguide, black textured paint, as shown in Figure 3.7.
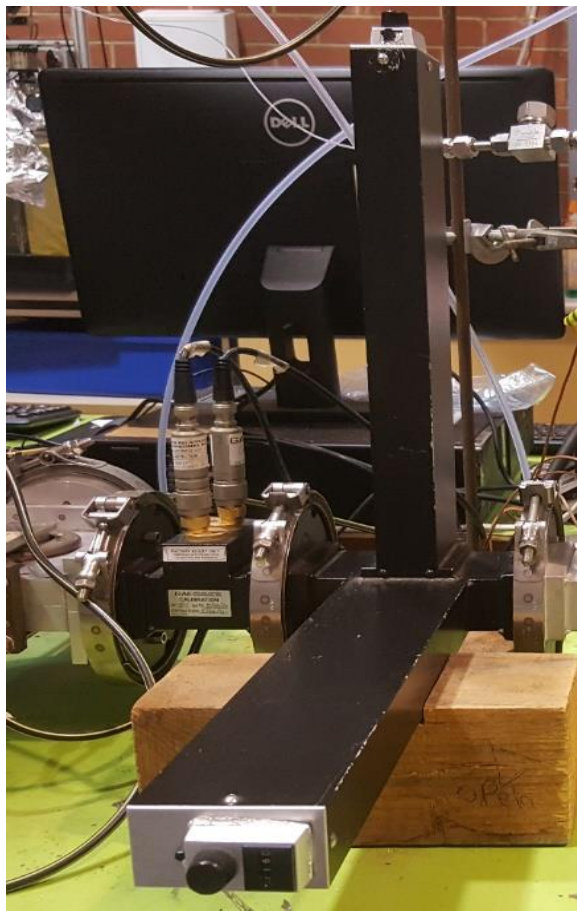
Figure 3. 7 Precision high power E-H tuner

3.2.1.6 Downstream plasma applicator

The downstream plasma applicator (GA6102) was designed as a general-purpose tool for plasma process development, as shown in Figure 3.8 (a and b). It features a quartz plasma tube fitted between standard stainless steel vacuum fittings that are easily disassembled for tube replacement, as shown in Figure 3.8a. Standard stainless steel

Swagelok fittings are provided for water-cooling as well as waveguide perforations for viewing and/or additional forced air-cooling of the plasma tube (Figure 3.8b). The downstream plasma applicator (GA6102) was designed to drive at a nominal frequency of 2.45 GHz and continuously input power of 1.5 kW at maximum value. In addition, it was a dip brazed aluminium waveguide and finished with chemical film; black textured paint, as shown in Figure 3.8 (a and b).

(a)   (b)
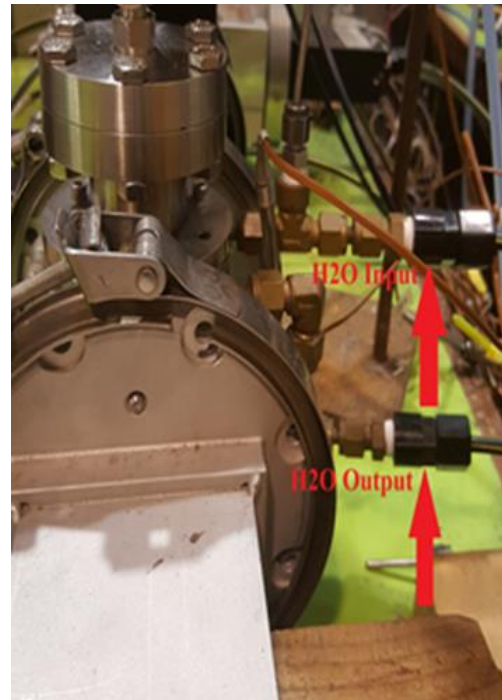
Figure 3. 8 Plasma reactor (a) downstream plasma applicator and (b) water cooling system for plasma reactor

3.2.1.7 Quartz Reactor

The cylindrical reactor was located inside the downstream plasma applicator (GA6102), and it was made of quartz (100 % quartz) with a wall thickness of 1.68 mm, an outer diameter of 25.5 mm, and a height of 126 mm, as shown in Figure 3.9. Quartz is a good dielectric material, and its low electrical conductivity close to 10^{-10} S/m means that it has almost no free charge on its surface and therefore does not interfere

with the electric field within the reactor (C. R. Paul & Nasar, 1987). In addition, quartz can withstand high temperatures because its melting point is close to 1600 °C.

Figure 3. 9 Microwave plasma reactor

3.2.1.8 Precision sliding short circuit

GAE's family of precision sliding short circuits is designed for use in high power microwave networks to establish a standing wave in the waveguide and adjust its relative phase angle continuously throughout a range of more than 1/2-guide wavelength, as shown in Figure 3.10. The precision sliding short circuit (GA1205B) is designed to drive the frequency of 2.45 GHz nominal and power 3 kW continuously. In addition, it is made of an aluminium waveguide, stainless steel actuator screw and brass, and aluminium plunger, as shown in Figure 3.10.

Figure 3. 10 Precision sliding short circuit

3.2.1.9 Feeding Gas

The four gases CH_2 (99.99%), CO_2 (99.99%), N_2 (99.99%), and Ar (99.99%) are fed from the cylinders, and they were controlled by mass flow controllers, as shown in Figure 3.11 (a and b). Then, they are sent into the gas tank to achieve the desired composition before entering the gas vortex inductor. The gas tanker is made from stainless steel, and its capacity is 5 L, as shown in Figure 3.11b.

(a)

(b)

Figure 3. 11 Feeding gas system (a) feeding gases system and (b) gas mixing tank

3.2.1.10 Mass Flow Rate Controller

The mass flow controller (MFC Alicat Scientific, MCS-Series) controls the feed flow rates for the four gases before entering the system, as shown in Figure 3.12. MFC has a high accuracy of ±0.4% of reading and ±0.2 of full scale over a wide temperature and pressure range. To ensure accuracy and reproducibility, the zero-flow point of each mass flow controller is checked before each experiment.

Figure 3. 12 Mass flow rate controller

3.2.1.11 Gas Vortex Inductor

Before entering the reactor, the gas passes through the static in a stainless-steel line mixer, as shown in Figure 3.13. That contains a series of geometric mixing elements fixed within a tubing, which uses the energy of the flow stream to create mixing between two or more fluids.
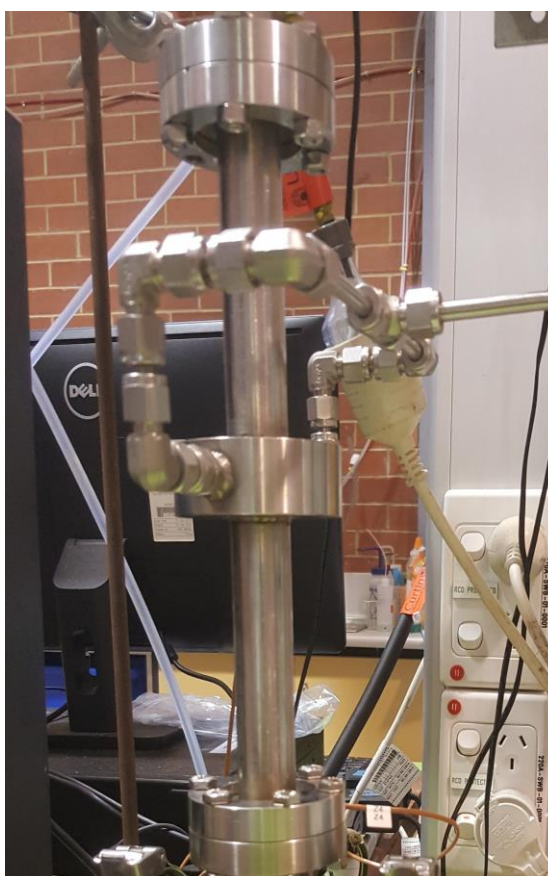
Figure 3. 13 Gas vortex inductor

3.2.1.12 Water Addition Line

The water addition line was contained of two parts, including an LC pump and a heated pipeline, as shown in Figure 3.14 (a–c). The deionised water was sent into a vaporizer, which works at the set temperature of 300 °C, by using an LC pump (Shimadzu LC-20AT) (Figure 3.14a). In addition, the steam was mixed with the gases in a final feed

mixer before entering the plasma reactor, as shown in Figure 3.14b. To avoid water recondensation before the reactor, heated tubing was used (Figure 3.14b). The temperature entering the heated tubing was controlled via the heat controller device, as shown in Figure 3.14c.

(a)

(b)   (c)

Figure 3. 14 Water addition line (a) LC pump, (b) heated pipeline and (c) heat controller

3.2.1.13 Temperature Monitory System

A K-type thermocouple is the most common type of thermocouple. It's inexpensive, accurate, reliable, and has a wide temperature range (maximum is around 1100 °C), as shown in Figure 3.15 (a and b). In addition, the K-type is commonly found in nuclear applications because of its relative radiation hardness. The K-type thermocouples were installed at different positions on all parts of the instrument to observe and control the temperatures during the reaction (Figure 3.15a). The temperature readings are displayed along with the operating condition via a portable device in Figure 3.15b.

(a)   (b)
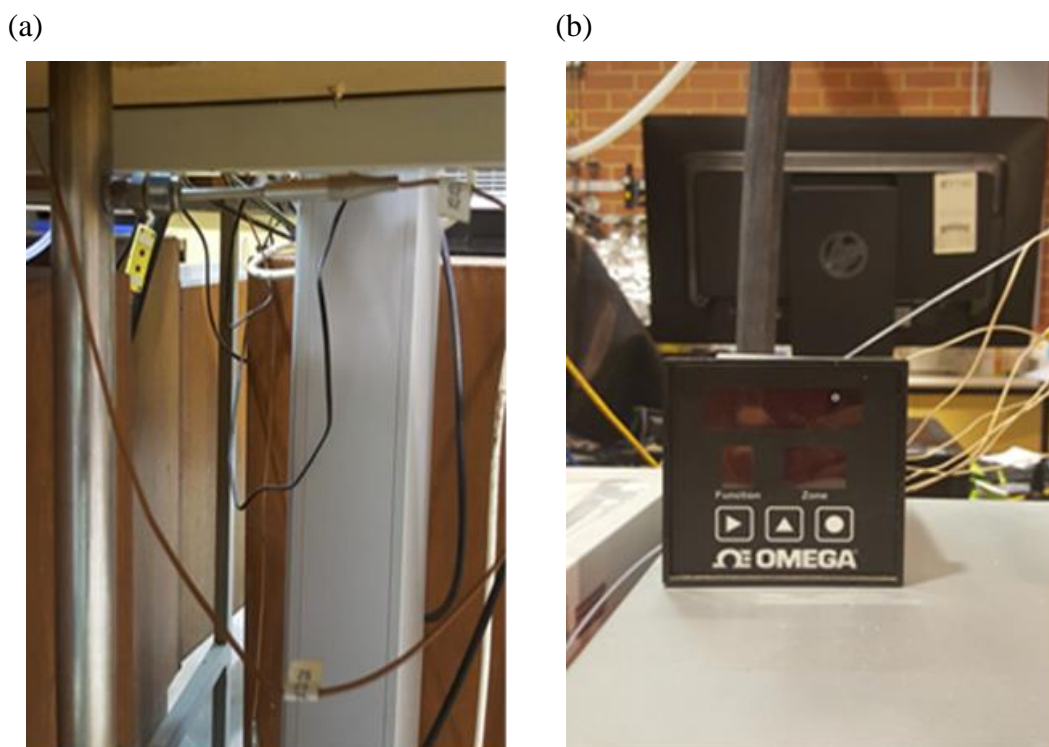
Figure 3. 15 Temperature monitory system (a) K-type thermocouple and (b) portable device for temperature reading

3.2.1.14 Product Gas Cooling System

The liquid trap was used to produce gas cooling, which works at 0 °C, and was installed between the reactor outlet and product sampling port to distinguish the produced gases from water, which may be produced as a side product, as shown in Figure 3.16. Then,

the trapped liquid was analysed by the gas chromatographic mass selective detector (GC-MSD).

Figure 3. 16 Product gas cooling system

3.2.1.15 Product Sampling Point System

The product sampling was taken through a sample port by a gasbag and then injected into the gas chromatographic (GC-MSD and gas chromatographic thermal conductivity detector (GC-TCD)) analysis system, as shown in Figure 3.17.

Figure 3. 17 Product sampling point system

3.2.1.16 Chemical Analysis

The gas sample was drawn by a gas bag sampling device and then injected into the GC/MSD-TCD analysers. Agilent 7890 GC/MS equipped with an HP-5 MS capillary column (30 m×0.32 mm×0.25 μm) was used in this work, as shown in Figure 3.18. GC is chromatography combined online with a MSD. GC can separate and identify gases such as CH_4, CO_2, H_2, CO, and N_2 by using a TCD. In contrast, the structure information was determined by using the MSD, as shown in Figure 3.18.

Figure 3. 18 GC MSD-TCD analyzer

3.2.2 Microwave Radiation

Although microwave radiation is necessary to generate the plasma flame, these radiations are too dangerous and harmful to human health. Therefore, a leak test was performed every three months to identify and apply additional controls when any power flux density above 2 GHZ (50 W/m^2) was detected. Microwave leakage detectors (ETS HI-1501 & Gerling GA3202) were used for the leak tests. Their procedure to follow to complete a microwave leak test is presented below:

1. Turn on the main power.
2. Turn on the transformer.
3. Turn on the cooling water system.
4. Turn on the power supply for the microwave.
5. Turn on the microwave generator start at 400 W.
6. Turn on the microwave leak detector system. Carry out a leak test to ensure there is no leak in the microwave generator.
7. Increase the microwave generator at 600, 800, 1000, 1200, 1400 to 1600 W and perform the leak test using the microwave detector to determine if there is any leak at many points in the microwave plasma reactor.
8. Turn off the microwave generator.
9. Open the top and bottom of the reactor.

10. Turn on the microwave generator starting at 400 W and do a leak test at the microwave and flanges.

11. Increase the microwave generator from 600 to 1600 W and perform the leak test using the microwave detector to determine if there is any leak at any point.

12. Download the microwave generator at 800 W and check the leak test again.

13. Turn on the power for MFC for the three gases.

14. Turn on a little bit the three-needle valves for the three gases.

15. Turn on 1.5 L min^{-1} of N_2.

16. Do the leak test for the microwave generator at 800 W.

17. Do a gas leak test for CH_4 by the detector to check if there any leak in the CH_4 tubing.

18. Perform a flammable leak test for the reactor at the flanges.

19. Gradually increase the flow rate of gases to reach 2.5 L min^{-1} of CH_4 and 5 L min^{-1} of CO_2 with a constant flow rate of N_2 1.5 of L min^{-1}.

20. Take a sample of the syngas using a gas bag sampling device after 20 min for analysis by the gas chromatographic (GC-MSD and GC-TCD) analysis system.

3.2.3 Experimental Conditions

All experiments were performed at atmospheric pressure. In our experimental runs, generally, a small amount of carbon powder (soot) can be observed in the reactor at the end of the experimental because CO_2 cannot be completely converted to syngas. Each measurement was repeated three times to improve data accuracy. To investigate and attempt to optimise a dry reforming reaction performed in a microwave plasma reactor, the following parameters have been studied in the present work, as shown in Tables 3.1–3.3.

Table 3. 1 Experimental runs for microwave-assisted DRM

Experimental type	Flow Rate [Lmin^{-1}]			MWP [W]	R [-]	TFR [L min^{-1}]	Sampling Time [min]
	CO$_2$	CH4	N$_2$				
Effect of input MWP	**0.4**	**0.2**	**1.5**	**700** 800 900 1000 1100 1200	**2/1**	**2.1**	**20**
Effect of R	**0.4** 0.5 0.6 0.7 0.8 0.9 1	**0.2**	**1.5**	**700**	**2/1** 2.5/1 3/1 3.5/1 4/1 4.5/1 5/1	**2.1** 2.2 2.3 2.4 2.5 2.6 2.7	**20**
Effect of TFR	0.1 0.15 0.2 0.25 0.3 0.35 **0.4**	0.05 0.075 0.1 0.125 0.15 0.175 **0.2**	0.3 0.5 0.7 0.9 1.1 1.3 **1.5**	**700**	**2/1**	0.45 0.725 1 1.275 1.55 1.825 **2.1**	**20**
DRM performance stability	**0.4**	**0.2**	**1.5**	**700**	**2/1**	**2.1**	**480**

Table 3. 2 Different experimental runs for microwave-assisted DRM using N_2 and Ar

Experiment type	Flow Rate [Lmin^{-1}]				MWP [W]	R [-]	TFR [L min^{-1}]	Sampling Time [min]
	CO₂	**CH₄**	**N₂**	**Ar**				
Different N₂ flow rate	**0.4**	**0.2**	0.5 0.75 1 1.25 **1.5**	-	**700**	**2/1**	1.1 1.35 0.7 1.85 **2.1**	**20**
Different Ar flow rate	**0.4**	**0.2**	-	0.5 0.75 1 1.5 **1.5**	**700**	**2/1**	1.1 1.35 0.7 1.85 **2.1**	**20**
Different MWP	**0.4**	**0.2**	**1.5**	-	**700** 800 900 1000 1100 1200	**2/1**	**2.1**	**20**
			-	**1.5**		**2/1**	**2.1**	**20**
Different R	**0.4** 0.5 0.6 0.7 0.8 0.9 1	**0.2**	**1.5**	-	**700**	**2/1** 2.5/1 3/1 3.5/1 4/1 4.5/1 5/1	**2.1** 2.2 2.3 2.4 2.5 2.6 2.7	**20**
			-	**1.5**				
DRM performance stability	**0.4**	**0.2**	**1.5**	-	**700**	**2/1**	**2.1**	**480**
			-	**1.5**				

Table 3. 3 Different experimental runs for microwave-assisted DRM with Adding Steam

Experiment type	Flow Rate [mole min^{-1}]				TFR [mole min^{-1}]	SC [%]	MWP [W]	Sampling Time [min]
	CO$_2$	CH$_4$	N$_2$	Steam				
Effect of TFR	0.004	0.002	0.0124	0.005	0.02	**42.62**	**700**	**20**
	0.006	0.003	0.020	0.015	0.04			
	0.008	0.004	0.029	0.025	0.06			
	0.010	0.005	0.037	0.035	0.08			
	0.012	0.006	0.045	0.045	0.1			
	0.014	0.007	0.054	0.055	0.13			
	0.016	**0.008**	**0.062**	**0.065**	**0.15**			
SC	**0.016**	**0.008**	**0.062**	0.005	0.02	5.4	**700**	**20**
				0.015	0.04	14.63		
				0.025	0.06	22.22		
				0.035	0.08	28.56		
				0.045	0.1	33.96		
				0.055	0.13	38.59		
				0.065	**0.15**	42.62		
Effect of input MWP	**0.016**	**0.008**	**0.062**	**0.065**	**0.161**	**42.62**	**700**	**20**
							800	
							900	
							1000	
							1100	
							1200	
Stability of plasma	**0.016**	**0.008**	**0.062**	**0.065**	**0.161**	**42.62**	**700**	**480**

3.2.4 Calculation Methods

The conversions of CH_4 and CO_2; selectivities and yields of H_2, CO, and CO; and H_2/CO ratio are defined as follows:

$$CH_4 \text{ \% Conversion} = \frac{\text{moles of CH4 converted}}{\text{moles of CH4 introduced}} \times 100 \tag{3-1}$$

$$CO_2 \text{ \% Conversion} = \frac{\text{moles of CO2 converted}}{\text{moles of CO2 introduced}} \times 100 \tag{3-2}$$

$$H_2 \text{ \% Selectivity} = \frac{\text{moles of H2 produced}}{2 \times \text{moles of CH4 converted}} \times 100 \tag{3-3}$$

$$CO \text{ \% Selectivity} = \frac{\text{moles of CO produced}}{[\text{moles of CH4 + moles of CO2] converted}} \times 100 \tag{3-4}$$

$$H_2 \text{ \% Yield} = \frac{\text{moles of H2 produced}}{2 \times \text{moles of CH4 introduced}} \times 100 \tag{3-5}$$

$$CO \text{ \% Yield} = \frac{\text{moles of CO produced}}{[\text{moles of CH4 + moles of CO2]introduced}} \times 100 \tag{3-6}$$

$$\frac{H_2}{CO} \text{ Ratio} = \frac{\text{moles of H2 produced}}{\text{moles of CO produced}} \tag{3-7}$$

3.3 Experimental design and regression analysis

RSM with BBD was applied to optimise the performance process via the DRM microwave plasma technique. This method was used to investigate the interactive impacts of the three independent variables on plasma stability and syngas production. The present research consists of two parts; the first part used the input MWP (x_1), R (x_2), and TFR (x_3) on DRM. In addition, the second used the three feed flow rates of CH_4 (x_1), CO_2 (x_2), and N_2 (x_3) gases. Because these variables can significantly influence plasma stability and the syngas production process, they were selected as critical factors.

To achieve these aims, 15 experimental tests were averaged, and they were performed at random by varying MWP from 600 to 800 W with a central point of 700 W, R from

1 to 3 with a central point of 2, and TFR from 1.9 to 2.3 L min^{-1} with a central point 2.1 L min^{-1}. In addition, CH$_4$ was varied from 0.1 to 0.3 L min^{-1} with a central point 0.2 L min^{-1}, CO$_2$ from 0.2 to 0.6 L min^{-1} with a central point 0.4 L min^{-1}, and N$_2$ (x$_3$) from 1.4 to 1.6 L min^{-1} with a central point 1.5 L min^{-1}.

The conversions of CO$_2$ and CH$_4$, selectivities and yields of H$_2$, CO, and H$_2$/CO ratio were selected as the response variables. The actual values of independent factors (Xi) were coded as (x$_i$) by applying the following equation (Tanyildizi, Özer, & Elibol, 2005).

$$x_i = \frac{X_i - X_o}{\Delta X_I}, \qquad i = 1, 2, ..., k \tag{3-8}$$

Where x$_i$ is the coded value of the actual value for factor x$_i$, x$_o$ is the actual value of the factor at the centre point, Δx_i is the step change value, and i = 1, 2, …, k. A second-order polynomial equation (Equation (3-9)) was used to calculate the predicted responses (Alketife, Judd, & Znad, 2017).

$$Y = \beta_0 + \sum_{j=1}^{k} \beta_j X_j + \sum_{j=1}^{k} \beta_{jj} X_j^2 + \sum_{i=1}^{k-1} \sum_{j=i+1}^{k} \beta_{ij} X_i X_j + \varepsilon \tag{3-9}$$

Here, Y is the predicted response variable; β_0 is the constant interception coefficient; βj, βjj and βij are the interaction coefficients of linear, quadratic, and the second-order terms, respectively; x$_i$ is the initial input parameters; and ε is the standard error (El Hassani, Beakou, & Anouar, 2018). The reaction performance was predicted for different process conditions by this model (Mallieswaran, Padmanabhan, & Balasubramanian, 2018).

The actual and coded values of the independent variables in the Box–Behnken design with the experimental and predicted responses value are shown in Tables 3.4 and 3.5. All experiments were replicated in triplicate to reduce the effect of temporal related absolute errors, and the coefficients of Equation (3-8) were generated. In this research, BBD experimental design and regression analysis were performed by JMP statistical

discovery software from SAS (version 13.1.0). The effects of the process parameters were studied by plotting the 3D response surface graphs and the 2D contour plots. The calculations of CH_4 and CO_2 conversions, the H_2 and CO selectivities and yields, and the H_2/CO ratio were presented in Section 3.2.4.

Table 3. 4 Actual and coded levels of factors in the Box-Behnken design matrix with experimental and predicted results

Run order	Actual Values[a]			Coded Values[b]		
	X_1	X_2	X_3	X_1	X_2	X_3
1	800	2	1.9	+	0	−
2	700	3	2.3	0	+	+
3	600	2	2.3	−	0	+
4	600	1	2.1	−	−	0
5	800	2	2.3	+	0	+
6	700	1	2.3	0	-	+
7	600	2	1.9	−	0	−
8	700	1	1.9	0	−	−
9	600	3	2.1	−	+	0
10	800	3	2.1	+	+	0
11	700	3	1.9	0	+	−
12	800	1	2.1	+	−	0
13[*]	700	2	2.1	0	0	0
14[*]	700	2	2.1	0	0	0
15[*]	700	2	2.1	0	0	0

[*]**Replicated experimental runs (Run order 13-15); [a]x_1, x_2, x_3 are actual values of MWP (W), R (-) and TFR (L min^{-1}), respectively. [b]Coded values x_1, x_2, and x_3.**

Table 3. 5 Actual and coded levels of factors in the Box-Behnken design matrix with experimental and predicted results

Run order	Actual Values[a]			Coded Values[b]		
	X_1	X_2	X_3	X_1	X_2	X_3
1[*]	0.2	0.4	1.5	0	0	0
2[*]	0.2	0.4	1.5	0	0	0
3	0.1	0.6	1.5	_	+	0
4	0.3	0.6	1.5	+	+	0
5	0.1	0.4	1.4	_	0	_
6	0.1	0.4	1.6	_	0	+
7	0.3	0.4	1.4	+	0	_
8	0.3	0.4	1.6	+	0	+
9	0.2	0.2	1.4	0	_	_
10	0.2	0.6	1.4	0	+	_
11[*]	0.2	0.4	1.5	0	0	0
12	0.2	0.6	1.6	0	+	+
13	0.1	0.2	1.5	_	_	0
14	0.3	0.2	1.5	+	_	0
15	0.2	0.2	1.6	0	_	+

[*]**Replicated experimental runs (Run order 1, 2 and 11); [a]x_1, x_2, x_3 are actual values of CH_4 (L min^{-1}), CO_2 (L min^{-1}) and N_2 (L min^{-1}), respectively. [b]Coded values x_1, x_2, and x_3.**

4

Chapter 4: Modelling and optimization of different parameters on the syngas production by plasma dry reforming of methane using a response surface methodology

4.1 Introduction

The DoE work is commonly performed for process optimisation by varying a single parameter while setting all other parameters at fixed values (Montgomery, 2017). Thus, RSM has been used to design experiments to investigate the interactive impacts of factors and determine optimum experimental conditions. The chemical model requires a significantly lower number of experiments compared to using traditional methods (Mei et al., 2016). RSM is considered one of the most used methodologies in DoE. This methodology is based on the Box–Behnken design (BBD) and takes the various input parameters and output responses that could interpolate the impact of individual factors and their interactions on the responses by three-dimensional and contour interpretations (Rowshanzamir & Eikani, 2009). However, as mentioned in the literature review chapter, the use of the DoE method to optimise the plasma chemical reactions in the microwave is still limited. Therefore, the main objective of this chapter is to discuss the effects of three parameters, namely MWP, R, and TFR via DBD on the plasma stability and syngas production by the DRM microwave plasma method. Moreover, the effects of these parameters and their interactions on the conversions of CH_4 and CO_2, selectivities and yields of H_2 and CO, and H_2/CO ratio are also investigated and discussed.

4.2 Material and methods
4.2.1 Experimental setup

A commercial microwave reactor system (Alter, SM 1150T, Canada) consists of a feed gas system, plasma reactor, microwave generator, and gas chromatographic (GCMS) analysis system. Further details about the experimental design and the calculation methodology can be found elsewhere in Chapter 3.

4.2.2 Experimental design

RSM with BBD was applied to optimise the syngas production process via dry reforming plasma microwave technique and to investigate interactive impacts of the three independent variables. Because MWP (X_1), R (X_2), and TFR (X_3) can significantly affect plasma stability and the syngas production process, they were selected as the critical factors. To achieve these aims, an average of 15 experimental tests were accomplished at random by varying MWP from 600 to 800 W with a central point of 700 W, R from 1 to 3 with a central point of 2, and TFR from 1.9 to 2.3 with a central point of 2.1. The actual and coded values of the independent variables in the Box–Behnken design with the experimental and predicted response values are shown in Table 1.

4.3 Results and Discussion
4.3.1 Multiple regression analysis

Multiple regression analysis for determining the real relationships between the three response parameters of MWP, R, and TFR concerning the CO_2 and CH_4 conversions (Y_1 and Y_2), H_2 and CO selectivities (Y_3, Y_4), H_2 and CO yields (Y_5, Y_6), and H_2/CO ratio (Y_7) generated second-order polynomial equations based on the BBD method of actual data (Table 4.1):

$$Y_1 = 43.38 + 14.59x_1 + 4.73x_2 + 0.26x_3 + 0.53x_1x_2 - 2.90x_1x_3 - 0.32x_2x_3 - 22.89x_1^2 - 7.48x_2^2 - 12.89x_3^2 \tag{4-1}$$

$$Y_2 = 77.80 + 9.45x_1 + 2.28x_2 - 18.78x_3 + 0.17x_1x_2 - 6.24x_1x_3 + 0.55x_2x_3 - 16.04x_1^2 - 17.17x_2^2 - 38.41x_3^2 \tag{4-2}$$

$$Y_3 = 37.52 + 0.97x_1 - 0.69x_2 - 9.67x_3 + 0.06x_1x_2 - 0.50x_1x_3 + 0.88x_2x_3 - 8.72x_1^2 - 9.57x_2^2 - 18.70x_3^2 \tag{4-3}$$

$$Y_4 = 48.78 + 4.40x_1 - 0.67x_2 - 18.57x_3 + 0.87x_1x_2 - 3.11x_1x_3 + 0.67x_2x_3 - 7.45x_1^2 - 6.90x_2^2 - 23.03x_3^2 \tag{4-4}$$

$$Y_5 = 57.35 + 2.80x_1 - 1.69x_2 - 22.14x_3 + 0.59x_1x_2 - 0.81x_1x_3 + 3.00x_2x_3 - 7.53x_1^2 - 8.70x_2^2 - 27.08x_3^2 \tag{4-5}$$

$$Y_6 = 29.50 + 0.82x_1 + 0.12x_2 - 8.80x_3 + 0.022x_1x_2 - 0.85x_1x_3 + 0.07x_2x_3 - 6.36x_1^2 - 6.21x_2^2 - 14.50x_3^2 \tag{4-6}$$

$$Y_7 = 0.84 + 0.05x_1 - 0.0075x_2 - 0.31x_3 - 0.02x_1x_2 - 0.03x_1x_3 - 0.02x_2x_3 - 0.14x_1^2 - 0.09x_2^2 - 0.40x_3^2 \tag{4-7}$$

Where, x_1, x_2, and x_3 are the coded values, as shown in Table 4.1 (calculated according to Equation (3-8) and defined in Table 3.4), of the initial values of MWP, R, and TFR, respectively. The determination coefficients (R^2) of the regression equations of CO_2 and CH_4 conversions, H_2 and CO selectivities and yields, and the H_2/CO ratio were 0.99, 0.99, 0.98, 0.99, 0.97, 0.97, and 0.97 respectively, indicating that the regression models (Equations (4-1) to (4-7)) can adequately explain the relationship between independent parameters and responses. The predicted values from Equations (4-1) to (4-7) are in good agreement with those determined experimentally, as shown in Figure 4.1(a–g).

4.3.2 Analysis of variance (ANOVA)

The ANOVA for the second-order polynomial equations and significance, interactive, quadratic, and adequacy terms of the progression equations are presented in Tables 4.2 to 4.8. The level of significance of each term of fitting models was indicated by p-value. The impact is considered significant if the p-value is less than 0.05. Tables 4.2 to 4.8 show that the linear term coefficients (x_1 and x_3) significantly influenced the CO_2 and CH_4 conversions, H_2 selectivity, and H_2/CO ratio; while the linear term coefficient (x_3) was identified as significant parameters in the CO selectivity and H_2, CO yields. In contrast, the quadratic term coefficients (x_1^2, x_2^2, and x_3^2) had significant impacts on the CO_2 and CH_4 conversions, H_2 and CO selectivities and yields, and the H_2/CO ratio (p<0.005), as shown in Tables 4.2 to 4.8. However, this implies that the interactive term coefficients (x_1x_3) have a significant effect on the H_2 selectivity, whereas the interactive term coefficients (x_1x_2, x_1x_3, and x_2x_3) did not have a

significant impact on the CO_2 and CH_4 conversions, CO selectivity, H_2 and CO yields, and the H_2/CO ratio ($p>0.005$) (Tables 4.2 to 4.8).

In other words, the MWP and TFR were significantly affected by the linear terms of CO_2 and CH_4 conversions, H_2 selectivity, and H_2/CO ratio, while R had the most significant impact on CO selectivity and H_2 and CO yields with a p-value <0.05, as shown in Tables 4.2 to 4.8. The quadratic terms of MWP, R, and TFR were identified as significant parameters on the conversion of CO_2 and CH_4, selectivities and yields of H_2 and CO, and the H_2/CO ratio (p-value< 0.05) (Tables 4.2 to 4.8).

Table 4. 1 Actual and coded levels of factors in the Box-Behnken design matrix with experimental and predicted results

Run no.	Response Values, [%]													
	CO_2 conv.a	CO_2 conv.b	CH_4 conv.a	CH_4 conv.b	H_2 selc.a	H_2 selc.b	CO selc.a	CO selc.b	H_2 yielda	H_2 yieldb	CO yielda	CO yieldb	H_2/CO ratioa	H_2/CO ratiob
1	38.14	39.19	59.17	61.81	42.83	44.39	47.08	48.48	20.20	21.25	19.38	18.67	0.65	0.69
2	0	0	0	-0.29	0.00	0.27	0.00	0.72	0	-0.23	0	0.11	0.00	-0.00
3	0	0	0	-2.64	0.00	-1.56	0.00	0.00	0	-0.05	0	0.06	-1.40	-0.04
4	27.34	25.68	32.11	35.59	30.21	31.5	37.3	40.59	18.34	19.01	17.65	16.39	0.53	0.52
5	0	0	0	3.77	0.00	1.01	0.00	2.57	0	0.89	0	-4.08	0.00	-0.00
6	0	0	0	0.83	0.00	0.27	0.00	-1.89	0	-0.61	0	-0.16	0.00	0.05
7	26.53	28.34	34.21	30.43	30.38	29.36	43.84	41.26	19.18	18.28	15.96	14.32	0.51	0.53
8	24.38	25.99	45.54	45.83	39.04	38.76	49.13	48.40	20.26	22.49	18.57	17.46	0.64	0.66
9	25.32	24.67	31.75	34.69	27.27	28.55	35.34	36.02	19.21	17.49	16.36	15.19	0.51	0.56
10	38.89	38.11	57.42	53.94	40.25	38.96	46.11	42.81	20.24	19.57	20.41	18.31	0.62	0.62
11	26.67	27.09	43.33	44.16	36.35	36.07	37.12	39.08	16.71	17.33	17.54	15.70	0.72	0.66
12	38.76	37.42	57.09	54.15	39.99	38.70	45.7	45.01	21.11	20.83	18.43	17.59	0.74	0.69
13[*]	41.56	42.79	75.58	77.81	46.89	50.94	54.65	53.35	35.08	37.52	26.77	29.50	0.82	0.84
14[*]	44.82	46.85	79.35	83.12	50.12	51.35	58.42	57.21	39.77	38.41	32.89	30.72	0.86	0.87
15[*]	43.78	42.32	78.49	77.81	49.34	52.78	51.24	57.58	37.71	38.52	28.85	29.50	0.84	0.85

[*]**Replicated experimental runs (Run order 13-15); CO_2 conv.a, CH_4 conv.a, H_2 selc.a, CO selc.a and H_2/CO Ratioa show experimental values of CO_2 conversion (%), CH_4 conversion (%), H_2 selectivity (%), CO selectivity (%), and H_2/CO ratio, respectively. While CO_2 conv.b, CH_4 conv.b, H_2 selc.b, CO selc.b and H_2/CO ratiob are predicted values of H_2 selectivity (%), CO selectivity (%) and H_2/CO ratio, respectively**

(a)

(b)

(c)

Predicted H₂ Selectivity, %

(d)

Predicted CO Selectivity, %

(e)

Predicted H₂ Yield, %

(f)

Predicted CO Yield, %

(g)
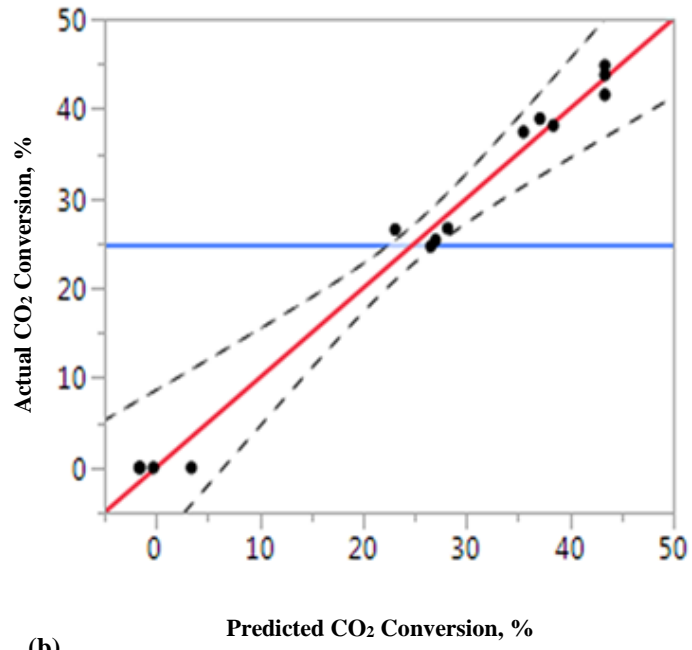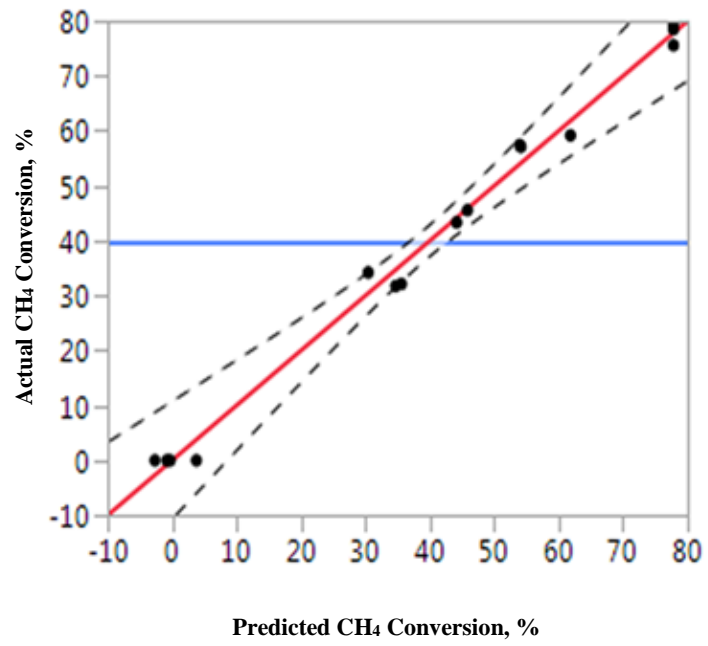
Predicted H₂/CO Ratio
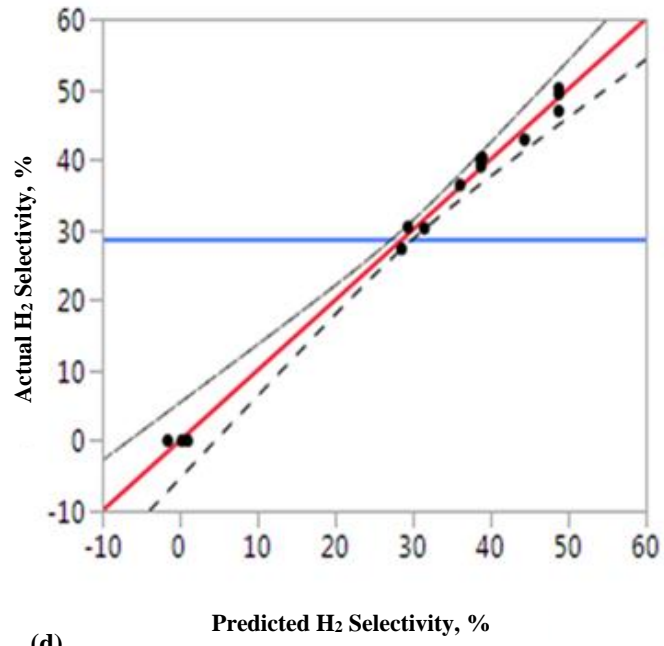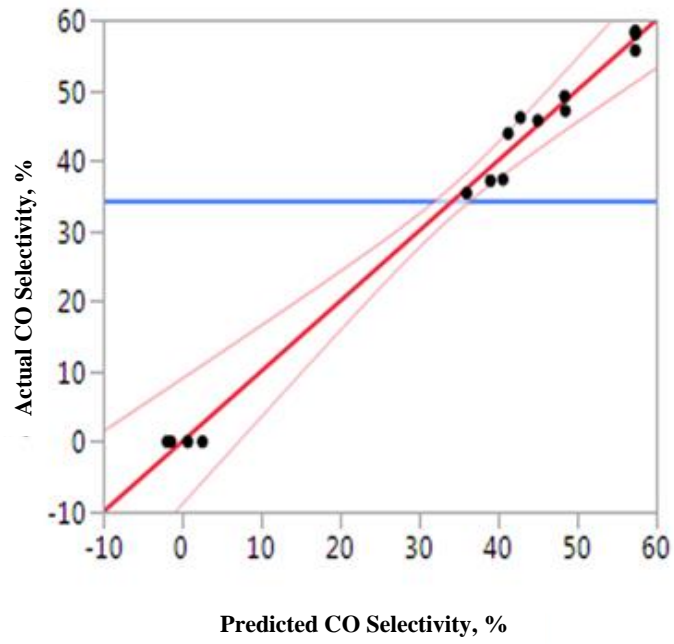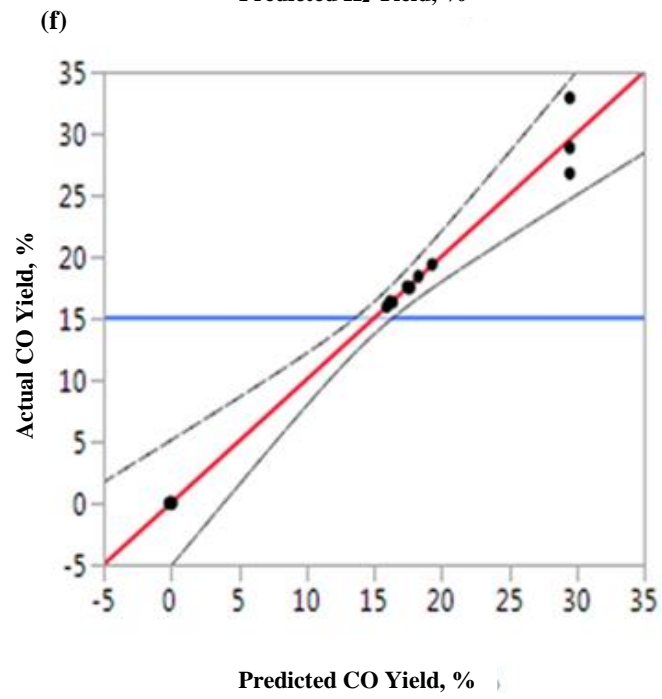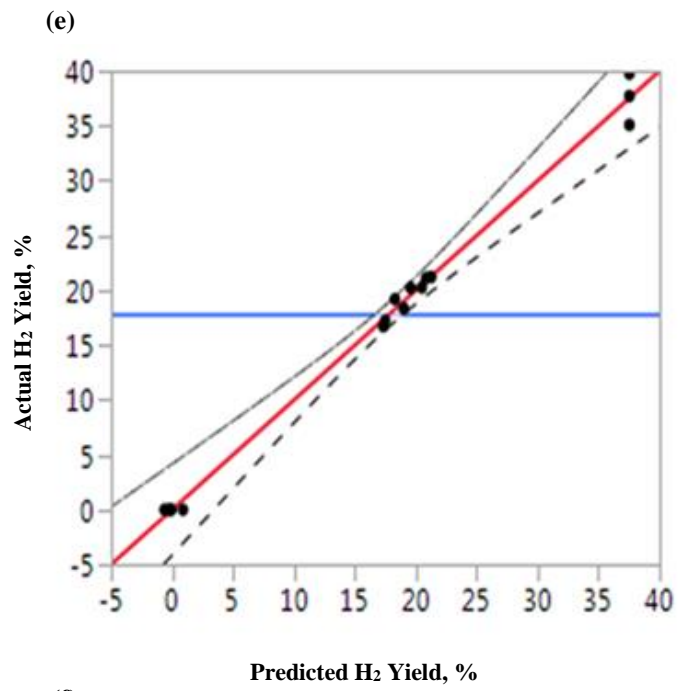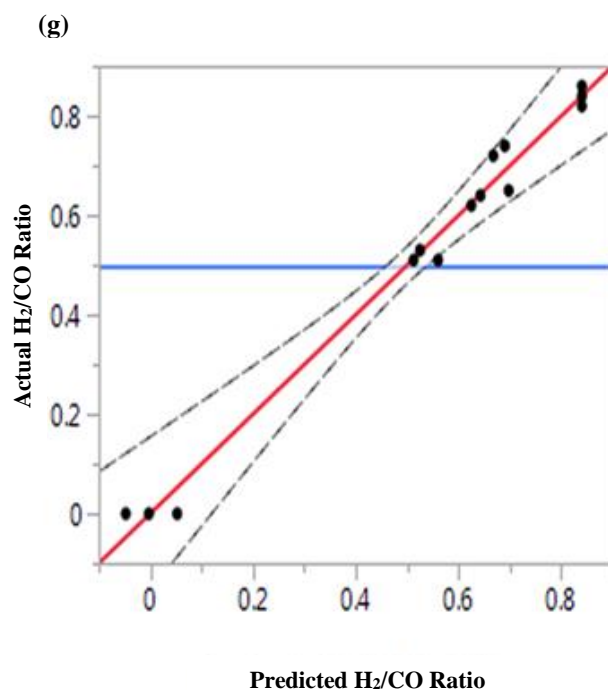
Figure 4. 1 Comparison between experimental and predicted values of (a) CO_2 conversion; (b) CH_4 conversion; (c) H_2 selectivity; (d) CO selectivity; (e) H_2 yield; (f) CO yield; (g) H_2/CO ratio [(.) experimental values, (–) confidence bands, (–) fit line, Equations (4-1 to 4-7), (–) mean of the Y leverage residuals]

The interactive terms of MWP and TFR significantly influenced the H_2 selectivity and H_2/CO ratio with a p-value >0.05, while the interactive terms of MWP, R, and TFR did not significantly influence the CO_2 and CH_4 conversions, CO selectivity, H_2 and CO yields, and H_2/CO ratio with a p-value >0.05, as shown in Tables 4.2 to 4.8. Therefore, all three factors (MWP, R, and TFR) were found to have significant impacts on CO_2 and CH_4 conversions, H_2 and CO selectivities and yields, and H_2/CO ratio (Tables 4.2 to 4.8).

Table 4. 2 ANOVA analysis for the model of CO_2 conversion using BBD

Model term CO₂ conversion	Estimate	Standard error	F-value	P-value
Intercept	43.386667	1.870088	-	-
x_1	4.73875	2.14519	258.2387	0.0090*
x_2	0.26125	1.14519	222.1336	0.8286
x_3	-14.59	1.14519	125.0673	<.0001*
$x_1 x_2$	0.535	1.619544	120.0064	0.7545
$x_1 x_3$	-2.9025	1.619544	8.3342	0.1331
$x_2 x_3$	-0.3225	1.619544	0.0653	0.8500
x_1^2	-4.325833	2.685675	250.8537	<.0001*
X_2^2	-7.480833	1.685675	158.2527	0.0068*
X_3^2	-22.89333	1.685675	131.6151	<.0001*

*Significant at p-value <0.05

Table 4. 3 ANOVA analysis for the model of CH_4 conversion using BBD

Model term CH₄ conversion	Estimate	Standard error	F-value	P-value
Intercept	77.806667	1.495869	-	-
x_1	9.45125	2.528401	227.1765	0.0016*
x_2	-0.28	2.528401	235.3123	0.8618
x_3	-22.78125	1.528401	122.1232	<.0001*
$x_1 x_2$	0.1725	2.161486	120.0064	0.9395
$x_1 x_3$	-6.24	1.161486	8.3342	0.3343
$x_2 x_3$	0.5525	1.161486	0.0653	0.8084
x_1^2	-16.04333	2.249746	242.6645	0.0008*
X_2^2	-17.17083	2.249746	134.3462	0.0006*
X_3^2	-38.41833	1.249746	124.5675	<.0001*

*Significant at p-value <0.05

Table 4. 4 ANOVA analysis for the model of H_2 selectivity using BBD

Model term H_2 selectivity	Estimate	Standard error	F-value	P-value
Intercept	48.783333	1.141997	-	-
x_1	4.40125	0.699327	705.6088	0.0015[*]
x_2	-0.67125	0.699327	650.9213	0.3812
x_3	-18.575	0.699327	558.4996	<.0001[*]
x_1x_2	0.8	0.988998	0.6543	0.4553
x_1x_3	-3.1125	0.988998	9.9044	0.0055[*]
x_2x_3	0.6725	0.988998	0.4624	0.5267
x_1^2	-7.449167	1.029382	52.3676	0.0008[*]
X_2^2	-6.904167	1.029382	44.9852	0.0011[*]
X_3^2	-23.03167	1.029382	500.6080	<.0001[*]

[*]**Significant at p-value <0.05**

Table 4. 5 ANOVA analysis for the model of CO selectivity using BBD

Model term CO selectivity	Estimate	Standard error	F-value	P-value
Intercept	57.35	1.871808	-	-
x_1	2.80125	1.146244	373.9724	0.0084
x_2	-1.695	1.146244	322.1867	0.1993
x_3	-22.14625	1.146244	216.2902	<.0001[*]
x_1x_2	0.5925	1.621033	0.1336	0.7297
x_1x_3	-0.81	1.621033	0.2497	0.6385
x_2x_3	3.0025	1.621033	3.4307	0.1232
x_1^2	-7.535	1.687225	19.9444	0.0066[*]
X_2^2	-8.7025	1.687225	26.6037	0.0036[*]
X_3^2	-27.085	1.687225	257.6984	<.0001[*]

[*]**Significant at p-value <0.05**

Table 4. 6 ANOVA analysis for the model of H_2 yield using BBD

Model term	Estimate	Standard error	F-value	P-value
H_2 yield				
Intercept	37.523916	0.985009	-	-
x_1	0.9767622	1.603193	132.6222	0.1663
x_2	-0.694526	0.603193	111.3258	0.3016
x_3	-9.67081	0.603193	117.0477	<.0001*
x_1x_2	0.0634162	0.853043	0.0055	0.9436
x_1x_3	-0.505278	0.853043	0.3508	0.5794
x_2x_3	0.8871152	0.853043	1.0815	0.3460
x_1^2	-8.722329	1.887875	116.5075	0.0002*
X_2^2	-9.570763	0.887875	16.1955	0.0001*
X_3^2	-18.70656	0.887875	13.8987	<.0001*

*Significant at p-value <0.05

Table 4. 7 ANOVA analysis for the model of CO yield using BBD

Model term	Estimate	Standard error	F-value	P-value
CO yield				
Intercept	29.503333	0.14095	-	-
x_1	0.82625	1.698686	158.3985	0.2901
x_2	0.1275	0.698686	110.0333	0.8624
x_3	-8.80625	0.698686	118.8612	<.0001*
x_1x_2	0.2275	0.988091	0.0530	0.8270
x_1x_3	-0.855	0.988091	0.7488	0.4264
x_2x_3	0.0075	0.988091	0.0001	0.9942
x_1^2	-6.161667	1.028438	135.8955	0.0019*
X_2^2	-6.219167	0.028438	14.5686	0.0018*
X_3^2	-14.50667	0.028438	21.9660	<.0001*

*Significant at p-value <0.05

Table 4. 8 ANOVA analysis for the model of H_2/CO ratio using BBD

Model term H_2/CO ratio	Estimate	Standard error	F-value	P-value
Intercept	0.84	0.032558	-	-
x_1	0.0575	0.019937	249.3176	0.0044*
x_2	-0.0075	0.019937	187.1415	0.7222
x_3	-0.315	0.019937	94.6226	<.0001*
x_1x_2	-0.025	0.028196	0.7862	0.4159
x_1x_3	-0.035	0.028196	1.5409	0.2695
x_2x_3	-0.02	0.028196	0.5031	0.5098
x_1^2	-0.145	0.029347	24.4122	0.0043*
X_2^2	-0.095	0.029347	10.4790	0.0030*
X_3^2	-0.405	0.029347	190.4499	<.0001*

*Significant at p-value <0.05

However, for the CO_2 and CH_4 conversions and H_2 and CO selectivities, the most important factors were MWP and TFR, followed by R, as shown in Tables 4.2 to 4.8. In contrast, for the H_2 and CO yields and H_2/CO ratio, R had a greater impact than other factors, followed by MWP and TFR (Tables 4.2 to 4.8). The synergistic effect of MWP-TFR was significant on the H_2 selectivity (p-value <0.05), while the synergistic effects of MWP-R, MWP-TFR, and R-TFR had a weak significant effect on the CO_2 and CH_4 conversions, CO selectivity, H_2 and CO yields, and H_2/CO ratio because it had the lowest f-value (0.7545, 0.1331, and 0.8500 for CO_2 conversion; 0.9395, 0.3343, and 0.8084 for CH_4 conversion; 0.7297, 0.6385, and 0.1232 for CO selectivity; 0.9436, 0.5794, and 0.3460 for H_2 yield; 0.8270, 0.4264, and 0.9942 for CO yield; and 0.4159, 0.2695, and 0.5098 for H_2/CO ratio, respectively), as shown in Tables 4.2 to 4.8. The quadratic term coefficients of MWP, R, and TFR on the CO_2 conversion, CH_4 conversion, H_2 yield, and CO yield were more significant factors (<.0001, 0.0068, and <.0001 for CO_2 conversion; 0,0008, 0.0006, and <.0001 for CH_4 conversion; 0.0008, 0.0011 and <.0001 for H_2 selectivity; 0.0066, 0.0036 and <.0001 for CO selectivity; 0.0002, 0.0001, and <.0001 for H_2 yield; 0.0019, 0.0018, and <.0001 for CO yield; and 0.0043, 0.0030, and <.0001 for H_2/CO ratio, respectively), as illustrated in Tables 4.2 to 4.8.

The 3D response surfaces and 2D contour lines plots shown in Figures 4.2 to 4.8 (a, b, and c) are based on Equations (4.3) to (4.9), respectively, with one independent parameter kept at a constant level (coded zero levels), while the other two parameters were changed within the experiential values ranges. These figures show the effects of MWP and R, MWP and TFR, and R and TFR, respectively, on the conversions of CO_2 and CH_4, selectivities and yields of H_2 and CO, and H_2/CO ratio. The responses enhanced as corresponding parameters increased until the maximum was reached. Afterwards, they decreased even when both parameters continued to increase, as presented in Figures 4.2 to 4.8 (a, b, and c). For instance, Figures 4.2 to 4,8 (a and b) indicate that CO_2 and CH_4 conversions, H_2 and CO selectivities and yields, and H_2/CO ratio increase rapidly when MWP was extended from 600 to 724 W and then slightly declined when MWP continued to increase from 724 to 800 W. The possible reason for this behaviour might be the electron collisions for the molecules of CO_2 and CH_4 at 724 W till reaching the optimum value and then gradually declining with increasing MWP.

Previous studies (Aziznia et al., 2012; S. M. Chun et al., 2017; Jiang et al., 2002; Moshrefi et al., 2013; A. Ozkan et al., 2015; Qi et al., 2006; Shapoval & Marotta, 2015; X Tu & Whitehead, 2012; Xin Tu & Whitehead, 2014; Q. Wang et al., 2009b; A.-J. Zhang et al., 2010) have shown that increasing input MWP leads to enhance the electric field, electron density, and the gas temperature in the discharge zone (Xin Tu & Whitehead, 2014). Shorter residence time translates to a shorter reaction time and lower frequency of collisions between CH_4 and CO_2 with energetic species such as electrons, OH, O, and O- that lead to dissociations of CH_4 and CO_2, as represented by possible reactions listed in Equations (4-8) to (4-13) and Equations (4-14) to (4-19) for CH_4 and CO_2, respectively (G. Chen et al., 2015). After reaching the optimum value, the collision molecules of CO_2 and CH_4 decreased with increased MWP, as shown in Figures 4.2 to 4.8 (a and b). Therefore, the possibility of interaction molecules of CO_2 and CH_4 could be enhanced.

$$CH_4 + e \rightarrow CH_3 + H + e \tag{4-8}$$

$$CH_4 + e \rightarrow CH_2 + H + e \tag{4-9}$$

$$CH_4 + e \rightarrow CH + H + e \tag{4-10}$$

$$CH_4 + e \rightarrow C + H + e \qquad (4\text{-}11)$$

$$CH_4 + O \rightarrow CH_3 + OH \qquad (4\text{-}12)$$

$$CH_4 + OH \rightarrow CH_3 + H_2O \qquad (4\text{-}13)$$

$$CO_2 + e \rightarrow CO + O + e \qquad (4\text{-}14)$$

$$CO_2 + e \rightarrow O + 2O + e \qquad (4\text{-}15)$$

$$CO_2 + e \rightarrow CO + O^- \qquad (4\text{-}16)$$

$$CO_2 + O \rightarrow CO + O_2 \qquad (4\text{-}17)$$

$$CO + O^- \rightarrow CO_2 + e \qquad (4\text{-}18)$$

$$CO + O \rightarrow CO_2 \qquad (4\text{-}19)$$

Similarly, the conversions of CO_2, CH_4, the selectivities and yields of H_2, CO, and the H_2/CO ratio initially increased when R ranged from 1 to 1.99 and then decreased with increasing values of R, as shown in Figures 4.2 to 4.8 (b and c). The reason for this behaviour could be that the number of collisions between the molecules of CO_2 and CH_4 increased until reaching the optimum value. Afterwards, the collisions interaction decreased with increased R, as shown in Figures 4.2 (b and c). Similar results have been reported by other researchers (Serrano-Lotina & Daza, 2014; Shapoval & Marotta, 2015; Yunpeng Xu, Tian, Xu, & Lin, 2002; Zeng, Zhu, Mei, Ashford, & Tu, 2015). These transitions can be caused by increasing the initial concentration of CO_2, enhancing the collisions between the CO_2 and CH_4 molecules and the energetic electrons(Q. Wang et al., 2009b; A. Wu et al., 2014).

(a)

(b)

(c)
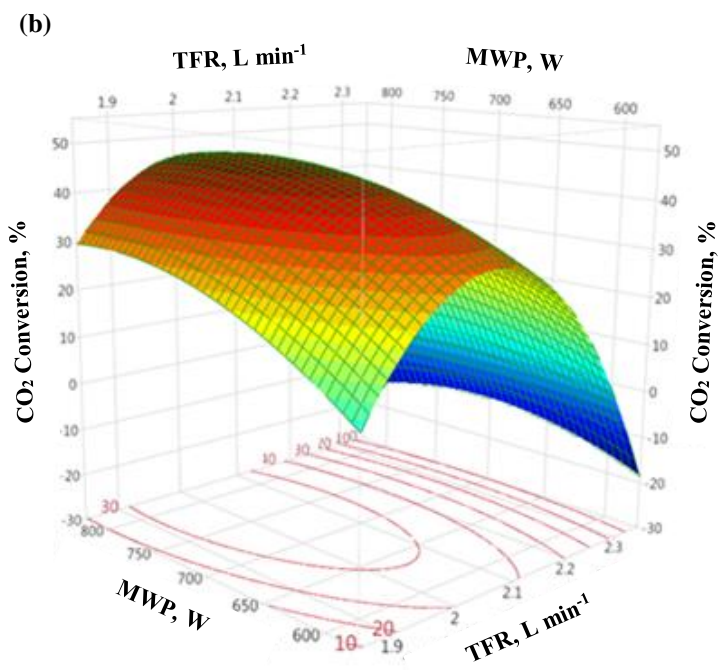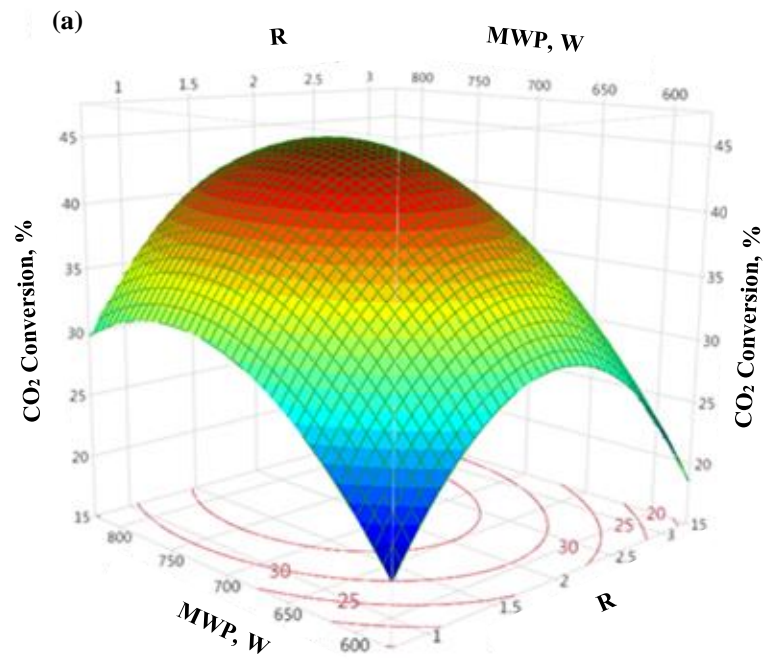
Figure 4. 2 Effect of MWP, R, and TFR and their interaction on CO_2 conversion [(3D surface plots; 2D projected contour plots (a, b, and c)]

(a)

(b)

(c)

Figure 4. 3 Effect of MWP, R, and TFR and their interaction on CH_4 conversion [(3D surface plots; 2D projected contour plots (a, b, and c)]

(a)

(b)

(c)
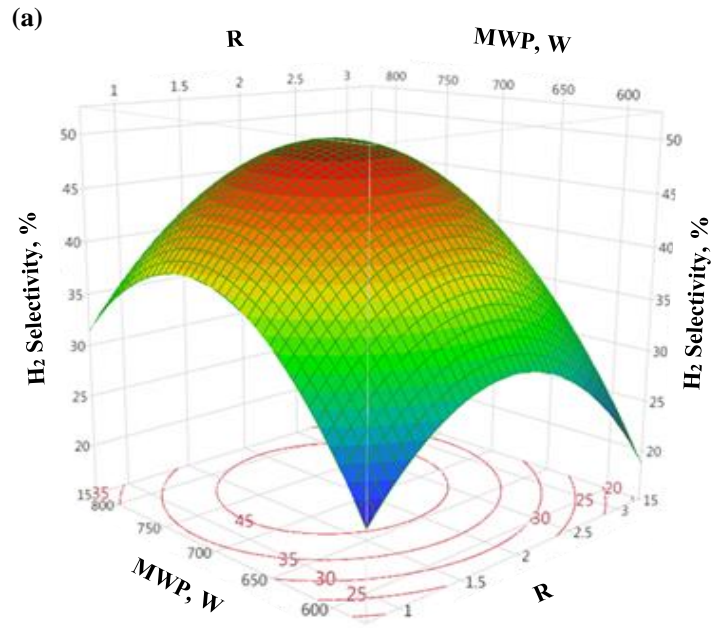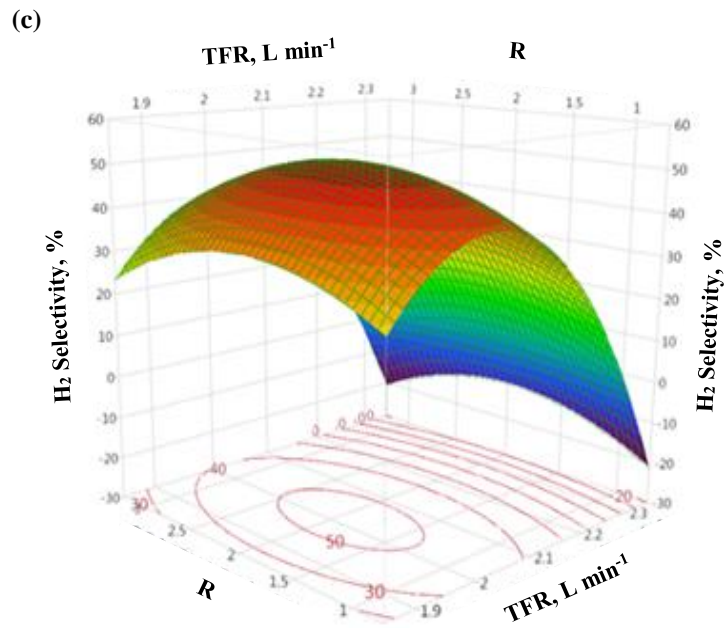
Figure 4. 4 Effect of MWP, R, and TFR and their interaction on H_2 selectivity [(3D surface plots; 2D projected contour plots (a, b, and c)]

(a)
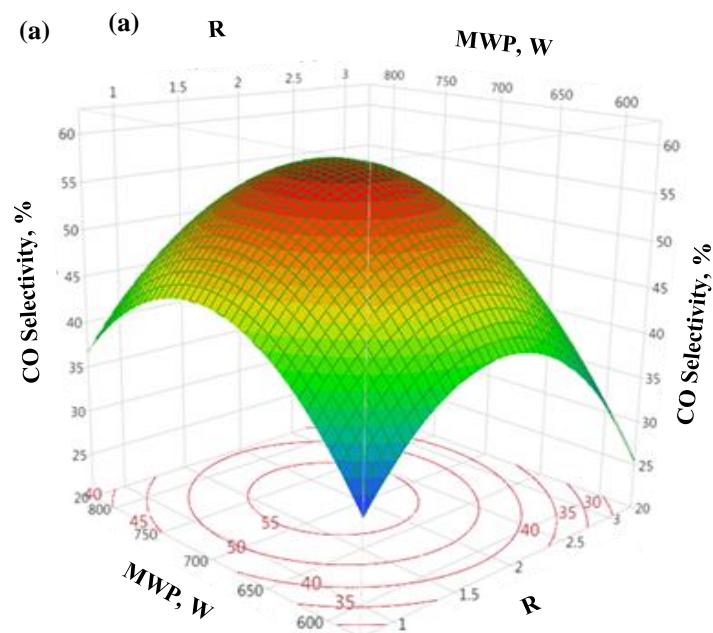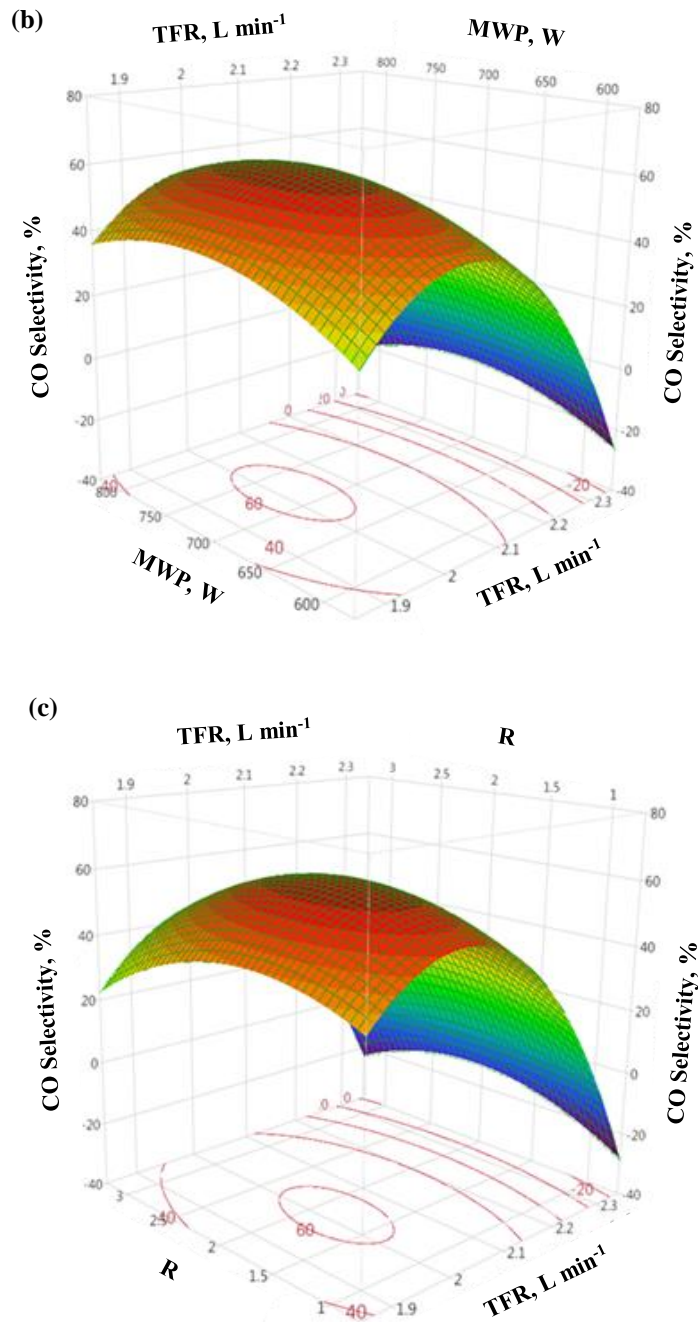
Figure 4. 5 Effect of MWP, R, and TFR and their interaction on CO selectivity [(3D surface plots; 2D projected contour plots (a, b, and c)]

(a)

(b)
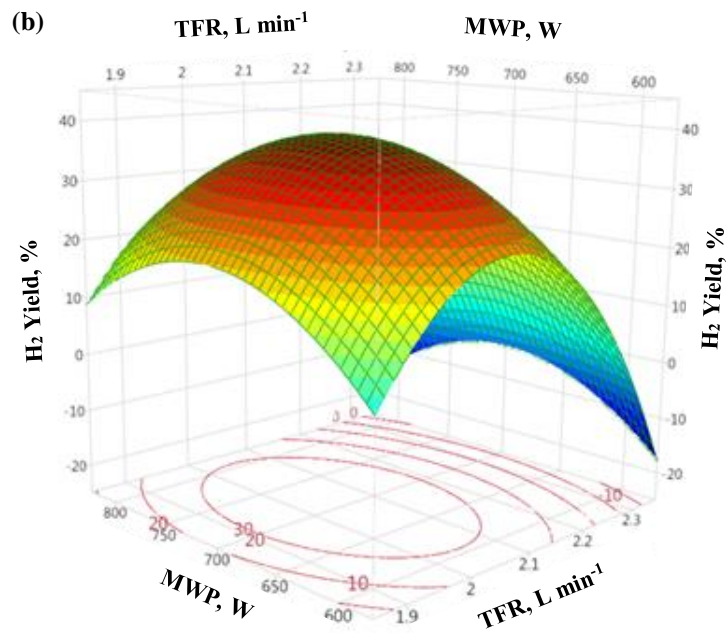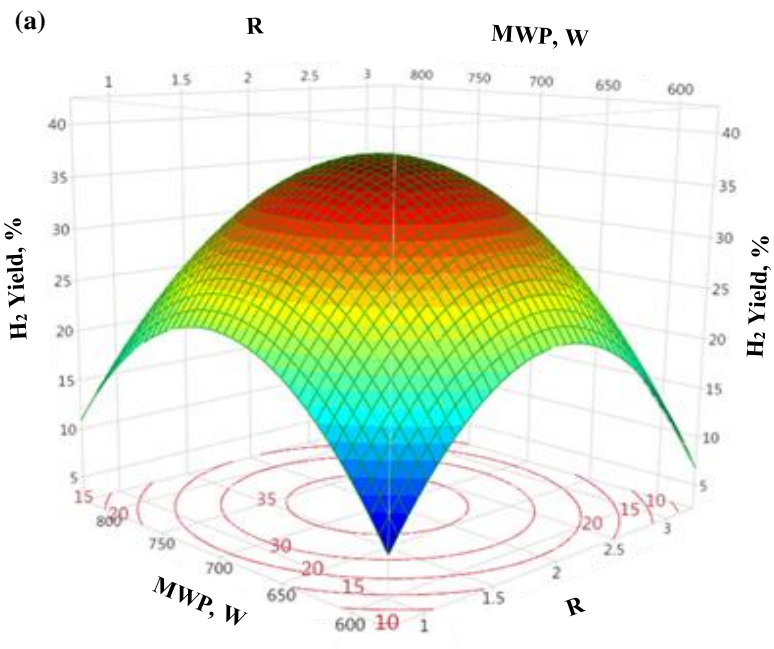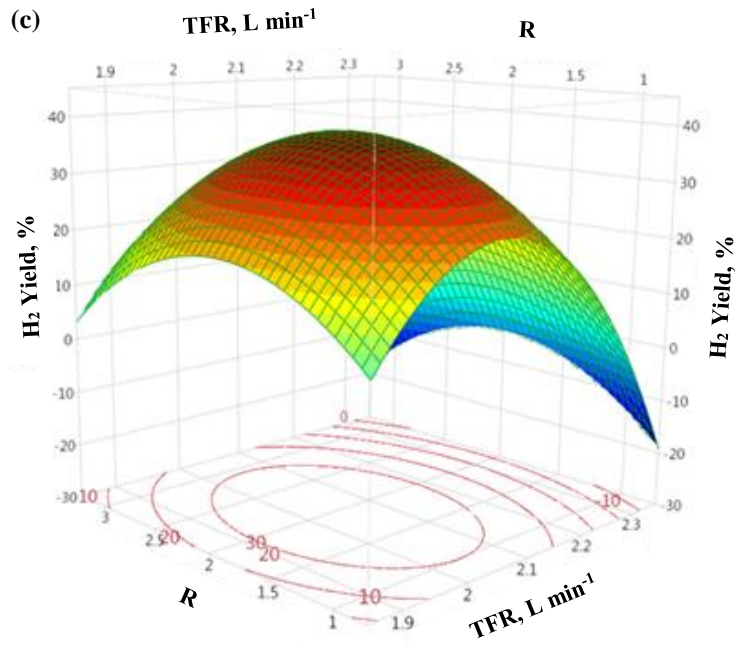
Figure 4. 6 Effect of MWP, R, and TFR and their interaction on H_2 yield [(3D surface plots; 2D projected contour plots (a, b, and c)]
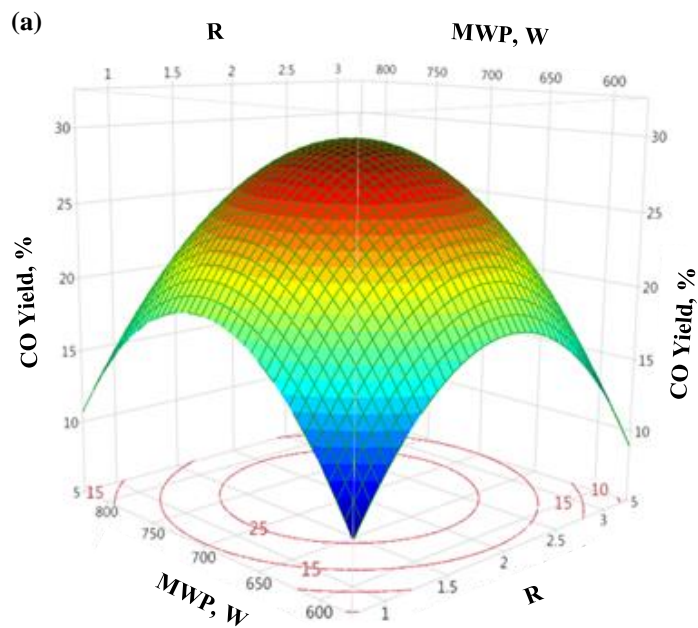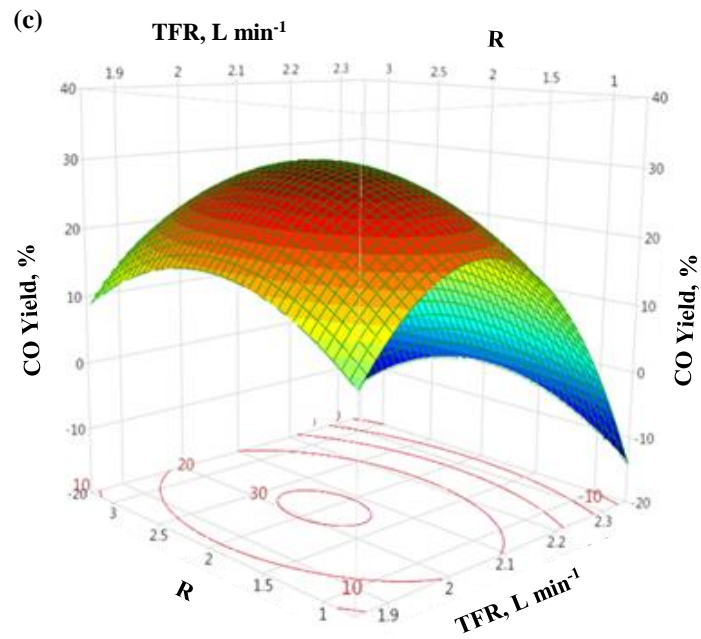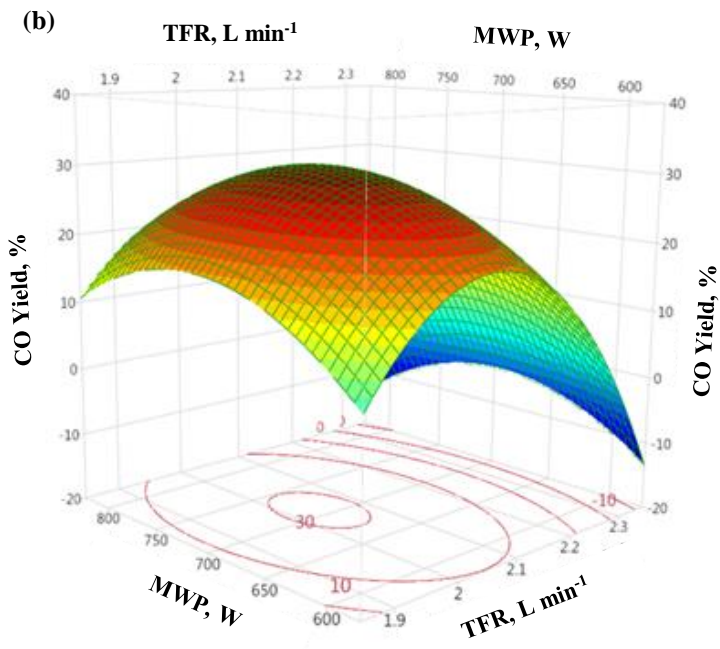
Figure 4. 7 Effect of MWP, R, and TFR and their interaction on CO yield [(3D surface plots; 2D projected contour plots (a, b, and c)]
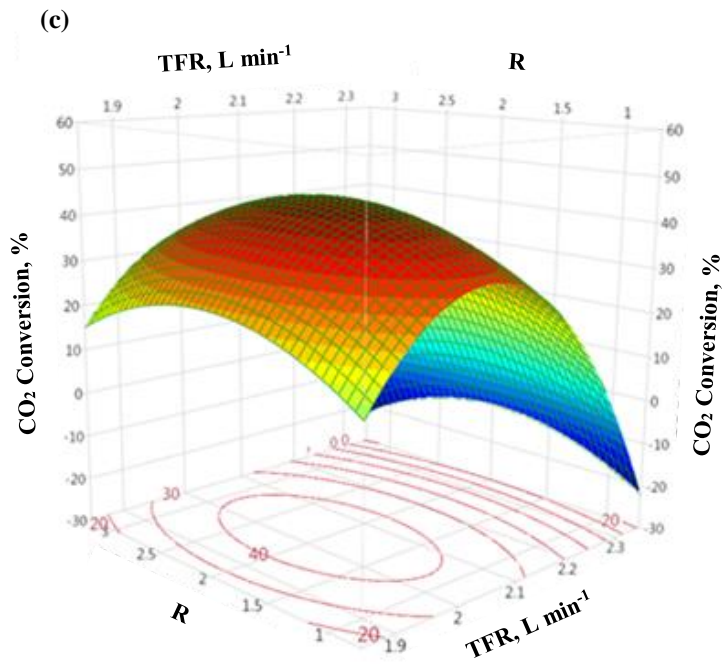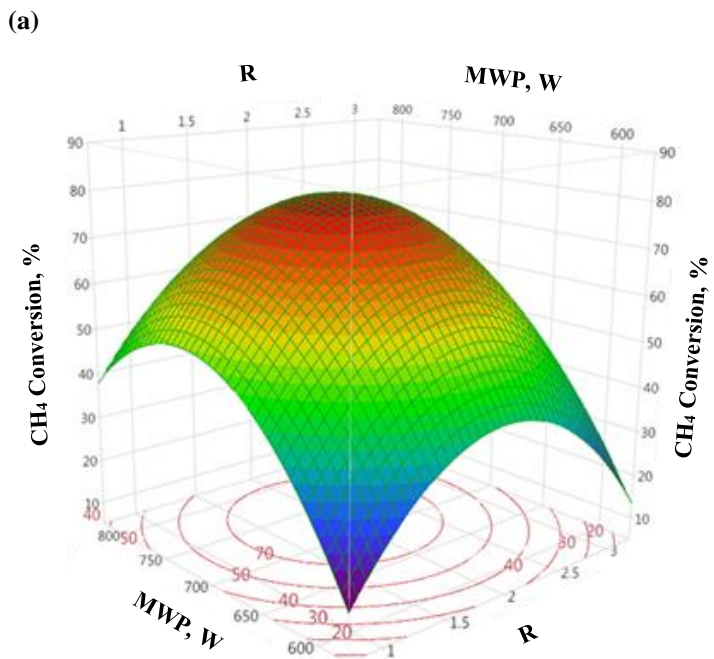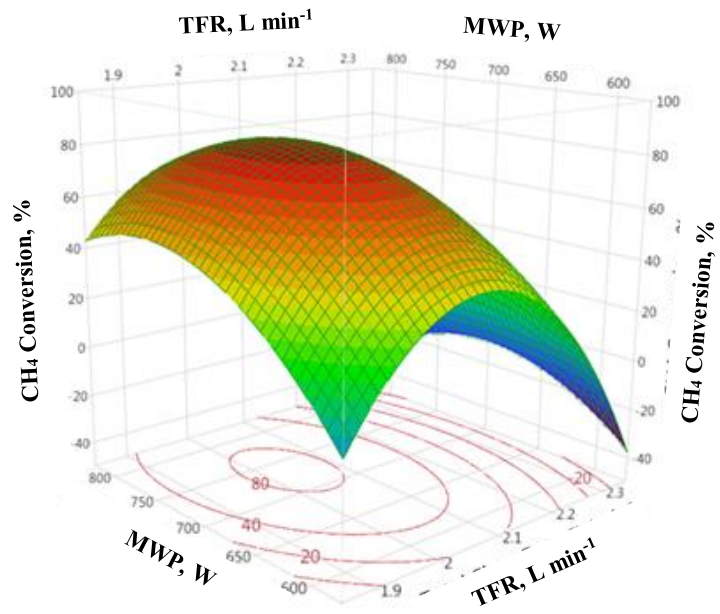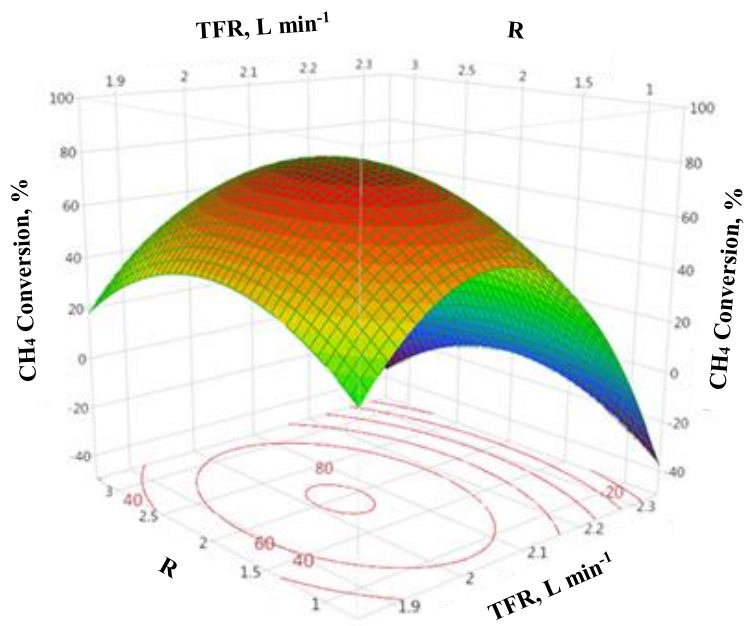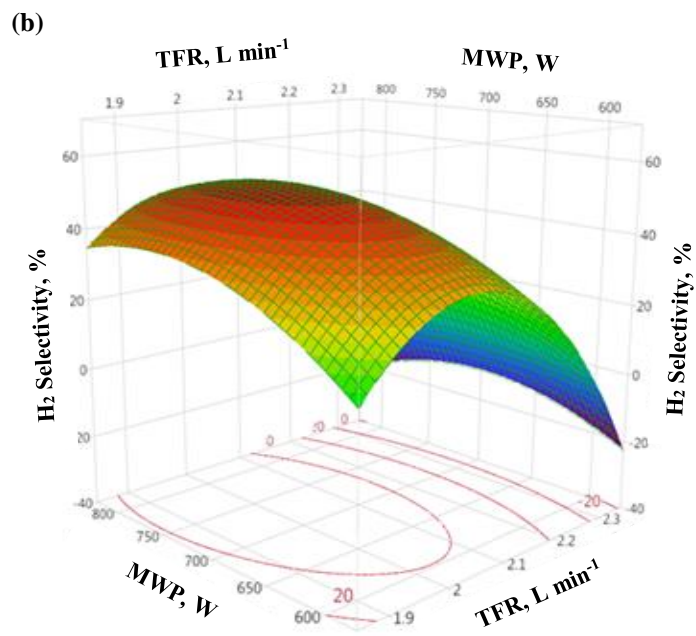
(a)

(b)
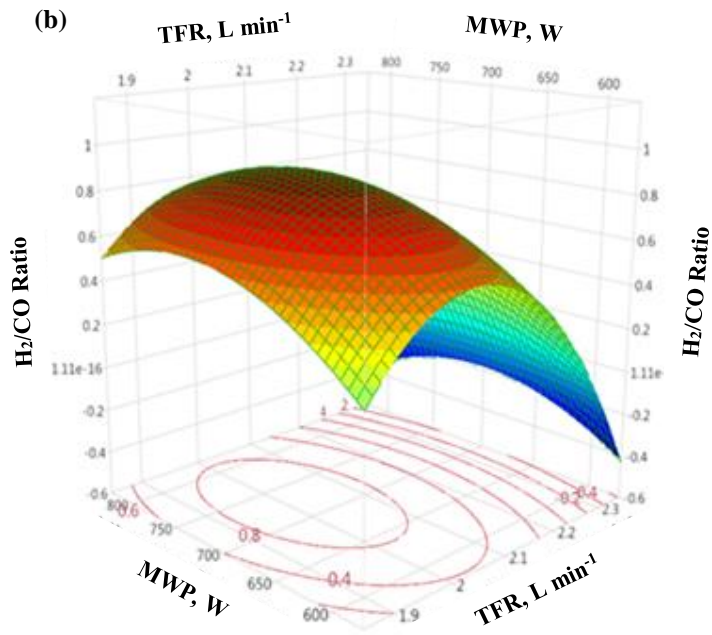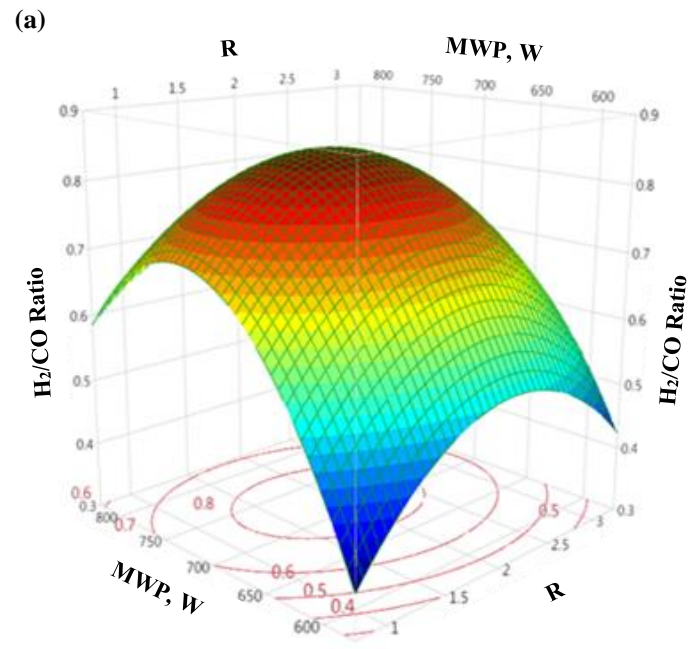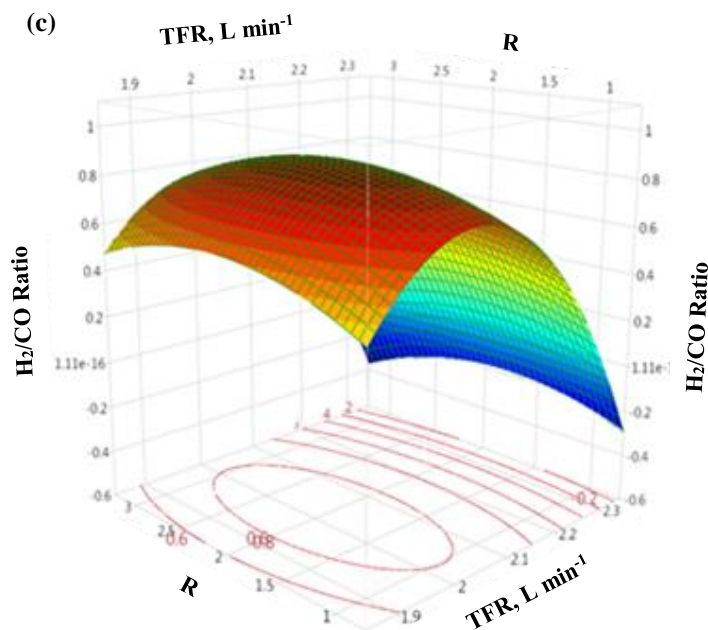
Figure 4. 8 Effect of MWP, R, and TFR and their interaction on H2/CO ratio [(3D surface plots; 2D projected contour plots (a, b, and c)]

As depicted in Figures 4.2 to 4.8 (a and c), CO_2 and CH_4 conversions, H_2 and CO selectivities and yields, and the H_2/CO ratio increased with increasing TFR from 1.9 to 2.07 L min^{-1} and then declined with increased TFR 2.07 to 2.3 L min^{-1}. The reason for this behaviour might be the residence time of the gas mixture molecules inside the microwave discharge zone (L. Li et al., 2017; Pakhare & Spivey, 2014; Serrano-Lotina & Daza, 2014; Timmermans et al., 1998), which increased with escalated TFR till reaching the highest value, and then started to decrease with increasing TFR. This is consistent with previous studies (Aziznia et al., 2012; Chung & Chang, 2016; Long et al., 2008; Pan, Chung, & Chang, 2014; Shapoval & Marotta, 2015; Xin Tu & Whitehead, 2014; Zeng et al., 2015; A.-J. Zhang et al., 2010).

Tables 4.2 to 4.8, respectively, indicate the F-values for the regression model for CO_2 conversion were 258.2387, 222.1336, and 125.0673; for CH_4 conversion were 227.1765, 235.3123, and 122.1232, for H_2 selectivity were 705.6088, 650.9213, and 558.4996, for CO selectivity were 373.9724, 322.1867, and 216.2902, for H_2 yield were 132.6222, 111.3258, and 117.0477; for CO yield were 158.3985, 110.0333, and 118.8612; and for H_2/CO ratio were 249.3176, 187.1415, and 94.6226, respectively. The results of the F-value suggest that the model is statistically significant and

represent the correlation between the input process factors and the plasma performance process. These results show that the regression model is adequate for the prediction and optimisation of the plasma H_2 and CO selectivities and yields.

4.3.3 Optimization and validation of models

Lastly, the optimum operating values of the independent parameters for the syngas production process were determined, and the fitting ability models for predicting optimal values of responses were calculated. The desirability function (DF) method was used to prove the optimal approaches to multiple responses. In addition, DF values are dimensionless, and the scale of desirability function ranges between zero for unacceptable response values and one for a desirable response value (Ehrgott, 2005). The maximum desirable value of 0.93, and the optimal conditions of input MWP, R, and TFR were 700.02 W, 1.99, and 2.07 L min^{-1}, respectively. Under these conditions, the predicted responses of CO_2 and CH_4 conversions, H_2 and CO selectivities and yield, and H_2/CO ratio were 46.77%, 83.12 %, 52.78%, 57.35%, 38.41%, and 30.72 %, and 0.9, respectively.

A separate experiment was conducted in triplicate to validate the accuracy of the current optimisation analysis through the optimum values of MWP, R, and TFR. As shown in Table 4.9, the experimental response values are in good agreement with the predicted response values. These values confirm the validity of the second-order polynomial model equations applied in the current study. A higher agreement was observed for CO_2 and CH_4 conversions values with an error of around 4% and CO selectivity, H_2 yield, and H_2/CO Ratio values have an error of around 3.5% compared to the H_2 selectivity and CO yield values having an error of 5.03% and 6.60%, respectively (Table 4.9).

Table 4. 9 Comparison between the experimental and predicted data at optimum conditions

Optimum condition	Response [%]	Experimental Data [%]	Predicted Data [%] (Equations (4.3 to 4.9))	Error [%]
MWP = 700.24 [W] R = 1.99 [-] TFR = 2.07 [L min^{-1}]	CO_2 Conversion	44.82	46.77	4.16
	CH_4 Conversion	79.35	82.68	4.02
	H_2 Selectivity	50.12	52.78	5.03
	CO Selectivity	58.42	56.36	3.52
	H_2 Yield	39.77	38.35	3.57
	CO Yield	32.89	30.72	6.60
	H_2/CO Ratio [-]	0.86	0.83	3.48

4.4 Conclusion

The response of syngas production to different levels of CO_2, CH_4 conversions, H_2, CO selectivities, and yields, and the H_2/CO ratio has been successfully evaluated by using DoE. Response factors consist of MWP, R, and TFR. The optimisation was based on an MWP range of 600–800 W, R range of 1–3, and TFR range of 1.9–2.3. BBD and RSM have been applied to discern the nature of the synergies among MWP, R, and TFR. The analysis reveals that all three parameters (MWP, R, and TFR) were found to have significant impacts on the conversions of CO_2 and CH_4, selectivities and yields of H_2 and CO, and H_2/CO ratio, respectively. However, for MWP and TFR, the most important factors were CO_2 and CH_4 conversions, H_2 selectivity, and H_2/CO ratio, followed by R. While for CO selectivity and H_2 and CO yields, R had a greater impact than other factors, followed by MWP and TFR. In addition, MWP-R has a significant impact on the H_2 selectivity, while the MWP-TFR and R-TFR had a weak significant on the CO_2 and CH_4 conversions, H_2 and CO selectivities and yields, and H_2/CO ratio, respectively. The quadratic term coefficients of MWP, R, and TFR had a significant impact on the CO_2 and CH_4 conversions, H_2 and CO selectivities and yields, and H_2/CO ratio, respectively. The predicted optimal conditions of MWP, R, and TFR were 700 W, 2/1, and 2.1 L min^{-1}, respectively. Under these conditions, the experimental responses of CO_2 and CH_4 conversions, H_2 and CO selectivities and yields, and H_2/CO ratio were 44.82%, 79.35%, 50.12%, 58.42%, 39.77%, 32.89, and 0.86, respectively. This was confirmed through experimental validation. The

conversions of CO_2 and CH_4, selectivities and yields of H_2 and CO, and H_2/CO ratio were well described by quadratic models developed using BBD according to multiple linear regression analysis of the outputs, with ANOVA analysis confirming the relative importance of the different parameters. Optimising and balancing the MWP, R, and TFR appear to be critical in achieving higher CO_2 and CH_4 conversions, H_2 and CO selectivities and yields, and H_2/CO ratio.

5

Chapter 5: Optimization and modelling of Feed Flow Rate for the Dry Reforming of Methane by a Microwave Plasma Technique Using a Box-Behnken Design

5.1 Introduction

The optimization of the reaction parameters has been executed by using multivariate statistic techniques (Kwak, 2005). DoE studies have increased lately to find the optimum value for the process fewer experiments (Montgomery, 2017). RSM is based on many mathematical and statistical techniques that fit a polynomial equation which depends on the experimental data (Challiwala et al., 2017). However, to the best of authors' knowledge, a limit reports have been found so far using DoE method to optimize the plasma chemical reactions in the microwave technique such as H_2/CO ratio. Therefore, the present work aims to investigate and optimise the effect of the feed gas flow rate upon the CO_2, CH_4 conversions, the selectivities, the yields of H_2 and CO, and the H_2/CO molar ratio. This study also explores and discusses the impact of different process parameters and their interaction on plasma stability and syngas production via DRM microwave plasma technology.

5.2 Experimental Work
5.2.1 Experimental design

In this study, the microwave plasma system fundamentally consists of a gas cylinders, mass flow controllers, gas mixer, feed gas system, steam vapour unit, plasma reactor, microwave generator, and gas chromatographic (GC-MSD and GC-TCD) analysis system. Further details about the experimental design and the calculation methodology can be found elsewhere in Chapter 3.

5.2.2 Approximate Model Function

The RSM is a set of mathematical and statistical tool that is helpful for the modelling and analysis of problems (Montgomery, 2017). RSM refers to a function of independent parameters as described in Equation 5-1 (Ramachandran et al., 2011):

$$y = f(x_1, x_2, x_3, \ldots., xi) \tag{5-1}$$

Where y is the response variable, f is the response function, and x_1, x_2, …, x_i is the independent input parameters. RSM is a very beneficial and helpful method for controlling experimental variables and to optimize the operating parameters with as little errors as possible (Sidik et al., 2016). The relationship between the independent parameters and the response surface is essential because it gives the real functional relationship. Additionally, the second-order model is used in the RMS (Abbasi et al., 2017).

In this study, three factors in the three-level BBD were utilized to investigate the interaction impact among these factors on the performance process of CO_2 and CH_4 conversions, H_2 and CO selectivities and yields and the ratio of H_2/CO. In this work, the flow rates of CH_4 (x_1), CO_2 (x_2), and N_2 (x_3) have been identified as the three independent variables affecting the conversions of CH_4, CO_2, the selectivities and yields of H_2, CO and, the H_2/CO ratio. Therefore, they were selected as the input parameters for the BBD, while conversions of CH_4 (Y_1), CO_2 (Y_2), selectivities of H_2 (Y_3) and CO (Y_4), yields of H_2 (Y_5) and CO (Y_6) and H_2/CO ratio (Y_7) are identified as responses. Each variable contains on the three different levels, which are coded as a low (-1), centre (0) and high (+1), as shown in Table 5.1.

Table 5. 1 Experimental range and levels of the independent input variables in the Box-Behnken design

Independent Variables	Symbols	Level and Range		
		Low [-1]	Centre [0]	High [+1]
CH_4 [L/min.]	x_1	0.1	0.2	0.3
CO_2 [L/min.]	x_2	0.2	0.4	0.6
N_2 [L/min.]	x_3	1.4	1.5	1.6

The BBD, the regression (quadratic) model describes the relationship between the input process variables and each response. The quadratic model used to predict the optimal values is presented by Equation (4-2) chapter 4.

Analysis of variance (ANOVA) is used to estimate the indication of adequacy and modelling fitting. Response surfaces were generated by JMP statistical discovery™ software from SAS (version 13.1.0), which was used in the regression analysis and to plot the contour and 3D surface figures. The multiple coefficients of determination

(R^2) values were found by the variance of variables and identified the interaction between the parameters within the particular experimental boundary conditions. The interaction between parameters was obtained by using the model equation to determine the optimum response values.

5.3 Results and Discussion
5.3.1 Analysis of Multiple Regressions

Fifteen experimental samples were selected randomly for the BBD, including triplicate experimental runs, as shown in Table 5-2. The real relationships between the input and output values are presented in eight equations based on the DoE analysis. The CH_4 and CO_2 (Y_1 and Y_2), the selectivity of H_2 and CO (Y_3, Y_4), the yield of H_2 and CO (Y_5, Y_6) and the ratio of H_2/CO (Y_7) are presented in Equations (5-2 to 5-8).

$$Y_1 = 77.80 + 6.41x_1 - 32.32x_2 + 2.63x_3 + 0.64x_1x_2 + 7.13x_1x_3 - 0.91x_2x_3 - 9.84x_1^2 - 36.08x_2^2 - 8.93x_3^2 \tag{5-2}$$

$$Y_2 = 43.38 - 2.43x_1 - 12.19x_2 - 0.84x_3 + 1.28x_1x_2 - 0.32x_1x_3 - 0.85x_2x_3 - 4.35x_1^2 - 25.54x_2^2 - 6.94x_3^2 \tag{5-3}$$

$$Y_3 = 48.78 + 0.58x_1 - 16.24x_2 + 0.26x_3 + 0.107x_1x_2 + 1.005x_1x_3 - 0.38x_2x_3 - 5.03x_1^2 - 25.75x_2^2 - 8.54x_3^2 \tag{5-4}$$

$$Y_4 = 57.35 + 0.23x_1 - 21.1x_2 + 0.05x_3 + 0.02x_1x_2 + 0.28x_1x_3 - 0.38x_2x_3 - 6.05x_1^2 - 29.09x_2^2 - 8.26x_3^2 \tag{5-5}$$

$$Y_5 = 37.524 + 1.31125x_1 - 10.26375x_2 + 0.0125x_3 - 07875x_1x_2 + 0.925x_1x_3 + 0.16x_2x_3 - 9.190708x_1^2 - 19.94071x_2^2 - 5.448208x_3^2 \tag{5-6}$$

$$Y_6 = 29.5034 - 0.7575x_1 - 6.37375x_2 - 0.44875x_3 + 0.4275x_1x_2 - 1.3975x_1x_3 + 0.61x_2x_3 - 6.691667x_1^2 - 15.41917x_2^2 - 8.729167x_3^2 \tag{5-7}$$

$$Y_7 = 0.65 - 0.1125x_1 - 0.26875x_2 + 0.0075x_3 + 0.015x_1x_2 - 0.0025x_1x_3 - 0.0025x_2x_3 - 0.045x_1^2 - 0.335x_2^2 - 0.0475x_3^2 \tag{5-8}$$

ANOVAs were used to determine the significance and adequacy of the quadratic models (Tables 5.3 to 5.9). The coefficient of determination (R^2) of the regression equations for the process parameters (conversions of CH_4 and CO_2) and process

performances (selectivities and yields of H_2, CO, and H_2/CO ratio) were 0.97, 0.99, 0.98, 0.98, 0.99, 0.98 and 0.99, respectively. The relationship between the variables and responses is described by the second-order equation, and this shows a good agreement between the experimental and predicted values because R^2 is close to 1, as shown in Figure 5.1. These results indicate that the quadratic models are statistically significant also able to predict and optimize the CH_4, CO_2 conversions, selectivities, and yields of H_2, CO, and H_2/CO ratio, as shown in Figure 5.1.

5.3.2 Effects of Plasma Process Parameters on DRM Process
5.3.2.1 CH_4 and CO_2 Conversions

The coefficient (β), standard error (ST), the squares sum (SS), the degree of freedom (*DF*), f-values and p-values are created by ANOVA, as presented in Table 5.3. The importance of this factor is indicated by its f-value and the p-value, which gives the level of significance of the parameter. The influence is considered significant on the performance of process if the p-value of a term (individual parameter x_i or interaction of two parameters x_ix_j) is below 0.05, while it is not significant if the p-value is above 0.05.

For the CH_4, CO_2 conversions, the variable x_2 is an identified as a significant factors (p<0.005), while the variables x_1 and x_3 are not significant (p>0.005), as shown in Tables 5.3 and 5.4. The Tables 5.3 and 5.4 were showed that the interactions of CH_4-CO_2, CH_4-N_2, and CO_2-N_2 have a very weak effect on CH_4, CO_2 conversions. Also, the quadratic term coefficients of x_1^2, x_2^2, and x_3^2 are as a significant on the CH_4, CO_2 conversions, as shown in Tables 5.3 and 5.4. These results suggest that the term of CO_2 is the most significant impact on conversions of CH_4 and CO_2, followed by CH_4 and N_2.

Table 5. 2 Actual values of the independent variables with the experimental and predicted values in the Box-Behnken Design

Run order	Actual Values			Response Values, CH_4 Conversion [%]		Response Values, CO_2 Conversion [%]		Response Values, H_2 Selectivity [%]		Response Values, CO Selectivity [%]	
	X_1	X_2	X_3	[d]Experimental of CH_4 Conversion	Predicated of CH_4 Conversion	[d]Experimental of CO_2 Conversion	Predicted of CO_2 Conversion	[d]Experimental of H_2 Selec.	Predicted of H_2 Selec.	[d]Experimental of CO Selec.	Predicted of CO Selec.
1[a]	0.2	0.4	1.5	70.21	72.36	38.65	40.35	43.61	45.36	51.75	53.33
2[b]	0.2	0.4	1.5	72.10	71.54	40.71	41.65	45.88	44.19	53.92	53.01
3	0.1	0.4	1.6	39.77	44.74	32.69	31.63	30.75	31.49	39.04	39.58
4	0.1	0.2	1.5	60.49	54.33	27.47	27.35	33.67	31.39	41.33	40.07
5	0.2	0.2	1.6	62.68	63.85	18.69	19.89	27.64	29.16	37.91	38.62
6	0.3	0.2	1.5	58.09	65.07	22.71	20.43	33.27	32.28	41.26	40.46
7	0.2	0.6	1.6	0	-2.01	0	-1.21	0	-1.73	0	-1.33
8	0.1	0.4	1.4	44.94	53.11	33.67	32.62	32.35	32.88	40.11	40.01
9	0.2	0.6	1.4	0	-1.17	0	-1.21	0	-1.52	0	-0.71
10	0.3	0.4	1.6	68.81	69.94	25.41	26.48	34.99	34.46	40.47	40.55
11[c]	0.2	0.4	1.5	73.79	72.48	41.68	40.89	46.61	45.73	54.33	52.78
12	0.1	0.6	1.5	0	-6.98	0	-2.27	0	-0.98	0	-0.79
13	0.2	0.2	1.4	59.27	57.24	21.85	23.05	26.23	27.98	36.47	37.81
14	0.3	0.6	1.5	0	-6.14	0	0.13	0	2.27	0	1.26
15	0.3	0.4	1.4	56.74	51.77	27.59	30.83	32.85	34.52	40.46	42.92

[a-c]**Replicated experimental runs (Run order 1, 2, and 11); [d]Responses are shown as the means of three replicates with a standard deviation**

Continued to Table 5.2

Run order	Actual Values			Response Values, CH_4 Conversion [%]		Response Values, CO_2 Conversion [%]		Response Values, N_2 Conversion [%]	
	X_1	X_2	X_3	[d]Experimental of H_2 Yield	Predicated of H_2 Yield	[d]Experimental of CO Yield	Predicted of CO Yield	[d]Experimental of H_2/CO Ratio	Predicted of H_2/CO Ratio
1[a]	0.2	0.4	1.5	39.77	37.52	32.89	29.51	0.86	0.84
2[b]	0.2	0.4	1.5	35.08	34.36	26.77	28.95	0.82	0.83
3	0.1	0.4	1.6	20.31	20.66	16.28	15.78	0.54	0.55
4	0.1	0.2	1.5	15.21	16.55	15.64	14.95	0.64	0.61
5	0.2	0.2	1.6	23.95	22.25	9.49	10.67	0.52	0.54
6	0.3	0.2	1.5	18.36	20.75	13.93	12.58	0.61	0.58
7	0.2	0.6	1.6	0	2.04	0	-0.85	0	-0.03
8	0.1	0.4	1.4	21.79	22.48	14.06	13.89	0.53	0.55
9	0.2	0.6	1.4	0	1.69	0	-1.18	0	-0.02
10	0.3	0.4	1.6	25.83	25.13	11.31	11.47	0.53	0.52
11[c]	0.2	0.4	1.5	37.71	36.93	28.85	27.29	0.84	0.85
12	0.1	0.6	1.5	0	-2.39	0	1.34	0	0.02
13	0.2	0.2	1.4	24.59	22.54	11.93	12.78	0.51	0.54
14	0.3	0.6	1.5	0	-1.34	0	0.68	0	0.03
15	0.3	0.4	1.4	23.61	23.25	14.68	15.17	0.56	0.55

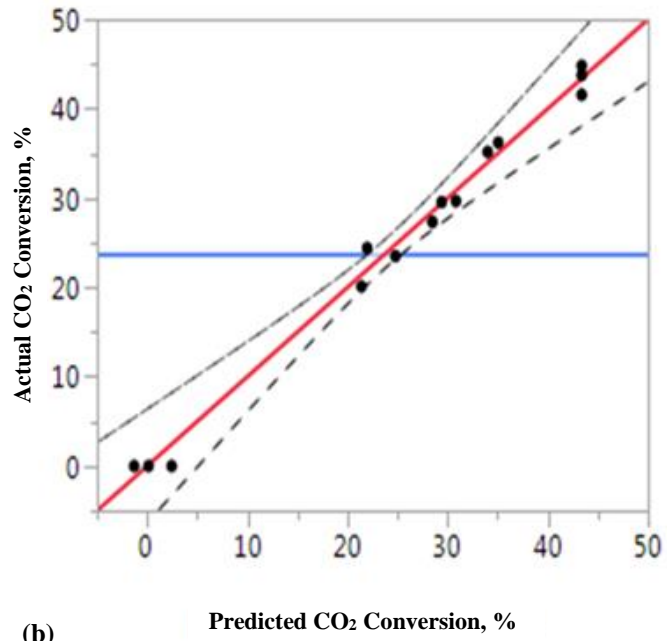[a-c]**Replicated experimental runs (Run order 1, 2, and 11); [d]Responses are shown as the means of three replicates with a standard deviation**

(a)

Predicted CO₂ Conversion, %

(b)

Predicted CH₄ Conversion, %

(c)

Predicted H₂ Selectivity, %

(d)

Predicted CO Selectivity, %

(e)

Predicted H₂ Yield, %

(f)

Predicted CO Yield, %

(g)
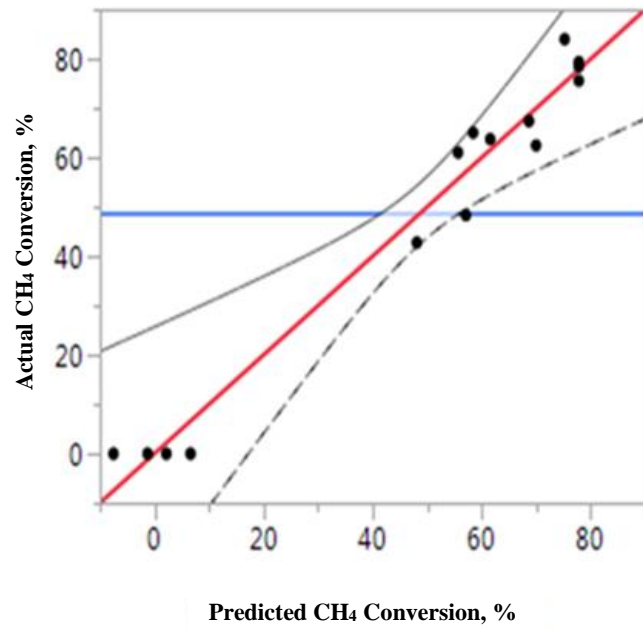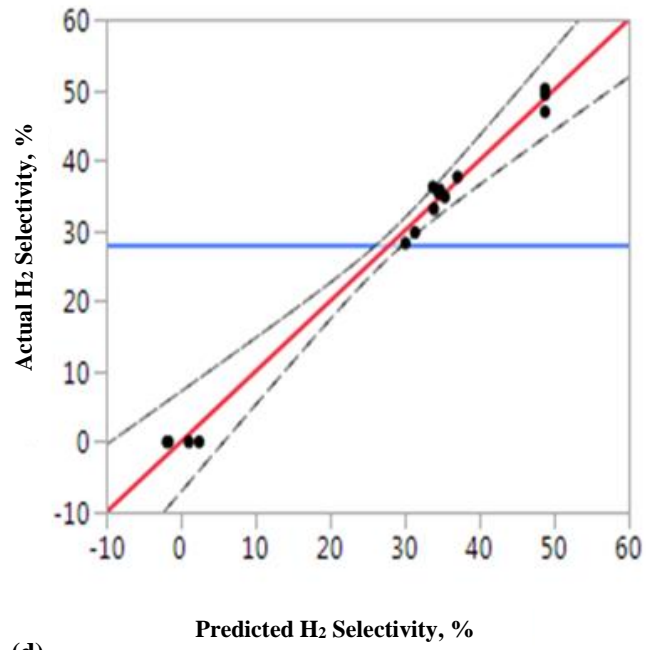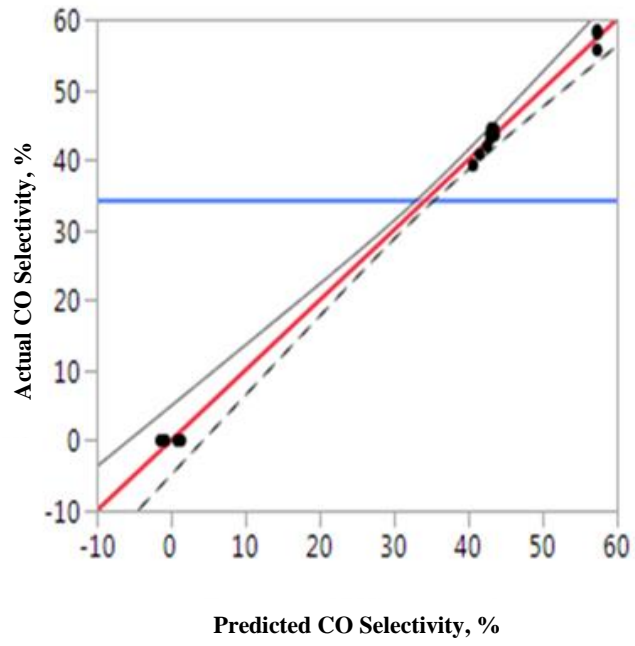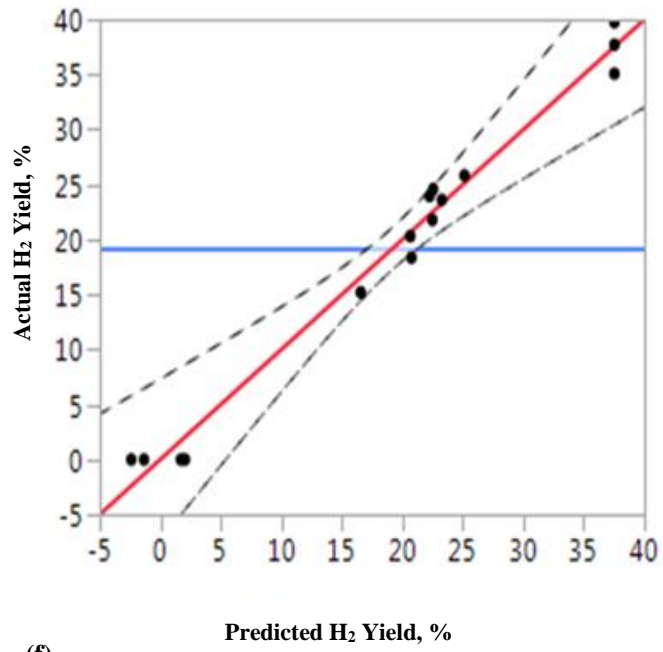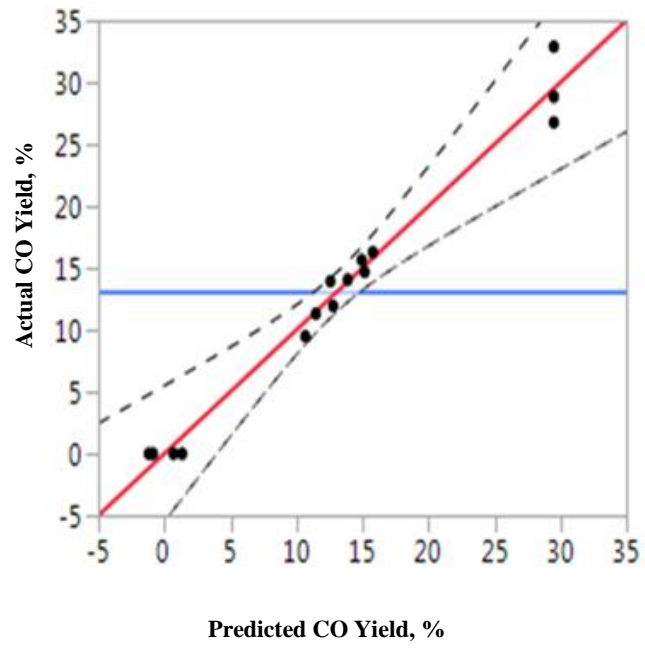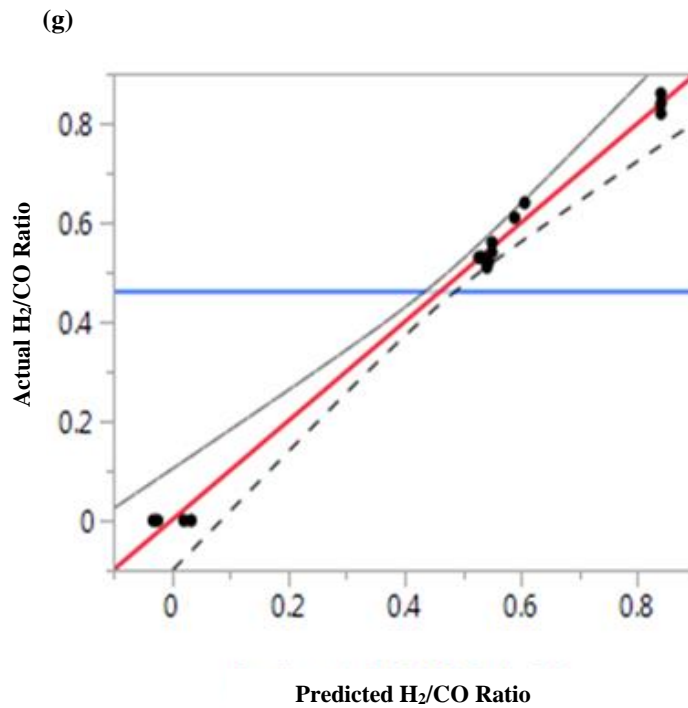
Figure 5. 1 Comparison between experimental and predicted values of (a) CO_2 conversion; (b) CH_4 conversion; (c) H_2 selectivity; (d) CO selectivity; (e) H_2 yield; (f) CO yield; (g) H_2/CO ratio [(.) experimental values, (–) confidence bands, (–) fit line, Equations (5-1 to 5-7), (–) mean of the Y leverage residuals]

The reason for that it has the highest f-value among the CH_4 and CO_2 conversions that are 96.78 and 200.87, as shown in Tables 5.3 and 5.4. The 3D response surface and 2D contour lines are based on Equations 5-2 and 5-3 plots in Figures 5.2, and 5.3 (a to f), respectively with one independent factor kept at a constant level (coded zero levels), while the other two factors were changed within the experimental ranges.

Table 5. 3 ANOVA results for the quadratic regression model of CH_4 conversion

Model Terms	β^a	SE^b	SS^c	DF^d	F-Value	P-Value
Intercept	77.806667	5.366206	-	-	-	-
X_1	6.41625	3.286116	329.3461	1	3.8124	0.1083
X_2	-32.32875	3.286116	8361.1846	1	96.7859	<.0001[*]
X_3	2.635	3.286116	55.5458	1	0.6430	0.4590
$X_1 X_2$	0.645	4.64727	1.6641	1	0.0193	0.8950
$X_1 X_3$	7.1375	4.64727	203.7756	1	2.3588	0.1852
$X_2 X_3$	-0.9175	4.64727	3.3672	1	0.0390	0.8513
X_1^2	-9.845833	4.837032	357.9339	1	4.1433	0.0974[*]
X_2^2	-36.08583	4.837032	4808.0764	1	55.6564	0.0007[*]
X_3^2	-8.938333	4.837032	294.9925	1	3.4147	0.1239[*]

R^2, 0.97; [a]Coefficient; [b]Standard error; [c]Sum of Squares; [d]Degrees of freedom; f-values and p-values

Table 5. 4 ANOVA results for the quadratic regression model of CO_2 conversion

Model Terms	β^a	SE^b	SS^c	DF^d	F-Value	P-Value
Intercept	43.386667	1.404953	-	-	-	-
X_1	-2.4375	0.860354	47.5312	1	8.0267	0.0365
X_2	-12.19375	0.860354	1189.5003	1	200.8722	<.0001[*]
X_3	-0.84875	0.860354	5.7630	1	0.9732	0.3692
$X_1 X_2$	1.2825	1.216725	6.5792	1	1.1110	0.3401
$X_1 X_3$	-0.3225	1.216725	0.4160	1	0.0703	0.8015
$X_2 X_3$	0.85	1.216725	2.8900	1	0.4880	0.5160
X_1^2	-4.353333	1.266407	69.9748	1	11.8167	0.0185[*]
X_2^2	-25.54583	1.266407	1109.5616	1	106.9052	<.0001[*]
X_3^2	-6.940833	1.266407	177.8775	1	30.0384	0.0028[*]

R^2, 0.99; [a]Coefficient; [b]Standard error; [c]Sum of Squares; [d]Degrees of freedom; f-values and p-values

These figures show the effects of CH_4, CO_2 and N_2 feed flow rates on CH_4 and CO_2 conversions at a CO_2:CH_4 ratio of 2:1 and the microwave power at 700 W. Figures 5.2 and 5.3 (a, b, and c) show that the responses enhanced as corresponding factors (flow rate of CH_4, CO_2, and N_2) peaked, and after that, they decreased when it (the corresponding factor) increased to more than 0.19, 0.38 and 1.49 L min^{-1}, respectively. Figures 5.2 and 5.3 (a, b, and c) indicate that the CH_4 and CO_2 conversion increased rapidly when the CH_4, CO_2, and N_2 flow rates ranged from 0.1 to 0.19, 0.2 to 0.38 and

1.4 to 1.49 L min^{-1}, respectively, and then declined when the flow rate increased to higher than 0.19, 0.38 and 1.49 L min^{-1}, respectively. The reason for this behavior was explained previously in chapter 4. In this work, we observed the amount of water formed and the amount of solid carbon powder (according to Equations 2-1 to 2-4, chapter 2) out the quartz tube of the microwave plasma reactor.

Maximum CH_4 and CO_2 conversions of 84.91% and 44.40% were achieved at the highest gas feed flow rates of 0.19, 0.38 and 1.49 L min^{-1} for CH_4, CO_2, and N_2, respectively. The conversion of CH_4 and CO_2 decreased with increasing the feed flow rates for CH_4, CO_2 and N_2 from 0.05 to 0.19, 0.1 to 0.38 and 0.3 to 1.49 L min^{-1}, respectively. The reason for this was explain before in chapter 4, as plotted in Figures 5.2 and 5.3 (a, b, and c). These results indicate that the interactions of the conversion of CH_4 (0.1083, 0.4590, 0.8950, 0.1852 and 0.8513) as shown in Table 5.3 i.e., the terms x_1, x_3, x_1x_2, x_1x_3 and x_2x_3 are not significant. Likewise, the interaction of the two parameters on the plasma process is not considered significant on the CO_2 conversion as shown by the high p-values (0.0365, 0.3692, 0.3401, 0.8015 and 0.5160) of the terms x_1, x_3, x_1x_2, x_1x_3, and x_2x_3, respectively, as listed in Tables 5.4.

(a)
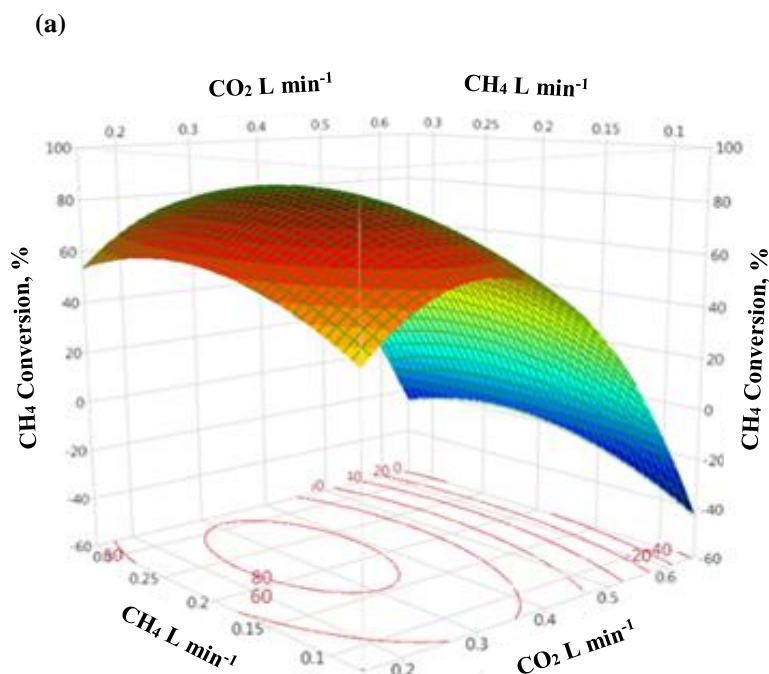
(b)
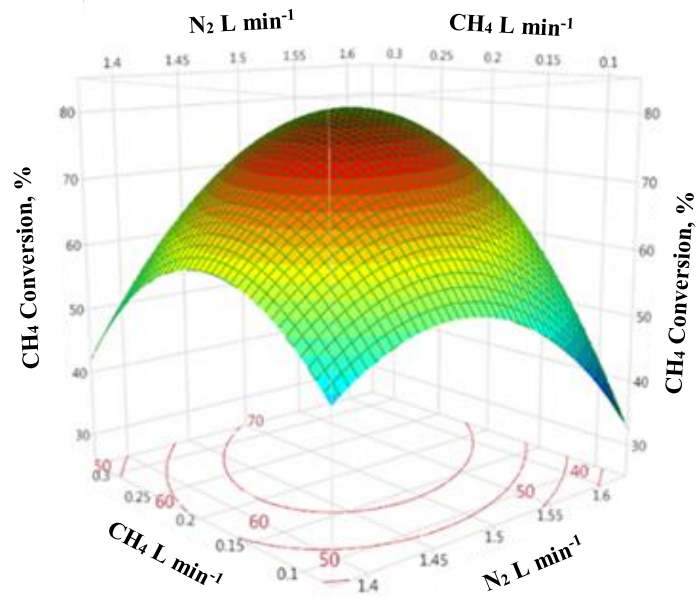
(c)
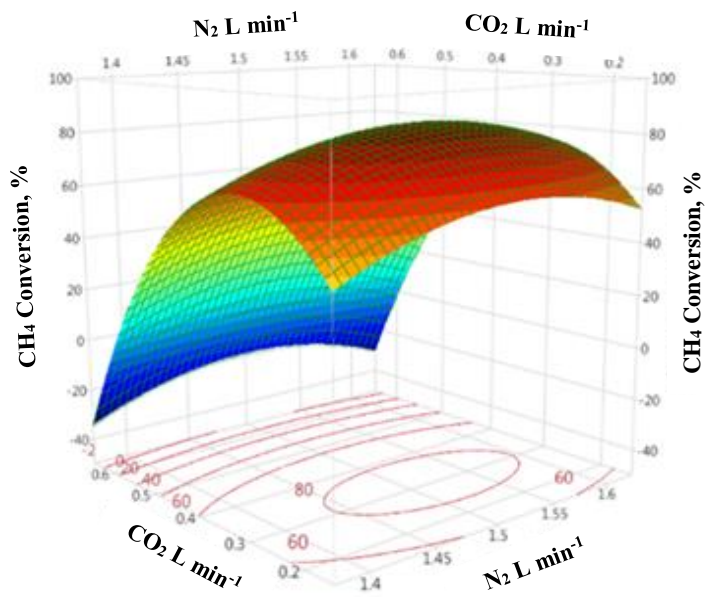
Figure 5. 2 Effect of feed gas flow rates and their interaction on CH_4 conversion at a $CO_2:CH_4$ ratio of 2:1 and microwave plasma of 700 W [3D surface plots; 2D projected contour plots (a, b, and c)]

(a)
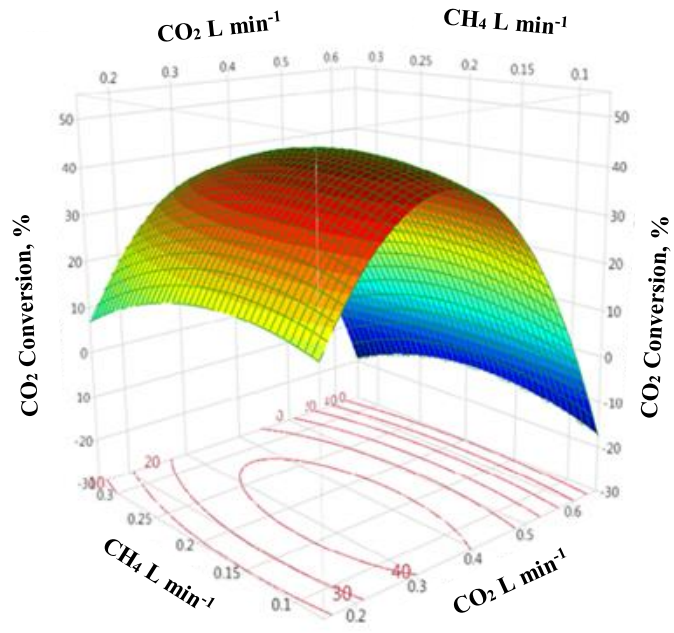
(b)
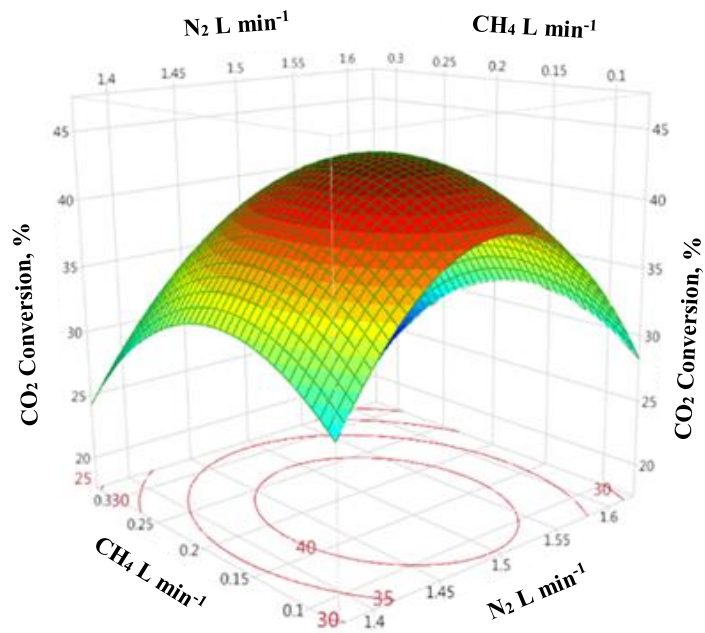
(c)
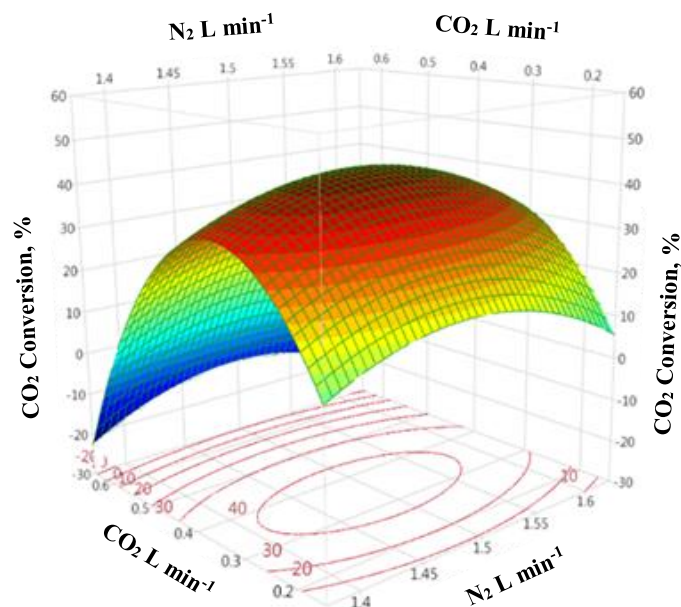
Figure 5. 3 Effect of feed gas flow rates and their interaction on CO_2 conversion at a $CO_2:CH_4$ ratio of 2:1 and microwave plasma of 700 W [3D surface plots; 2D projected contour plots (a, b, and c)]

5.3.2.2 H_2 and CO Selectivities

The ANOVA analysis is performed to determine the significance and adequacy of the progression models, as shown in Tables 5.5 and 5.6. In H_2 and CO selectivities, the term of x_2 is an identified as significant, while the terms x_1 and x_3 are not considered significant. As shown in Tables 5.5 and 5.6, the interactions of CH_4-CO_2, CH_4-N_2, and CO_2-N_2 have a very weak effect on H_2, CO selectivities. The quadratic term coefficients of x_1^2, x_2^2, and x_3^2 are significant on the H_2 and CO selectivities, as shown in Tables 5.5 and 5.6. These results indicate that the CO_2 term is more important, followed by CH_4 and N_2 in term of selectivities of H_2 and CO, as shown in Tables 5.5 and 5.6. The CO_2 flow rate has the highest F-value while it is 307.7060 and 1141.848 for H_2 and CO respectively, so it has reflected the most significant effect on selectivities of H_2 and CO, as shown in Tables 5.5 and 5.6.

The highest H_2 and CO selectivities of 51.31% and 61.17% were achieved at the optimal gas feed flow rate of CH_4 (0.19 L min^{-1}), CO_2 (0.38 L min^{-1}) and N_2 (1.49 L min^{-1}), respectively. The effect of different factors and their interaction on selectivities

of H_2 and CO are shown by the 3D response surface plots and 2D contour lines and represented by Equations 5-4 and 5-5, as shown in Figures 5.4 and 5.5 (a, b, and c). The selectivities of H_2 and CO decreased with increasing the feed flow rates for CH_4, CO_2 and N_2 from 0.05 to 0.19, 0.1 to 0.38 and 0.3 to 1.49 L min^{-1}, respectively, as shown in Figures 5.4 and 5.5 (a, b, and c). The reason for this behavior has been explained in detail previously in chapter 4. This behavior is similar to that reported previously (Allah & Whitehead, 2015; Hwang et al., 2010; Indarto et al., 2006; Long et al., 2008; Rieks, Bellinghausen, Kockmann, & Mleczko, 2015; Sun et al., 2012; Tao et al., 2008; Yan Xu et al., 2013); these studies have shown that the conversions of CH_4 and CO_2, selectivities and yields of H_2 and CO were decreased with increasing gas feed flow rates. The interactions between the two parameters on the selectivities of H_2 and CO are not considered significant as illustrated in Tables 5.5 and 5.6 respectively. This was confirmed when high p-values (p-values for x_1, x_3, x_1x_2, x_1x_3, and x_2x_3) for H_2 and CO selectivity were obtained. It was 0.5561, 0.7881, 0.9378, 0.4774 and 0.7833 for H_2 and 0.7263, 0.9378, 0.9828, 0.7579 and 0.6810 for CO.

Table 5. 5 ANOVA result for the quadratic regression model of H_2 selectivity

Model Terms	β^a	SE^b	SS^c	DF^d	*F*-Value	*P*-Value
Intercept	48.783333	1.511944	-	-	-	-
X_1	0.58375	0.925873	2.7261	1	0.3975	0.5561
X_2	-16.24125	0.925873	2110.2256	1	307.7060	<.0001*
X_3	0.2625	0.925873	0.5513	1	0.0804	0.7881
$X_1 X_2$	0.1075	1.309382	0.0462	1	0.0067	0.9378
$X_1 X_3$	1.005	1.309382	4.0401	1	0.5891	0.4774
$X_2 X_3$	-0.38	1.309382	0.5776	1	0.0842	0.7833
X_1^2	-5.032917	1.362848	93.5271	1	13.6378	0.0141*
X_2^2	-25.75292	1.362848	1448.7854	1	257.0736	<.0001*
X_3^2	-8.545417	1.362848	269.6276	1	39.3162	0.0015*

R^2, 0.98; [a]Coefficient; [b]Standard error; [c]Sum of Squares; [d]Degrees of freedom; f-values and p-values

Table 5. 6 ANOVA result for the quadratic regression model of CO selectivity

Model Terms	β^a	SE^b	SS^c	DF^d	F-Value	P-Value
Intercept	57.35	1.019677	-	-	-	-
X_1	0.23125	0.624422	0.4278	1	0.1372	0.7263
X_2	-21.1	0.624422	3561.6800	1	1141.848	<.0001*
X_3	0.05125	0.624422	0.0210	1	0.0067	0.9378
$X_1 X_2$	0.02	0.883066	0.0016	1	0.0005	0.9828
$X_1 X_3$	0.2875	0.883066	0.3306	1	0.1060	0.7579
$X_2 X_3$	-0.385	0.883066	0.5929	1	0.1901	0.6810
X_1^2	-6.05375	0.919125	135.3153	1	43.3811	0.0012*
X_2^2	-29.09125	0.919125	3124.8031	1	1001.788	<.0001*
X_3^2	-8.26375	0.919125	252.1461	1	80.8361	0.0003*

R^2, 0.98; [a]Coefficient; [b]Standard error; [c]Sum of Squares; [d]Degrees of freedom; f-values and p-values

(a)

(b)

(c)
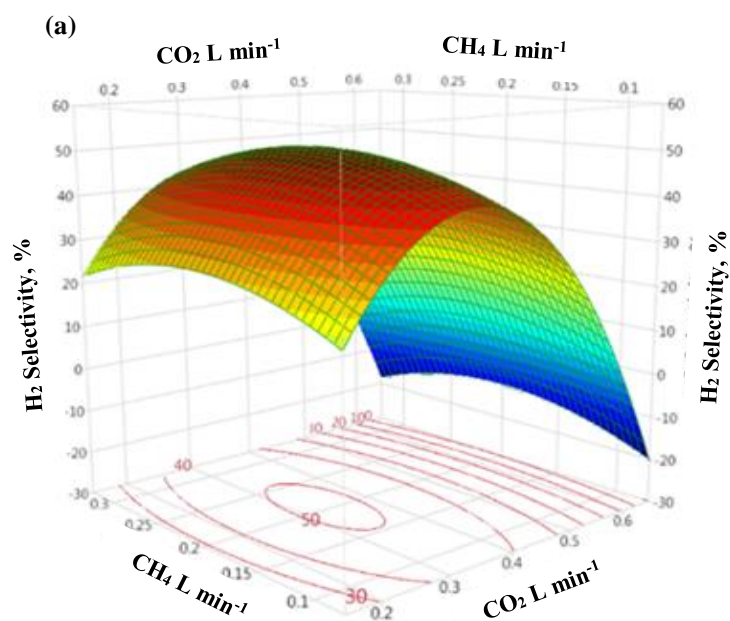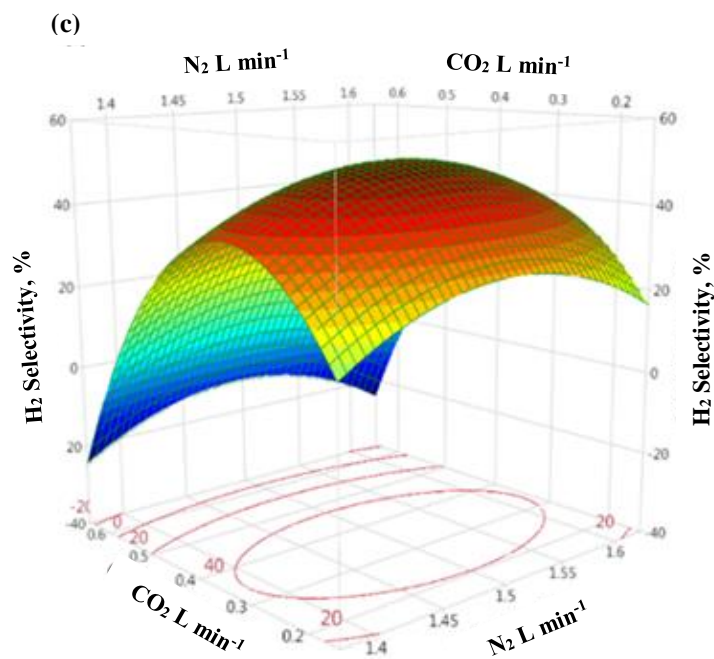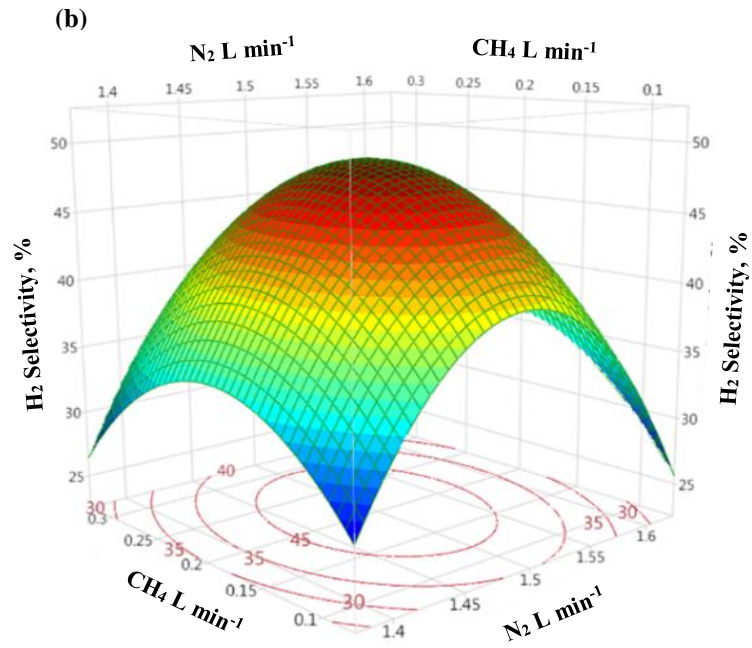
Figure 5. 4 Effect of feed gas flow rates and their interaction on H_2 selectivity at a CO_2/CH_4 ratio of 2:1 and microwave plasma of 700 W [3D surface plots; 2D projected contour plots (a, b, and c)]

(a)

(a)

(b)

(c)
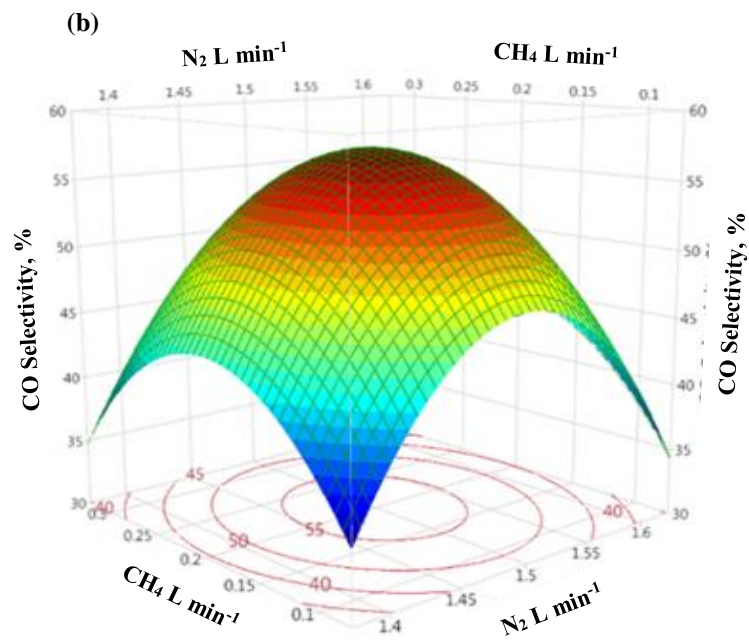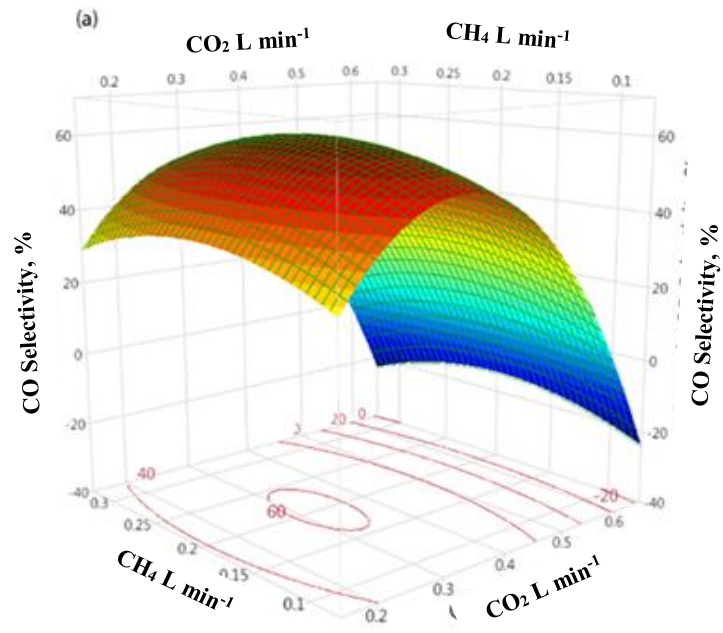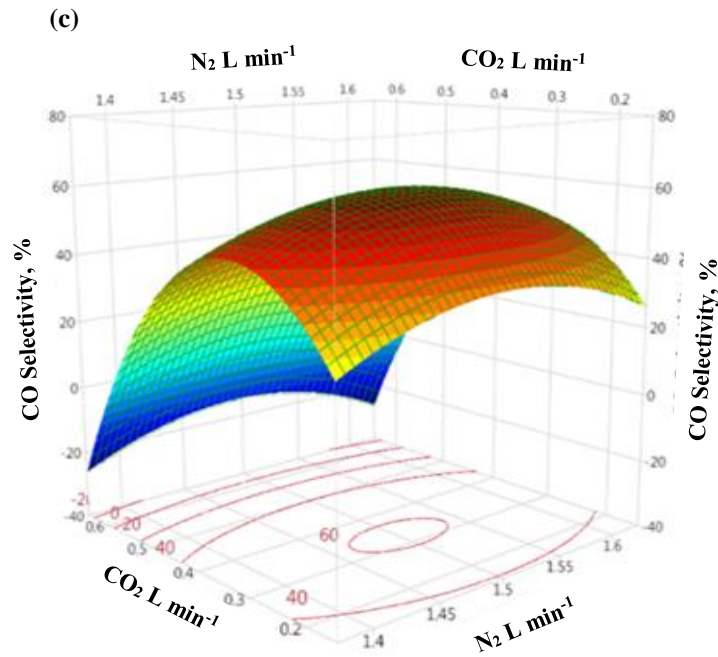
Figure 5. 5 Effect of feed gas flow rates and their interaction on CO selectivity at a CO_2/CH_4 ratio of 2:1 and microwave plasma of 700 W [3D surface plots; 2D projected contour plots (a, b, and c)]

5.3.2.3 H_2 and CO Yields

Tables 5.7 and 5.8, present the ANOVA results for the quadratic model. In the H_2 and CO yields, the effect of x_2 is a significant, while the terms x_1, x_3, are not considered significant. Tables 5.7 and 5.8 show that the interactions of CH_4-CO_2, CH_4-N_2, and CO_2-N_2 have a very weak effect on H_2 and CO yields. The quadratic term coefficients of x_1^2, x_2^2, and x_3^2 are as a significant on the H_2 and CO yields, as shown in Tables 5.7 and 5.8. According to these results, CO_2 effect is more significant compared with other variables, followed by CH_4 and N_2. As Tables 5.7 and 5.8, respectively indicate, the F-value for the regression model of H_2 and CO yields are 101.57, and 56.52, which suggests that both models are statistically significant and represent the correlation between the input process parameters and the performance of the plasma process. These results show that both regression models are statistically significant and adequate for the prediction and optimization of the plasma H_2 and CO yields.

Table 5. 7 ANOVA result for the quadratic regression model of H_2 yield

Model Terms	β^a	SE^b	SS^c	DF^d	F-Value	P-Value
Intercept	37.524	1.66	-	-	-	-
X_1	1.311	1.01	13.75	1	1.65	0.25
X_2	-10.26	1.01	842.75	1	101.57	0.0002*
X_3	0.01	1.01	0.001	1	0.0002	0.9907
$X_1 X_2$	-0.78	1.43	2.48	1	0.29	0.6080
$X_1 X_3$	0.92	1.46	3.42	1	0.41	0.5490
$X_2 X_3$	0.16	1.44	0.10	1	0.01	0.9159
X_1^2	-9.19	1.48	311.88	1	37.59	0.0017*
X_2^2	-19.94	1.5	1468.17	1	76.95	<.0001*
X_3^2	-5.44	1.49	109.59	1	13.20	0.0150*

R^2, 0.99; [a]Coefficient; [b]Standard error; [c]Sum of Squares; [d]Degrees of freedom; f-values and p-values

Table 5. 8 ANOVA result for the quadratic regression model of CO yield

Model Terms	β^a	SE^b	SS^c	DF^d	F-Value	P-Value
Intercept	29.5	1.38	-	-	-	-
X_1	-0.75	0.83	4.59	1	0.79	0.41
X_2	-6.37	0.85	324.99	1	56.52	0.0007*
X_3	-0.44	0.84	1.61	1	0.28	0.6192
$X_1 X_2$	0.42	1.19	0.73	1	0.12	0.7360
$X_1 X_3$	-1.39	1.12	7.81	1	1.35	0.2963
$X_2 X_3$	0.61	1.19	1.48	1	0.25	0.6326
X_1^2	-6.69	1.26	165.33	1	28.75	0.0030*
X_2^2	-15.41	1.24	877.84	1	52.67	<.0001*
X_3^2	-8.72	1.25	281.34	1	48.93	0.0009*

R^2, 0.98; [a]Coefficient; [b]Standard error; [c]Sum of Squares; [d]Degrees of freedom; f-values and p-values

A maximum H_2 and CO yields of 37.52% and 29.50%, respectively are achieved at the highest feed flow rates for CH_4, CO_2, and N_2 of 0.19, 0.38 and 1.49 L min^{-1}, as shown in Figures 5.6 and 5.7 (a, b, and c). The three-dimension response surface and two dimension contour lines base on Equations 5-6 and 5-7 plots in Figures 5.6 and 5.7 (a, b, and c), respectively.

As showed in Figures 5.6 and 5.7 (a, b, and c), it can be seen that when the gas feed flow rate was increased the H_2 and CO yields decreased slightly as depicted in Figures 5.6 and 5.7 (a, b, and c). The reason for this behavior is explained in detail previously in chapter 4. The results show that the interaction between two variables does not significantly effect on the H_2 and CO yields, as shown with high p-values (0.25, 0.9907, 0.6080, 0.5490 and 0.9159) for H_2 and (0.41, 0.6192, 0.7360, 0.2963 and 0.6326) for CO, of the terms x_1, x_3, x_1x_2, x_1x_3 and x_2x_3, respectively, as listed in Tables 5.7 and 5.8, respectively.

(a)

(b)

(c)
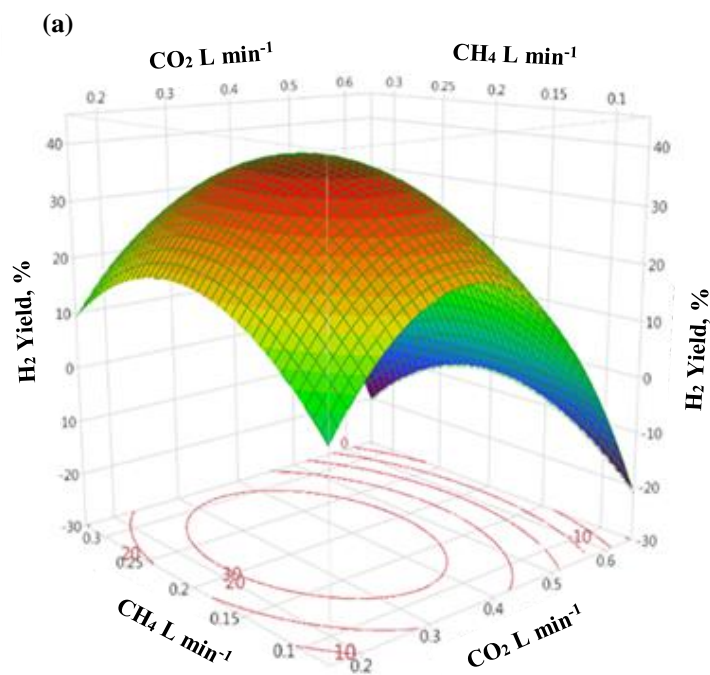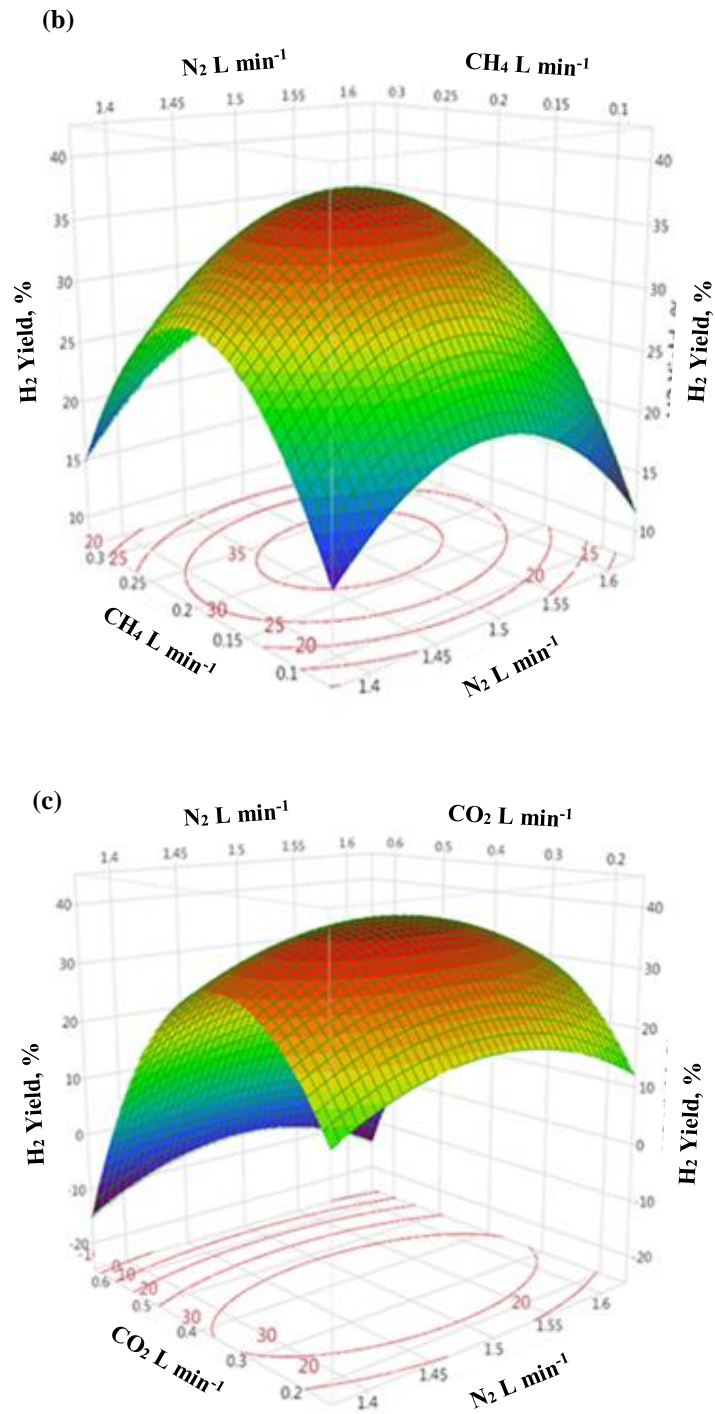
Figure 5. 6 Effect of feed gas flow rates and their interaction on H_2 yield at a CO_2/CH_4 ratio of 2:1 and microwave plasma of 700 W [3D surface plots; 2D projected contour plots (a, b, and c)]

(a)

(b)
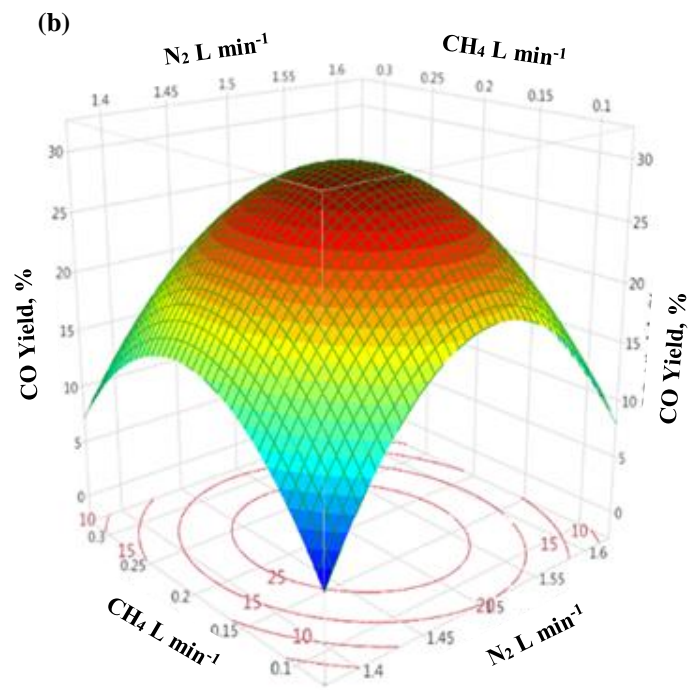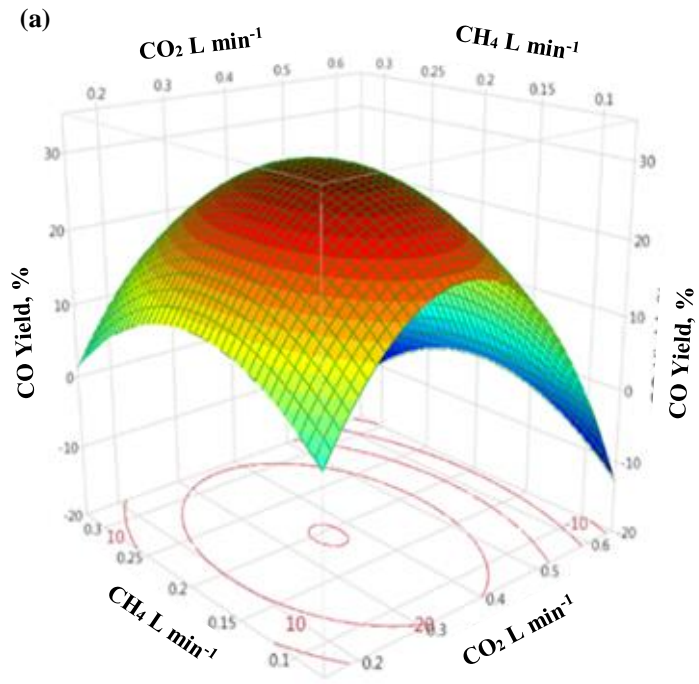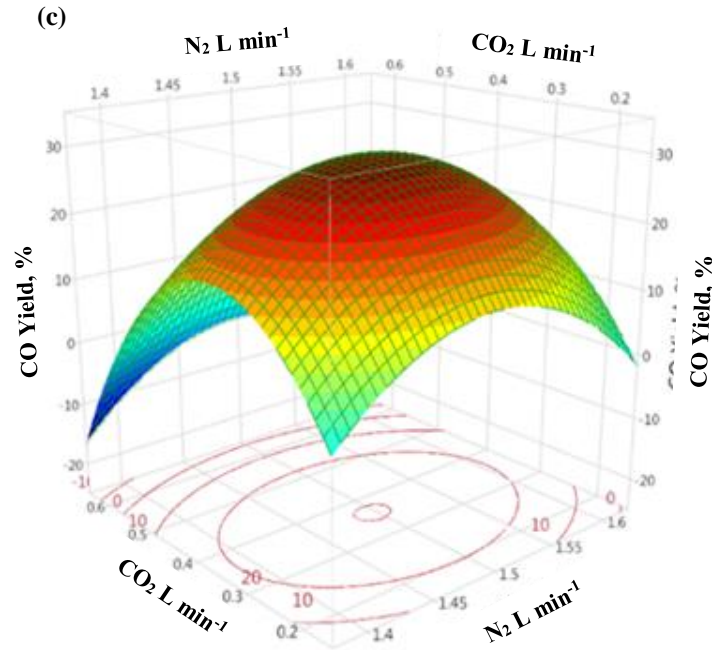
Figure 5. 7 Effect of feed gas flow rates and their interaction on CO yield at a CO_2/CH_4 ratio of 2:1 and microwave plasma of 700 W [3D surface plots; 2D projected contour plots (a, b, and c)]

5.3.2.4 H_2/CO Ratio

The results of the ANOVA analysis are showed in Table 5.9. The x_2 is a significant term ($P < 0.05$) with respect to its effect on the H_2/CO ratio, while x_1 and x_3 are the less significant term ($P > 0.05$), as shown in Table 5.9. It appears from Table 5.9 that, all the interactions of CH_4-CO_2, CH_4-N_2, and CO_2-N_2 have a very weak effect on H_2/CO ratio. The quadratic term coefficients of x_1^2, x_2^2, and x_3^2 are significant impact on the H_2/CO ratio, as illustrated in Tables 5.9. As shown in Table 5.9, the F-value is 383.92 for the H_2/CO molar ratio, and the high F-value gives the most significant parameter that effects on ratio of H_2/CO. The influence of feed gas flow rate parameters and their interactions on H_2/CO ratio is presented in Figure 5.8 (a, b, and c) by 3D response surface plots and 2D contour lines (based on Equation 5-8). The contour lines are plotted in Figure 5.8 (a, b, and c) show that x_2 strongly interact with the H_2/CO ratio due to the elliptical contour produced by the equation model. An optimum H_2/CO ratio of 0.7 was achieved at 0.19, 0.38 1.49 L min^{-1} of CH_4, CO_2, and N_2, respectively.

Table 5. 9 ANOVA result for the quadratic regression model of H_2/CO ratio

Model Terms	β^a	SE^b	SS^c	DF^d	F-Value	P-Value
Intercept	0.65	0.0223	-	-	-	-
X_1	-0.0112	0.013	0.0010	1	0.67	0.4494
X_2	-0.2687	0.013	0.5778	1	383.92	<.0001*
X_3	0.0075	0.013	0.0004	1	0.29	0.6080
$X_1 X_2$	0.015	0.019	0.0009	1	0.59	0.4743
$X_1 X_3$	-0.0025	0.019	0.00002	1	0.01	0.9025
$X_2 X_3$	-0.0025	0.019	0.00002	1	0.01	0.9025
X_1^2	-0.045	0.020	0.00747	1	4.96	0.0163*
X_2^2	-0.335	0.020	0.41436	1	275.32	<.0001*
X_3^2	-0.0475	0.020	0.00833	1	5.53	0.0053*

R^2, 0.99; [a]Coefficient; [b]Standard error; [c]Sum of Squares; [d]Degrees of freedom; f-values and p-values

In Figure 5.8 (a, b, and c), we find that the H_2/CO ratio decreased slightly with increasing the feed gas flow rates. Both effects of the reverse RWGS and reverse boudouard reactions (Equations 2-1 to 2-4, chapter 2) might contribute to the higher conversion of CH_4 and selectivity of CO with the lower conversion of CO_2 and selectivity of H_2. As shown in Table 5.9, the interaction between two parameters are not significant with respect to the effect on H_2/CO ratio according to the p-values (0.4494, 0.6080, 0.4743, 0.9025 and 0.9025) of x_1, x_3, x_1x_2, x_1x_3 and x_2x_3, respectively. According to the results, the CO_2 feed flow rate (x_2) is considered the most significant impact on H_2/CO ratio due to it has the highest F-value (Table 5.9).

(a)

(b)
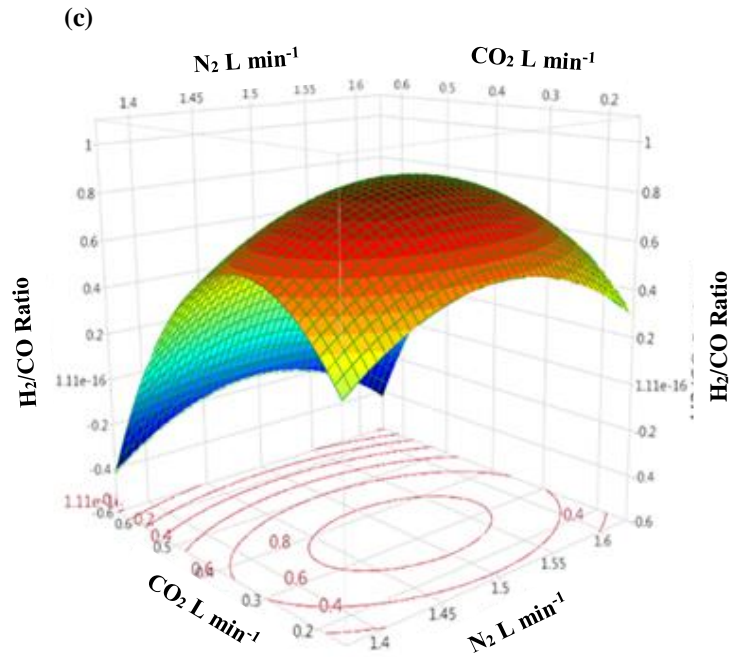
Figure 5. 8 Effect of feed gas flow rates and their interaction on the H_2/CO ratio at a CO_2/CH_4 ratio of 2:1 and microwave plasma of 700 W [3D surface plots; 2D projected contour plots (a, b, and c)]

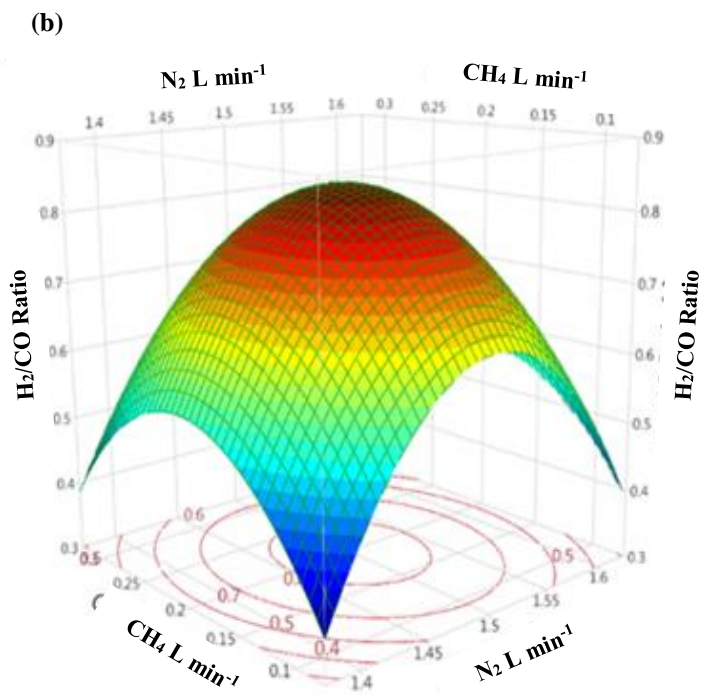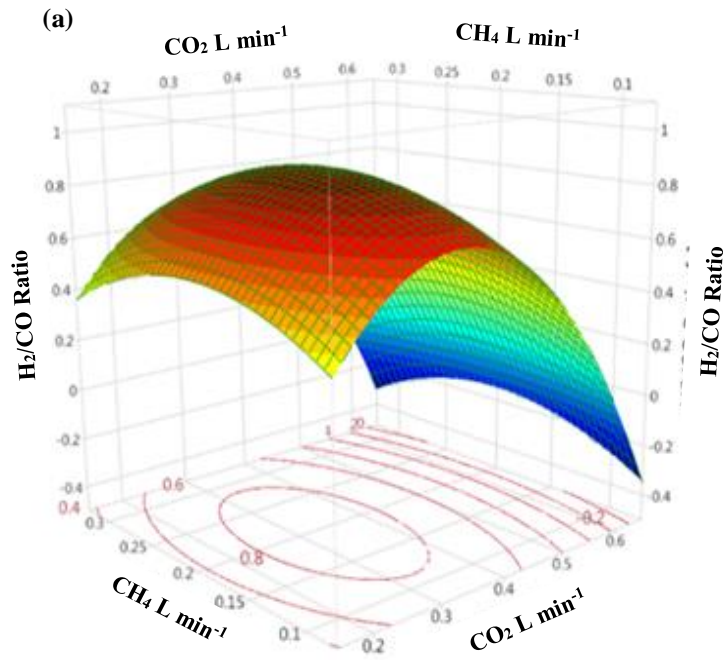## 5.3.3 Desirability and Optimum conditions

The optimum operating conditions were determined for several input variables, which led to obtaining the desired output response values. Desirability Function (DF) method is used to prove the optimal approaches to multiple responses. Also, the values of DF are dimensionless and ranged from zero to one (zero means the unacceptable response value while one represents gaining the goal) (Ehrgott, 2005).

In this research, the maximized desirability flow rates of CO_2, CH_4, and N_2 is 0.92. This value for the desirability gives strong support to the fitting model. The optimal experimental conditions were achieved at $CH_4 = 0.19$ L/min, $CO_2 = 0.38$ L/min and $N_2 = 1.49$ L/min, respectively. The validity of the equations of the model (Equations 5-3 to 5-9) is good with a reasonable error, as shown in Table 5.10.

Therefore, the balance between conversions (CH_4, CO_2), selectivities and yields (H_2, CO), and ratio of H_2/CO are important in the development of an active plasma process. Thus, the performance of the plasma process generally depends on a wide range of operating conditions and especially on the flow rates. It is necessary and fundamental

for optimizing the performance plasma process with multiple inputs and multiple responses. This study aims to optimize the plasma process variables (various parameters) that jointly optimize the CH_4 and CO_2 conversions, selectivities, and yields of H_2 and CO and H_2/CO ratio (various responses). Also, the present work aims to investigate the effect of these parameters and their interaction on plasma stability and syngas production via the DRM microwave plasma method.

Table 5. 10 Comparison between the experimental and predicted data at optimum conditions

Parameters [Lmin^{-1}]	Response [%]	Experimental Data [%]	Predicted Data [%] (Equations (5-3 to 5-9))	Error [%]
CH$_4$ = 0.19 CO$_2$ = 0.38 N$_2$ = 1.49	CH$_4$ Conversion	79.35	80.64	1.59
	CO$_2$ Conversion	44.82	43.15	3.72
	H$_2$ Selectivity	50.12	50.24	0.23
	CO Selectivity	58.42	57.33	1.86
	H$_2$ Yield	39.77	40.52	1.88
	CO Yield	32.89	32.37	1.58
	H$_2$/CO Ratio	0.86	0.85	1.16

Table 5.11 summarises the results of conversions, selectivities, yields, and syngas ratios results of the previous studies compared with those in this work. It has been demonstrated that this study obtained acceptable results amongst others. All previous works were done at different operating conditions, which are higher than those used in this study including the flow rates, CO_2/CH_4 ratios, and microwave power. In this research, the total feed flow rate of 2.04 L min^{-1}, CO_2/CH_4 ratio of 2/1 and microwave power of 700 W were used for producing microwave plasma with a good performance. The conversions of CH_4 and CO_2 were 84.91% and 44.40%, in sequence while the selectivities and yields of H_2 and CO and H_2/CO ratio were 51.31%, 61.17%, 37.52%, 29.50% and 0.7, respectively. Hwang et al. (2010) claimed that the highest selectivities could be achieved at a high feed flow rate and input power. Although they used an input power of 1000 W and a total flow rate of 20 L min^{-1} which were higher than those in the present work, however, the conversion in this study is greater than their conversion. Besides, Long et al. (2008) found that the conversions of CH_4 and CO_2, selectivities and yields of H_2 and CO and molar ratio of H_2/CO changed with increasing flow rates also the optimum flow rate and input power were 16.667 L min$^-$

[1] and 770 W respectively. However, as shown in Table 5.11, the present conversions were higher than their conversions.

Moreover, Y. N. Chun and Lim (2018) reported that the microwave discharge affected the stability of plasma and the process performance. It can be shown in Table 5.11, that their conversions of CH_4 and CO_2 at a low total flow rate (2.25 ml. min^{-1}) and high microwave energy (2000 W) were lower than the conversions of CH_4 and CO_2 in this study. Furthermore, Fidalgo and Menéndez (2012) investigated how the flow rate and microwave energy affected the CH_4 and CO_2 conversions, selectivities, and yields of H_2 and CO and H_2/CO ratio. They claimed that the maximum CH_4 and CO_2 conversions, the selectivities and yields of H_2 can be obtained at high total flow rate of 33.34 L min^{-1} and microwave power of 83000 W. Their results were higher than on present results although they used lower specific energy which was due to using a microwave laboratory pilot plant with CO_2 gas as the plasma generation gas. Eventually, S. M. Chun et al. (2017) pointed out that microwave power affected the plasma stability and performance of the process. They noticed that the CH_4 and CO_2 conversions, the H_2 and CO selectivities and yields, and H_2/CO ratio were improved at the total flow rate of 30 L min^{-1} and the high microwave power of 6000 W. They used feed flow rates and power higher than in this work but the results in term conversions, selectivities, yields, and syngas ratio were fairly close, as shown in Table 5.11. It seems that the results of this research are more reliable for the conversion of CO_2 and CH_4 and producing H_2 and CO with high selectivities, yields, and syngas ratio.

Table 5. 11 Comparison between previous studies with the current study

Production method	Feed Gas Flow Rate [L min^{-1}]			R [-]	TFR [L min^{-1}]	*Specific energy [kJ L^{-1}]	MWP [W]	Conversion [%]			Selectivity [%]		Yield [%]		H$_2$/CO Ratio [-]	Refs
	CO$_2$	CH$_4$	N$_2$					CH$_4$	CO$_2$	N$_2$	H$_2$	CO	H$_2$	CO		
Arc Jet Plasma (AJP)	2	2	16	1/1	20	0.00083	1000	50.74	35.55	-	80.98	78.31	-	-	0.5	Hwang et al. (2010)
Cold Plasma Jet (CPJ)	3.334	5	8.334	2/3	16.667	0.0008	770	45.68	34.03	-	78.11	85.41	36.17	33.81	-	(Long et al., 2008)
Microwave reformer	1.5	0.75	-	2/1	2.25	0.00148	2000	79.41	61.7	-	-	-	-	-	0.6	(Choi et al.)
Microwave pilot plant	16.67	16.67	-	1/1	33.34	0.00415	8300	88.13	93.36	-	75.37	69.72	-	-	1	(Fidalgo & Menéndez, 2012)
Microwave plasma torch	15	15	-	1/1	30	0.00334	6000	86.84	48.41	-	54.61	65.92	-	-	-	(S. M. Chun et al., 2017)
Microwave Plasma	0.38	0.17	1.49	2/1	2.04	0.00571	700	84.91	44.40	3.37	51.31	61.17	37.52	29.50	0.7	This study

5.4 Conclusion

The effect of the feed gas flow rates (CO_2, CH_4, and N_2) and their interactions on process performance to produce syngas (H_2 and CO) has been investigated by using a microwave plasma reactor at atmospheric pressure. The conversions of CH_4, CO_2, and N_2, selectivities and yields of H_2 and CO, and H_2/CO ratio were determined and optimized. The Behnken-Box design and response surface methodology have been used to determine the interactions of the feed flow rate variables in the dry reforming of methane technology. Regression models have been developed to describe the relationships between the feed flow rate variables and reaction performance (conversions, selectivities, yields, and H_2/CO ratio). ANOVAs were applied to estimate a significant interaction flow rates of CO_2 with CH_4 to produce H_2 and CO via the plasma process. The results show that the CO_2 and CH_4 conversion, selectivity, yield of H_2 and CO and molar ratio of H_2/CO decrease with the increasing the gas feed flow rate. The most significant effect on process parameters and process performances was the flow rate of CO_2, followed by CH_4 and N_2. Also, the interactions CH_4-CO_2, CH_2-N_2, and CO_2-N_2 had a very weak effect on the CH_4, CO_2 conversions, the H_2, CO selectivities, yields, and the H_2/CO ratio. The quadratic term coefficients of x_1^2, x_2^2, and x_3^2 are as significant with respect to their effect on the CO_2 and CH_4 conversion, selectivity, yield of H_2 and CO and molar ratio of H_2/CO. The optimum coefficient of determination (R^2) of the regression equations for the CH_4 and CO_2 conversion were 0.97 and 0.99, while those of the selectivity, yield of H_2 and CO and H_2/CO ratio were 0.99, 0.99, 0.89, 0.99 and 0.99, respectively. The optimal CH_4 and CO_2 conversions were 84.91% and 44.40%, the selectivity and yield of H_2 and CO and molar ratio of H_2/CO were 51.31%, 61.17%, 37.52%, 29.50% and 0.7, respectively. The optimal plasma condition was achieved when the gas feed flow rates of CH_4, CO_2, and N_2 were 0.19, 0.38, and 1.49 L min.$^{-1}$, respectively. The experimental results under the theoretical optimal conditions have explained the ability and reliability of the DoE for understanding the effect of process variables and their interaction on the process parameters and performances.

6

Chapter 6: Stability of Nitrogen-Plasma Dry Reforming of Methane in a Horizontal Microwave Irradiation Reactor

6.1 Introduction

Recently, the DRM technique is one of the most important modern technologies used to convert CO_2 and CH_4 to syngas (Equation 1-3, Chapter 1) (L. Li et al., 2017; Usman et al., 2015). Plasma technology has been used widely in the reforming of CH_4 process because it is considered the best method for a suitable conversion for CO_2 and CH_4 to produce syngas by microwave discharge (Snoeckx et al., 2015). In the presence of microwave irradiation, dissociative collisions of molecules occur, leading to the formation of reactive atoms, ionised gases, free electrons, and free positive and negative ions that activate the plasma-induced reaction (Eliasson & Kogelschatz, 1991; Ghorbanzadeh et al., 2005; Shapoval & Marotta, 2015; Tao et al., 2011; Thornton, 1983). As we mentioned previously in Chapters 1 and 2, there are many parameters affecting the plasma stability and syngas production such as MWP, R, TFR, and reaction time (RT). In this study, the effects of input parameters (N_2 feed flow rate, MWP, R, TFR, and RT) on the performance of processes such as conversions of CH_4 and CO_2, the product selectivities and yields of H_2 and CO, and H_2/CO ratio, were investigated at long-running times under microwave plasma at atmospheric pressure. The results could be important information for closing the knowledge gap of plasma stability, plasma condition and side reactions in the complex microwave plasma DRM reaction zone.

6.2 Experimental set up

The microwave plasma system consisted of gas cylinders, mass flow controllers, gas mixer, feed gas system, plasma reactor, microwave generator, and gas chromatographic (GC-MSD and GC-TCD) analysis system. The three feeding gases (CH_4, CO_2, and N_2) were controlled by an MFC (MFC Alicat Scientific, MCS-Series) and send into the gas mixer. Further details about the experimental design and the calculation methodology are presented in Chapter 3.

6.3 Results and Discussions
6.3.1 Effect of N_2 Feed Flow Rate

The effect of using N_2 as an inert gas on plasma stability and syngas production was investigated in this work under microwave-assisted plasma DRM. Figure 6.1(a–d) displays CO_2 and CH_4 conversions, H_2 and CO selectivities and yields, and H_2/CO ratio, respectively, as a function of N_2 flow rate between 0.3 and 1.5 L min^{-1}. These data were obtained at a constant microwave power of 700 W and constant CO_2 and CH_4 flow rates of 0.4 and 0.2 L min^{-1}, respectively (Table 3.2, Chapter 3). A five-fold increase in the N_2 flow rate from 0.3 to 1.5 L min^{-1} translates to a minor reduction in CO_2 and CH_4 conversions from 56.69 to 44.82% and from 88.01 to 79.35%, respectively, as shown in Figure 6.1(a). These trends reproduce the trends reported elsewhere and can be attributed to the reduction in the residence time of the gases in the microwave-exposed region (Yunpeng Xu et al., 2002). The reason for this behaviour is explained in detail previously in Chapter 4.

At the N_2 flow rate between 0.3 and 1.5 L min^{-1}, CH_4 conversion was always higher than CO_2 conversion. Such discrepancy can be attributed to the lower bond dissociation energy for CH_4 (4.5 eV) than that for CO_2 (5.5 eV) (Aziznia et al., 2012). H_2 and CO selectivities also decreased from 62.94 to 50.12% and from 70.43 to 58.42%, respectively, with an increase in N_2 flow rate from 0.3 to 1.5 L min^{-1}, as shown in Figure 6.1(b), agreeing with the reduction of the selectivities with increasing total gases flow rate observed by others (Chung & Chang, 2016; Shapoval & Marotta, 2015; Yunpeng Xu et al., 2002; Zeng et al., 2015; A.-J. Zhang et al., 2010). The decrease in H_2 and CO yields over the same flow rate region was more pronounced from 55.39 to 39.77% and from 47.26 to 32.89%, respectively, as shown in Figure 6.1(c).

The H_2/CO ratio decreases from 0.97 to 0.86 with increasing N_2 flow rate from 0.3 to 1.5 L min^{-1} (Figure 6.1(d)), as is observed elsewhere (Aziznia et al., 2012; Jiang et al., 2002; Moshrefi et al., 2013; Pan et al., 2014; Qi et al., 2006). Such a decrease may come from the production of additional CO (and H_2O) from RWGS reaction (Equation (2-2), Chapter 2) and reverse Boudouard reaction (Equation (2-3), Chapter 2). Water and carbon powder presence was observed at the end of DRM experiments.
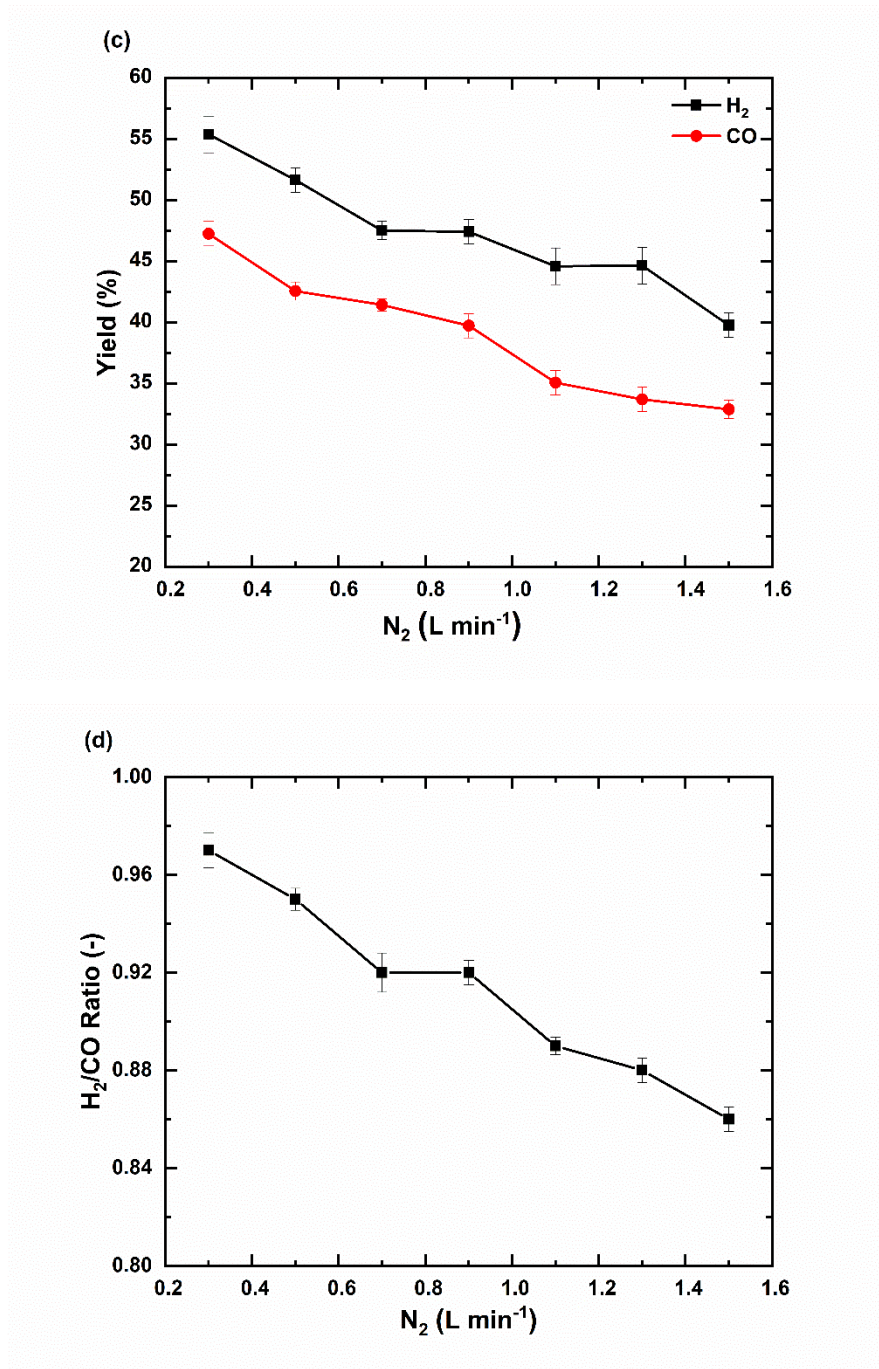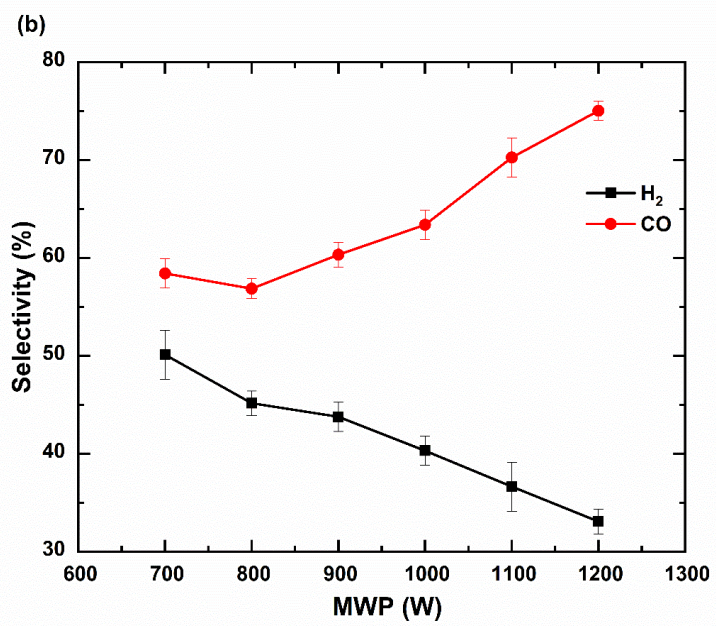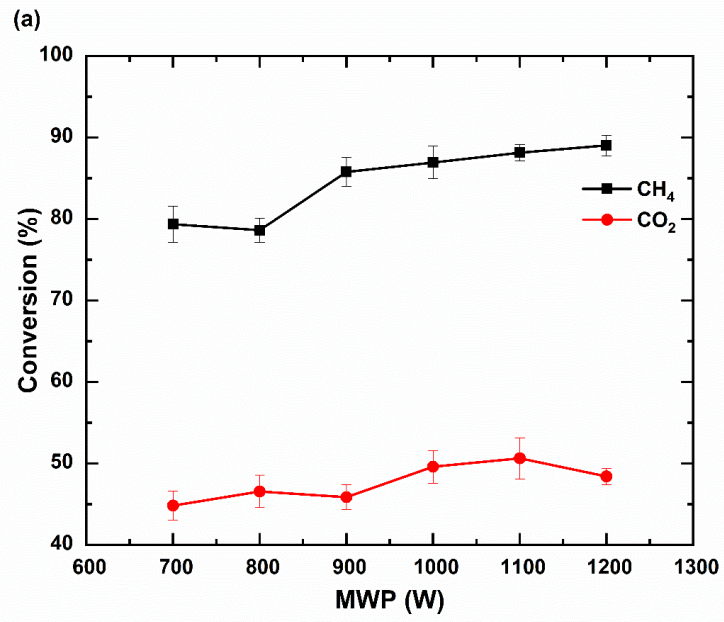
(a)

(b)
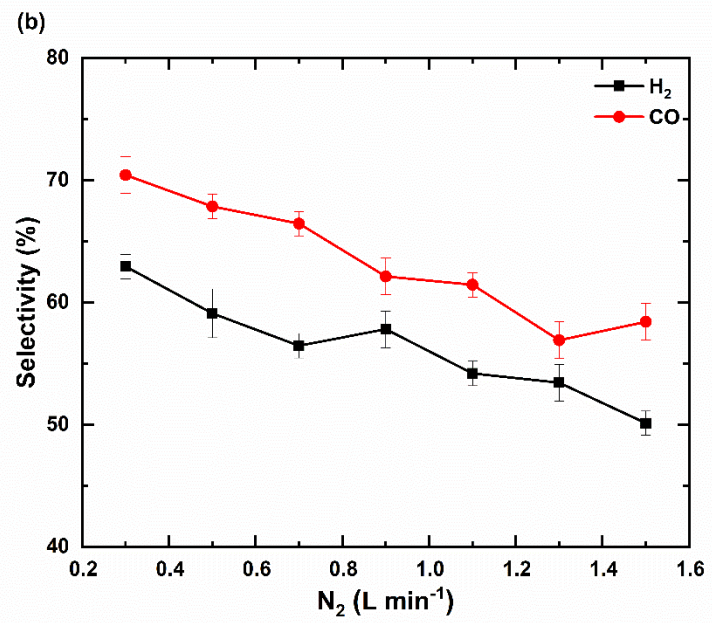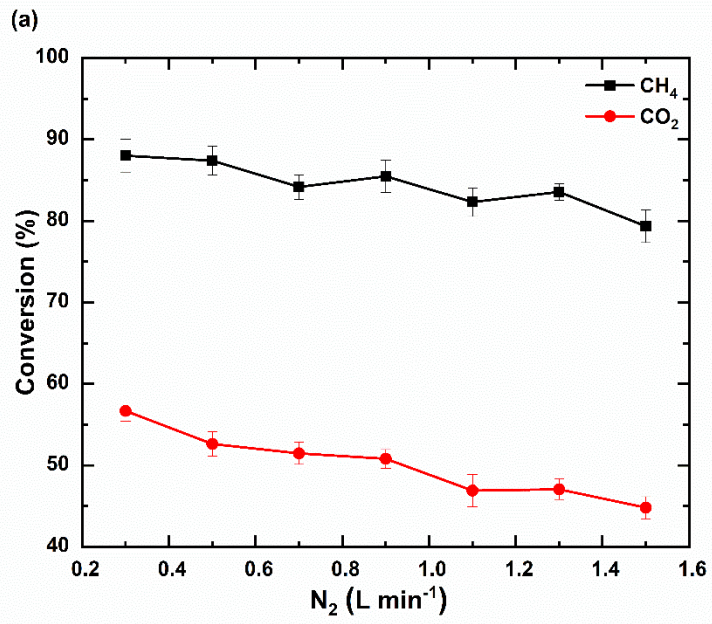
Figure 6. 1 Effect of N_2 feed flow rate on the microwave-assisted plasma DRM; (a) CH_4 and CO_2 Conversions; (b) H_2 and CO Selectivity; (c) H_2 and CO Yield; and (d) H_2/CO Ratio (R: 2/1; input MWP: 700 W)

6.3.2 Effect of Microwave Power

The input power is one of the most important factors affecting the stability of plasma and syngas production that was used for this experiment. Figure 2(a–d) shows CH_4 and CO_2 conversions, H_2 and CO selectivities, H_2 and CO yields, and H_2/CO ratio, respectively, as a function of MWP between 700 and 1200 W. These data were obtained at constant TFR of 2.1 L min^{-1} and R of 2/1 (Table 3.1, Chapter 3). An increase in MWP from 700 to 1200 W leads to a minor increase in CO_2 and CH_4 conversions from 44.82 to 48.41% and from 79.35 to 89.03% respectively, as shown in Figure 6.2(a). The reason for this behaviour has been explained previously in Chapter 4.

H_2 selectivity decreases from 50.12 to 33.08%, while CO selectivity increases from 58.42 to 75.04% with increased MWP from 700 to 1200 W (Figure 6.2(b)). Such behaviour has been observed in previous works and can be attributed to the higher dissociation energy of CO (11.1 eV) than H_2 (4.5 eV) as well as the possible subsequent reactions between CO_2 and H_2 to form H_2O via RWGS reaction (Equation (2-2), Chapter 2) and between CO_2 and C to form CO *via* reverse Boudouard reaction (Equation (2-3), Chapter 2) (Aziznia et al., 2012; Moshrefi et al., 2013). Likewise, H_2 yield decreases from 39.77 to 29.45%, while CO yield increases from 32.89 to 46.47% over the same MWP range increase, as shown in Figure 6.2(c). Water and carbon powder presence was again observed at the end of DRM.

Decreasing H_2 yield accompanied by increasing CO yield over an increase in MWP from 700 to 1200 W translates to the significant reduction in H_2/CO ratio from 0.86 to 0.44 also observed by others (Figure 6.2(d)) (Aziznia et al., 2012; Jiang et al., 2002; Moshrefi et al., 2013; Qi et al., 2006). Because MWP increase affects marginally CO_2 and CH_4 conversions and significantly affects H_2 and CO selectivities, low microwave power is desirable to maintain balanced H_2 and CO selectivities.
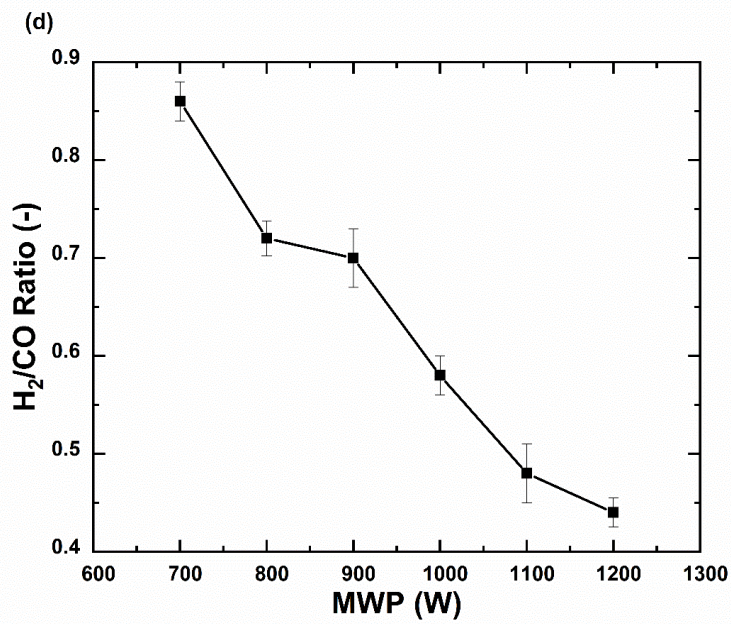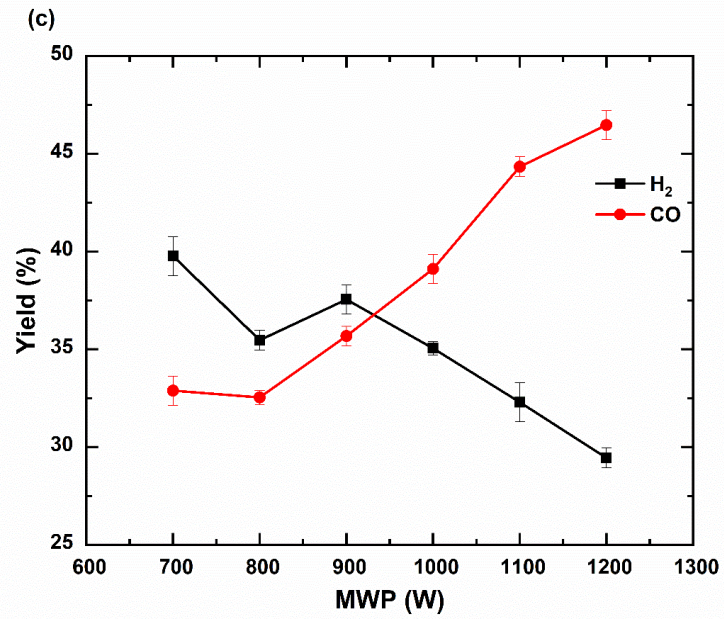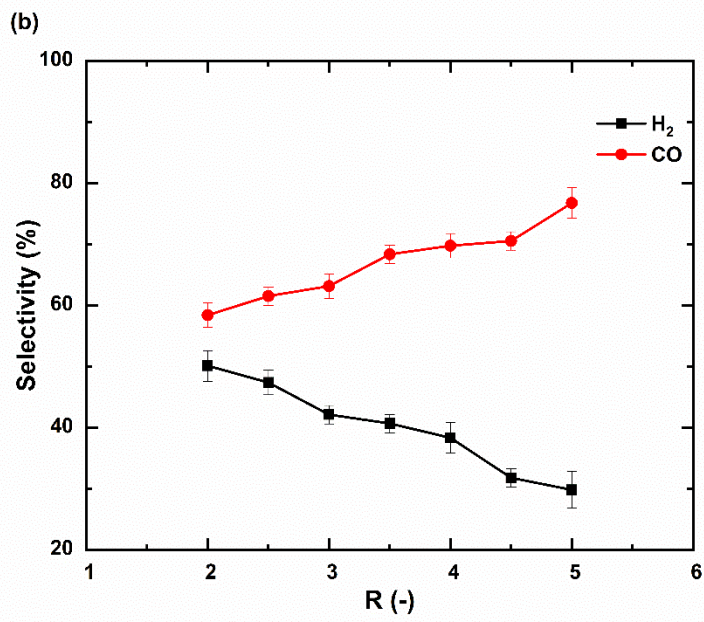
(a)

(b)

Figure 6. 2 Effect of MWP on the microwave-assisted plasma DRM (a) CH_4 and CO_2 Conversions; (b) H_2 and CO Selectivity; (c) H_2 and CO Yield; and (d) H_2/CO Ratio (R: 2/1; TFR: 2.1 L min^{-1})

6.3.3 Effect of CO_2/CH_4 Ratio

For a better understanding of the feed composition on the stability of plasma and syngas production, test series with varying R from 2/1 to 5/1 in the feed gas at MWP of 700 W was performed. Figure 6.3(a–d) shows CO_2 and CH_4 conversions, H_2 and CO selectivities and yields, and H_2/CO ratio, respectively, as a function of R inlet supply ratio between 2 and 5. These data were obtained for a change of CO_2 flow rate from 0.4 to 1 L min^{-1}, constant MWP of 700 W, and constant CH_4 and N_2 flow rates of 0.2 and 1.5 L min^{-1} (Table 3.1, Chapter 3). With an increase in R from 2 to 5, CH_4 conversion increases from 79.35 to 96.31%, and CO_2 conversion decreases from 44.82 to 21.18%, as shown in Figure 6.3(a). Such trends mirror the trends observed in other DRM studies (Serrano-Lotina & Daza, 2014; Shapoval & Marotta, 2015; Yunpeng Xu et al., 2002). The decrease in CO_2 conversion happened because the main reaction of CH_4 and CO_2 under microwave plasma at atmospheric pressure was the dry reforming reaction (Equation (1-3, Chapter 1)) when the CO_2 amount exceeds the reaction stoichiometry of the main reaction, the conversion of CO_2 decreases while the conversion of CH_4 increases (Serrano-Lotina & Daza, 2014; Yunpeng Xu et al., 2002). H_2 selectivity decreases from 50.12 to 29.83% while CO selectivity increases from 58.42 to 76.77% with an increase in R from 2 to 5 (Figure 6.3(b)). Increase in CO selectivity comes mainly from increasing the amount of CO_2 reactant, favouring the production of CO product via DRM reaction (Equation (1-3, Chapter 1)) as is observed in other works (Khoja et al., 2017; A. Wu et al., 2014; Yunpeng Xu et al., 2002; X. Zhu, Li, Liu, Li, & Zhu, 2014). H_2 and CO yields nonetheless decreased from 39.77 to 28.72% and from 32.89 to 25.85% over the increase in the same R region, as shown in Figure 6.3(c). As shown in Figure 6.3(d), increasing R from 2 to 5 also decreases H_2/CO ratio from 0.86 to 0.36, agreeing with the results by others (Serrano-Lotina & Daza, 2014; Zeng et al., 2015). The increasing amount of CO_2 in the reactor favours the formation of water *via* RWGS (Equation (2-2, Chapter 2)). Water was clearly present at the reactor tube at the end of the DRM reaction.
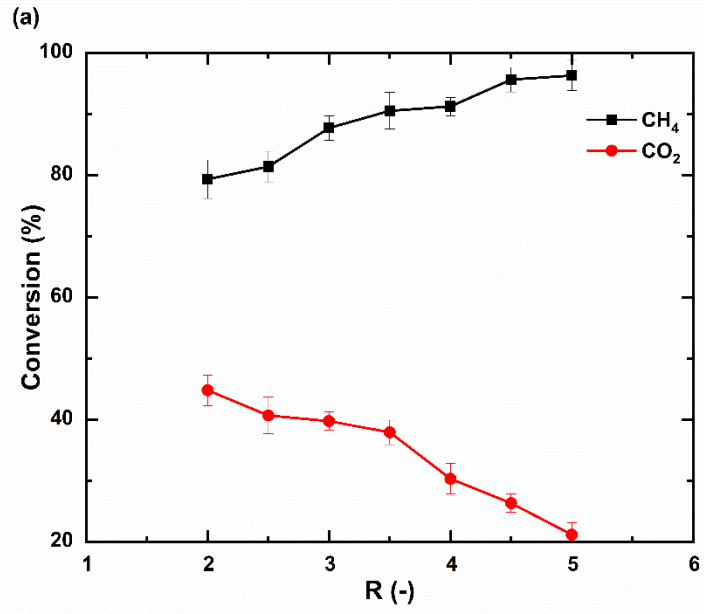
(a)

(b)

Figure 6. 3 Effect of R on the microwave-assisted plasma DRM (a) CH_4 and CO_2 Conversions; (b) H_2 and CO Selectivity; (c) H_2 and CO Yield; and (d) H_2/CO Ratio (MWP: 700 W; CH_4 and N_2 flow rates of 0.2 and 1.5 L min^{-1})

6.3.4 Effect of Total Feed Flow Rates

The effects of the TFR on the stability of plasma and syngas production under microwave-assisted plasma DRM were determined at a constant R of 2/1 and the input MWP of 700 W at atmospheric pressure. Figures 6.4(a–d) displays the conversion of CH_4 and CO_2, selectivities and yields of H_2 and CO, and H_2/CO ratio, respectively, as a function of TFR between 0.45 and 2.1 L min^{-1}. As shown in Figure 6.4(a–c), the conversions of CH_4 and CO_2 and the selectivities and yields of H_2 and CO slightly decreased from 94.67%, 65.24%, 70.85%, 75.32%, 67.07% and 56.51% to 79.35%, 44.82%, 50.12%, 58.42%, 39.77% and 32.89%, respectively with increasing TFR. While the H_2/CO ratio reveals opposite trends which increased slightly from 0.78 to 0.86 with increasing TFR, as shown in Figure 6.4(d). A similar conversion tendency has also been reported previously (Aziznia et al., 2012; Chung & Chang, 2016; Long et al., 2008; Pan et al., 2014; Shapoval & Marotta, 2015; Xin Tu & Whitehead, 2014; Yunpeng Xu et al., 2002; Zeng et al., 2015; A.-J. Zhang et al., 2010). The reason for this behaviour has been previously explained in Chapter 4.
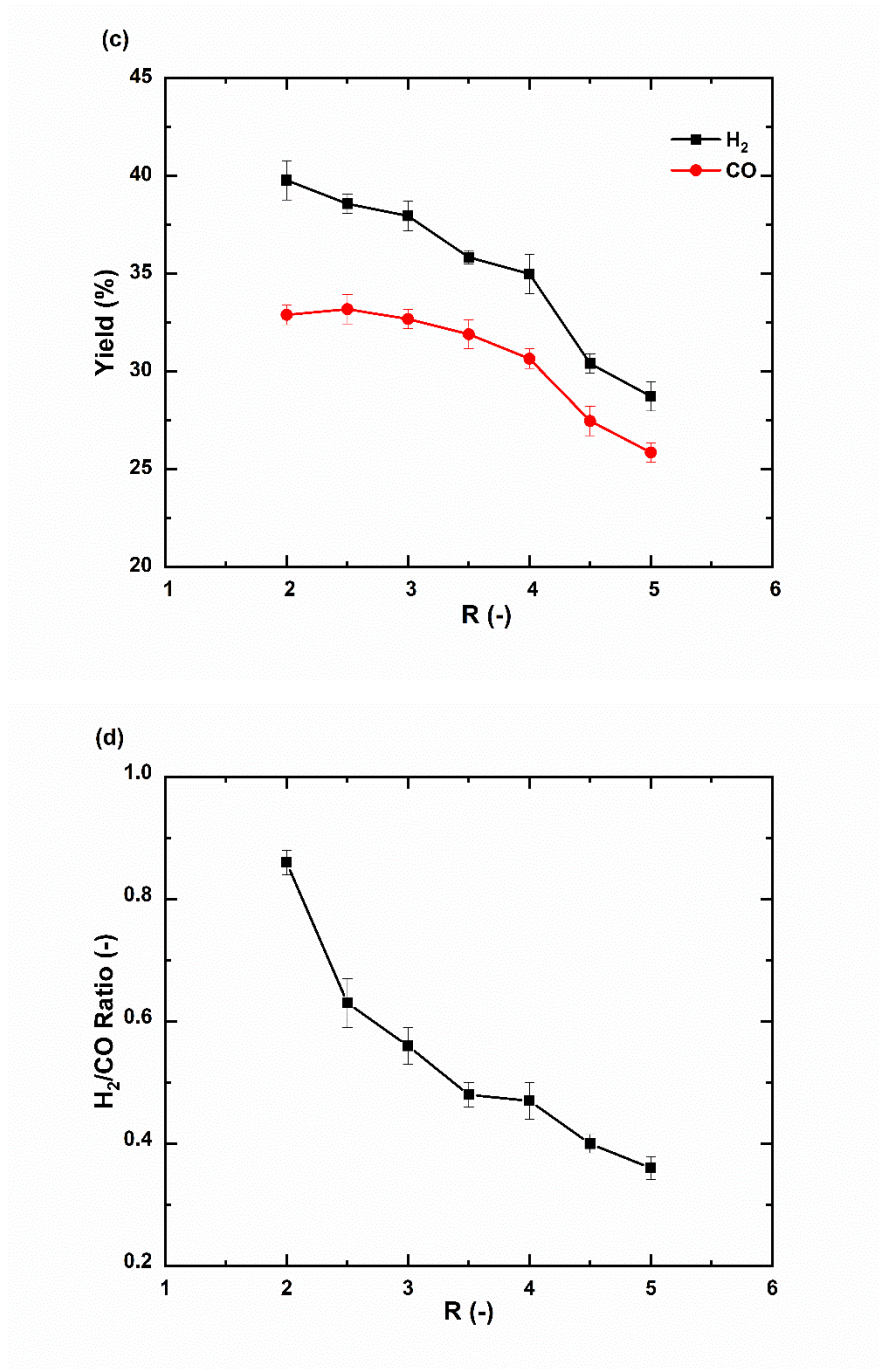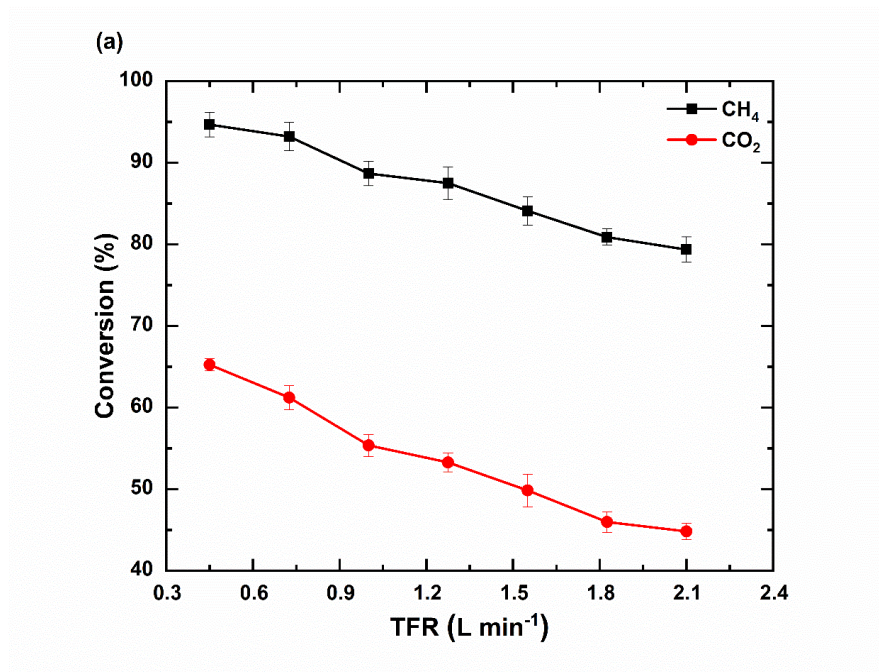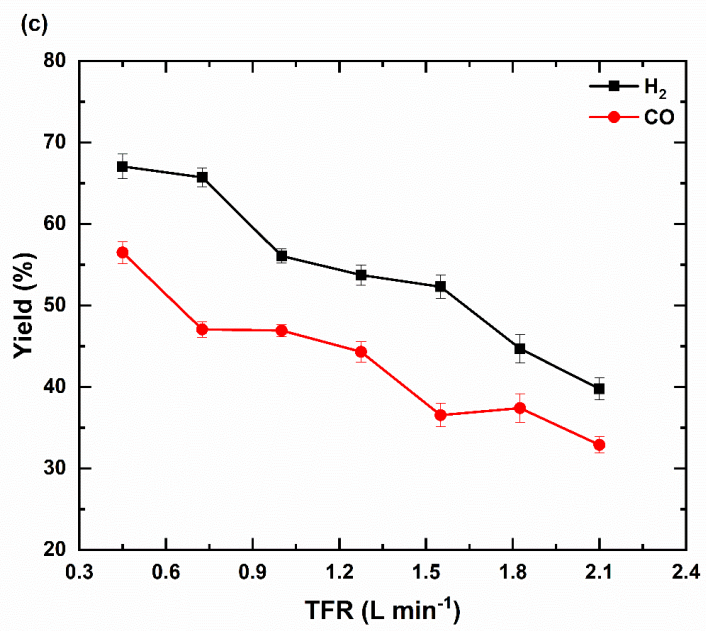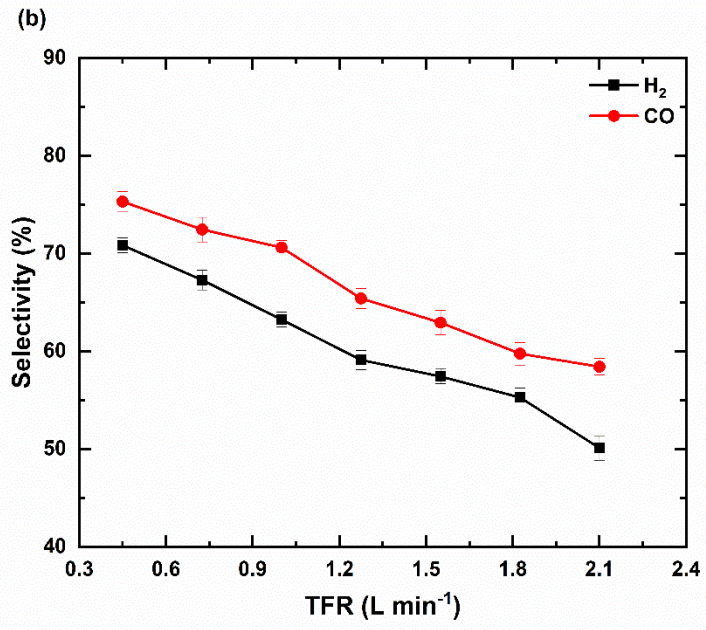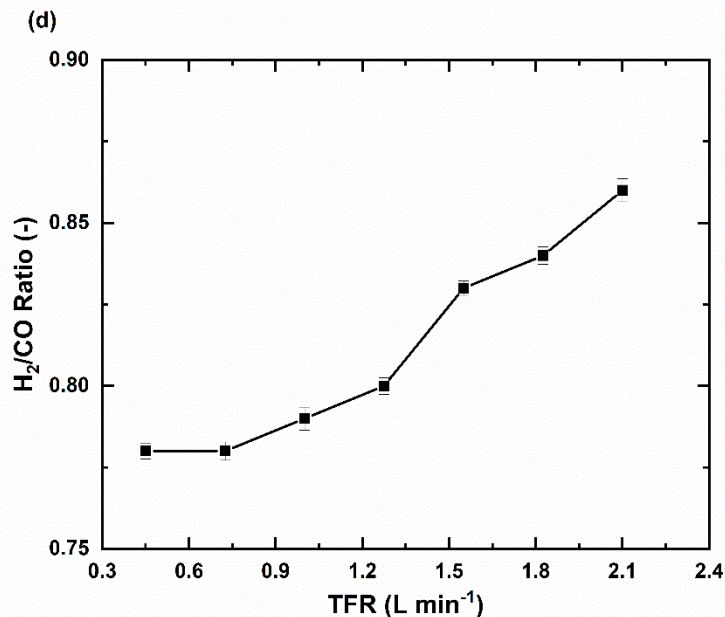
Figure 6. 4 Effect of TFR on the microwave-assisted plasma DRM (a) CH_4 and CO_2 Conversions; (b) H_2 and CO Selectivity; (c) H_2 and CO Yield; and (d) H_2/CO Ratio (MWP: 700 W; R: 2/1)

6.3.5 Effect of DRM Performance Stability

The stability of DRM performance was also evaluated as a function of RT at a constant MWP of 700 W, constant R of 2/1, and constant TFR of 2.1 L min^{-1}, respectively. Figure 6.5(a–d) shows CH_4 and CO_2 conversions, H_2 and CO selectivities and yields, and H_2/CO ratio, respectively, as a function of RT from 20 to 480 min (up to 8 h). The data point was recorded after 20 min-RT to ensure that steady-state condition was achieved. Over this time period, CH_4 and CO_2 conversions fluctuated marginally around median values of 80 and 44%, respectively (Figure 6.5(a)), while H_2 and CO selectivities fluctuated around median values of 50 and 59%, respectively (Figure 6.5(b)). Likewise, over this same time period, H_2 and CO yields also fluctuated slightly around median values of 39.5 and 34.5%, respectively (Figure 6.5(c)), while the H_2/CO ratio fluctuated around 0.85 (Figure 6.5(d)). In essence, stable microwave-assisted DRM performance can be observed for up to 8 h-reaction duration.

(a)

(b)
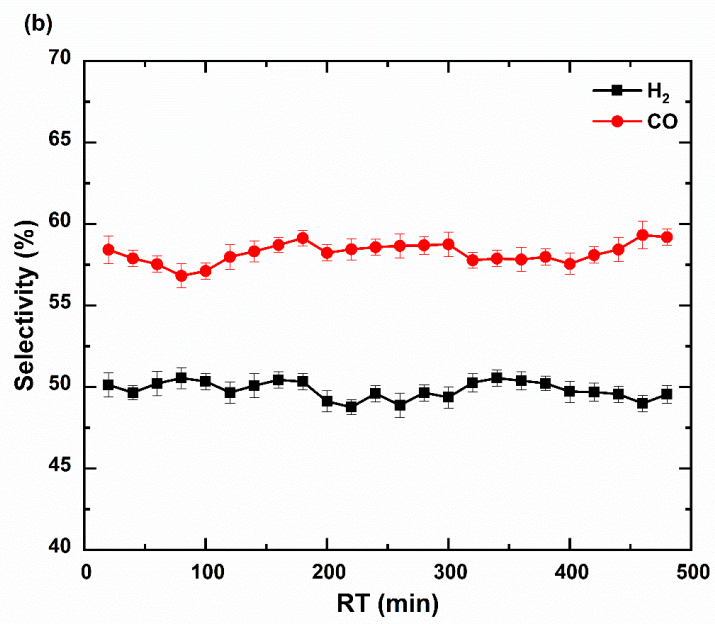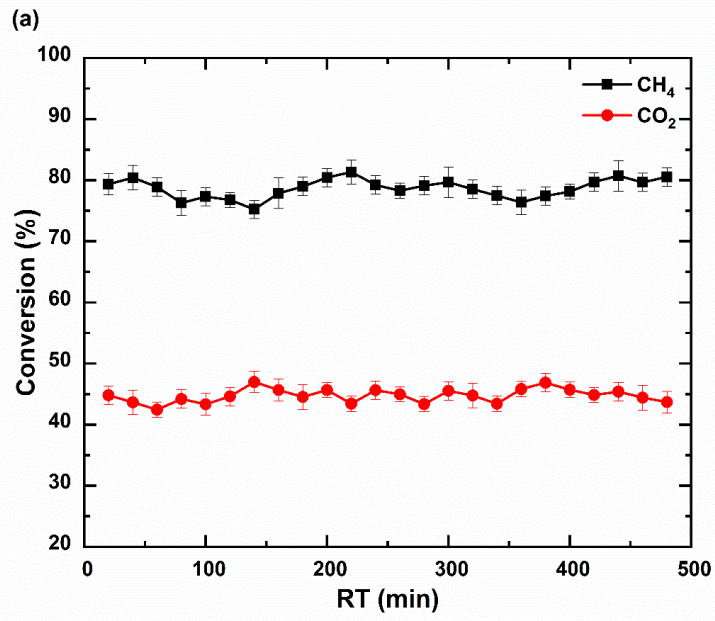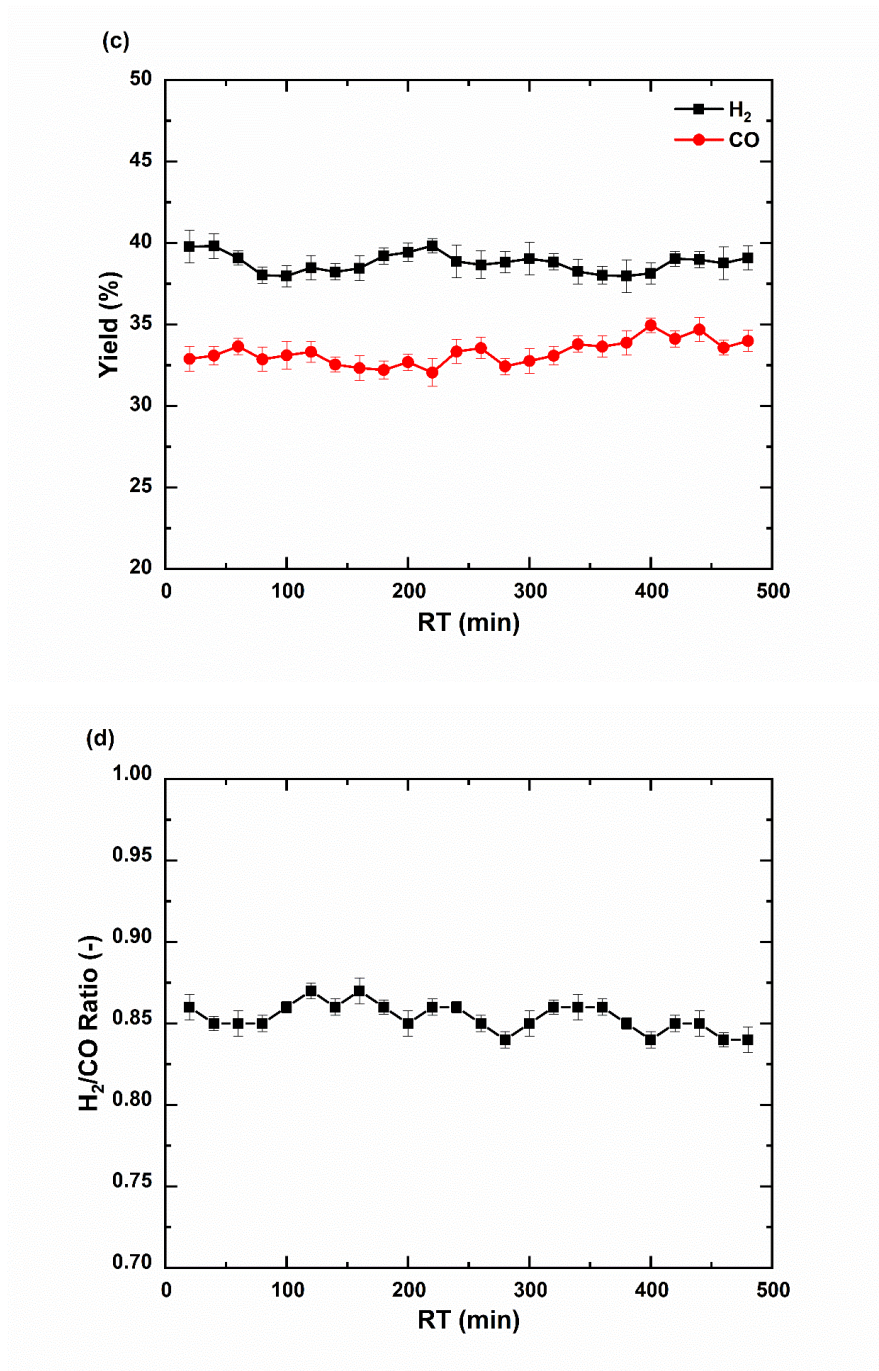
Figure 6. 5 Effect of DRM performance stability on the microwave-assisted plasma DRM (a) CH_4 and CO_2 Conversions; (b) H_2 and CO Selectivity; (c) H_2 and CO Yield; and (d) H_2/CO Ratio (MWP: 700 W; R: 2/1; TFR: 2.1 L min^{-1})

6.4 Comparison of DRM performance in N_2-Plasma with Different Plasma Forms

The performance of microwave-assisted DRM performed here in N_2 atmosphere was compared against other works in N_2 atmosphere in Table 6.1 (Chung & Chang, 2016; Hwang et al., 2010; Indarto et al., 2006; X. S. Li et al., 2011; Long et al., 2008; Sun et al., 2012; Tao et al., 2008; Yan Xu et al., 2013; B. Zhu et al., 2012). Sun et al. (2012), for example, reported maximum CO_2 and CH_4 conversions of 88.18 and 92.06%, respectively, and an H_2 yield of 60.12% in a DC arc thermal plasma reactor were obtained at a discharge power of 3400 W, TFR of 16 L min^{-1}, and R of 1/1. These highest conversions and yields were achieved at a very high flow rate. Li et al. (2011), on the other hand, they reported CO_2 and CH_4 conversions of 55.84 and 65.27%, respectively, and an H_2 yield of 40.35% in an AC spark discharge plasma reactor was obtained at a low-discharge power of 45 W and low TFR of 0.15 L min^{-1}. Zhu et al. (2012) reported that CO_2 and CH_4 conversions of 70.78 and 75.33%, respectively, and an H_2 yield of 62.78% in a kHz spark discharge reactor were obtained at a relatively high discharge power of 1344 W and a low TFR of 0.15 L min^{-1}. Our maximum CO_2 and CH_4 conversions of 44.82 and 79.35%, respectively, and an H_2 yield of 39.77% are comparable with the values reported in these works. The discrepancies between this work and previous works reflect the different equipment setup and operating conditions.

Table 6. 1 Comparison of DRM performance in N_2 atmosphere reported here with the others in the literature

Plasma Form	MWP [W]	R [-]	TFR [L min^{-1}]	Conversion [%]			Selectivity [%]		Yield [%]		H_2/CO Ratio [-]	References
				CH$_4$	CO$_2$	N$_2$	H$_2$	CO	H$_2$	CO		
Gliding Arc Discharge (GAD)	182	1/1	1	40.63	29.32	NA	50.25	62.41	20.53	NA	0.9	(Indarto et al., 2006)
DC Arc Thermal Plasma	3,400	1/1	16	92.06	88.18	NA	65.16	66.53	60.12	NA	NA	(Sun et al., 2012)
Arc Jet Plasma (AJP)	1000	1/1	4	50.74	35.55	NA	80.98	78.31	40.51	NA	1.1	(Hwang et al., 2010)
Cold Plasma Jet (CPJ)	770	2/3	16.667	45.68	34.03	NA	78.11	85.41	36.73	33.09	0.8	(Long et al., 2008)
Single-Anode Thermal Plasma Jet	9,600	3/2	30	89.82	80.14	NA	68.60	88.37	62.34	NA	0.7	(Tao et al., 2008)
Binod-anode Thermal Plasma+ Ni/Al$_2$O$_3$	1,440	3/2	83.334	77.1	62.4	NA	88.6	96.7	86.15	NA	NA	(Yan Xu et al., 2013)
Spark Discharge Plasma (SDP)	26.6	1/1	0.2	53.43	58.8	NA	79.2	61.7	42.64	NA	NA	(Chung & Chang, 2016)
AC Spark Discharge Plasma (SDP)	45	1.5/1	0.15	65.27	55.84	-	62.35	87.63	40.83	NA	2	(X. S. Li et al., 2011)
kHz Spark Discharge	1,344	2/3	0.15	75.33	70.78	-	82.78	70.32	62.57	NA	NA	(B. Zhu et al., 2012)
Microwave Discharge Plasma	700	2/1	2.1	79.35	44.82	-	50.12	58.42	39.77	32.89	0.86	This study

6.5 Conclusion

In this work, N_2-plasma dry CH_4 reforming was investigated for microwave-assisted plasma DRM at atmospheric pressure. The effects of different reaction conditions such as N_2 feed flow rate, MWP, R, TFR, and DRM performance stability on the conversions of CH_4 and CO_2, selectivities and yields of H_2 and CO, and H_2/CO ratio were demonstrated. For the standard conditions (700 W of input MWP, 2/1 of R, and 2.1 L min^{-1} of TFR), the microwave-assisted DRM performance stability is excellent, and the plasma flame lasting for up to 8 h-duration in N_2 atmosphere was achieved. In addition, the CH_4 and CO_2 conversions, H_2 and CO selectivities and yields, and H_2/CO ratio decreased with increased N_2 flow rate from 0.3 to 1.5 L min^{-1}. The study also found that the MWP significantly affected the CH_4 and CO_2 conversions and the selectivity and yield of CO. In contrast, the MWP has a negative effect on the selectivity and yield of H_2 and CO and the ratio of H_2/CO. The R increased from 2/1 to 5/1 at 700 W and the conversion of CH_4 and the selectivity of CO increased rapidly, while the conversion of CO_2, selectivity of H_2, yield of H_2 and CO, and ratio of H_2/CO exhibited opposite behaviours. Moreover, the TFR slightly affects the conversions of CH_4 and CO_2 and the selectivities and yields of H_2 and CO, respectively. In addition, the H_2/CO ratio sharply increased with increasing TFR. The findings from this study contribute to the current literature. The effects of N_2 feed flow rate, MWP, R, and TFR is useful for plasma stability, syngas production, and avoiding the carbon-formation-free condition on the inner wall of the quartz tube.

7

Chapter 7: Stability of Argon-Plasma Dry Reforming of Methane in a Horizontal Microwave Irradiation Reactor

7.1 Introduction

In this study, Ar was chosen as additive gas because N_2 and Ar are the first and the third most abundant gases in the atmosphere. Plasma generation in N_2 and Ar would also require a lower power consumption relative to those performed in He and H_2 plasma. (A.-J. Zhang et al., 2010). Furthermore, they are relatively cheap and safe when used as additives gases compared with other additives gases. Numerous works are available that report the performance of plasma-induced DRM in terms of CH_4 and CO_2 conversions, H_2 and CO selectivities and yields, and molar ratio of H_2/CO in Ar and/or N_2 atmosphere(s) (Allah & Whitehead, 2015; Hwang et al., 2010; Long et al., 2008; Moshrefi et al., 2013; Seyed-Matin et al., 2010; Sun et al., 2012; Tao et al., 2009; Tao et al., 2008; Yan Xu et al., 2013; B. Yan et al., 2010). None of these works, however, evaluated the effects of the additive gas type and flowrate in syngas production from CH_4 and CO_2 using microwave plasma sources. Therefore, in this work, the use of Ar as an additive gas is compared against N_2. DRM performance is also evaluated as a function of MWP, different R, TFR, and RT at atmospheric pressure.

7.2 Experimental set up

A commercial microwave reactor system (Alter, SM 1150T, Canada) consisting of a feed gas system, plasma reactor, microwave generator, and gas chromatographic (GCMS) analysis system was used. Further details about the experimental design and the calculation methodology can be found elsewhere in Chapter 3.

7.3 Results and Discussions
7.3.1 Effect of Ar Feed Flow Rate

The effects of adding Ar as an inert gas on plasma stability and syngas production were investigated under microwave-assisted plasma DRM. Figure 7.1(a–d) displays the CH_4 and CO_2 conversions, H_2 and CO selectivities and yields, and H_2/CO ratio,

respectively, as a function of Ar flow rate between 0.3 and 1.5 L min^{-1}. These data were obtained at a constant MWP of 700 W and constant CO_2 and CH_4 flow rates of 0.4 and 0.2 L min^{-1}, respectively (Table 3.2, Chapter 3). Marginal variations in CH_4 and CO_2 conversions from the median values of 77.66 to 76.94% and of 43.85 to 41.11%, respectively, manifest when the Ar flow rate increased from 0.3 to 1.5 L min^{-1} (Figure 7.1(a)). Marginal fluctuation can also be observed for H_2 and CO selectivities (median values of 59.85% to 62.87% and 67.32% to 69.62%, respectively) (Figure 7.1(b)) as well as for H_2 and CO yields (median values of 46.47 to 48.37% and 37.09% to 40.56%, respectively) (Figure 7.1(c)). The increase in CO yield over this Ar flow rate region, however, is still slightly larger than the increase in H_2 yield, which translates to a minor decrease in H_2/CO ratio from 1.02 to 0.91 over this region (Figure 7.1(d)). Such reduction in H_2 yield and H_2/CO ratio with increasing flow rate was also observed in another work (Zeng et al., 2015).

(b)

(c)
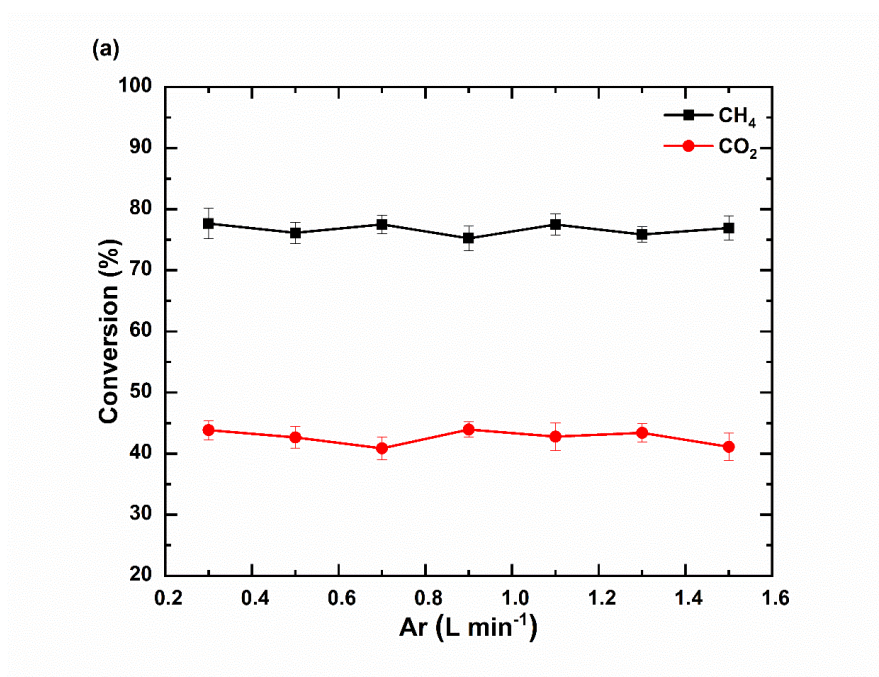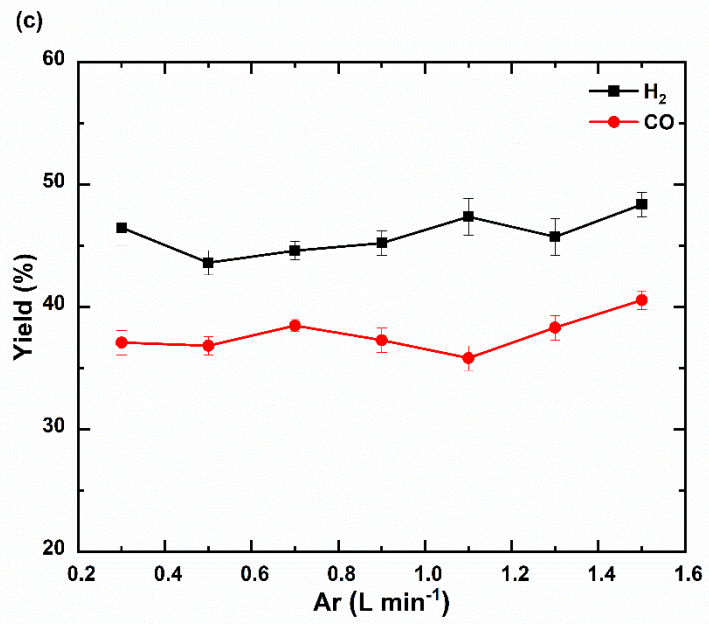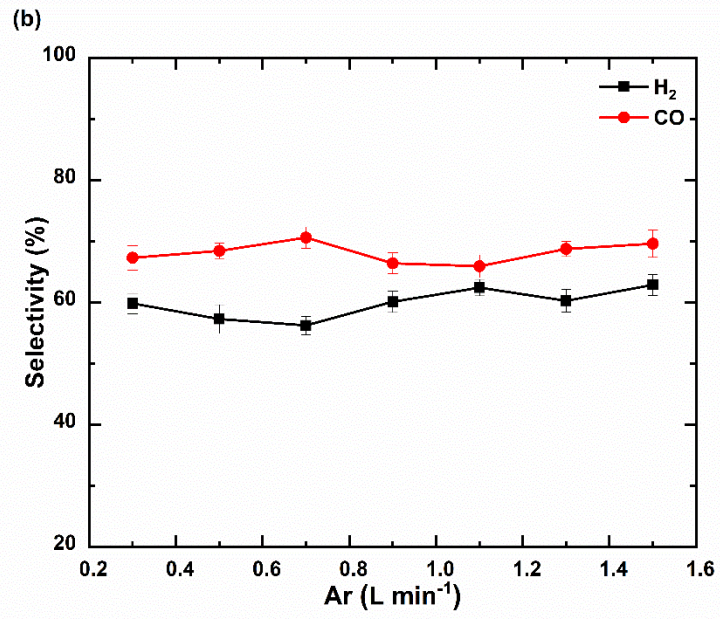
Figure 7. 1 Effect of Ar feed flow rate on the microwave-assisted plasma DRM; (a) CH_4 and CO_2 Conversions; (b) H_2 and CO Selectivity; (c) H_2 and CO Yield; and (d) H_2/CO Ratio (R: 2/1; input MWP: 700 W)

7.3.2 Effect of Microwave Power

The effect of input MWP had been found to be another significant variable affecting the plasma stability and syngas production. Figure 7.2(a–d) shows CH_4 and CO_2 conversions, H_2 and CO selectivities, H_2 and CO yields, and H_2/CO ratio, respectively, as a function of MWP between 700 and 1200 W. These data were obtained at constant TFR of 2.1 L min^{-1} and R of 2/1 (Table 3.2, Chapter 3). A minor increase in CH_4 and CO_2 conversions from 76.94 to 87.55% and from 41.11 to 52.47% occur as MWP increased from 700 to 1200 W (Figure 7.2(a)). The reason for this behaviour is explained in detail previously in Chapter 4. CH_4 conversion was always higher than CO_2 conversion, as observed earlier when DRM was performed in an Ar atmosphere. H_2 selectivity decreases from 62.87 to 44.79%, while CO selectivity increased from 69.62 to 81.93% with an increase in MWP from 700 to 1200 W (Figure 7.2(b)).

Such reversed behaviour between H_2 and CO reflects the occurrence of RWGS reaction and reverse Boudouard reaction. Likewise, H_2 and CO yields show the same reversed behaviour, i.e. H_2 yield decreases from 48.37 to 39.21%, while CO yields increased from 40.56 to 52.55% with increasing MWP (Figure 7.2(c)). A concurrent increase in CO yield and decrease in H_2 yield with an increase in MWP from 700 to

1200 W essentially leads to a reduction in H_2/CO ratio from 0.91 to 0.49 over this power region (Figure 7.2(d)). Water was again observed at the end of DRM.
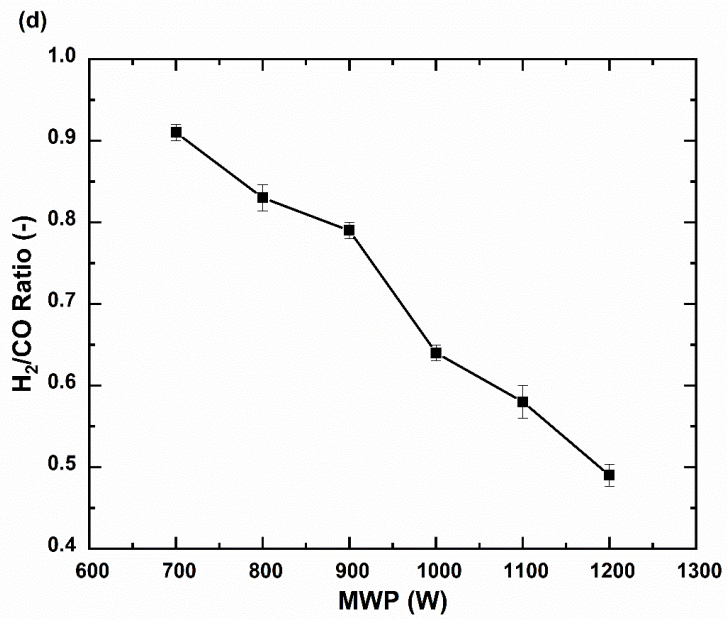
Figure 7. 2 Effect of MWP on the microwave-assisted plasma DRM (a) CH_4 and CO_2 Conversions; (b) H_2 and CO Selectivity; (c) H_2 and CO Yield; and (d) H_2/CO Ratio (R: 2/1; TFR: 2.1 L min^{-1})

7.3.3 Effect of CO_2/CH_4 Ratio

The R ratio has a significant effect on plasma stability and syngas production. Figure 7.3(a–d) shows CH_4 and CO_2 conversions, H_2 and CO selectivities, H_2 and CO yields, and H_2 to CO ratio, respectively, as a function of R inlet supply between 2 and 5. These data were obtained for CO_2 flow rate change from 0.4 to 1 L min^{-1} at a constant MWP of 700 W, and a constant CH_4 and Ar flow rate of 0.2 and 1.5 L min^{-1} (Table 3.1, Chapter 3). Increasing R from 2 to 5 translates to an increase in CH_4 conversion from 76.94 to 95.11% and a decrease in CO_2 conversion from 41.11 to 18.79% (Figure 7.3(a)). While H_2 selectivity decreases from 62.87 to 37.83% with an increase in R from 2 to 5, CO selectivity increases from 69.62 to 90.77% (Figure 7.3(b)).

As observed, also in an Ar atmosphere case, enhanced CO selectivity is a result of a higher amount of CO_2 reactants, shifting the equilibrium towards CO product *via* DRM reaction (Equation (1.3, Chapter 1)). H_2 and CO yields, however, decrease from 48.37 to 36.44% and from 40.56 to 28.51%, respectively, with an increase in R from 2 to 5 (Figure 7.3(c)). Increasing the CO_2/CH_4 ratio from 2 to 5 leads to a reduction in H_2 to CO ratio from 0.91 to 0.42 (Figure 7.3(d)). The trends observed in Figure 7.3(a–d) as a function of R inlet supply between 2 and 5 in Ar atmosphere reproduce the trends observed in Figure 6.3(a–d), Chapter 6, in N_2 atmosphere.
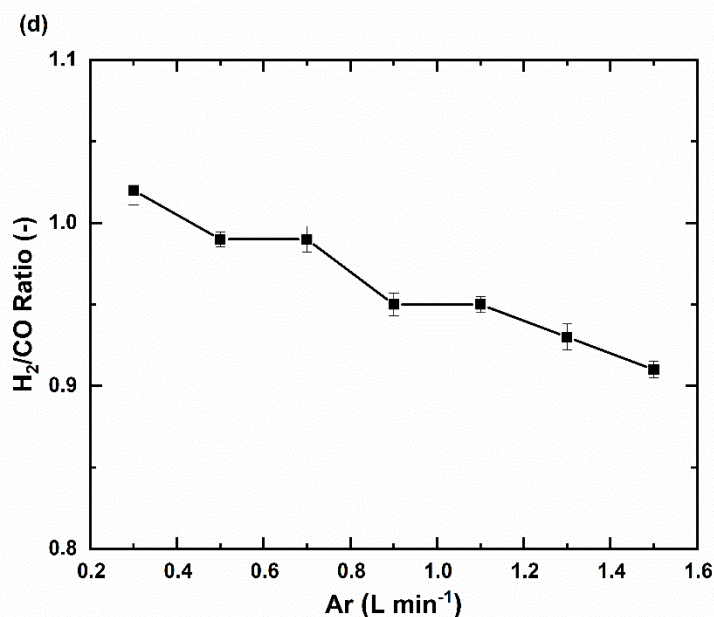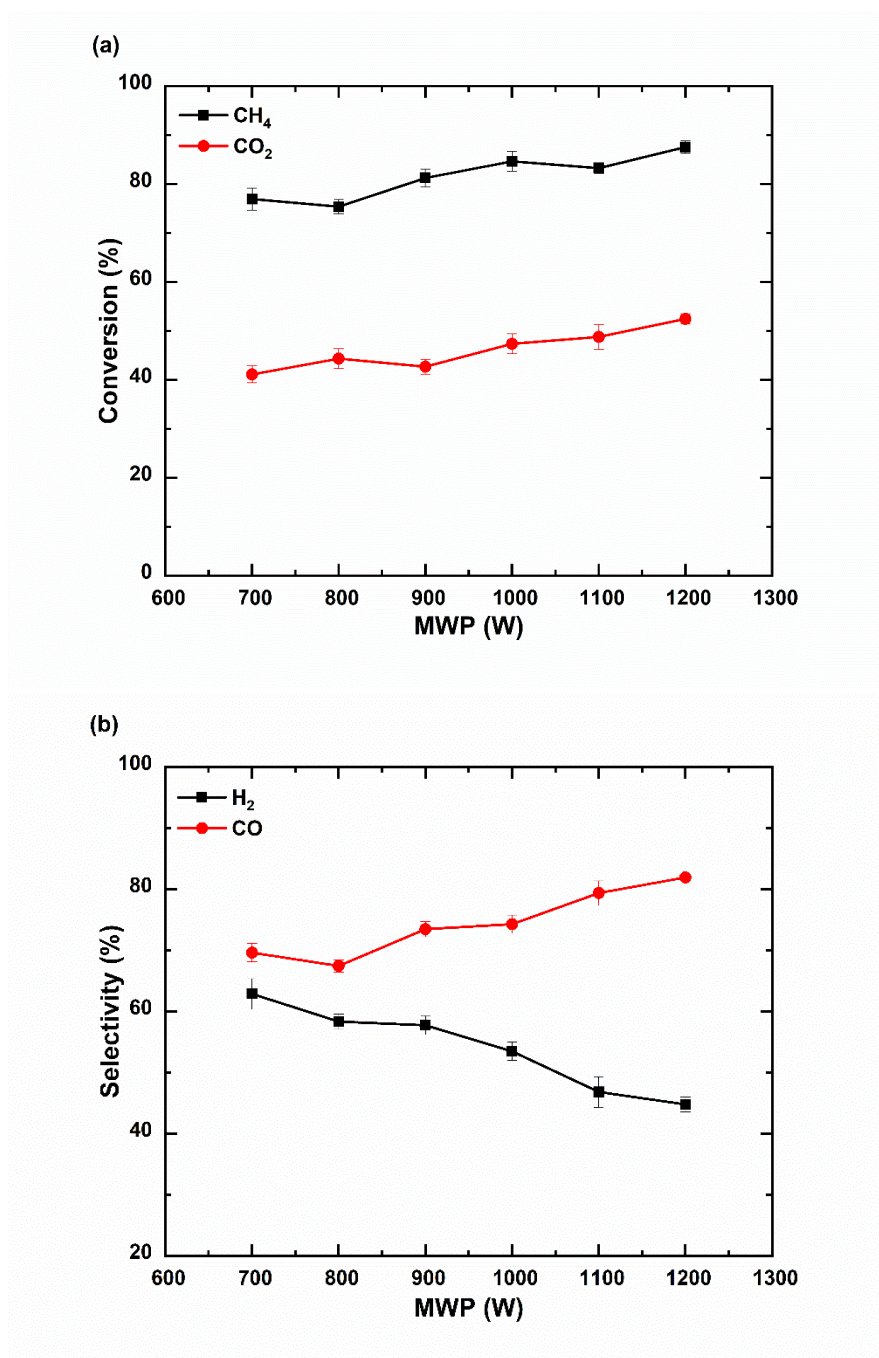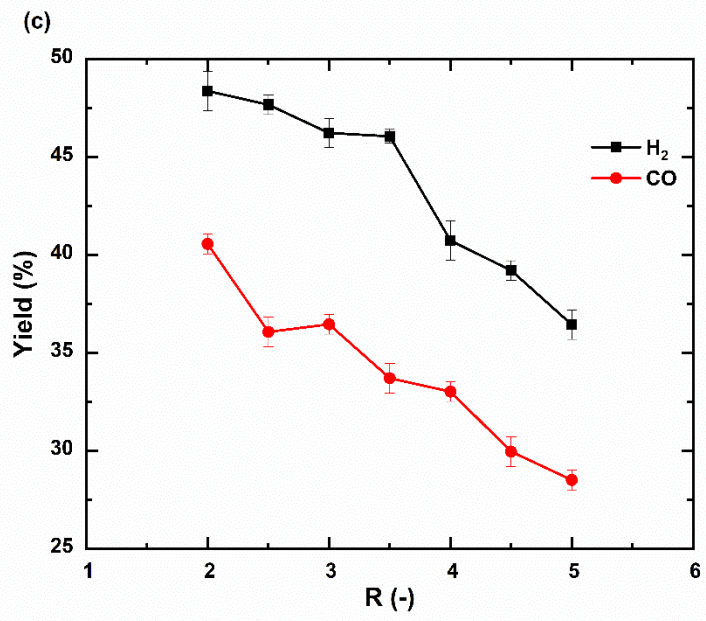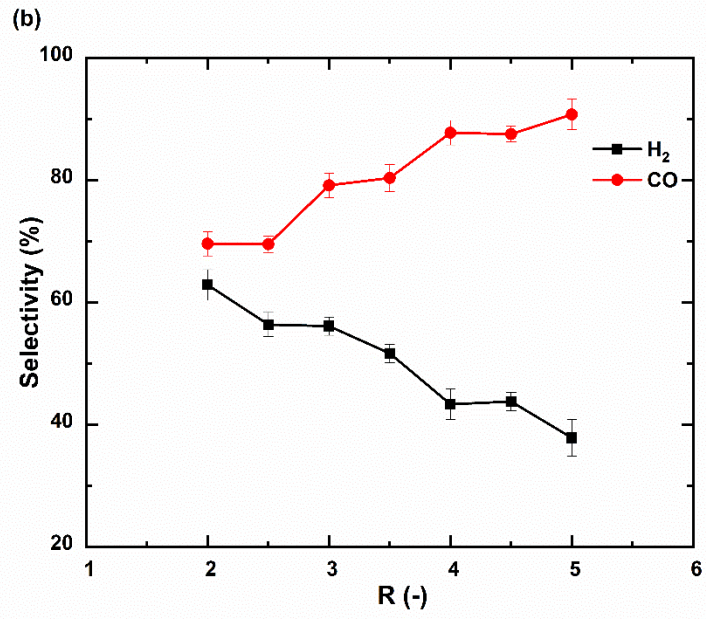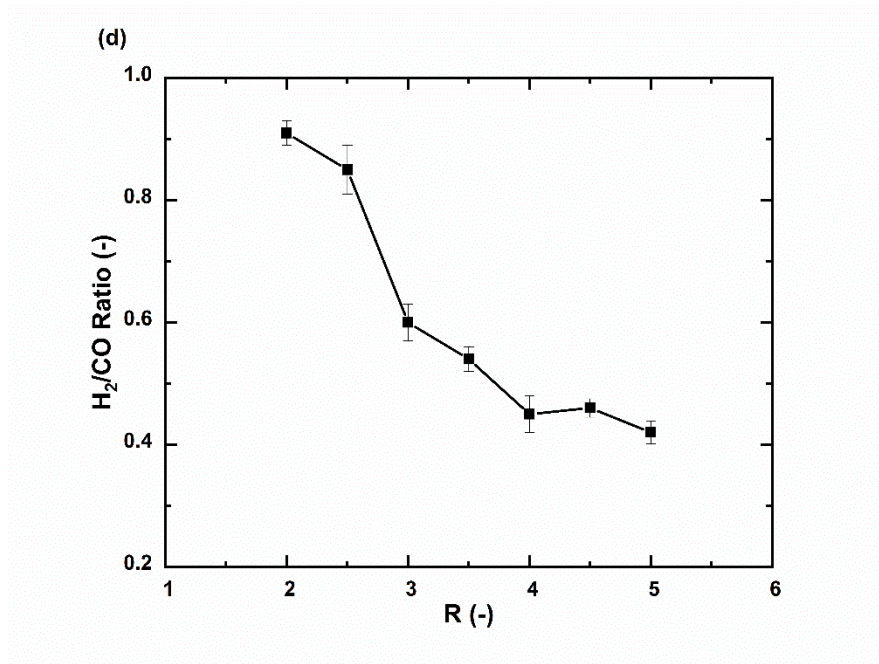
Figure 7. 3 Effect of R on the microwave-assisted plasma DRM (a) CH_4 and CO_2 Conversions; (b) H_2 and CO Selectivity; (c) H_2 and CO Yield; and (d) H_2/CO Ratio (MWP: 700 W; CH_4 and N_2 flow rates of 0.2 and 1.5 L min^{-1})

7.3.4 Effect of Total Feed Flow Rate

The effects of the TFR on the plasma stability and syngas production under microwave-assisted plasma DRM were determined at constant R of 2/1 and the input MWP of 700 W at atmospheric pressure. Figure 7.4(a–d) shows the conversions of CH_4 and CO_2, the selectivities, yields of H_2 and CO, and the H_2/CO ratio, respectively, as a function of TFR between 0.45 to 2.1 L min^{-1}. Figure 7.4(a–c) show that the conversions of CH_4 and CO_2, selectivities and yields of H_2 and CO, and the H_2/CO ratio slightly decreased from 96.23%, 67.43%, 83.21%, 88.33%, 78.76% and 67.32% to 76.94%, 41.11%, 62.87%, 69.62%, 48.37%, and 40.56%, respectively, with increasing TFR. In addition, the H_2/CO ratio reveals opposite trends that increased slightly from 0.82 to 0.91 with increased TFR, as shown in Figure 6.4(d). A similar conversion tendency has also been previously reported (Aziznia et al., 2012; Chung & Chang, 2016; Long et al., 2008; Pan et al., 2014; Shapoval & Marotta, 2015; Xin Tu & Whitehead, 2014; Yunpeng Xu et al., 2002; Zeng et al., 2015; A.-J. Zhang et al., 2010). The reason for this behaviour is explained previously in detail in Chapter 4.

(a)

(b)

(c)

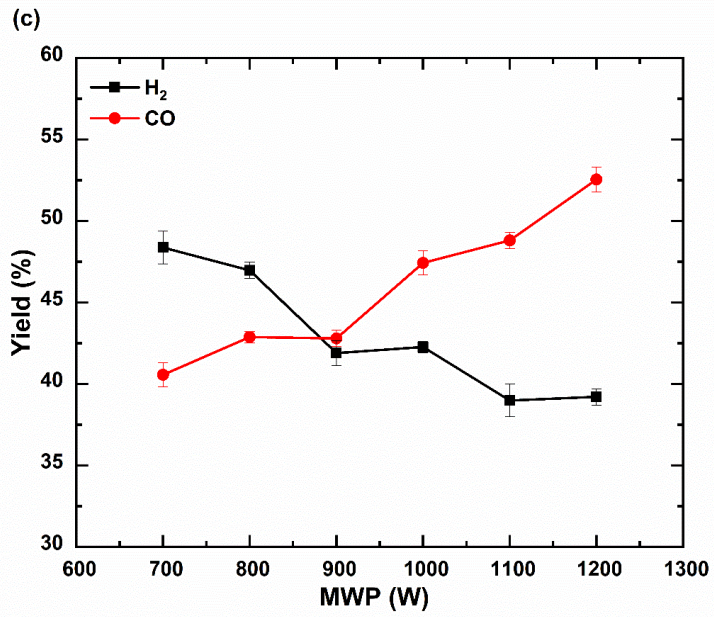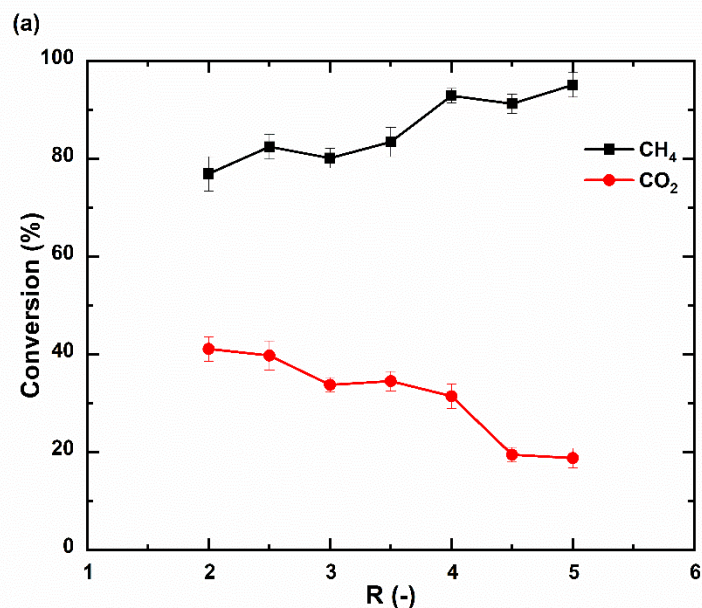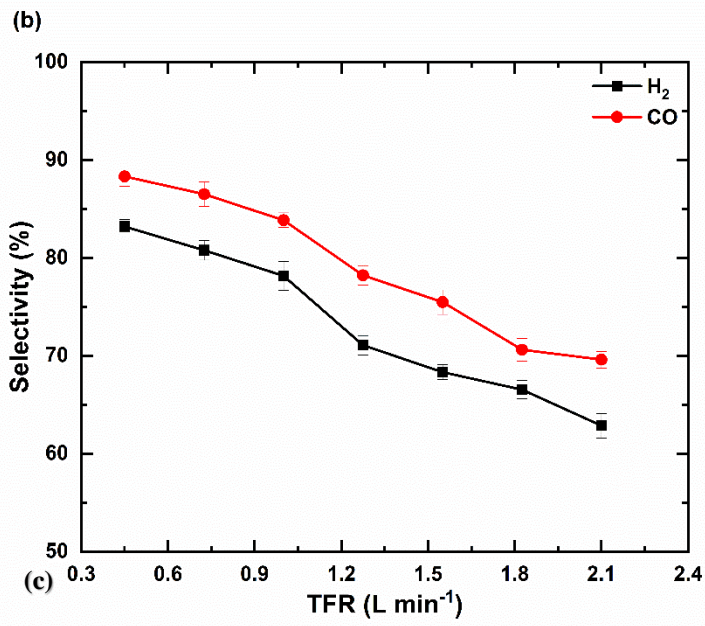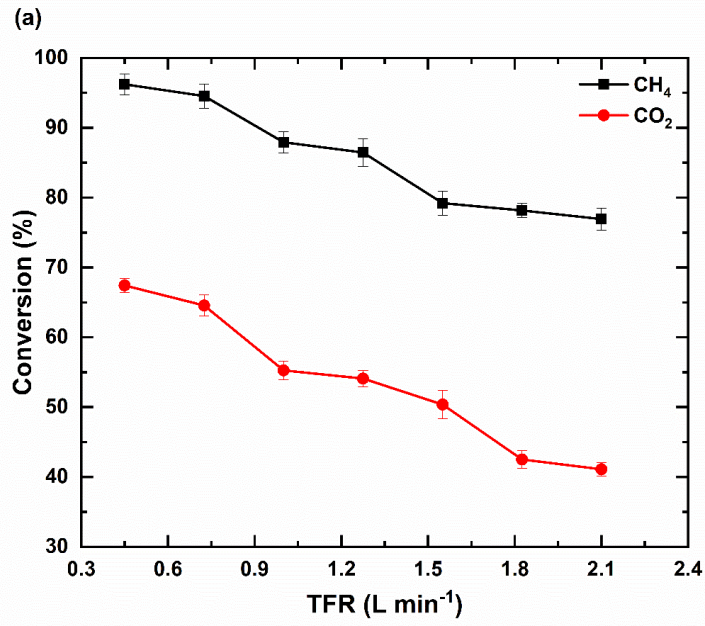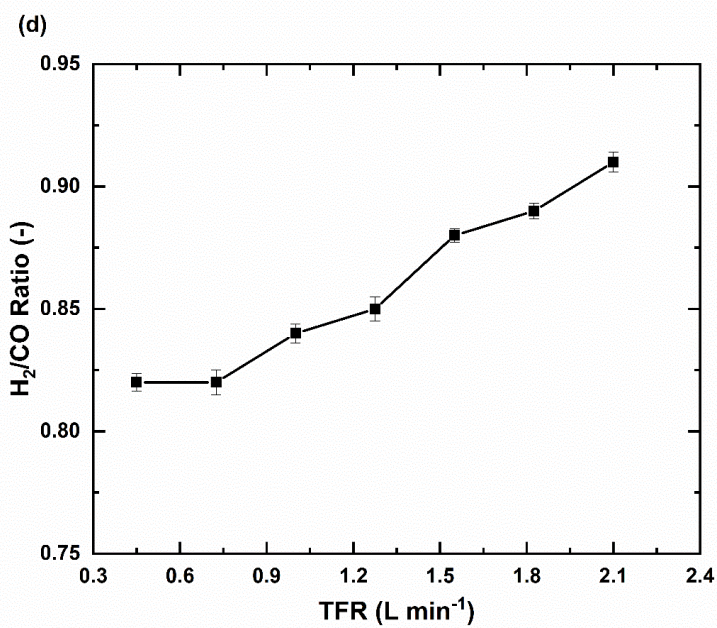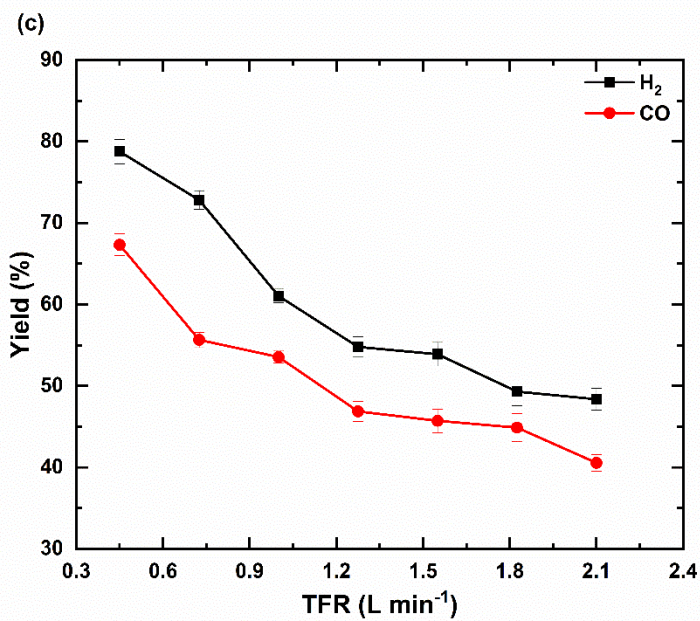Figure 7. 4 Effect of TFR on the microwave-assisted plasma DRM (a) CH_4 and CO_2 Conversions; (b) H_2 and CO Selectivity; (c) H_2 and CO Yield; and (d) H_2/CO Ratio (MWP: 700 W; R: 2/1)

7.3.5 Effect of DRM Performance Stability

The stability of DRM performance was also studied as a function of RT at a constant MWP of 700 W, constant R of 2/1, and constant TFR of 2.1 min^{-1}, respectively. Figure 7.5(a–d) displays CH_4 and CO_2 conversions, H_2 and CO selectivities, H_2 and CO yields, and H_2 to CO ratio, respectively, as a function of RT from 20 to 480 min (up to 8 h). Minor fluctuations are observed in CH_4 and CO_2 conversions, with median values of 76 and 41%, respectively (Figure 7.5(a)). H_2 and CO selectivities fluctuated in the same manner, with median values of 63 and 69%, respectively (Figure 7.5(b)). H_2 and CO yields also varied around the median values of 48 and 40% (Figure 7.5(c)). Similarly, the H_2 to CO ratio varied slightly around 0.91 (Figure 7.5(d)). As is the case for the N_2-based DRM studied, performing microwave-assisted DRM in Ar atmosphere also provides highly stable performance for up to 8 h.
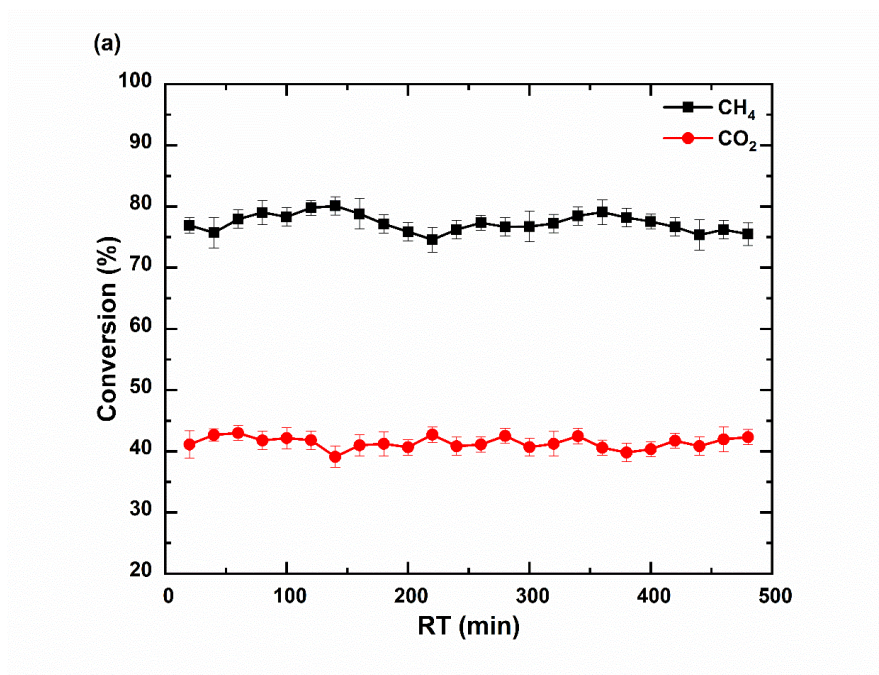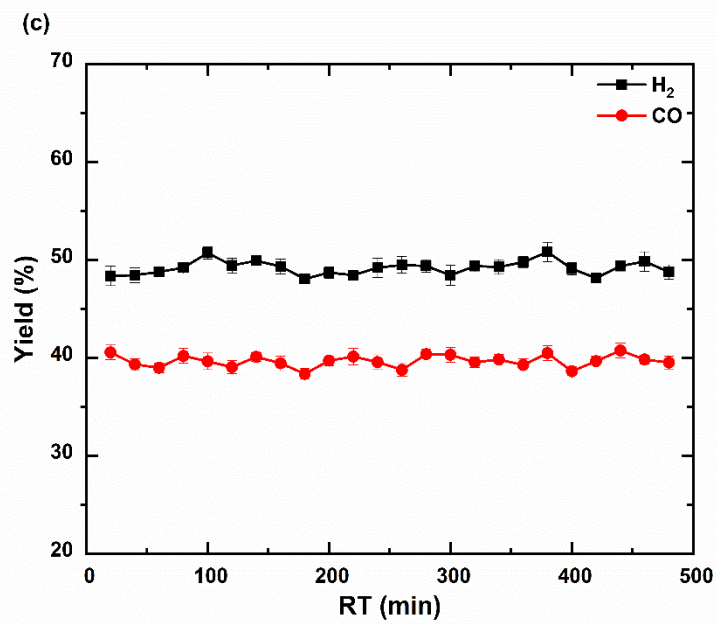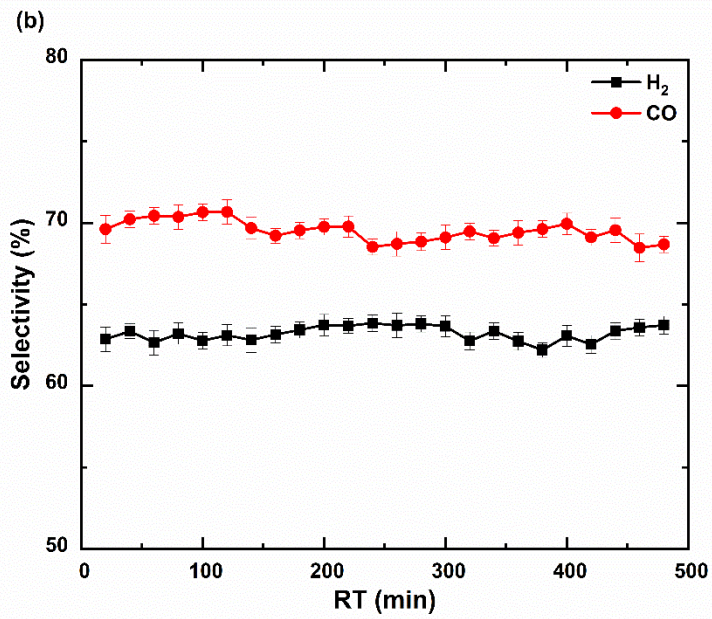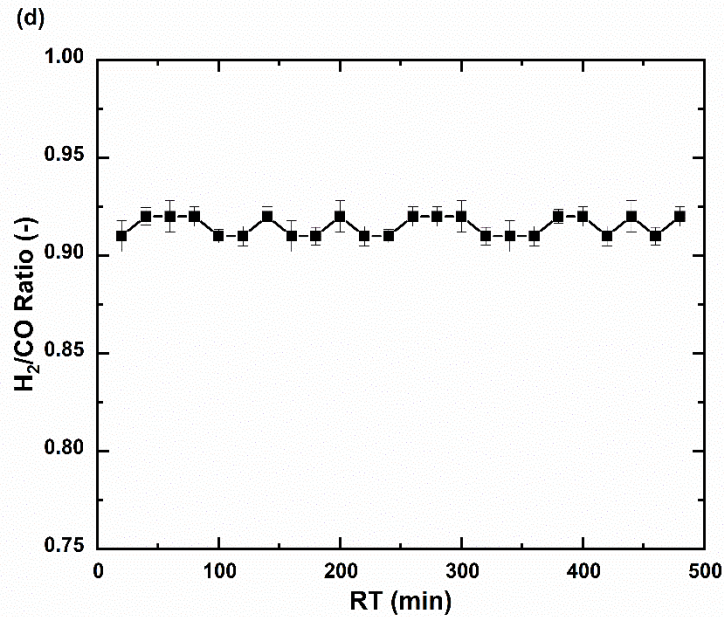
Figure 7. 5 Effect of DRM performance stability on the microwave-assisted plasma DRM (a) CH_4 and CO_2 Conversions; (b) H_2 and CO Selectivity; (c) H_2 and CO Yield; and (d) H_2/CO Ratio (MWP: 700 W; R: 2/1; TFR: 2.1 L min^{-1})

7.4 Comparison of DRM performance in Ar-Plasma with Different Plasma Forms

Table 7.1 provides a comparison between the performance of microwave-assisted DRM performed here in Ar atmosphere against other works in Ar atmosphere (Allah & Whitehead, 2015; Daihong Li et al., 2009; Moshrefi et al., 2013; Sentek et al., 2010; Seyed-Matin et al., 2010; Q. Wang et al., 2009a; B. Yan et al., 2010; A.-J. Zhang et al., 2010; Zhou et al., 1998). Our maximum CO_2 and CH_4 conversions of 41.11 and 76.94%, respectively, and H_2 yield of 48.37% are comparable with the values reported in these works. Zhou et al. (1998), for instance, have reported that the highest CO_2 and CH_4 conversions of 34.63 and 64.34%, respectively, and an H_2 yield of 33.79% in an AC DBD reactor were obtained at a low-discharge power of 500 W, TFR of 0.5 L min^{-1}, and R of 1/4. Daihong Li et al. (2009), in contrast, have reported that CO_2 and CH_4 conversions of 39.91 and 60.97%, respectively, and an H_2 yield of 54.44% in an AC atmospheric pressure glow discharge (APGD) plasma reactor was obtained at a low-discharge power of 69.85 W and a TFR of 2.2 L min^{-1}. Allah and Whitehead (2015) have reported that low CO_2 and CH_4 conversions of 15.93 and 12.36%, respectively,

and an H_2 yield of 6.43% in an AC GAD plasma reactor were obtained at a relatively low-discharge power of 190 W and a TFR of 4 L min^{-1}. Different equipment setup and operating conditions could be the main contributors between the observed different performances.

Table 7. 1 Comparison of DRM performance in Ar atmosphere reported here with the others in the literature

Plasma Form	MWP [W]	R [-]	TFR [L min^{-1}]	Conversion [%]		Selectivity [%]		Yield [%]		H$_2$/CO Ratio	References
				CH$_4$	CO$_2$	H$_2$	CO	H$_2$	CO		
AC Dielectric Barrier Discharge (DBD)	500	1/4	0.5	64.34	34.63	52.8	23.38	33.79	NA	0.5	(Zhou et al., 1998)
AC Atmospheric Pressure Glow Discharge (APGD)	69.85	6/4	2.2	60.97	39.91	89.3	72.58	54.44	NA	1.5	(Daihong Li et al., 2009)
DC Pulsed Plasma	21	1/1	0.18	33.26	23.55	68.15	65.67	22.44	NA	1.2	(Seyed-Matin et al., 2010)
Dielectric Barrier Discharge	71.5	1/1	0.03	~63	~35	~88	~95	~55.44	NA	~0.58	(Q. Wang et al., 2009b)
AC Gliding Arc Discharge (GAD)	~190	1/1	4	12.36	15.93	50.13	47.52	6.43	NA	NA	(Allah & Whitehead, 2015)
DC Spark Discharge (SD)	16	2/1	0.12	48.34	37/05	84.25	100	40.32	NA	0.5	(Moshrefi et al., 2013)
AC Dielectric Barrier Discharge (DBD)	19	2/1	0.0167	58.53	33.32	32.8	39.62	19.02	NA	NA	(Sentek et al., 2010)
Pulsed DC Arc Discharge	204	1/1	0.1	99.6	99.3	~100	~100	9.96	NA	NA	(B. Yan et al., 2010)
Dielectric Barrier Discharge	60	1/1	0.06	15.09	3.11	34	40.13	5.1	NA	NA	(A.-J. Zhang et al., 2010)
Microwave Discharge Plasma	700	2/1	2.1	76.94	41.11	62.87	69.62	48.37	40.56	0.91	This study

7.5 DRM performance comparison overview

Figure 7.6(a–d) compare CH_4 and CO_2 conversions, H_2 and CO selectivities, H_2 and CO yields, and H_2 to CO ratio, respectively, between DRM performed in N_2 atmosphere against that performed in Ar atmosphere at a constant MWP of 700 W, R of 2/1, and constant TFR of 2.1 L min^{-1}, respectively. Although DRM in N_2 gave slightly higher CH_4 and CO_2 conversions relative to DRM in Ar (Figure 7.6(a)), the latter clearly provided higher H_2 and CO selectivities and yields (Figure 7.6(b) and (c)), translating to higher H_2 to CO ratio relative to the former (Figure 7.6(d)).

(b)

(c)
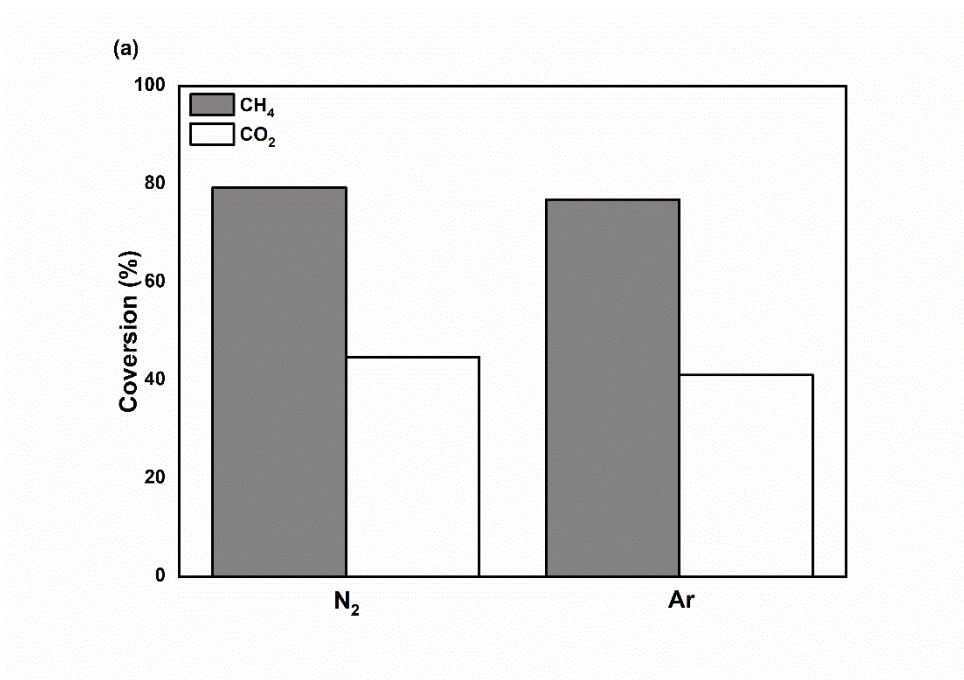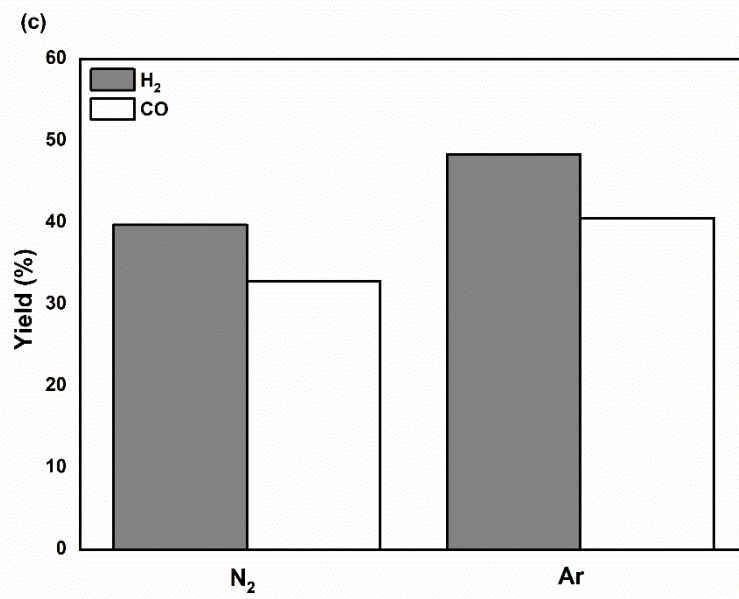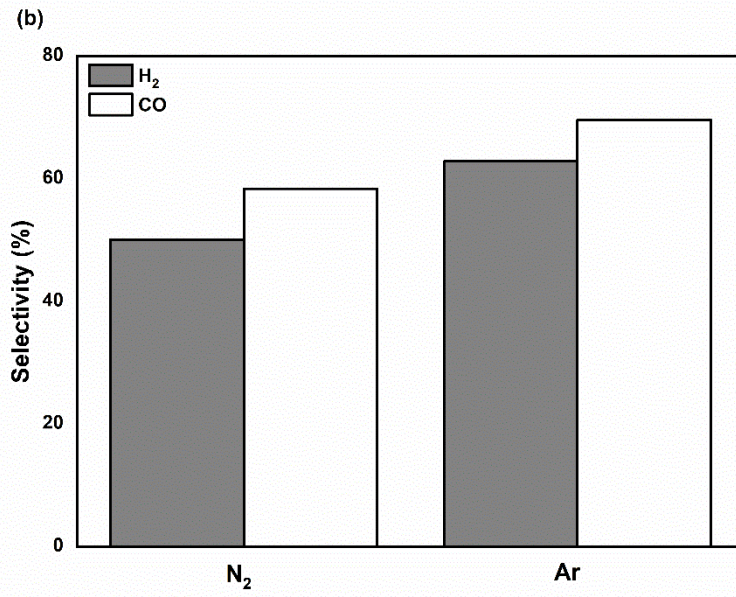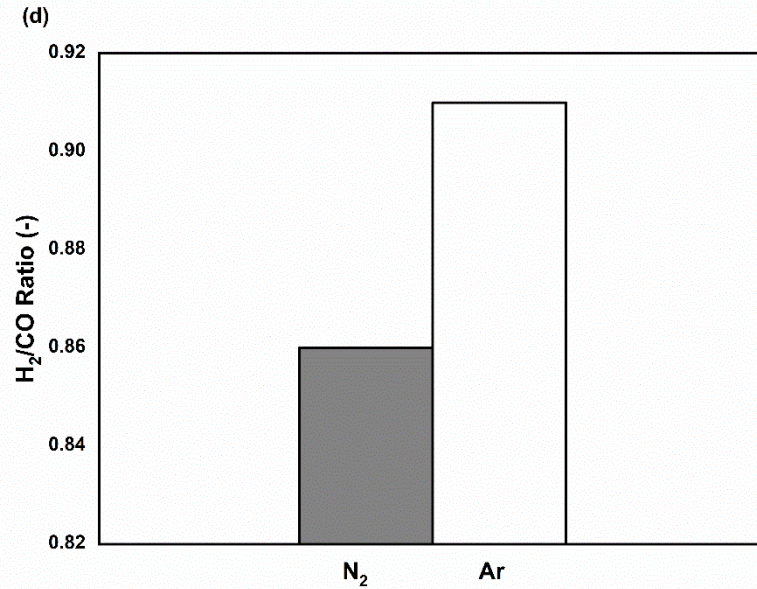
Figure 7. 6 Comparison overview between microwave-assisted DRM performed in N_2 atmosphere against that performed in Ar atmosphere (a) CH_4 and CO_2 Conversions; (b) H_2 and CO Selectivity; (c) H_2 and CO Yield; and (d) H_2/CO Ratio (MWP: 700 W; R: 2/1; TFR: 2.1 L min^{-1})

These results showed that the Ar case gave better performance relative to the N_2 case because in the N_2 case, ammonia and cyanide may be produced as side products (Equations (7-1) to (7-3)) (Indarto et al., 2006; Wnukowski & Jamróz, 2018). Moreover, it is also possible that in the N_2 case, N_2 reacts with O_2 to form various oxides of N_2 (Equation (7-4)) (Greenwood & Earnshaw, 2012). In the Ar case, however, Ar first collides with electrons and becomes excited (Desai, 1969) (Equation (7-5)). Then, the CH_4 and CO_2 molecules obtain energy from the excited Ar atoms instead of electrons (Equations (7-6) and (7-7)) (Zou, Zhang, & Liu, 2007). Therefore, Ar does not react with CH_4 and CO_2 to form any side products (Meija & Possolo, 2017).

$$N_2 + 3H_2 \rightarrow 2NH_3 \qquad\qquad (7\text{-}1)$$

$$N_2 + CO \rightarrow CN + NO \qquad\qquad (7\text{-}2)$$

$$CN + H_2 \rightarrow HCN + H \qquad\qquad (7\text{-}3)$$

$$N_2 + O_2 \rightarrow 2NO \qquad\qquad (7\text{-}4)$$

$$Ar + e \rightarrow Ar^* + e \qquad\qquad (7\text{-}5)$$

$$CH_4 + Ar^* \rightarrow CH_3 + H + Ar \qquad\qquad (7\text{-}6)$$

$$CO_2 + Ar^* \rightarrow CO + O + Ar \qquad\qquad (7\text{-}7)$$
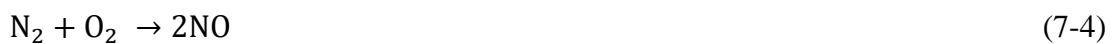
7.6 Conclusion

The results show that microwave-assisted dry reforming of CH_4 (DRM) in Ar atmosphere show identical performance trends as a function of additive gas flow rate, MWP, R inlet supply, TFR, and DRM performance stability. For example, as the Ar flow rate increased from 0.3 to 1.5 L min^{-1}, there are slight fluctuations in CH_4 and CO_2 conversions, H_2 and CO selectivities, and H_2 and CO yields as well as a minor reduction in H_2/CO ratio. Increasing MWP from 700 to 1200 W, in contrast, increased CH_4 and CO_2 conversions and CO selectivity and yield and decreased H_2 selectivity and yield, translating to a significant reduction in H_2/CO ratio. Furthermore, increasing the R inlet supply from 2 to 5 led to an apparent reduction in CO_2 conversion, H_2 selectivity, H_2 and CO yields, and H_2/CO ratio and an increase in CH_4 conversion and CO selectivity. In addition, increasing TFR from 0.45 to 2.1 L min^{-1} decreased the CH_4 and CO_2 conversions, H_2 and CO selectivities, yields, and H_2/CO ratio, while the H_2/CO ratio increased. Microwave-assisted DRM performance showed stability for up to 8 h-duration in Ar atmosphere. Despite these identical trends, at a constant MWP of 700 W, R of 2/1, and constant TFR of 2.1 L min^{-1}, respectively, DRM in Ar gave higher H_2 and CO selectivities and yields and higher H_2/CO ratio than DRM in N_2.

8

Chapter 8: Syngas Formation by Dry and Steam Reforming of Methane using Microwave Plasma Technology

8.1 Introduction

As mentioned previously (Chapters 1 and 2), there are many reforming technologies that can be used to produce syngas including SRM, POM, and DRM (Centi et al., 2013; Pacheco et al., 2015; Rowshanzamir & Eikani, 2009). These methods were explained deeply in Chapters 1 and 2. Anyway, the SRM (Equation 1-1, Chapter 1) is the most important process for syngas production at large scale because of its stability. The drawbacks of this highly endothermic reaction are the high-energy consumption and syngas ratio H_2/CO, which is not suitable for the F–T synthetic process. In recent years, the DRM (Equation 1-3, Chapter 1) has become an important technique that produces syngas from two main greenhouse gases (CH_4 and CO_2) (Hubert, Moisan, & Ricard, 1979; Usman et al., 2015). The reason for this is that it has environmental, economic, technical, and industrial advantages (Oyama et al., 2012). The limitation of DRM is the low-syngas ratio H_2/CO, which cannot be used to feed to the F–T process without H_2 addition. As a result, the combined SRM and DRM, abbreviated as CSDRM (Equation 2-5, Chapter 2), also known as bi-reforming of CH_4, has recently appeared as a promising technique because it can generate a suitable syngas for F–T process by using greenhouse gases and water (Noureldin et al., 2013; Olah et al., 2015). The syngas production with H_2/CO ratios of 2.0 can be produced and controlled by changing the composition of the feed gas (H_2O, CO_2, and CH_4) *via* the CSDRM method (Choudhary & Mondal, 2006; A. R. Kim et al., 2015; Pour & Mousavi, 2015). In recent days, some research results on CH_4 reforming by CO_2 and water by using microwave plasma are reported in the literature (Czylkowski et al., 2016; L. Li et al., 2016). From these studies, adding steam into DRM is effective and leads to increasing the conversion of CH_4, selectivity, and yield of H_2. Unfortunately, some knowledge gaps about the combined effects of the steam concentration and input MWP on the process performance and product quality have remained unknown. Therefore, the main aims of the present work will study the combined influence of the SC, MWP, TFR, and RT on the plasma stability and syngas production under microwave irradiation at atmospheric pressure. Moreover, the CSDRM and DRM results are compared.

8.2 Experimental set up

A microwave plasma system consisting of the following eight essential units were used: gas cylinders system, mass flow controllers system, gas mixer system, feed gas system, steam vapour system, plasma reactor system, microwave generator system, and gas chromatographic (GC-MSD and GC-TCD) analysis system. Further details about the experimental design and the calculation methodology can be found elsewhere in Chapter 3.

8.3 Results and Discussions
8.3.1 Steam Concentration

To understand the reaction pathway of CSDRM, the steam concentration was varied (5.5 – 42.5 vol. %) at a fixed feed flow rate of CH_4, CO_2, and N_2 of 0.008, 0.016, 0.062 mole min^{-1}, respectively; R of 2/1; and input MWP of 700 W (Table 3.3, Chapter 3). Figure 8.1(a–d) exhibit the effects of SC on the conversions of CH_4 and CO_2, the selectivities, yields of H_2 and CO, and the H_2/CO ratio. As shown in Figure 8.1(a–d), CH_4 conversion, selectivity and yield of H_2, and H_2/CO mole ratio increased from 74.35%, 66.78%, 49.65% and 1.4 to 82.74%, 98.79%, 81.73% and 5.23, respectively; whereas the conversion of CO_2 and the selectivity and yield of CO slightly decreased from 32.41%, 25.77%, and 35.34% to 19.23%, 18.87%, and 9.04% respectively, with increased SC. This difference is because the steam has more reductive and oxidative radicals (H, OH, and O) in the CSDRM process, and these radicals lead to increased CH_4 conversion, H_2, and CO selectivity, yield, and H_2/CO ratio (Jiang et al., 2002).

(a)

(b)
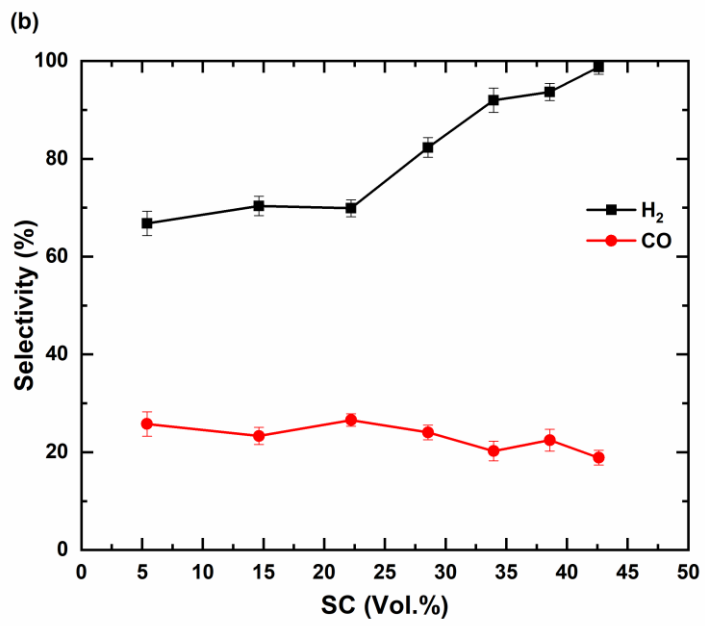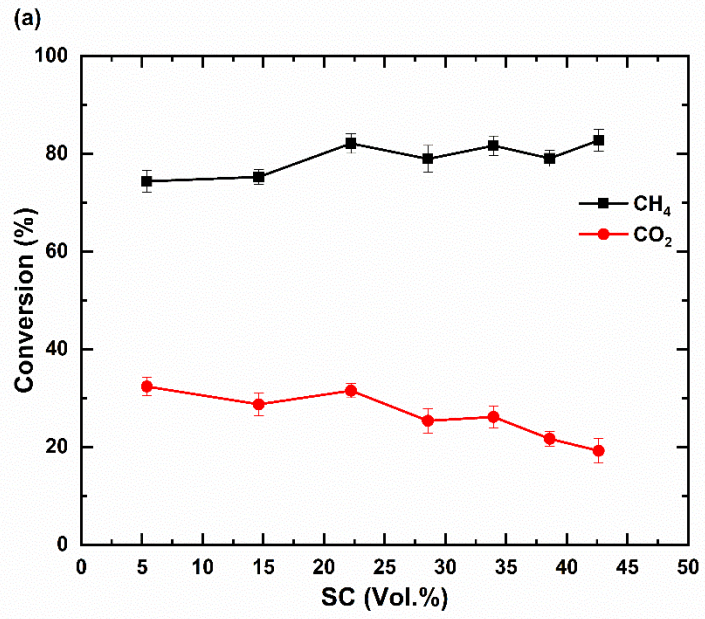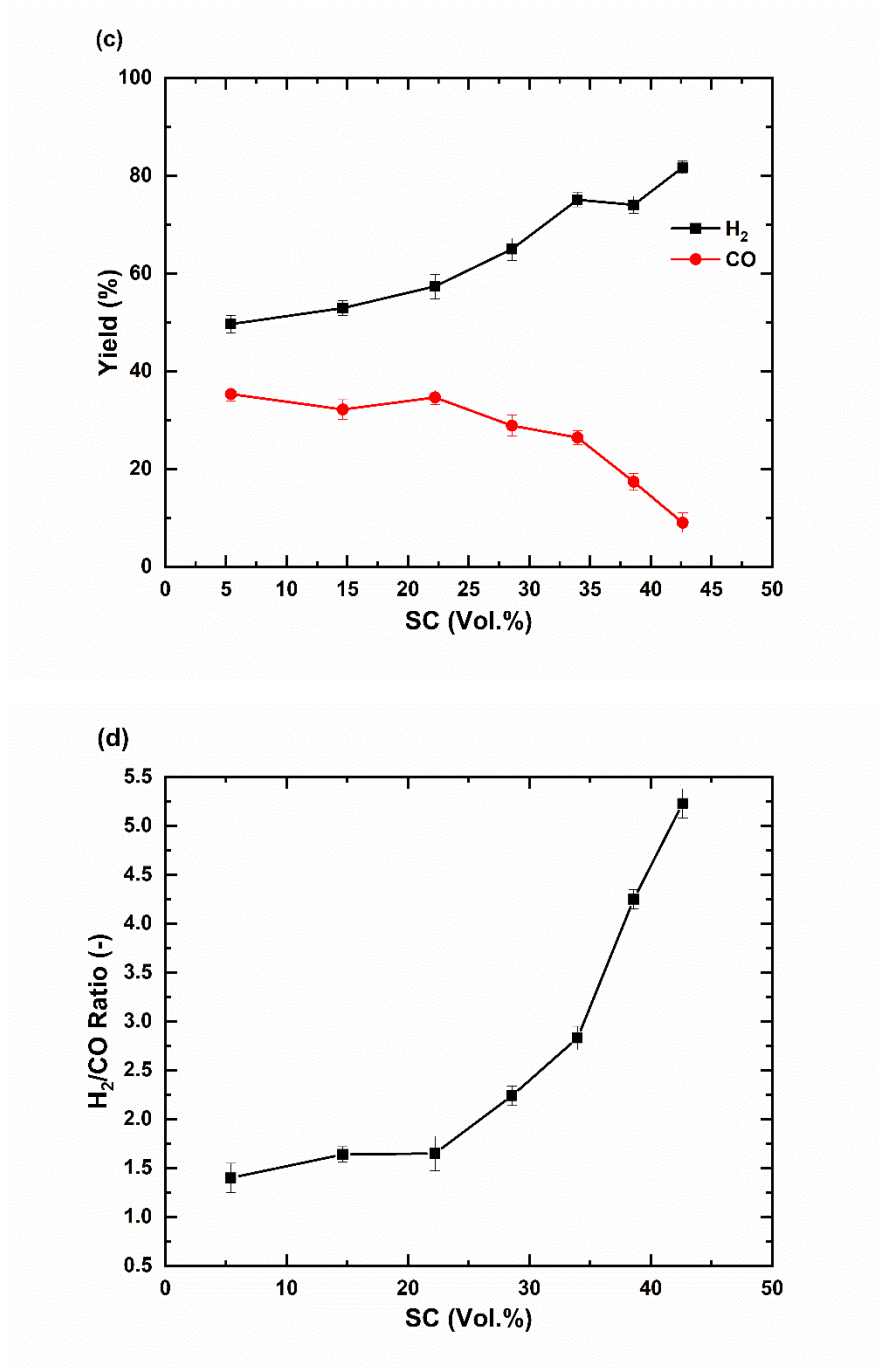
Figure 8. 1 Effect of SC on the microwave-assisted plasma SRM (a) Conversion of CH_4 and CO_2; (b) Selectivity of H_2 and CO; (C) Yield of H_2 and CO; (d) H_2/CO Ratio; (MWP at 700 W, R at 2/1 and TFR of CH_4, CO_2, N_2 at 0.086 mole min^{-1})

8.3.2 Effect of Microwave Power

It is well known, the input MWP is an important factor, which affects the plasma DRM and SRM as it supplies the requested energy for plasma formation. In other words, the input power will influence the density of the active species for the reaction. The conversions of CH_4 and CO_2, the selectivities and yields of H_2 and CO, and the H_2/CO ratio as a function of input microwave power under Ar of 2/1, and the TFR of 0.15 mole min^{-1}, respectively, as shown in Figure 8.2(a–d). The input MWP changed from 700 to 1200 W (Table 3.3, Chapter 3). Figure 8.2(a–c) depict the conversions of CH_4 and CO_2, the selectivity of CO and yields of H_2 and CO increased from 82.74%, 19.23%, 18.87%, 81.73% and 9.04% to 92.58%, 29.78%, 38.87%, 90.43% and 19.04%. While the ratio of H_2/CO decreased from 5.23 to 2.51with increasing the input MWP (Figure 8.2(d)). The reason for this has been explained previously (Chapter 6). The selectivity of H_2 is mostly constant (98.79% to 97.68%) with an increase in the MWP, as shown in Figure 8.2(b). In this study, we observed the amount of water, and the amount of solid carbon powder out the quartz tube low compared with the DRM, Chapter 6.

(b)

(c)
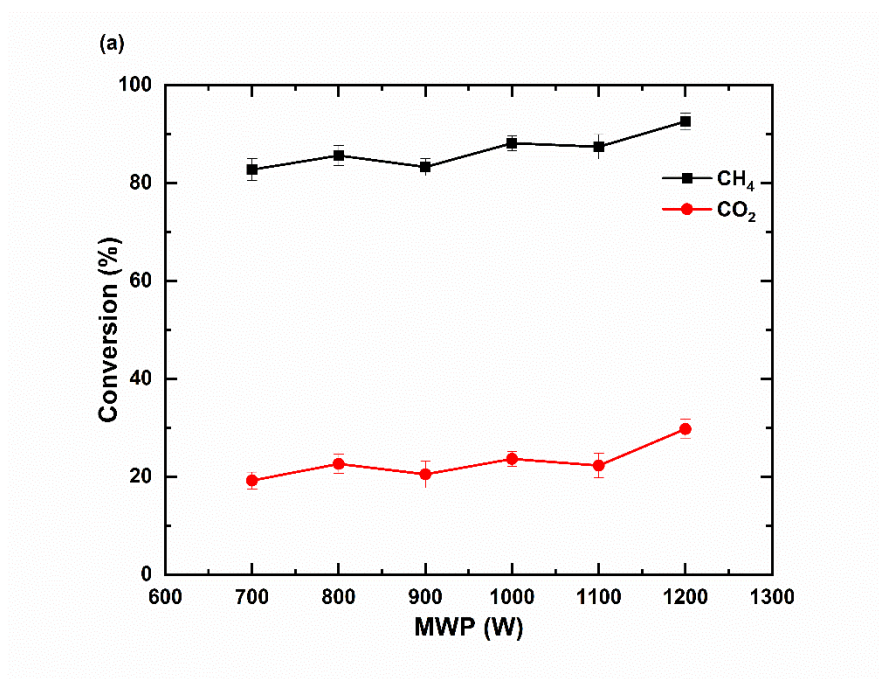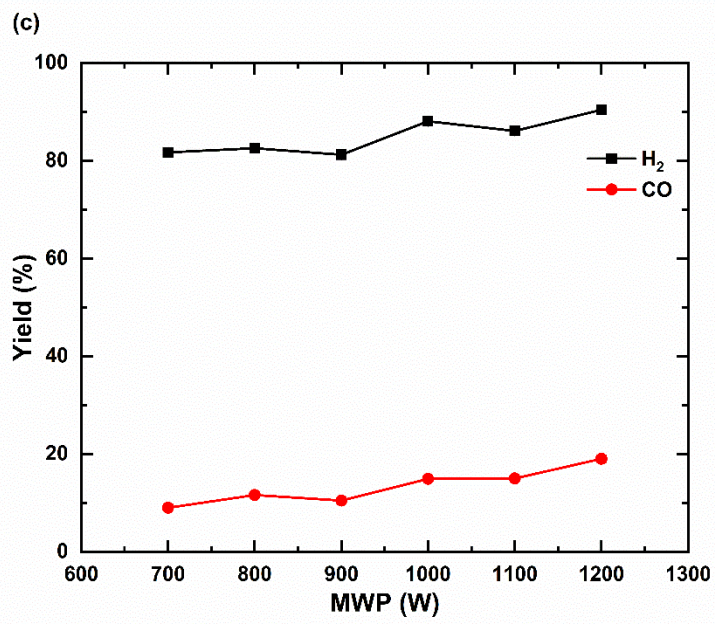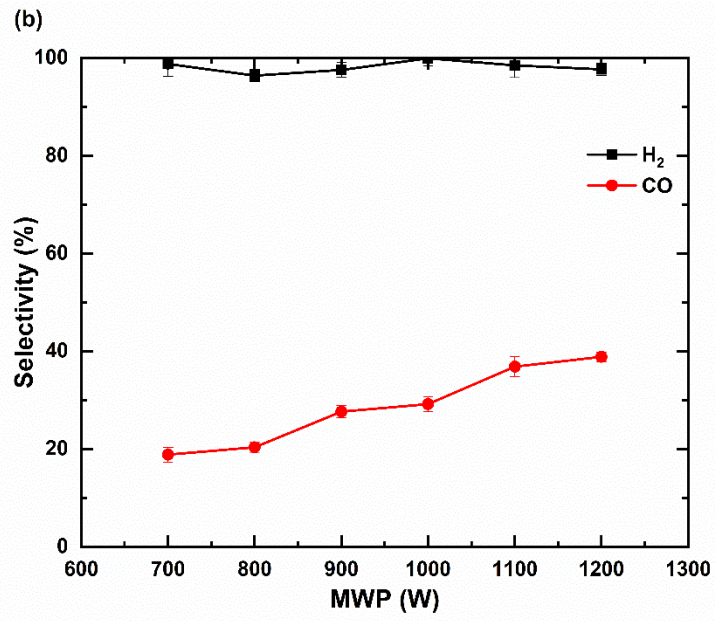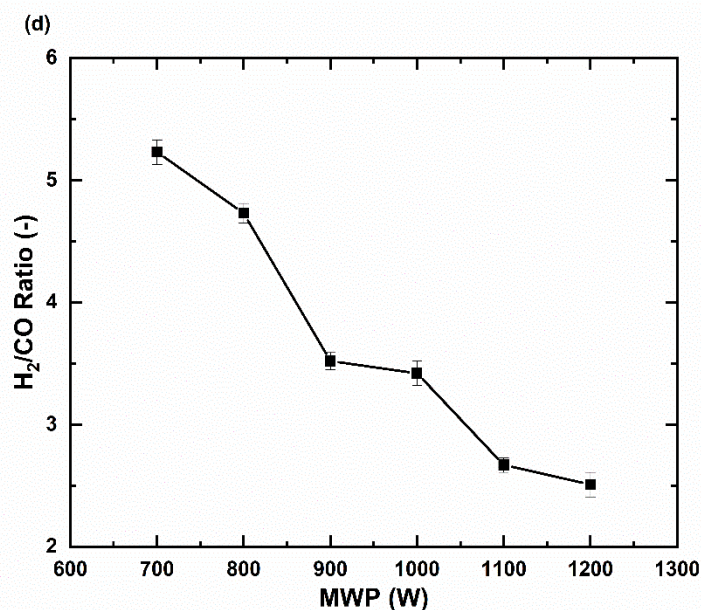
Figure 8. 2 Effect of MWP on the microwave-assisted plasma SRM (a) CH_4 and CO_2 Conversions; (b) H_2 and CO Selectivity; (c) H_2 and CO Yield; and (d) H_2/CO Ratio (R: 2/1; TFR at 0.15 mole min^{-1})

8.3.3 Effect of Total Feed Flow Rates

The steam additions have a noteworthy effect on the conversions of CH_4, and CO_2, the selectivities, yields of H_2 and CO, and the H_2/CO ratio are shown in Figure 8.3(a–d), respectively. The TFR of H_2O, CO_2, CH_4, and N_2 ranged from 0.02 to 0.15 mole min^{-1}, as keeping constant the input MWP of 700 W and R of 2/1 (Table 3.3, Chapter 3). As is expected, the CH_4 conversion, the H_2 selectivity and yield, and the H_2/CO ratio are enhanced from 69.23%, 63.21%, 43.76% and 1.39 to 82.74%, 98.79%, 81.73% and 5.23, respectively with increasing the TFR, pointing to the fact that combined reforming by H_2O and CO_2 is stronger than dry reforming (Figure 8.3(a–d)). This is because the steam molecules could dissociate into OH and H radicals, reacting with CH_4 and resulting in the lower probability of CH_4 recombination due to the production of CH_3 and other by-products (Bonard, Daële, Delfau, & Vovelle, 2002; Sutherland, Su, & Michael, 2001). The CH_4 reacted with H_2O instead of CO_2 with an increasing amount of steam in the feed stream because of the more stable nature of CO_2. In contrast, the increase of steam content caused a considerable decrease in the conversion of CO_2, CO selectivity and yield from 27.43 %, 28.33 % and 31.32 % to

19.23 %, 18.87 % and 9.04 %, as shown in Figure 8.3(a–c). Although higher steam amounts resulted in the more CH_4 conversion, H_2 selectivity, H_2 yield, and the H_2/CO ratio, increasing steam content did not favour CO_2 conversion, selectivity, and yield of CO due to the fixed R in the feed. The conversion of CO_2 was dampened as a result of the RWGS reaction (Equation (2-2, Chapter 2)).

(a)

(b)
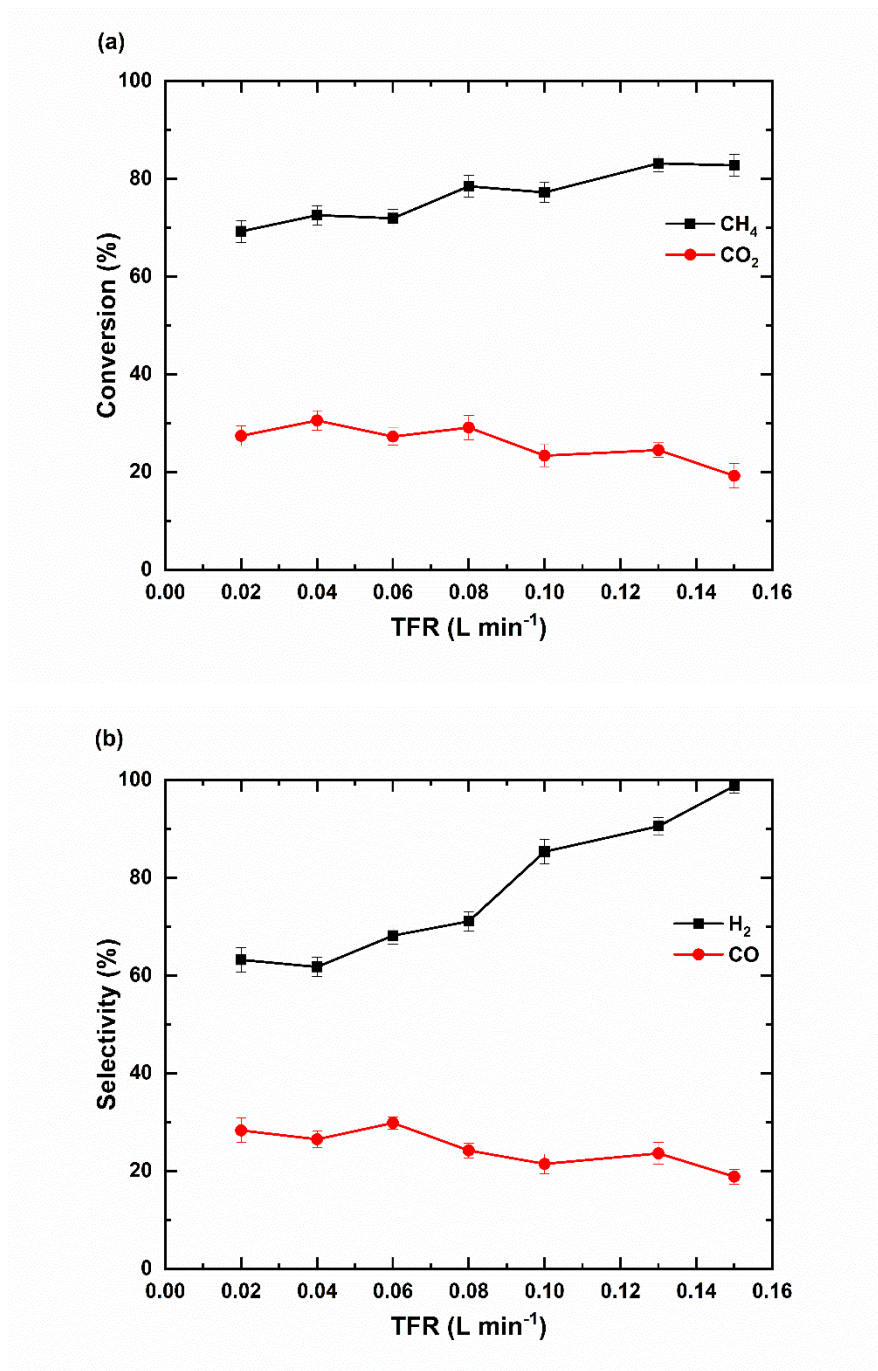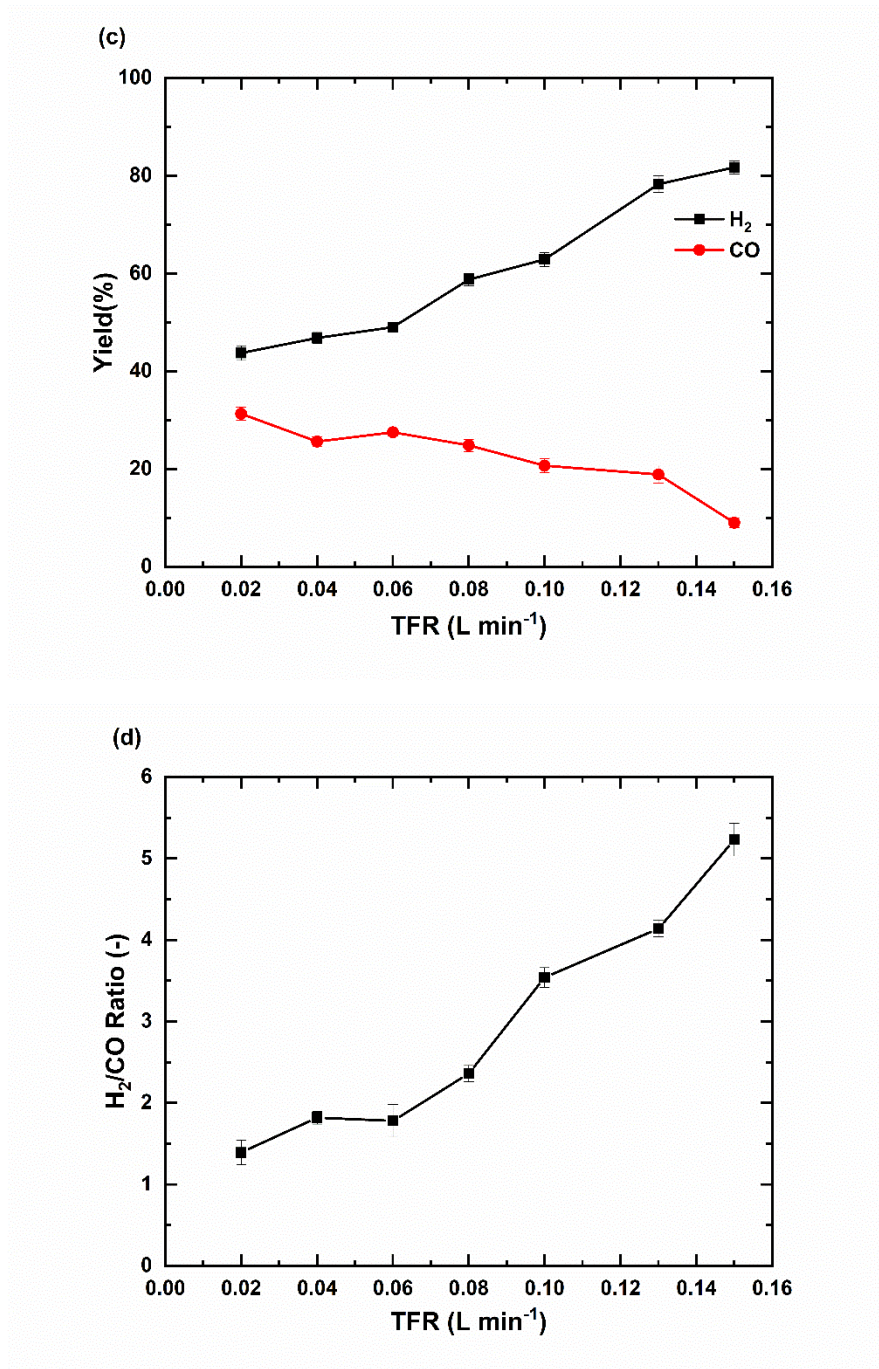
Figure 8. 3 Effect of TFR on the microwave-assisted plasma SRM (a) CH_4 and CO_2 Conversions; (b) H_2 and CO Selectivity; (c) H_2 and CO Yield; and (d) H_2/CO Ratio (MWP: 700 W; R: 2/1)

8.3.4 Effect of SRM Performance Stability

Stability of plasma with RT on the performance of SRM (CH_4 and CO_2 conversions, H_2 and CO selectivities and yields, and H_2/CO ratio) in the microwave plasma reactor at atmospheric pressure, the MWP (700 W), the R (2/1), and the TFR (0.15 mole min^{-1}) were investigated (Table 3.3, Chapter 3), as shown in Figure 8.4(a–d). The conversion of CH_4 and CO_2 are somewhat stable tend around median values of 82% and 19% with increase the RT from 20 min to 480 min, as shown in Figure 8.4(a). Also, the selectivities of H_2 and CO were somewhat stable tend around median values of 98% to 97%, and 18%, respectively with increase the RT, is illustrated in Figure 8.4(b). In Figure 8.4(c), the yields of H_2 and CO were somewhat stable tend also around median values of 81% to 83% and 9%, respectively. Moreover, the H_2/CO ratio is an almost stable trend from 5 with increase the RT, as shown in Figure 8.4(d). In brief, these results were found that all these parameters had a little effect following 8 h continuous reaction while the plasma flame remained stable.
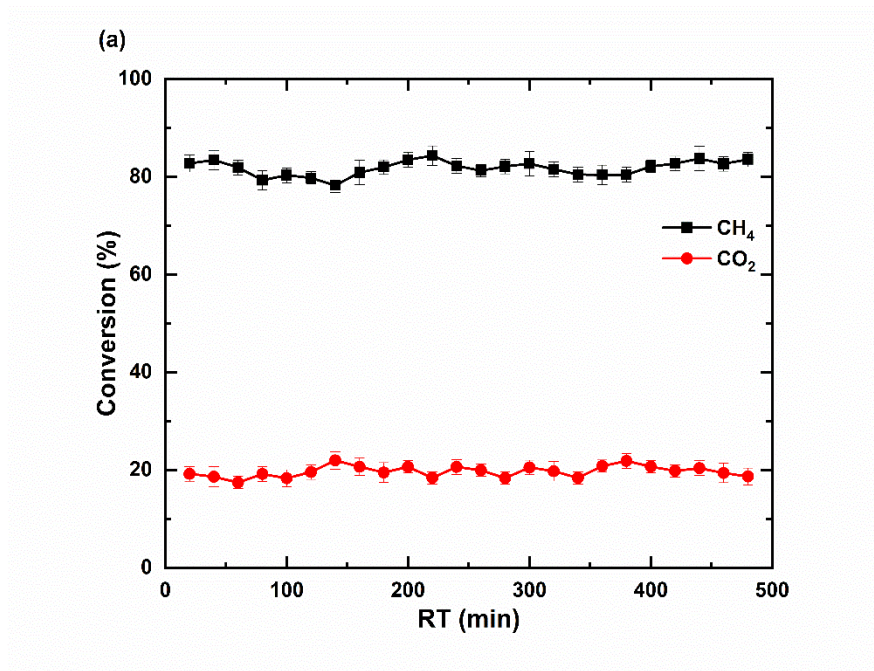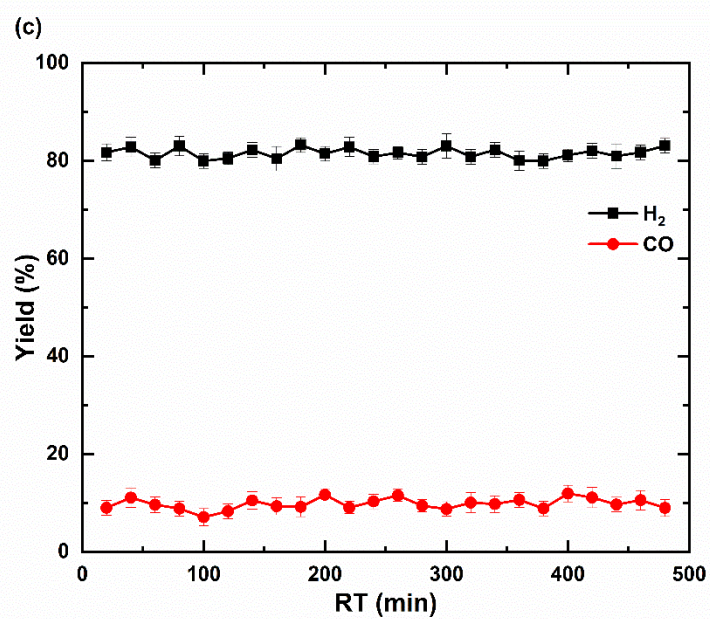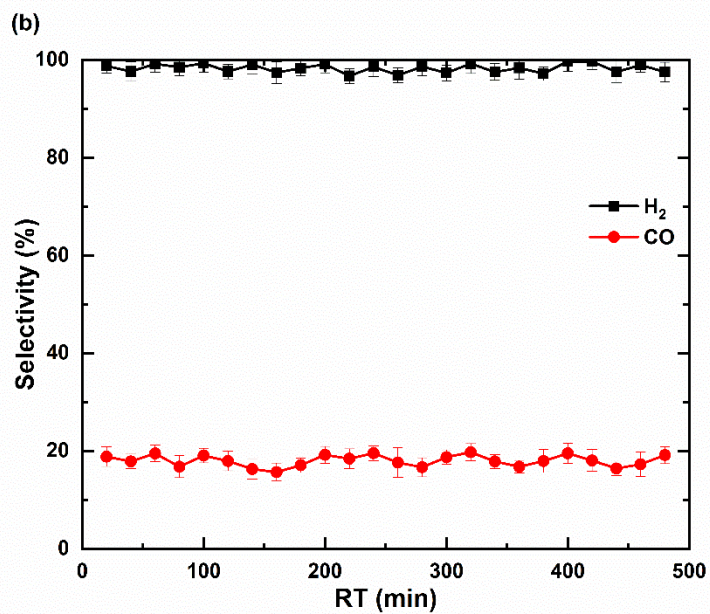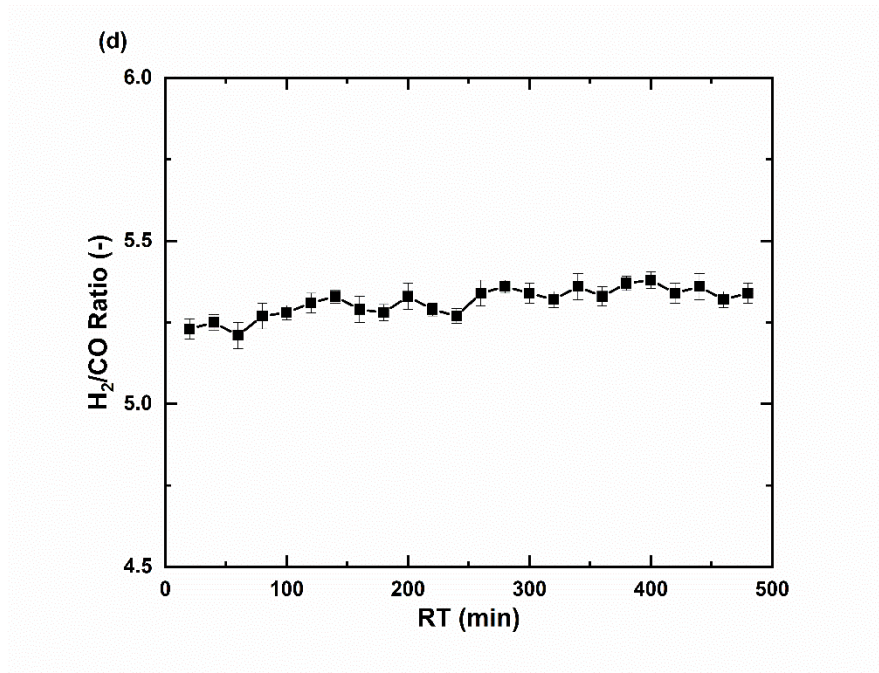
Figure 8. 4 Effect of SRM performance stability on the microwave-assisted plasma DRM (a) CH_4 and CO_2 Conversions; (b) H_2 and CO Selectivity; (c) H_2 and CO Yield; and (d) H_2/CO Ratio (MWP: 700 W; R: 2/1; TFR: 0.15 mole min^{-1})

8.4 SRM performance comparison overview

The combined effects of microwave plasma SRM with DRM (Chapter 6) were compared and are displayed in Figure 8.5(a–d). The combined DRM-SRM as a function of MWP at 700 W, R: 2/1, the TFR at 2.1 L min^{-1}, and the TFR at 0.15 mole min^{-1}, as shown in Figure 8.5(a–d). The conversions of CH_4 and CO_2 over DRM were 79.35%, and 44.82%, respectively, and the selectivities and yields of H_2 and CO, and the H_2/CO ratio were 50.12%, 58.42%, 39.77%, 32.89%, and 0.86, respectively. When the steam was added to DRM, the conversion of CH_4, selectivity and yield of H_2, and synthesis ratio improved, as shown in Figure 8.5(a–c), respectively. The conversions of CH_4 and CO_2 were 82.74% and 19.23% respectively. The selectivities, yields of H_2 and CO and the H_2/CO ratio were 98.79%, 18.87%, 81.73%, 9.04%, and 5.23, respectively. The conversions of CH_4 were 82.74% under combined steam and dry reforming of CH_4, which was higher than using the dry reforming of CH_4. Similar tendencies in the selectivity and yield of H_2 and H_2/CO ratio were also improved under combined steam and dry reforming of CH_4. However, the conversion of CO_2 decreased

by adding steam. The selectivity of H_2 was 98.79%, and that of H_2/CO ratio was 5.23, which was even higher than that obtained in DRM, which was presented in Chapter 6.
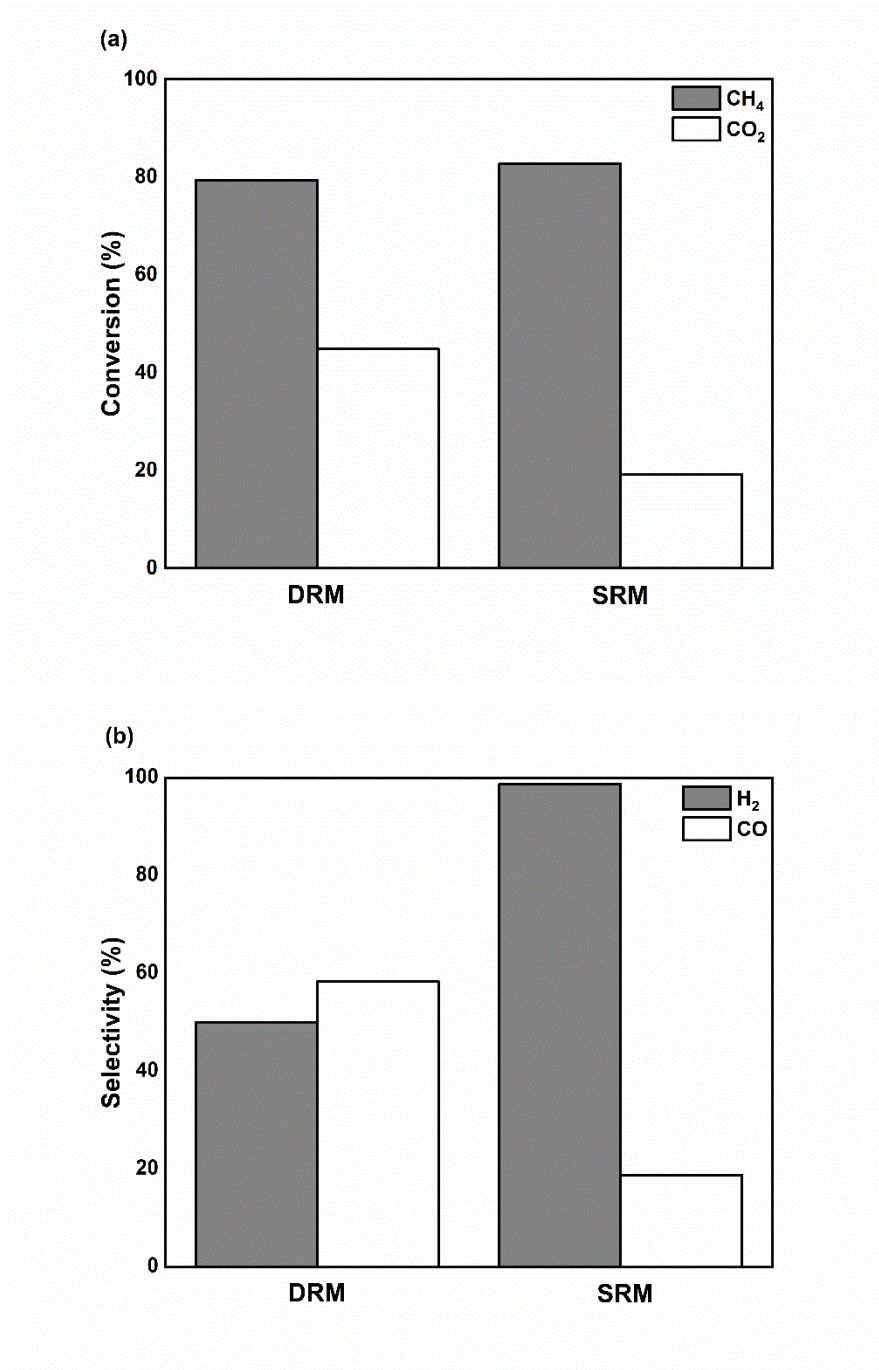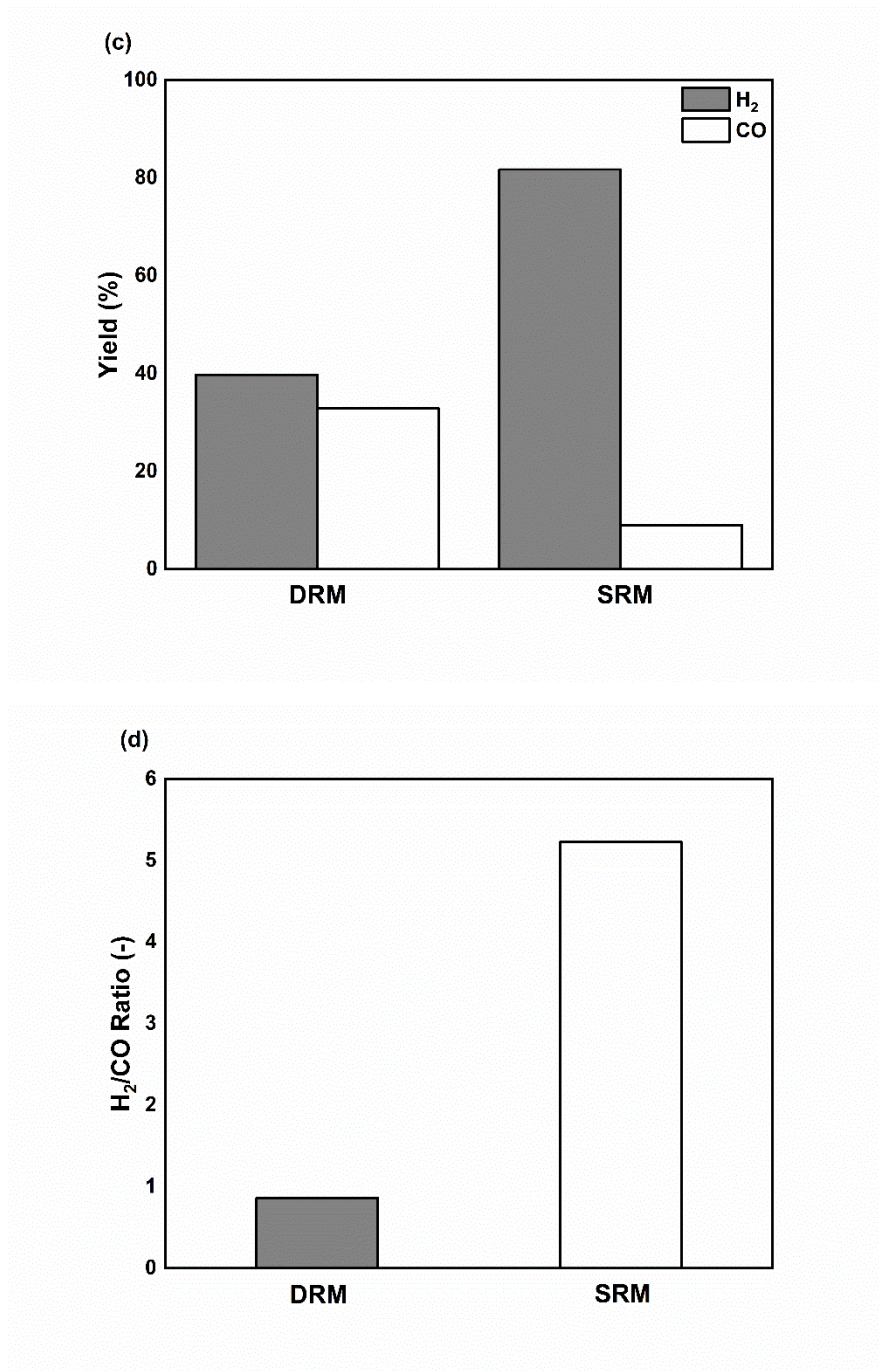
Figure 8. 5 Effect of H_2O on equilibrium (a) CH_4 and CO_2 Conversions; (b) H_2 and CO Selectivities; (c) H_2 and CO Yields and (d) H_2/CO Ratio for combined DR-SR as a function of MWP at 700 W (R: 2/1; the TFR at 2.1 L min^{-1} and the TFR at 0.15 mole min^{-1})

8.5 Conclusion

In this work, the effect of adding steam into the feed mixture i.e., CH_4 and CO_2 on the syngas formation has been studied by using a microwave-assisted plasma reactor at atmospheric pressure for syngas production. Based on the measured results, the following conclusions can be made:

1- With H_2O addition, the SRM can achieve high CH_4 and CO_2 conversions of 82.74% and 19.23%, respectively. At these conversion levels, the selectivities and yields of H_2 and CO, and H_2/CO ratio were 98.79%, 18.87%, 81.73%, 9.04%, and 5.23, respectively.

2- The CH_4 conversion, H_2, and CO selectivity, yields, and H_2/CO ratio were affected by the H_2O concentration in the feed significantly.

3- The combined SRM and DRM processes are very sensitive to operating conditions such as the input MWP and TFR.

4- The microwave-assisted plasma DRM performance was stable for up to 8 h at a constant MWP of 700 W, R of 2/1 and constant TFR of 0.15 mole min^{-1}, respectively.

5- The desired syngas ratio H_2/CO for the F–T process can be reached by optimising the H_2O concentration in the feed and input MWP.

9

Chapter 9: Conclusions and Recommendations for Future Work

9.1 Introduction

The DRM using plasma technology to produce syngas has been investigated widely in previous studies. However, research on the microwave-assisted plasma DRM at atmospheric pressure is very limited. Furthermore, studies on modelling and optimising microwave-assisted plasma DRM at different parameters such as MWP, R, TFR, and CH_4, CO_2, and N_2 flow rates are very limited. Therefore, this study strived to determine the optimum experimental conditions on plasma stability and syngas production. To accomplish this goal, a series of experimental and analytical tests were conducted on the microwave-assisted plasma DRM in a wide range of the MWP, R, and TFR. Moreover, the relationship between the impact of different process parameters and their interaction was investigated by the BBD method on the terms of the CH_4 and CO_2 conversions, H_2 and CO selectivities and yields, and H_2/CO ratio. In addition, the effects of additive gas at the same experimental conditions on the process performance by using different feed gas flow rates for N_2 and Ar flow rates of MWP, R, and TFR were studied and discussed. The findings of using the N_2 and Ar gases in terms of the process performance were also compared. Furthermore, the combined effect of adding the steam into DRM in terms of steam concentration, MWP, and TFR was investigated. The CSDRM and DRM were also compared in terms of MWP. In addition, based on the conclusions from this research, several recommendations are suggested for future work to improve the knowledge in this research area.

9.2 Conclusions

1- The results showed that the effects of MWP and TFR were significant on the CO_2 and CH_4 conversions, H_2 selectivity, and H_2/CO ratio, while the R had a significant effect on the CO selectivity and H_2 and CO yields. The CO_2 and CH_4 conversions, H_2 selectivity, and H_2/CO ratio increased with increased MWP and TFR, while they decreased with increased R. In contrast, the CO selectivity and H_2 and CO yields were increased with increased R, but they decreased with increased MWP and TFR. In addition, the interactive term coefficient of MWP-R has a significant effect on the H_2 selectivity, while the

MWP-TFR and R-TFR had a weak significant on the CO_2, CH_4 conversions, H_2 and CO selectivities and yields, and H_2/CO ratio. The effects of the MWP, R, and TFR quadratic term coefficients had significant effects on the CO_2, CH_4 conversions, H_2 and CO selectivities and yields, and H_2/CO ratio, respectively.

2- Experimental results exhibited that for the CO_2 and CH_4 conversions, H_2 and CO selectivities, and H_2 and CO yields, the molar ratio of H_2/CO are decreased with increased gas feed flow rate. The CO_2 flow rate has a significant effect on the CO_2 and CH_4 conversions, H_2 and CO selectivities and yields, and H_2/CO ratio, followed by CH_4 and N_2 flow rates. In addition, the interactions CH_4-CO_2, CH_2-N_2, and CO_2-N_2 gas flow rates have a very weak effect on CH_4 and CO_2 conversions, H_2 and CO selectivities and yields, and H_2/CO ratio. The quadratic term coefficients of CH_4, CO_2, and N_2 are significant on the conversions of CO_2 and CH_4, selectivity and yield of H_2 and CO, and molar ratio of H_2/CO.

3- Although the regression models were successful in predicting the CO_2 and CH_4 conversions, H_2 and CO selectivities and yields, and H_2/CO ratio, they still have certain limitations. The limitations in the present work might be related to some sources such as the plasma stability, input MWP, amount of CO_2/CH_4 ratio, flow rate of CH_4, CO_2, and N_2 gases, amount of data, type of software, and type of regression analysis. Therefore, the findings of this work should be used carefully to account for the limitations presented.

4- It was found that the CH_4 and CO_2 conversions, H_2 and CO selectivities and yields, and H_2/CO ratio decreased with increased N_2 flow rate. The results also demonstrated that the CH_4 and CO_2 conversions, selectivity, and yield of CO increased with increased MWP; while the selectivity and yield of H_2 and CO and the ratio of H_2/CO decreased. With increased R, the conversion of CH_4 and the selectivity of CO increased, but the conversion of CO_2, selectivity of H_2, yields of H_2 and CO, and ratio of H_2/CO decreased. Moreover, the conversions of CH_4 and CO_2 and the selectivities and yields of H_2 and CO changed little with increasing the TFR while clearly increasing the H_2/CO ratio.

5- Adding Ar slightly improved in the CH_4 and CO_2 conversions, and H_2 and CO selectivities H_2 and CO yields increased with increasing Ar flow rate; however, the H_2/CO ratio slightly decreased as Ar was added. In addition, the CH_4 and CO_2 conversions, CO selectivity, and yield increased, but the H_2 selectivity and

yield and the H_2/CO ratio decreased with increased MWP. Furthermore, the CH_4 conversion and CO selectivity increased with increased R, while the CO_2 conversion, H_2 selectivity, H_2 and CO yields, and H_2/CO ratio decreased. In addition, the CH_4 and CO_2 conversions, H_2 and CO selectivities, yields, and H_2/CO ratio decreased with increasing TFR, but the H_2/CO ratio increased. When comparing the results of Ar with N_2 at the same experimental conditions, the results showed that the Ar gave a higher H_2, CO selectivities and yields, and H_2/CO ratio than N_2.

6- The presence of steam also improved the conversion of CH_4, selectivity, and yield of H_2, and synthesis ratio, while the CO_2 conversion, selectivity, and yield of CO reduced with increased steam concentration. Furthermore, the CH_4 and CO_2 conversions, H_2 yield, CO yield, and selectivity increased, but the H_2/CO ratio decreased with increasing MWP. In contrast, there was not a noticeable increase in H_2 selectivity with increased MWP. In addition, the conversion of CH_4, selectivity and yield of H_2, and H_2/CO ratio increased, while the CO_2 conversion, CO selectivity, and yield decreased with increasing TFR. The results of SRM were higher with DRM at the same experimental conditions.

9.3 Recommendations for Future Work

1- Because some parameters may affect the plasma stability and syngas production, an additional study can be conducted by using a wide range of feed flow rate, microwave power, and CO_2/CH_4 ratio.

2- Further experimental study on the effects of using catalyst on plasma stability and syngas production is required. Moreover, a comparison with and without a catalyst on the process performance is highly recommended to perform.

3- Further experimental investigations on the effects of microwave irradiation direction on plasma stability and syngas production are required. In addition, a comparison between the horizontal and vertical microwave irradiation direction should be done.

4- The effect of the syngas ratio on liquid fuel production by the Fischer–Tropsch synthesis process under a wide range of temperatures and pressures has not

been investigated in this thesis. Therefore, additional investigations considering these conditions are required.

5- Presenting a mathematic model for the process and comparing the created model based on the experimental data will be of interest to the field.

6- Further RSM modelling by using other software programs and a wide range of input datasets is required.

References

Aasberg-Petersen, K., Christensen, T. S., Nielsen, C. S., & Dybkjær, I. (2003). Recent developments in autothermal reforming and pre-reforming for synthesis gas production in GTL applications. *Fuel Processing Technology, 83*(1-3), 253-261.

Abbasi, M., Niaei, A., Salari, D., Hosseini, S., Abedini, F., & Marmarshahi, S. (2017). Modeling and optimization of synthesis parameters in nanostructure La 1− xBaxNi 1− yCuyO 3 catalysts used in the reforming of methane with CO 2. *Journal of the Taiwan Institute of Chemical Engineers, 74*, 187-195.

Abdullah, B., Ghani, N. A. A., & Vo, D.-V. N. (2017). Recent advances in dry reforming of methane over Ni-based catalysts. *J. Clean Prod., 162*, 170-185.

Abedini, F., Hosseini, S. A., Niaei, A., Salari, D., Abbasi, M., & Marmarshahi, S. (2017). Design and optimization of new La1− xCexNi1− yFeyO3 (x, y= 0–0.4) nano catalysts in dry reforming of methane. *International Journal of Green Energy*, 1-8.

Abolentsev, V., Korobtsev, S., & Medvedev, D. (1995). Pulsed {open_quotes} wet {close_quotes} discharge as an effective means of gas purification from H {sub 2} S and organosulfur impurities. *High Energy Chemistry, 29*(5).

Adris, A., Elnashaie, S., & Hughes, R. (1991). A fluidized bed membrane reactor for the steam reforming of methane. *The Canadian Journal of Chemical Engineering, 69*(5), 1061-1070.

Ahmadpour, J., & Taghizadeh, M. (2015). Catalytic conversion of methanol to propylene over high-silica mesoporous ZSM-5 zeolites prepared by different combinations of mesogenous templates. *Journal of Natural Gas Science and Engineering, 23*, 184-194.

Akande, A., Aboudheir, A., Idem, R., & Dalai, A. (2006). Kinetic modeling of hydrogen production by the catalytic reforming of crude ethanol over a co-precipitated Ni-Al2O3 catalyst in a packed bed tubular reactor. *International Journal of Hydrogen Energy, 31*(12), 1707-1715.

Akbari-Emadabadi, S., Rahimpour, M., Hafizi, A., & Keshavarz, P. (2017). Production of hydrogen-rich syngas using Zr modified Ca-Co bifunctional catalyst-sorbent in chemical looping steam methane reforming. *Applied Energy, 206*, 51-62.

Al-Sobhi, S., & Elkamel, A. (2015). Simulation and optimization of natural gas processing and production network consisting of LNG, GTL, and methanol facilities. *Journal of Natural Gas Science and Engineering, 23*, 500-508.

Alketife, A. M., Judd, S., & Znad, H. (2017). Synergistic effects and optimization of nitrogen and phosphorus concentrations on the growth and nutrient uptake of a freshwater Chlorella vulgaris. *Environmental technology, 38*(1), 94-102.

Allah, Z. A., & Whitehead, J. C. (2015). Plasma-catalytic dry reforming of methane in an atmospheric pressure AC gliding arc discharge. *Catalysis Today, 256*, 76-79.

Alper, E., & Orhan, O. Y. (2017). CO2 utilization: Developments in conversion processes. *Petroleum, 3*(1), 109-126.

Álvarez Galván, M. C., Trunschke, A., Falcon, H., Sánchez Sánchez, M., Campos Martín, J. M., Schlögl, R., & García Fierro, J. L. (2018). Microwave-assisted coprecipitation synthesis of LaCoO3 nanoparticles and their catalytic activity for syngas production by partial oxidation of methane.

Aparna, K., Basak, T., & Balakrishnan, A. (2007). Role of metallic and composite (ceramic–metallic) supports on microwave heating of porous dielectrics. *International Journal of Heat and Mass Transfer, 50*(15-16), 3072-3089.

Araszkiewicz, M., Koziol, A., Lupinska, A., & Lupinski, M. (2007). IR technique for studies of microwave assisted drying. *Drying technology, 25*(4), 569-574.

Aresta, M., Dibenedetto, A., & Angelini, A. (2013). The use of solar energy can enhance the conversion of carbon dioxide into energy-rich products: stepping towards artificial photosynthesis. *Phil. Trans. R. Soc. A, 371*(1996), 20120111.

Ashcroft, A., Cheetham, A. K., Green, M., & Vernon, P. (1991). Partial oxidation of methane to synthesis gas using carbon dioxide. *Nature, 352*(6332), 225-226.

Aw, M. S., Crnivec, I. G. O., Djinovic, P., & Pintar, A. (2014). Strategies to enhance dry reforming of methane: Synthesis of ceria-zirconia/nickelecobalt catalysts by freeze-drying and NO calcination. *International Journal of Hydrogen Energy, 39*(12636), e12647.

Ayodele, B. V., Khan, M. R., Nooruddin, S. S., & Cheng, C. K. (2017). Modelling and optimization of syngas production by methane dry reforming over samarium oxide supported cobalt catalyst: response surface methodology and artificial neural networks approach. *Clean Technologies and Environmental Policy, 19*(4), 1181-1193.

Aziznia, A., Bozorgzadeh, H. R., Seyed-Matin, N., Baghalha, M., & Mohamadalizadeh, A. (2012). Comparison of dry reforming of methane in low temperature hybrid plasma-catalytic corona with thermal catalytic reactor over Ni/γ-Al 2 O 3. *J. Nat. Gas Chem., 21*(4), 466-475.

Beenakker, C. (1976). A cavity for microwave-induced plasmas operated in helium and argon at atmospheric pressure. *Spectrochimica Acta Part B: Atomic Spectroscopy, 31*(8-9), 483-486.

Behroozsarand, A., & Zamaniyan, A. (2017). Simulation and optimization of an integrated GTL process. *Journal of cleaner production, 142*, 2315-2327.

Bo, Z., Yan, J., Li, X., Chi, Y., & Cen, K. (2008). Plasma assisted dry methane reforming using gliding arc gas discharge: effect of feed gases proportion. *International Journal of Hydrogen Energy, 33*(20), 5545-5553.

Bo, Z., Yang, Y., Chen, J., Yu, K., Yan, J., & Cen, K. (2013). Plasma-enhanced chemical vapor deposition synthesis of vertically oriented graphene nanosheets. *Nanoscale, 5*(12), 5180-5204.

Boenig, H. V. (1988). *Fundamentals of plasma chemistry and technology*: CRC.

Bogaerts, A., & Alves, L. L. (2017). Special issue on numerical modelling of low-temperature plasmas for various applications—part II: Research papers on numerical modelling for various plasma applications. *Plasma Processes and Polymers, 14*(4-5), 1790041.

Bogaerts, A., Neyts, E., Gijbels, R., & van der Mullen, J. (2002). Gas discharge plasmas and their applications. *Spectrochimica Acta Part B: Atomic Spectroscopy, 57*(4), 609-658.

Bonard, A., Daële, V., Delfau, J.-L., & Vovelle, C. (2002). Kinetics of OH Radical Reactions with Methane in the Temperature Range 295− 660 K and with Dimethyl Ether and Methyl-tert-butyl Ether in the Temperature Range 295− 618 K. *The Journal of Physical Chemistry A, 106*(17), 4384-4389.

Bonizzoni, G., & Vassallo, E. (2002). Plasma physics and technology; industrial applications. *Vacuum, 64*(3-4), 327-336.

Boulos, M. I., Fauchais, P., & Pfender, E. (2013). *Thermal plasmas: fundamentals and applications*: Springer Science & Business Media.

Bradford, M., & Vannice, M. (1999). CO2 reforming of CH4. *Catal. Rev.-Sci. Eng., 41*(1), 1-42.

Bruggeman, P. J., Iza, F., & Brandenburg, R. (2017). Foundations of atmospheric pressure non-equilibrium plasmas. *Plasma Sources Science and Technology, 26*(12), 123002.

Budiman, A. W., Song, S.-H., Chang, T.-S., Shin, C.-H., & Choi, M.-J. (2012). Dry reforming of methane over cobalt catalysts: a literature review of catalyst development. *Catalysis Surveys from Asia, 16*(4), 183-197.

Caballero, A., & Pérez, P. J. (2013). Methane as raw material in synthetic chemistry: The final frontier. *Chemical Society Reviews, 42*(23), 8809-8820.

Caldeira, K., & Wickett, M. E. (2005). Ocean model predictions of chemistry changes from carbon dioxide emissions to the atmosphere and ocean. *Journal of Geophysical Research: Oceans, 110*(C9).

Centi, G., Quadrelli, E. A., & Perathoner, S. (2013). Catalysis for CO 2 conversion: a key technology for rapid introduction of renewable energy in the value chain of chemical industries. *Energy Environ. Sci., 6*(6), 1711-1731.

Cha-um, W., Rattanadecho, P., & Pakdee, W. (2009). Experimental analysis of microwave heating of dielectric materials using a rectangular wave guide (MODE: TE10)(case study: water layer and saturated porous medium). *Experimental Thermal and Fluid Science, 33*(3), 472-481.

Chabert, P., & Braithwaite, N. (2011). *Physics of radio-frequency plasmas*: Cambridge University Press.

Challiwala, M. S., Ghouri, M. M., Sengupta, D., El-Halwagi, M. M., & Elbashir, N. O. (2017). A Process Integration Approach to the Optimization of CO2 Utilization via Tri-Reforming of Methane. In *Computer Aided Chemical Engineering* (Vol. 40, pp. 1993-1998): Elsevier.

Chandrasekaran, S., Ramanathan, S., & Basak, T. (2012). Microwave material processing—a review. *AIChE Journal, 58*(2), 330-363.

Chandrasekaran, S., Ramanathan, S., & Basak, T. (2013). Microwave food processing—A review. *Food Research International, 52*(1), 243-261.

Chang, J.-S., Lawless, P. A., & Yamamoto, T. (1991). Corona discharge processes. *IEEE Transactions on plasma science, 19*(6), 1152-1166.

Chen, G., Silva, T., Georgieva, V., Godfroid, T., Britun, N., Snyders, R., & Delplancke-Ogletree, M. P. (2015). Simultaneous dissociation of CO2 and H2O to syngas in a surface-wave microwave discharge. *International Journal of Hydrogen Energy, 40*(9), 3789-3796.

Chen, H.-L., Li, T., Liang, Y., Sun, B., & Li, Q.-L. (2017). Experimental study of temperature distribution in rubber material during microwave heating and vulcanization process. *Heat and Mass Transfer, 53*(3), 1051-1060.

Chen, W., Zhao, G., Xue, Q., Chen, L., & Lu, Y. (2013). High carbon-resistance Ni/CeAlO3-Al2O3 catalyst for CH4/CO2 reforming. *Applied Catalysis B, 136*, 260-268.

Chen, X., Lan, L., Lu, H., Wang, Y., Wen, X., Du, X., & He, W. (2017). Numerical simulation of Trichel pulses of negative DC corona discharge based on a plasma chemical model. *Journal of Physics D: Applied Physics, 50*(39), 395202.

Chhawchharia, S., Sahoo, S. K., Balamurugan, M., Sukchai, S., & Yanine, F. (2018). Investigation of wireless power transfer applications with a focus on renewable energy. *Renewable and Sustainable Energy Reviews, 91*, 888-902.

Choi, D. H., Chun, S. M., Ma, S. H., & Hong, Y. C. (2016). Production of hydrogen-rich syngas from methane reforming by steam microwave plasma. *Journal of Industrial and Engineering Chemistry, 34*, 286-291.

Choudhary, V. R., & Mondal, K. C. (2006). CO2 reforming of methane combined with steam reforming or partial oxidation of methane to syngas over NdCoO3 perovskite-type mixed metal-oxide catalyst. *Applied Energy, 83*(9), 1024-1032.

Choudhary, V. R., & Rajput, A. M. (1996). Simultaneous Carbon Dioxide and Steam Reforming of Methane to Syngas over NiO− CaO Catalyst. *Industrial & engineering chemistry research, 35*(11), 3934-3939.

Chun, S. M., Hong, Y. C., & Choi, D. H. (2017). Reforming of methane to syngas in a microwave plasma torch at atmospheric pressure. *Journal of CO2 Utilization, 19*, 221-229.

Chun, Y. N., & Lim, M. S. (2018). Produced Gas Conversion of Microwave Carbon Receptor Reforming. *World Academy of Science, Engineering and Technology, International Journal of Environmental, Chemical, Ecological, Geological and Geophysical Engineering, 12*(1), 17-23.

Chung, W.-C., & Chang, M.-B. (2016). Dry reforming of methane by combined spark discharge with a ferroelectric. *Energy Conversion and Management, 124*, 305-314.

Clark, D. E., Folz, D. C., & West, J. K. (2000). Processing materials with microwave energy. *Materials Science and Engineering: A, 287*(2), 153-158.

Clark, D. E., & Sutton, W. H. (1996). Microwave processing of materials. *Annual Review of Materials Science, 26*(1), 299-331.

Cleiren, E., Heijkers, S., Ramakers, M., & Bogaerts, A. (2017). Dry Reforming of Methane in a Gliding Arc Plasmatron: Towards a Better Understanding of the Plasma Chemistry. *ChemSusChem, 10*(20), 4025-4036.

Conrads, H., & Schmidt, M. (2000). Plasma generation and plasma sources. *Plasma Sources Science and Technology, 9*(4), 441.

Crabtree, R. H. (1995). Aspects of methane chemistry. *Chemical Reviews, 95*(4), 987-1007.

Croslyn, A., Smith, B., & Winefordner, J. (1997). A review of microwave plasma sources in atomic emission spectrometry: literature from 1985 to the present. *Critical Reviews in Analytical Chemistry, 27*(3), 199-255.

Culp, R. C., & Ng, K. C. (1995). Recent developments in analytical microwave-induced plasmas. *Adv. At. Spectrosc., 2*, 215.

Czylkowski, D., Hrycak, B., Jasiński, M., Dors, M., & Mizeraczyk, J. (2016). Microwave plasma-based method of hydrogen production via combined steam reforming of methane. *Energy, 113*, 653-661.

Datta, A. K. (2001). *Handbook of microwave technology for food application*: CRC Press.

De Bie, C., van Dijk, J., & Bogaerts, A. (2015). The dominant pathways for the conversion of methane into oxygenates and syngas in an atmospheric pressure dielectric barrier discharge. *The Journal of Physical Chemistry C, 119*(39), 22331-22350.

Desai, S. V. (1969). *Thermodynamic and kinetic behavior of an argon plasma jet. Decomposition of nitric oxide between 1300-1750 degrees K in an argon plasma.* California Institute of Technology, USA.

Ehrgott, M. (2005). *Multicriteria optimization* (Vol. 491): Springer Science & Business Media.

El Hassani, K., Beakou, B., & Anouar, A. (2018). Analysis of adsorption of azo dye onto NiAl-CO3 using Box-Behnken design approach and desirability function.

Eliasson, B., & Kogelschatz, U. (1991). Nonequilibrium volume plasma chemical processing. *IEEE transactions on plasma science, 19*(6), 1063-1077.

Espiau, F. M., & Chang, Y. (2009). Microwave energized plasma lamp with dielectric waveguide. In: Google Patents.

Fakeeha, A. H., Ibrahim, A. A., Naeem, M. A., & Al–Fatesh, A. S. (2014). *Energy Source from Hydrogen Production by Methane Dry Reforming.* Paper presented at the Proceedings of the 2014 International Conference on Industrial Engineering and Operations Management Bali, Indonesia.

Falk, M., & Issels, R. (2001). Hyperthermia in oncology. *International Journal of Hyperthermia, 17*(1), 1-18.

Ferreira, C. M., & Moisan, M. (2013). *Microwave discharges: fundamentals and applications* (Vol. 302): Springer Science & Business Media.

Fidalgo, B., & Menéndez, J. (2012). Study of energy consumption in a laboratory pilot plant for the microwave-assisted CO2 reforming of CH4. *Fuel processing technology, 95*, 55-61.

Figen, H. E., & Baykara, S. Z. (2018). Effect of ruthenium addition on molybdenum catalysts for syngas production via catalytic partial oxidation of methane in a monolithic reactor. *International Journal of Hydrogen Energy, 43*(2), 1129-1138.

Fleisch, T., Sills, R., & Briscoe, M. (2002). A review of global GTL developments. *journal of natural gas chemistry, 11*, 1-14.

Foest, R., Schmidt, M., & Becker, K. (2006). Microplasmas, an emerging field of low-temperature plasma science and technology. *International Journal of Mass Spectrometry, 248*(3), 87-102.

Freitas, A. C., & Guirardello, R. (2014). Thermodynamic analysis of methane reforming with CO2, CO2+ H2O, CO2+ O2 and CO2+ air for hydrogen and synthesis gas production. *Journal of CO2 utilization, 7*, 30-38.

Fridman, A. (2008). *Plasma chemistry*: Cambridge university press.

Fridman, A., Chirokov, A., & Gutsol, A. (2005). Non-thermal atmospheric pressure discharges. *Journal of Physics D: Applied Physics, 38*(2), R1.

Gangadharan, P., Kanchi, K. C., & Lou, H. H. (2012). Evaluation of the economic and environmental impact of combining dry reforming with steam reforming of methane. *Chemical engineering research and design, 90*(11), 1956-1968.

Ghorbanzadeh, A., Norouzi, S., & Mohammadi, T. (2005). High energy efficiency in syngas and hydrocarbon production from dissociation of CH4–CO2 mixture in a non-equilibrium pulsed plasma. *Journal of Physics D: Applied Physics, 38*(20), 3804.

Ghouri, M. M., Afzal, S., Hussain, R., Blank, J., Bukur, D. B., & Elbashir, N. O. (2016). Multi-scale modeling of fixed-bed Fischer Tropsch reactor. *Computers & Chemical Engineering, 91*, 38-48.

Godyak, V. A. (2006). Nonequilibrium EEDF in gas discharge plasmas. *IEEE transactions on plasma science, 34*(3), 755-766.

Goossens, M. (2012). *An introduction to plasma astrophysics and magnetohydrodynamics* (Vol. 294): Springer Science & Business Media.

Gousset, G., Panafieu, P., Touzeau, M., & Vialle, M. (1987). Plasma Chem. Plasma Process. In.

Green, K. M., Borras, M. C., Woskov, P. P., Flores, G. J., Hadidi, K., & Thomas, P. (2001). Electronic excitation temperature profiles in an air microwave plasma torch. *IEEE transactions on plasma science, 29*(2), 399-406.

Greenwood, N. N., & Earnshaw, A. (2012). *Chemistry of the Elements*. London: Elsevier.

Grill, A. (1994). *Cold plasma in materials fabrication* (Vol. 151): IEEE Press, New York.

Gupta, M., & Leong, E. W. W. (2008). *Microwaves and metals*: John Wiley & Sons.

Hafizi, A., Rahimpour, M., & Hassanajili, S. (2016). Hydrogen production by chemical looping steam reforming of methane over Mg promoted iron oxygen carrier: Optimization using design of experiments. *Journal of the Taiwan Institute of Chemical Engineers, 62*, 140-149.

Hammer, T. (1999). Application of plasma technology in environmental techniques. *Contributions to Plasma Physics, 39*(5), 441-462.

Hamzehlouia, S., Jaffer, S. A., & Chaouki, J. (2018). Microwave Heating-Assisted Catalytic Dry Reforming of Methane to Syngas. *Scientific reports, 8*(1), 8940.

Hazeltine, R. D. (2018). *The framework of plasma physics*: CRC Press.

Hegarty, M., O'Connor, A., & Ross, J. (1998). Syngas production from natural gas using ZrO2-supported metals. *Catalysis Today, 42*(3), 225-232.

Heijkers, S., Snoeckx, R., Kozák, T. s., Silva, T., Godfroid, T., Britun, N., . . . Bogaerts, A. (2015). CO2 conversion in a microwave plasma reactor in the presence of N2: elucidating the role of vibrational levels. *The Journal of Physical Chemistry C, 119*(23), 12815-12828.

Hesas, R. H., Daud, W. M. A. W., Sahu, J., & Arami-Niya, A. (2013). The effects of a microwave heating method on the production of activated carbon from agricultural waste: a review. *Journal of Analytical and Applied pyrolysis, 100*, 1-11.

Hippler, R., Pfau, S., Schmidt, M., & Schoenbach, K. H. (2001). Low temperature plasma physics: fundamental aspects and applications. *Low Temperature Plasma Physics: Fundamental Aspects and Applications, by Rainer Hippler (Editor), Sigismund Pfau (Editor), Martin Schmidt (Editor), Karl H. Schoenbach (Editor), pp. 530. ISBN 3-527-28887-2. Wiley-VCH, June 2001.*, 530.

Holladay, J. D., Hu, J., King, D. L., & Wang, Y. (2009). An overview of hydrogen production technologies. *Catalysis today, 139*(4), 244-260.

Horikoshi, S., Schiffmann, R. F., Fukushima, J., & Serpone, N. (2018). Microwave Materials Processing in Solid Media. In *Microwave Chemical and Materials Processing* (pp. 213-241): Springer.

Hu, Y. H. (2010). *Advances in CO2 conversion and utilization*: ACS Publications.

Hubert, J., Moisan, M., & Ricard, A. (1979). A new microwave plasma at atmospheric pressure. *Spectrochimica Acta Part B: Atomic Spectroscopy, 34*(1), 1-10.

Hwang, N., Song, Y.-H., & Cha, M. S. (2010). Efficient Use of $\hbox {CO} _ {2} $ Reforming of Methane With an Arc-Jet Plasma. *IEEE Transactions on Plasma Science, 38*(12), 3291-3299.

Indarto, A., Choi, J.-W., Lee, H., & Song, H. K. (2006). Effect of additive gases on methane conversion using gliding arc discharge. *Energy, 31*(14), 2986-2995.

Iravani, S., Korbekandi, H., Mirmohammadi, S. V., & Zolfaghari, B. (2014). Synthesis of silver nanoparticles: chemical, physical and biological methods. *Research in pharmaceutical sciences, 9*(6), 385.

Ismail, N., & Ani, F. N. (2015). A Review on Plasma Treatment for the Processing of Solid Waste. *Jurnal Teknologi (Sciences & Engineering), 41*, 49.

Itkulova, S., Zakumbaeva, G., Nurmakanov, Y., Mukazhanova, A., & Yermaganbetova, A. (2014). Syngas production by bireforming of methane over Co-based alumina-supported catalysts. *Catalysis Today, 228*, 194-198.

Iwarere, S. A., Rohani, V.-J., Ramjugernath, D., & Fulcheri, L. (2015). Dry reforming of methane in a tip–tip arc discharge reactor at very high pressure. *International Journal of Hydrogen Energy, 40*(8), 3388-3401.

Jamróz, P., Kordylewski, W., & Wnukowski, M. (2018). Microwave plasma application in decomposition and steam reforming of model tar compounds. *Fuel Processing Technology, 169*, 1-14.

Jankowski, K. J., & Reszke, E. (2010). *Microwave induced plasma analytical spectrometry*: Royal Society of Chemistry.

Jašek, O., Eliáš, M., Zajíčková, L., Kudrle, V., Bublan, M., Matějková, J., . . . Kadlečíková, M. (2006). Carbon nanotubes synthesis in microwave plasma torch at atmospheric pressure. *Materials Science and Engineering: C, 26*(5-7), 1189-1193.

Jasiński, M., Dors, M., & Mizeraczyk, J. (2009). Application of atmospheric pressure microwave plasma source for production of hydrogen via methane reforming. *The European Physical Journal D, 54*(2), 179-183.

Javanbakht, M., Fathollahi, F., Divsar, F., Ganjali, M. R., & Norouzi, P. (2013). A selective and sensitive voltammetric sensor based on molecularly imprinted polymer for the determination of dipyridamole in pharmaceuticals and biological fluids. *Sensors and Actuators B: Chemical, 182*, 362-367.

Javier, F., Moreno, S. H., Stankiewicz, A. I., & Stefanidis, G. D. (2016). Reduction of CO2 with hydrogen in a non-equilibrium microwave plasma reactor. *International Journal of Hydrogen Energy, 41*(46), 21067-21077.

Javier, F., Moreno, S. H., Stankiewicz, A. I., & Stefanidis, G. D. (2017). On the improvement of chemical conversion in a surface-wave microwave plasma reactor for CO2 reduction with hydrogen (The Reverse Water-Gas Shift reaction). *International Journal of Hydrogen Energy, 42*(18), 12943-12955.

Jena, S., Gupta, A., Pippara, R. K., & Pal, P. (2019). Wireless Sensing Systems: A Review. In *Sensors for Automotive and Aerospace Applications* (pp. 143-192): Springer.

Jiang, T., Li, Y., Liu, C.-j., Xu, G.-h., Eliasson, B., & Xue, B. (2002). Plasma methane conversion using dielectric-barrier discharges with zeolite A. *Catalysis Today, 72*(3), 229-235.

Jin, Q., Zhu, C., Border, M. W., & Hieftje, G. M. (1991). A microwave plasma torch assembly for atomic emission spectrometry. *Spectrochimica Acta Part B: Atomic Spectroscopy, 46*(3), 417-430.

Johnsen, K., Ryu, H., Grace, J., & Lim, C. (2006). Sorption-enhanced steam reforming of methane in a fluidized bed reactor with dolomite as CO2-acceptor. *Chemical Engineering Science, 61*(4), 1195-1202.

Jones, D. A., Lelyveld, T., Mavrofidis, S., Kingman, S., & Miles, N. (2002). Microwave heating applications in environmental engineering—a review. *Resources, conservation and recycling, 34*(2), 75-90.

Jonkers, J., De Regt, J., Van der Mullen, J., Vos, H., De Groote, F., & Timmermans, E. (1996). On the electron temperatures and densities in plasmas produced by the "torche à injection axiale". *Spectrochimica Acta Part B: Atomic Spectroscopy, 51*(11), 1385-1392.

Kappe, C. O., Stadler, A., & Dallinger, D. (2012). *Microwaves in organic and medicinal chemistry*: John Wiley & Sons.

Karamé, I., Shaya, J., & Srour, H. (2018). Carbon Dioxide Chemistry, Capture and Oil Recovery.

Kasht, A., Hussain, R., Ghouri, M., Blank, J., & Elbashir, N. O. (2015). Product analysis of supercritical Fischer-Tropsch synthesis: utilizing a unique on-line and off-line gas chromatographs setup in a bench-scale reactor unit. *American Journal of Analytical Chemistry, 6*(08), 659.

Khalil, M. A. K. (2013). *Atmospheric methane: sources, sinks, and role in global change* (Vol. 13): Springer Science & Business Media.

Khoja, A. H., Tahir, M., & Amin, N. A. S. (2017). Dry reforming of methane using different dielectric materials and DBD plasma reactor configurations. *Energy Conversion and Management, 144*, 262-274.

Kim, A. R., Lee, H. Y., Lee, D. H., Kim, B.-W., Chung, C.-H., Moon, D. J., . . . Bae, J. W. (2015). Combined Steam and CO2 Reforming of CH4 on LaSrNiO x Mixed Oxides Supported on Al2O3-Modified SiC Support. *Energy & Fuels, 29*(2), 1055-1065.

Kim, J., Maiti, A., Lin, L.-C., Stolaroff, J. K., Smit, B., & Aines, R. D. (2013). New materials for methane capture from dilute and medium-concentration sources. *Nature Communications, 4*, 1694.

Kim, S., Sekiguchi, H., & Doba, Y. (2013). Development of ultra-high temperature SHS furnace using atmospheric-pressure microwave steam plasma. *Applied Thermal Engineering, 52*(1), 1-7.

Kirschke, S., Bousquet, P., Ciais, P., Saunois, M., Canadell, J. G., Dlugokencky, E. J., . . . Bruhwiler, L. (2013). Three decades of global methane sources and sinks. *Nature geoscience, 6*(10), 813.

Klemensø, T., Nielsen, J., Blennow, P., Persson, Å. H., Stegk, T., Christensen, B. H., & Sønderby, S. (2011). High performance metal-supported solid oxide fuel cells with Gd-doped ceria barrier layers. *Journal of Power Sources, 196*(22), 9459-9466.

Kraus, M., Egli, W., Haffner, K., Eliasson, B., Kogelschatz, U., & Wokaun, A. (2002). Investigation of mechanistic aspects of the catalytic CO 2 reforming of methane in a dielectric-barrier discharge using optical emission spectroscopy and kinetic modeling. *Physical Chemistry Chemical Physics, 4*(4), 668-675.

Kresnyak, S., Price, S., & Wagner, J. (2018). Enhancement of Fischer-Tropsch Process for Hydrocarbon Fuel Formulation in a GTL Environment. In: Google Patents.

Kustov, L., & Sinev, I. (2010). Microwave activation of catalysts and catalytic processes. *Russ. J. Phys. Chem. A, 84*(10), 1676-1694.

Kwak, J.-S. (2005). Application of Taguchi and response surface methodologies for geometric error in surface grinding process. *International journal of machine tools and manufacture, 45*(3), 327-334.

Langmuir, I. (1928). Oscillations in ionized gases. *Proceedings of the National Academy of Sciences, 14*(8), 627-637.

Laroussi, M., Sayler, G. S., Glascock, B. B., McCurdy, B., Pearce, M. E., Bright, N. G., & Malott, C. M. (1999). Images of biological samples undergoing sterilization by a glow discharge at atmospheric pressure. *IEEE Transactions on plasma science, 27*(1), 34-35.

Leonov, S. B., & Yarantsev, D. A. (2006). Plasma-induced ignition and plasma-assisted combustion in high-speed flow. *Plasma Sources Science and Technology, 16*(1), 132.

Li, D., Li, X., Bai, M., Tao, X., Shang, S., Dai, X., & Yin, Y. (2009). CO 2 reforming of CH 4 by atmospheric pressure glow discharge plasma: a high conversion ability. *International Journal of Hydrogen Energy, 34*(1), 308-313.

Li, D., Nakagawa, Y., & Tomishige, K. (2011). Methane reforming to synthesis gas over Ni catalysts modified with noble metals. *Applied Catalysis A: General, 408*(1), 1-24.

Li, L., Jiang, X., Wang, H., Wang, J., Song, Z., Zhao, X., & Ma, C. (2017). Methane dry and mixed reforming on the mixture of bio-char and nickel-based catalyst with microwave assistance. *Journal of Analytical and Applied Pyrolysis, 125*, 318-327.

Li, L., Wang, H., Jiang, X., Song, Z., Zhao, X., & Ma, C. (2016). Microwave-enhanced methane combined reforming by CO_2 and H_2O into syngas production on biomass-derived char. *Fuel, 185*, 692-700.

Li, L., Yang, Z., Chen, J., Qin, X., Jiang, X., Wang, F., . . . Ma, C. (2018). Performance of bio-char and energy analysis on CH_4 combined reforming by CO_2 and H_2O into syngas production with assistance of microwave. *Fuel, 215*, 655-664.

Li, M.-w., Xu, G.-h., Tian, Y.-l., Chen, L., & Fu, H.-f. (2004). Carbon dioxide reforming of methane using DC corona discharge plasma reaction. *The Journal of Physical Chemistry A, 108*(10), 1687-1693.

Li, X. S., Zhu, B., Shi, C., Xu, Y., & Zhu, A. M. (2011). Carbon dioxide reforming of methane in kilohertz spark-discharge plasma at atmospheric pressure. *AIChE Journal, 57*(10), 2854-2860.

Li, Y., Wang, Y., Zhang, X., & Mi, Z. (2008). Thermodynamic analysis of autothermal steam and CO2 reforming of methane. *International Journal of Hydrogen Energy, 33*(10), 2507-2514.

Lidström, P., Tierney, J., Watheyb, B., & Westmana, J. (2001). Microwave assisted organic synthesisÐa review. *Tetrahedron, 57*, 9225-9283.

Lieberman, M. A., & Lichtenberg, A. J. (1994). Principles of plasma discharges and materials processing. *MRS Bulletin, 30*(2), 899-901.

Lieberman, M. A., & Lichtenberg, A. J. (2005). *Principles of plasma discharges and materials processing*: John Wiley & Sons.

Liston, E. M. (1989). Plasma treatment for improved bonding: a review. *The Journal of Adhesion, 30*(1-4), 199-218.

Long, H., Shang, S., Tao, X., Yin, Y., & Dai, X. (2008). CO 2 reforming of CH 4 by combination of cold plasma jet and Ni/γ-Al 2 O 3 catalyst. *International Journal of Hydrogen Energy, 33*(20), 5510-5515.

Mabrouk, M., Lemont, F., & Baronnet, J. (2012). *Incineration of radioactive organic liquid wastes by underwater thermal plasma.* Paper presented at the Journal of Physics: Conference Series.

Malik, M. A., Ghaffar, A., & Malik, S. A. (2001). Water purification by electrical discharges. *Plasma Sources Science and Technology, 10*(1), 82.

Mallieswaran, K., Padmanabhan, R., & Balasubramanian, V. (2018). Friction stir welding parameters optimization for tailored welded blank sheets of AA1100 with AA6061 dissimilar alloy using response surface methodology. *Advances in Materials and Processing Technologies*, 1-16.

Maqbool, W., Park, S. J., & Lee, E. S. (2014). Gas-to-liquid process optimization for different recycling configurations and economic evaluation. *Industrial & Engineering Chemistry Research, 53*(22), 9454-9463.

Marafee, A., Liu, C., Xu, G., Mallinson, R., & Lobban, L. (1997). An experimental study on the oxidative coupling of methane in a direct current corona discharge reactor over Sr/La2O3 catalyst. *Industrial & engineering chemistry research, 36*(3), 632-637.

Markewitz, P., Kuckshinrichs, W., Leitner, W., Linssen, J., Zapp, P., Bongartz, R., . . . Müller, T. E. (2012). Worldwide innovations in the development of carbon capture technologies and the utilization of CO 2. *Energy & environmental science, 5*(6), 7281-7305.

Meger, R., Fernsler, R., Lampe, M., Leonhardt, D., Manheimer, W., Murphy, D., . . . Walton, S. (1999). *Beam Generated Plasmas for Large Area Materials Processing.* Paper presented at the APS Annual Gaseous Electronics Meeting Abstracts.

Mei, D., He, Y. L., Liu, S., Yan, J., & Tu, X. (2016). Optimization of CO2 conversion in a cylindrical dielectric barrier discharge reactor using design of experiments. *Plasma Processes and Polymers, 13*(5), 544-556.

Mei, D., Zhu, X., He, Y.-L., Yan, J. D., & Tu, X. (2014). Plasma-assisted conversion of CO2 in a dielectric barrier discharge reactor: understanding the effect of packing materials. *Plasma Sources Science and Technology, 24*(1), 015011.

Meichsner, J., Schmidt, M., Schneider, R., & Wagner, H.-E. (2012). *Nonthermal plasma chemistry and physics*: CRC Press.

Meija, J., & Possolo, A. (2017). Data reduction framework for standard atomic weights and isotopic compositions of the elements. *Metrologia, 54*(2), 229.

Menéndez, J., Arenillas, A., Fidalgo, B., Fernández, Y., Zubizarreta, L., Calvo, E. G., & Bermúdez, J. M. (2010). Microwave heating processes involving carbon materials. *Fuel Processing Technology, 91*(1), 1-8.

Meredith, R. J. (1998). *Engineers' handbook of industrial microwave heating*: Iet.

Metaxas, A. a., & Meredith, R. J. (1983). *Industrial microwave heating*: IET.

Mishra, R. R., & Sharma, A. K. (2016). Microwave–material interaction phenomena: heating mechanisms, challenges and opportunities in material processing. *Composites Part A: Applied Science and Manufacturing, 81*, 78-97.

Moisan, M., Hubert, J., Margot, J., Sauvé, G., & Zakrzewski, Z. (1992). Microwave Discharge: Fundamentals and Applications, edited by CM Ferreira and M. Moisan. In: Plenum, New York.

Moisan, M., Sauve, G., Zakrzewski, Z., & Hubert, J. (1994). An atmospheric pressure waveguide-fed microwave plasma torch: the TIA design. *Plasma Sources Science and Technology, 3*(4), 584.

Monette, E., Bartnikas, R., Czeremuszkin, G., Latreche, M., & Wertheimer, M. (1999). 14th Int. Symp. Plasma Chemistry. *Prague, M. Hrabovsky, M. Konrad, and V. Kopecky, eds, 2*, 991.

Montgomery, D. C. (2017). *Design and analysis of experiments*: John Wiley & Sons.

Moshrefi, M. M., Rashidi, F., Bozorgzadeh, H. R., & Haghighi, M. E. (2013). Dry reforming of methane by DC spark discharge with a rotating electrode. *Plasma Chem. Plasma Process., 33*(2), 453-466.

Motasemi, F., & Afzal, M. T. (2013). A review on the microwave-assisted pyrolysis technique. *Renew. Sust. Energ. Rev., 28*, 317-330.

Motasemi, F., & Ani, F. (2012). A review on microwave-assisted production of biodiesel. *Renew. Sust. Energ. Rev., 16*(7), 4719-4733.

Motshekga, S. C., Pillai, S. K., Ray, S. S., Jalama, K., & Krause, R. W. (2012). Recent trends in the microwave-assisted synthesis of metal oxide nanoparticles supported on carbon nanotubes and their applications. *Journal of Nanomaterials, 2012*, 51.

Moustakas, K., Fatta, D., Malamis, S., Haralambous, K., & Loizidou, M. (2005). Demonstration plasma gasification/vitrification system for effective hazardous waste treatment. *Journal of hazardous Materials, 123*(1-3), 120-126.

Mustafa, M. F., Fu, X., Liu, Y., Abbas, Y., Wang, H., & Lu, W. (2018). Volatile organic compounds (VOCs) removal in non-thermal plasma double dielectric barrier discharge reactor. *Journal of hazardous materials, 347*, 317-324.

Mustafa, M. F., Fu, X., Lu, W., Liu, Y., Abbas, Y., Wang, H., & Arslan, M. T. (2018). Application of non-thermal plasma technology on fugitive methane destruction: Configuration and optimization of double dielectric barrier discharge reactor. *Journal of Cleaner Production, 174*, 670-677.

Naeem, M. A., Al-Fatesh, A. S., Khan, W. U., Abasaeed, A. E., & Fakeeha, A. H. (2013). Syngas production from dry reforming of methane over nano Ni polyol catalysts. *International Journal of Chemical Engineering and Applications, 4*(5), 315.

Nawfal, M., Gennequin, C., Labaki, M., Nsouli, B., Aboukaïs, A., & Abi-Aad, E. (2015). Hydrogen production by methane steam reforming over Ru supported on Ni–Mg–Al mixed oxides prepared via hydrotalcite route. *International Journal of Hydrogen Energy, 40*(2), 1269-1277.

Nikolic, M., Popovic, S., Upadhyay, J., Vuskovic, L., Leiweke, R., & Ganguly, B. (2012). On a dielectric-barrier and a microwave-cavity discharge in synchronized operation—the case of a helium/oxygen mixture. *Plasma Sources Science and Technology, 21*(1), 015004.

Nizio, M. (2016). *Plasma catalytic process for CO2 methanation.* Université Pierre et Marie Curie-Paris VI,

Noronha, F. B., Shamsi, A., Taylor, C., Fendley, E. C., Stagg-Williams, S., & Resasco, D. E. (2003). Catalytic performance of Pt/ZrO 2 And Pt/Ce-ZrO 2 catalysts on CO 2 reforming of CH 4 coupled with steam reforming or under high pressure. *Catalysis letters, 90*(1-2), 13-21.

Noureldin, M. M., Elbashir, N. O., & El-Halwagi, M. M. (2013). Optimization and selection of reforming approaches for syngas generation from natural/shale gas. *Industrial & Engineering Chemistry Research, 53*(5), 1841-1855.

Nüchter, M., Ondruschka, B., Bonrath, W., & Gum, A. (2004). Microwave assisted synthesis–a critical technology overview. *Green Chemistry, 6*(3), 128-141.

Okamoto, Y. (1996). A microwave-induced unmagnetized plasma source for plasma processing. *Plasma Sources Science and Technology, 5*(4), 648.

Olah, G. A., Goeppert, A., Czaun, M., Mathew, T., May, R. B., & Prakash, G. S. (2015). Single step bi-reforming and oxidative bi-reforming of methane (natural gas) with steam and carbon dioxide to metgas (CO-2H2) for methanol synthesis: self-sufficient effective and exclusive oxygenation of methane to methanol with oxygen. *Journal of the American Chemical Society, 137*(27), 8720-8729.

Országh, J., Danko, M., Ribar, A., & Matejčík, Š. (2012). Nitrogen second positive system studied by electron induced fluorescence. *Nuclear Instruments and Methods in Physics Research Section B: Beam Interactions with Materials and Atoms, 279*, 76-79.

Oyama, S. T., Hacarlioglu, P., Gu, Y., & Lee, D. (2012). Dry reforming of methane has no future for hydrogen production: comparison with steam reforming at high pressure in standard and membrane reactors. *International Journal of Hydrogen Energy, 37*(13), 10444-10450.

Ozbek, N., & Akman, S. (2016). Microwave plasma atomic emission spectrometric determination of Ca, K and Mg in various cheese varieties. *Food chemistry, 192*, 295-298.

Ozkan, A., Dufour, T., Arnoult, G., De Keyzer, P., Bogaerts, A., & Reniers, F. (2015). CO2–CH4 conversion and syngas formation at atmospheric pressure using a multi-electrode dielectric barrier discharge. *J. CO2 Util., 9*, 74-81.

Ozkan, I. A., Akbudak, B., & Akbudak, N. (2007). Microwave drying characteristics of spinach. *Journal of Food Engineering, 78*(2), 577-583.

Pacheco, J., Soria, G., Pacheco, M., Valdivia, R., Ramos, F., Frías, H., . . . Hidalgo, M. (2015). Greenhouse gas treatment and H 2 production, by warm plasma reforming. *International Journal of Hydrogen Energy, 40*(48), 17165-17171.

Pakhare, D., & Spivey, J. (2014). A review of dry (CO 2) reforming of methane over noble metal catalysts. *Chemical Society Reviews, 43*(22), 7813-7837.

Palaskar, S., & Desai, A. (2016). APPLICATION OF NON-THERMAL ATMOSPHERIC PRESSURE PLASMA IN TEXTILES. *Journal of Magnetohydrodynamics and Plasma Research, 21*(2), 213.

Pan, K. L., Chung, W. C., & Chang, M. B. (2014). Dry reforming of CH 4 with CO 2 to generate syngas by combined plasma catalysis. *IEEE Transactions on Plasma Science, 42*(12), 3809-3818.

Pärnaste, M., Bäcklund, A., & Walenius, L. (2018). Radio-frequency electrode and cyclotron configured to reduce radiation exposure. In: Google Patents.

Patience, G. S., & Boffito, D. C. (2016). Gas-to-liquids processes: Preface. *The Canadian Journal of Chemical Engineering, 94*(4), 605-606.

Patil, B., Wang, Q., Hessel, V., & Lang, J. (2015). Plasma N2-fixation: 1900–2014. *Catalysis Today, 256*, 49-66.

Paul, C. R., & Nasar, S. A. (1987). *Introduction to electromagnetic fields*: McGraw-Hill.

Paul, J., & Pradier, C.-M. (1994a). *Carbon dioxide chemistry.* Paper presented at the International Symposium on CO_2 Chemistry (1993: Hemavan, Sweden).

Paul, J., & Pradier, C.-M. (1994b). Carbon dioxide chemistry: environmental issues: international symposium. In: Royal Society of Chemistry.

Paulmier, T., & Fulcheri, L. (2005). Use of non-thermal plasma for hydrocarbon reforming. *Chemical engineering journal, 106*(1), 59-71.

Pearlman, H., Demydovych, M., Rabinovich, A., & Shenoy, S. (2018). *A NON-THERMAL GLIDING ARC PLASMA REFORMER FOR SYNGAS PRODUCTION.* Paper presented at the ASTFE Digital Library.

Pei, X., Zhang, P., Chen, K., & Lu, X. (2013). Large-volume N2 plasma induced by electron beam at high pressure. *IEEE Trans. Plasma Sci, 41*(3), 494-497.

Pena, D., Griboval-Constant, A., Lecocq, V., Diehl, F., & Khodakov, A. (2013). Influence of operating conditions in a continuously stirred tank reactor on the formation of carbon species on alumina supported cobalt Fischer–Tropsch catalysts. *Catalysis today, 215*, 43-51.

Peratt, A. L. (1997). Advances in numerical modeling of astrophysical and space plasmas. In *Advanced Topics on Astrophysical and Space Plasmas* (pp. 92-163): Springer.

Petitpas, G., Rollier, J.-D., Darmon, A., Gonzalez-Aguilar, J., Metkemeijer, R., & Fulcheri, L. (2007). A comparative study of non-thermal plasma assisted reforming technologies. *International Journal of Hydrogen Energy, 32*(14), 2848-2867.

Pettinau, A., Mureddu, M., & Ferrara, F. (2017). Carbon dioxide conversion into liquid fuels by hydrogenation and photoelectrochemical reduction: Project description and preliminary experimental results. *Energy Procedia, 114*, 6893-6904.

Peymani, M., Alavi, S. M., & Rezaei, M. (2016). Preparation of highly active and stable nanostructured Ni/CeO 2 catalysts for syngas production by partial oxidation of methane. *International Journal of Hydrogen Energy, 41*(15), 6316-6325.

Porter, M., D'Angio, A., Binner, J., Cinibulk, M. K., & Mogilevsky, P. (2017). High-temperature ceramic matrix composites using microwave enhanced chemical vapor infiltration.

Pour, A. N., & Mousavi, M. (2015). Combined reforming of methane by carbon dioxide and water: Particle size effect of Ni–Mg nanoparticles. *International Journal of Hydrogen Energy, 40*(38), 12985-12992.

Pradier, J. P., & Pradier, C.-M. (2014). *Carbon dioxide chemistry: environmental issues*: Elsevier.

Prokisch, C., Bilgic, A., Voges, E., Broekaert, J., Jonkers, J., Van Sande, M., & Van der Mullen, J. (1999). Photographic plasma images and electron number density as well as electron temperature mappings of a plasma sustained with a modified argon microwave plasma torch (MPT) measured by spatially resolved Thomson scattering. *Spectrochimica Acta Part B: Atomic Spectroscopy, 54*(9), 1253-1266.

Qi, C., Wei, D., Xumei, T., Hui, Y., Xiaoyan, D., & Yongxiang, Y. (2006). CO2 reforming of CH4 by atmospheric pressure abnormal glow plasma. *Plasma Science and Technology, 8*(2), 181.

Rafiee, A., & Hillestad, M. (2012). Techno-Economic Analysis of a Gas-to-Liquid Process with Different Placements of a CO2 Removal Unit. *Chemical Engineering & Technology, 35*(3), 420-430.

Ramachandran, C., Balasubramanian, V., & Ananthapadmanabhan, P. (2011). Multiobjective optimization of atmospheric plasma spray process parameters to deposit yttria-stabilized zirconia coatings using response surface methodology. *Journal of thermal spray technology, 20*(3), 590-607.

Ramakers, M., Michielsen, I., Aerts, R., Meynen, V., & Bogaerts, A. (2015). Effect of argon or helium on the CO2 conversion in a dielectric barrier discharge. *Plasma Processes and Polymers, 12*(8), 755-763.

Rani, D. A., Gomez, E., Boccaccini, A., Hao, L., Deegan, D., & Cheeseman, C. R. (2008). Plasma treatment of air pollution control residues. *Waste management, 28*(7), 1254-1262.

Ravari, F., Fazeli, S. M., Bozorgzadeh, H. R., & Sadeghzadeh Ahari, J. (2017). Kinetic Model Study of Dry Reforming of Methane Using Cold Plasma. *Physical Chemistry Research, 5*(2), 395-408.

Riba, J.-R., Morosini, A., & Capelli, F. (2018). Comparative Study of AC and Positive and Negative DC Visual Corona for Sphere-Plane Gaps in Atmospheric Air. *Energies, 11*(10), 2671.

Rieks, M., Bellinghausen, R., Kockmann, N., & Mleczko, L. (2015). Experimental study of methane dry reforming in an electrically heated reactor. *International Journal of Hydrogen Energy, 40*(46), 15940-15951.

Roh, H.-S., Koo, K. Y., Jeong, J. H., Seo, Y. T., Seo, D. J., Seo, Y.-S., . . . Park, S. B. (2007). Combined reforming of methane over supported Ni catalysts. *Catalysis Letters, 117*(1-2), 85-90.

Rosenkranz, B., & Bettmer, J. (2000). Microwave-induced plasma–optical emission spectrometry–fundamental aspects and applications in metal speciation analysis. *TrAC Trends in Analytical Chemistry, 19*(2-3), 138-156.

Ross, J., Van Keulen, A., Hegarty, M., & Seshan, K. (1996). The catalytic conversion of natural gas to useful products. *Catalysis Today, 30*(1-3), 193-199.

Rostrup-Nielsen, J. R. (2000). New aspects of syngas production and use. *Catalysis today, 63*(2), 159-164.

Roth, J. R. (1995). Industrial Plasma Engineering: Principles vol 1 (Bristol and Philadelphia. In: Institute of Physics Publishing.

Roth, J. R. (2001). *Industrial plasma engineering: Volume 2: Applications to nonthermal plasma processing*: CRC press.

Roth, J. R. (2003). Aerodynamic flow acceleration using paraelectric and peristaltic electrohydrodynamic effects of a one atmosphere uniform glow discharge plasma. *Physics of plasmas, 10*(5), 2117-2126.

Rowshanzamir, S., & Eikani, M. (2009). Autothermal reforming of methane to synthesis gas: Modeling and simulation. *International Journal of Hydrogen Energy, 34*(3), 1292-1300.

Roy, R., Agrawal, D., Cheng, J., & Gedevanishvili, S. (1999). Full sintering of powdered-metal bodies in a microwave field. *Nature, 399*(6737), 668.

Ruj, B., & Ghosh, S. (2014). Technological aspects for thermal plasma treatment of municipal solid waste—A review. *Fuel Processing Technology, 126*, 298-308.

Safa, N. N., Ghomi, H., & Niknam, A. (2014). Effect of the q-nonextensive electron velocity distribution on a magnetized plasma sheath. *Physics of Plasmas, 21*(8), 082111.

Salehi, E. N., & Save, S. W. (2013). Viability of GTL for the North American gas market. *Hydrocarbon processing*.

Samuel, P. (2003). GTL technology-challenges and opportunities in catalysis. *Bulletin of Catalysis Society of India, 2*(5), 82-99.

Schmidt, M., Föste, T., Michel, P., & Šapkin, V. (1982). Device for producing and investigating an electron beam plasma discharge. *Beiträge aus der Plasmaphysik, 22*(5), 435-441.

Schunk, R., & Nagy, A. (2009). *Ionospheres: physics, plasma physics, and chemistry*: Cambridge university press.

Schutze, A., Jeong, J. Y., Babayan, S. E., Park, J., Selwyn, G. S., & Hicks, R. F. (1998). The atmospheric-pressure plasma jet: a review and comparison to other plasma sources. *IEEE transactions on plasma science, 26*(6), 1685-1694.

Scott, A. W. (1993). *Understanding microwaves*: Wiley New York.

Sellers, H., Spiteri, R. J., & Perrone, M. (2009). CO2+ CH4 chemistry over Pd: Results of kinetic simulations relevant to environmental issues. *The Journal of Physical Chemistry C, 113*(6), 2340-2346.

Senseni, A. Z., Fattahi, S. M. S., Rezaei, M., & Meshkani, F. (2016). A comparative study of experimental investigation and response surface optimization of steam reforming of glycerol over nickel nano-catalysts. *International Journal of Hydrogen Energy, 41*(24), 10178-10192.

Sentek, J., Krawczyk, K., Młotek, M., Kalczewska, M., Kroker, T., Kolb, T., . . . Schmidt-Szałowski, K. (2010). Plasma-catalytic methane conversion with carbon dioxide in dielectric barrier discharges. *Appl. Catal. B-Environ., 94*(1), 19-26.

Serrano-Lotina, A., & Daza, L. (2014). Influence of the operating parameters over dry reforming of methane to syngas. *International Journal of Hydrogen Energy, 39*(8), 4089-4094.

Seyed-Matin, N., Jalili, A. H., Jenab, M. H., Zekordi, S. M., Afzali, A., Rasouli, C., & Zamaniyan, A. (2010). DC-pulsed plasma for dry reforming of methane to synthesis gas. *Plasma Chemistry and Plasma Processing, 30*(3), 333-347.

Shamkhali, A., Omidkhah, M., Towfighi, J., & Jafari Nasr, M. (2012). The Production of Synthesis Gas by a Combination of Steam and Dry Reforming Using GHR. *Petroleum science and technology, 30*(6), 594-604.

Shapoval, V., & Marotta, E. (2015). Investigation on Plasma-Driven Methane Dry Reforming in a Self-Triggered Spark Reactor. *Plasma Process. Polym., 12*(8), 808-816.

Shapoval, V., Marotta, E., Ceretta, C., Konjević, N., Ivković, M., Schiorlin, M., & Paradisi, C. (2014). Development and Testing of a Self-Triggered Spark Reactor for Plasma Driven Dry Reforming of Methane. *Plasma Process. Polym., 11*(8), 787-797.

Sidik, S., Triwahyono, S., Jalil, A., Majid, Z., Salamun, N., Talib, N., & Abdullah, T. (2016). CO 2 reforming of CH 4 over Ni–Co/MSN for syngas production: Role of Co as a binder and optimization using RSM. *Chemical Engineering Journal, 295*, 1-10.

Sievenpiper, D., Zhang, L., Broas, R. F., Alexopolous, N. G., & Yablonovitch, E. (1999). High-impedance electromagnetic surfaces with a forbidden frequency band. *IEEE Transactions on Microwave Theory and techniques, 47*(11), 2059-2074.

Singh, S., Gupta, D., Jain, V., & Sharma, A. K. (2015). Microwave processing of materials and applications in manufacturing industries: a review. *Materials and Manufacturing Processes, 30*(1), 1-29.

Siores, E., & Do Rego, D. (1995). Microwave applications in materials joining. *Journal of Materials Processing Technology, 48*(1-4), 619-625.

Sivagami, K., Padmanabhan, K., Joy, A. C., & Nambi, I. M. (2019). Microwave (MW) remediation of hydrocarbon contaminated soil using spent graphite–An approach for waste as a resource. *Journal of environmental management, 230*, 151-158.

Snoeckx, R., Zeng, Y., Tu, X., & Bogaerts, A. (2015). Plasma-based dry reforming: improving the conversion and energy efficiency in a dielectric barrier discharge. *RSC Advances, 5*(38), 29799-29808.

Song, Z., Jing, C., Yao, L., Zhao, X., Wang, W., Mao, Y., & Ma, C. (2016). Microwave drying performance of single-particle coal slime and energy consumption analyses. *Fuel Processing Technology, 143*, 69-78.

Spath, P. L., & Dayton, D. C. (2003). *Preliminary screening-technical and economic assessment of synthesis gas to fuels and chemicals with emphasis on the potential for biomass-derived syngas*. Retrieved from

Sturrock, P. A. (1994). *Plasma physics: an introduction to the theory of astrophysical, geophysical and laboratory plasmas*: Cambridge University Press.

Suib, S. L., & Zerger, R. P. (1993). A direct, continuous, low-power catalytic conversion of methane to higher hydrocarbons via microwave plasmas. *Journal of catalysis, 139*(2), 383-391.

Sun, Y., Nie, Y., Wu, A., Ji, D., Yu, F., & Ji, J. (2012). Carbon dioxide reforming of methane to syngas by thermal plasma. *Plasma Science and Technology, 14*(3), 252.

Sutherland, J., Su, M. C., & Michael, J. (2001). Rate constants for H+ CH4, CH3+ H2, and CH4 dissociation at high temperature. *International Journal of Chemical Kinetics, 33*(11), 669-684.

Taghvaei, H., Jahanmiri, A., Rahimpour, M. R., Shirazi, M. M., & Hooshmand, N. (2013). Hydrogen production through plasma cracking of hydrocarbons: Effect of carrier gas and hydrocarbon type. *Chemical engineering journal, 226*, 384-392.

Tanios, C., Bsaibes, S., Gennequin, C., Labaki, M., Cazier, F., Billet, S., . . . Abi-Aad, E. (2017). Syngas production by the CO2 reforming of CH4 over Ni–Co–Mg–Al catalysts obtained from hydrotalcite precursors. *International Journal of Hydrogen Energy, 42*(17), 12818-12828.

Tanyildizi, M. S., Özer, D., & Elibol, M. (2005). Optimization of α-amylase production by Bacillus sp. using response surface methodology. *Process Biochemistry, 40*(7), 2291-2296.

Tao, X., Bai, M., Li, X., Long, H., Shang, S., Yin, Y., & Dai, X. (2011). CH4–CO2 reforming by plasma–challenges and opportunities. *Progress in Energy and Combustion Science, 37*(2), 113-124.

Tao, X., Bai, M., Wu, Q., Huang, Z., Yin, Y., & Dai, X. (2009). CO_2 reforming of CH_4 by binode thermal plasma. *International Journal of Hydrogen Energy, 34*(23), 9373-9378.

Tao, X., Qi, F., Yin, Y., & Dai, X. (2008). CO 2 reforming of CH 4 by combination of thermal plasma and catalyst. *International Journal of Hydrogen Energy, 33*(4), 1262-1265.

Tendero, C., Tixier, C., Tristant, P., Desmaison, J., & Leprince, P. (2006). Atmospheric pressure plasmas: A review. *Spectrochimica Acta Part B: Atomic Spectroscopy, 61*(1), 2-30.

Thornton, J. A. (1983). Plasma-assisted deposition processes: theory, mechanisms and applications. *Thin Solid Films, 107*(1), 3-19.

Thostenson, E., & Chou, T.-W. (1999). Microwave processing: fundamentals and applications. *Composites Part A: Applied Science and Manufacturing, 30*(9), 1055-1071.

Timmermans, E., Jonkers, J., Thomas, I., Rodero, A., Quintero, M., Sola, A., . . . Van Der Mullen, J. (1998). The behavior of molecules in microwave-induced plasmas studied by optical emission spectroscopy. 1. Plasmas at atmospheric pressure. *Spectrochimica Acta Part B: Atomic Spectroscopy, 53*(11), 1553-1566.

Tonks, L., & Langmuir, I. (1929). Note on" Oscillations in Ionized Gases". *Physical Review, 33*(6), 990.

Tu, X., & Whitehead, J. (2012). Plasma-catalytic dry reforming of methane in an atmospheric dielectric barrier discharge: Understanding the synergistic effect at low temperature. *Appl. Catal. B-Environ., 125*, 439-448.

Tu, X., & Whitehead, J. C. (2014). Plasma dry reforming of methane in an atmospheric pressure AC gliding arc discharge: co-generation of syngas and carbon nanomaterials. *International Journal of Hydrogen Energy, 39*(18), 9658-9669.

Uden, P. C. (1995). Element-specific chromatographic detection by atomic absorption, plasma atomic emission and plasma mass spectrometry. *Journal of Chromatography A, 703*(1-2), 393-416.

Uhm, H. S., Kwak, H. S., & Hong, Y. C. (2016). Carbon dioxide elimination and regeneration of resources in a microwave plasma torch. *Environmental Pollution, 211*, 191-197.

Urashima, K., & Chang, J.-S. (2000). Removal of volatile organic compounds from air streams and industrial flue gases by non-thermal plasma technology. *IEEE Transactions on Dielectrics and Electrical Insulation, 7*(5), 602-614.

Usman, M., Daud, W. W., & Abbas, H. F. (2015). Dry reforming of methane: influence of process parameters—a review. *Renewable and Sustainable Energy Reviews, 45*, 710-744.

van Dijk, J. (2017). *COMBINED PLASMA SOURCE FOR EMISSION SPECTROSCOPY: LASER-INDUCED PLASMA IN HOLLOW CATHODE DISCHARGE.* Institute of Solid State Physics,

Venkatesh, M., & Raghavan, G. (2004). An overview of microwave processing and dielectric properties of agri-food materials. *Biosystems engineering, 88*(1), 1-18.

Volynets, A., Lopaev, D., & Popov, N. (2016). *Mechanism of N2 dissociation and kinetics of N (4S) atoms in pure nitrogen plasma.* Paper presented at the Journal of Physics: Conference Series.

Wan, J. (1993). Microwaves and chemistry: the catalysis of an exciting marriage. *Research on chemical intermediates, 19*(2), 147.

Wang, Q., Yan, B.-H., Jin, Y., & Cheng, Y. (2009a). Dry reforming of methane in a dielectric barrier discharge reactor with Ni/Al2O3 catalyst: interaction of catalyst and plasma. *Energy & Fuels, 23*(8), 4196-4201.

Wang, Q., Yan, B.-H., Jin, Y., & Cheng, Y. (2009b). Investigation of dry reforming of methane in a dielectric barrier discharge reactor. *Plasma Chemistry and Plasma Processing, 29*(3), 217-228.

Wang, T., & Liu, J. (2000). A review of microwave curing of polymeric materials. *Journal of Electronics Manufacturing, 10*(03), 181-189.

Wang, W., Wang, S., Ma, X., & Gong, J. (2011). Recent advances in catalytic hydrogenation of carbon dioxide. *Chemical Society Reviews, 40*(7), 3703-3727.

Wang, Y.-F., Tsai, C.-H., Chang, W.-Y., & Kuo, Y.-M. (2010). Methane steam reforming for producing hydrogen in an atmospheric-pressure microwave plasma reactor. *International Journal of Hydrogen Energy, 35*(1), 135-140.

Wang, Z., Ashok, J., Pu, Z., & Kawi, S. (2017). Low temperature partial oxidation of methane via BaBi0. 05Co0. 8Nb0. 15O3− δ-Ni phyllosilicate catalytic hollow fiber membrane reactor. *Chemical Engineering Journal, 315*, 315-323.

Whitman, W. B., Bowen, T. L., & Boone, D. R. (2006). The methanogenic bacteria. *Prokaryotes, 3*(Chapter 9), 165-207.

Wilhelm, D., Simbeck, D., Karp, A., & Dickenson, R. (2001). Syngas production for gas-to-liquids applications: technologies, issues and outlook. *Fuel processing technology, 71*(1-3), 139-148.

Will, H., Scholz, P., & Ondruschka, B. (2004). Microwave-Assisted Heterogeneous Gas-Phase Catalysis. *Chemical Engineering & Technology: Industrial Chemistry-Plant Equipment-Process Engineering-Biotechnology, 27*(2), 113-122.

William, M. H., Lide, D., & Bruno, T. (2011). CRC handbook of chemistry and physics. In: CRC Press: Boca Raton, FL, USA.

Williams, M. J., Sánchez, E., Aluri, E. R., Douglas, F. J., MacLaren, D. A., Collins, O. M., . . . Michaelis, M. (2016). Microwave-assisted synthesis of highly crystalline, multifunctional iron oxide nanocomposites for imaging applications. *RSC Advances, 6*(87), 83520-83528.

Williams, N. H. (1967). Curing Epoxy Resin Impregnates Pipe at 2450 Megahertz. *Journal of Microwave Power, 2*(4), 123-127.

Winefordner, J. D., Wagner, E. P., & Smith, B. W. (1996). Status of and perspectives on microwave and glow discharges for spectrochemical analysis. Plenary lecture. *Journal of Analytical Atomic Spectrometry, 11*(9), 689-702.

Wnukowski, M., & Jamróz, P. (2018). Microwave plasma treatment of simulated biomass syngas: Interactions between the permanent syngas compounds and their influence on the model tar compound conversion. *Fuel Processing Technology, 173*, 229-242.

Woskov, P., Rhee, D., Thomas, P., Cohn, D., Surma, J., & Titus, C. (1996). Microwave plasma continuous emissions monitor for trace-metals in furnace exhaust. *Review of scientific instruments, 67*(10), 3700-3707.

Wu, A., Yan, J., Zhang, H., Zhang, M., Du, C., & Li, X. (2014). Study of the dry methane reforming process using a rotating gliding arc reactor. *International Journal of Hydrogen Energy, 39*(31), 17656-17670.

Wu, L., Yick, K.-l., Ng, S.-p., & Yip, J. (2012). Application of the Box–Behnken design to the optimization of process parameters in foam cup molding. *Expert Systems with Applications, 39*(9), 8059-8065.

Xiao, N., Luo, H., Wei, W., Tang, Z., Hu, B., Kong, L., & Sun, Y. (2015). Microwave-assisted gasification of rice straw pyrolytic biochar promoted by alkali and alkaline earth metals. *Journal of Analytical and Applied Pyrolysis, 112*, 173-179.

Xu, Y., Tian, Z., Xu, Z., & Lin, L. (2002). Reactions in a Mixture of CH~ 4 and CO~ 2 under the Action of Microwave Discharge at Atmospheric Pressure. *Journal of Natural Gas Chemistry, 11*(1/2), 28-32.

Xu, Y., Wei, Q., Long, H., Zhang, X., Shang, S., Dai, X., & Yin, Y. (2013). CO 2 reforming of CH 4 by synergies of binode thermal plasma and catalysts. *International Journal of Hydrogen Energy, 38*(3), 1384-1390.

Yabe, T., Mitarai, K., Oshima, K., Ogo, S., & Sekine, Y. (2017). Low-temperature dry reforming of methane to produce syngas in an electric field over La-doped Ni/ZrO 2 catalysts. *Fuel Processing Technology, 158*, 96-103.

Yagi, F., Kanai, R., Wakamatsu, S., Kajiyama, R., Suehiro, Y., & Shimura, M. (2005). Development of synthesis gas production catalyst and process. *Catalysis today, 104*(1), 2-6.

Yan, B., Wang, Q., Jin, Y., & Cheng, Y. (2010). Dry reforming of methane with carbon dioxide using pulsed DC arc plasma at atmospheric pressure. *Plasma Chemistry and Plasma Processing, 30*(2), 257-266.

Yan, K., Hui, H., Cui, M., Miao, J., Wu, X., Bao, C., & Li, R. (1998). Corona induced non-thermal plasmas: Fundamental study and industrial applications. *Journal of electrostatics, 44*(1-2), 17-39.

Yang, W., Zhang, H., Yu, A., & Jin, Q. (2000). Microwave plasma torch analytical atomic spectrometry. *Microchemical journal, 66*(1-3), 147-170.

Yap, D., Tatibouët, J.-M., & Batiot-Dupeyrat, C. (2018). Catalyst assisted by non-thermal plasma in dry reforming of methane at low temperature. *Catalysis Today, 299*, 263-271.

Yasuda, H. (1990). *Plasma polymerization and plasma interactions with polymeric materials.* Paper presented at the Symposium on Plasma Polymerization and Plasma Interactions with Polymeric Materials (1990: Boston, Mass.).

Yin, C. (2012). Microwave-assisted pyrolysis of biomass for liquid biofuels production. *Bioresource technology, 120*, 273-284.

Yin, J., Zhao, Z., Zhan, X., & Duan, Y. (2017). Exploration and performance evaluation of microwave-induced plasma with different discharge gases for ambient desorption/ionization mass spectrometry. *Rapid Communications in Mass Spectrometry, 31*(11), 919-927.

Yu, M., Zhu, Y.-A., Lu, Y., Tong, G., Zhu, K., & Zhou, X. (2015). The promoting role of Ag in Ni-CeO 2 catalyzed CH 4-CO 2 dry reforming reaction. *Applied Catalysis B, 165*, 43-56.

Zajíčková, L., Eliáš, M., Jašek, O., Kudrle, V., Frgala, Z., Matějková, J., . . . Kadlečíková, M. (2005). Atmospheric pressure microwave torch for synthesis of carbon nanotubes. *Plasma physics and controlled fusion, 47*(12B), B655.

Zeng, Y., Zhu, X., Mei, D., Ashford, B., & Tu, X. (2015). Plasma-catalytic dry reforming of methane over γ-Al2O3 supported metal catalysts. *Catalysis Today, 256*, 80-87.

Zhang, A.-J., Zhu, A.-M., Guo, J., Xu, Y., & Shi, C. (2010). Conversion of greenhouse gases into syngas via combined effects of discharge activation and catalysis. *Chemical Engineering Journal, 156*(3), 601-606.

Zhang, H., Zhao, K., Yan, X., Sun, Q., Li, Y., Zhang, Y., . . . Ke, F. (2013). Effects of nitrogen conversion and environmental factors on landfill CH4 oxidation and N2O emissions in aged refuse. *Journal of environmental management, 126*, 174-181.

Zhang, J.-Q., Zhang, J.-S., Yang, Y.-J., & Liu, Q. (2003). Oxidative coupling and reforming of methane with carbon dioxide using a pulsed microwave plasma under atmospheric pressure. *Energy & fuels, 17*(1), 54-59.

Zhang, X., Yang, C., Zhang, Y., Xu, Y., Shang, S., & Yin, Y. (2015). Ni–Co catalyst derived from layered double hydroxides for dry reforming of methane. *International Journal of Hydrogen Energy, 40*(46), 16115-16126.

Zhao, X., Song, Z., Liu, H., Li, Z., Li, L., & Ma, C. (2010). Microwave pyrolysis of corn stalk bale: A promising method for direct utilization of large-sized biomass and syngas production. *Journal of Analytical and Applied Pyrolysis, 89*(1), 87-94.

Zherlitsyn, A. G., Shiyan, V. P., & Demchenko, P. V. (2016). Microwave plasma torch for processing hydrocarbon gases. *Resource-Efficient Technologies, 2*(1), 11-14.

Zhou, L., Xue, B., Kogelschatz, U., & Eliasson, B. (1998). Nonequilibrium plasma reforming of greenhouse gases to synthesis gas. *Energy & Fuels, 12*(6), 1191-1199.

Zhu, B., Li, X.-S., Shi, C., Liu, J.-L., Zhao, T.-L., & Zhu, A.-M. (2012). Pressurization effect on dry reforming of biogas in kilohertz spark-discharge plasma. *International Journal of Hydrogen Energy, 37*(6), 4945-4954.

Zhu, D., Jin, W., Yu, B., Ying, Y., Yu, H., Shan, J., . . . Jin, Q. (2017). Development of a novel kilowatt microwave plasma torch source for atomic emission spectrometry. *Chemical Research in Chinese Universities, 33*(5), 709-713.

Zhu, X., Li, K., Liu, J.-L., Li, X.-S., & Zhu, A.-M. (2014). Effect of CO2/CH4 ratio on biogas reforming with added O2 through an unique spark-shade plasma. *International Journal of Hydrogen Energy, 39*(25), 13902-13908.

Zou, J.-J., Zhang, Y.-P., & Liu, C.-J. (2007). Hydrogen production from dimethyl ether using corona discharge plasma. *Journal of power sources, 163*(2), 653-657.

Appendix: Attribution Agreement

RESEARCH ARTICLE

WILEY Asia-Pacific Journal of **Chemical Engineering** | Curtin University

Optimisation of CH_4 and CO_2 conversion and selectivity of H_2 and CO for the dry reforming of methane by a microwave plasma technique using a Box–Behnken design

Nabil Majd Alawi[1,2] | Ahmed Barifcani[1] | Hussein Rasool Abid[1]

[1] Western Australian School of Mines: Minerals, Energy & Chemical Engineering, Department of Chemical Engineering, Curtin University, Bentley, Australia

[2] Petroleum Technology Department, University of Technology, Baghdad, Iraq

Correspondence
Nabil Majd Alawi, Western Australian School of Mines: Minerals, Energy & Chemical Engineering, Department of Chemical Engineering, Curtin University, Kent St, Bentley WA 6102, Australia.
Email: n.alawi@postgrad.curtin.edu.au

Present Address
Hussein Rasool Abid, Department of Environmental Health, Applied Medical Science College, Karbala University, Iraq.

Abstract

A microwave plasma was generated by N_2 gas. Synthesis gases (H_2 and CO) were produced by the interaction of CH_4 and CO_2 under plasma conditions at atmospheric pressure. The experimental pilot plant was set up, and the gases were sampled and analysed by gas chromatography–mass spectrometry. The Box–Behnken design (BBD) method was used to find the optimising conditions based on the experimental results. The response surface methodology based on a three-parameter and three-level BBD has been developed to find the effects of independent process parameters, which were represented by the gas flow rates of CH_4, CO_2, and N_2 and their effects on the process performance in terms of CH_4, CO_2, and N_2 conversion and selectivity of H_2 and CO. In this work, four models based on quadratic polynomial regression have been determined to understand the connection between the limits of the feed gas flow rate and the performance of the process. The results show that the most important factor influencing the CO_2, CH_4, and N_2 conversion and the selectivity of H_2 and CO was "CO_2 feed gas flow rate." At the maximum desirable value of 0.92, the optimum CH_4, CO_2, and N_2 conversion were 84.91%, 44.40%, and 3.37%, respectively, and the selectivities of H_2 and CO were 51.31% and 61.17%, respectively. This was achieved at a gas feed flow rate of 0.19, 0.38, and 1.49 L min^{-1} for CH_4, CO_2, and N_2, respectively.

KEYWORDS

Box–Behnken design, dry reforming of methane, microwave plasma, optimisation, syngas production

Nomenclature

Abbreviations: BBD, Box–Behnken design; RSM, response surface methodology; ANOVA, analysis of variance; Y, response
Symbol Description and units: CH_4, methane Gas, L min^{-1}; CO_2, carbon dioxide gas, L min^{-1}; N_2, nitrogen gas, L min^{-1}; H_2, hydrogen gas, L min^{-1}; CO, carbon monoxide, L min^{-1}
Greek Characters: β, coefficient
Subscripts: $β_0$, constant coefficient; $β_i$, coefficient for linear; x_i, initial input parameters; $β_{ii}$, quadratic coefficient; $β_{ij}$, coefficient for interactions

1 | INTRODUCTION

Due to the increasing demand for energy in recent years, there has been higher usage of fossil fuels. This has led to the release of greenhouse gases such as methane (CH_4) and carbon dioxide (CO_2), causing global warming and subsequent climate change.[1] Consequently, it has become imperative to depend on the modern and economical technologies using greenhouse gases as an alternative source

Published paper

1. **"Optimisation of CH₄ and CO₂ conversion and selectivity of H₂ and CO for the dry reforming of methane by a microwave plasma technique using a Box–Behnken design.** Asia-Pac J Chem. Eng. 2018; e2254".

Authors	Conception and design	Acquisition of data and method	Data conditioning and manipulation	Analysis & statistical method	Interpretation & discussion	Final Approval
Associate Professor Ahmed Barifcani						
I acknowledge that these represent my contribution to the above research output Singed.						
Dr. Hussein Rasool Abid						
I acknowledge that these represent my contribution to the above research output Singed.						

Syngas formation by dry and steam reforming of methane using microwave plasma technology

Nabil Majd Alawi[1,2], Gia Hung Pham[1], Ahmed Barifcani[1], Minh Hoang Nguyen[1] and Shaomin Liu[1]

[1]Department of Chemical Engineering, Curtin University, Perth, Western Australia 6845, Australia
[2]Petroleum Technology Department, University of Technology, Baghdad, Iraq

Corresponding author's e-mail address: n.alawi@postgrad.curtin.edu.au

Abstract. The combined dry and steam reforming of methane at atmospheric pressure was experimentally studied by using microwave plasma technology. The effect of the process parameters such as total feed gas flow rate, steam concentration and input microwave power on the synthesis gas H_2/CO ratio was investigated using a commercial microwave reactor system. In order to minimise the carbon formation and plasma instability, the concentration of methane and carbon dioxide in nitrogen plasma were kept at a low level in this study. The long-term test results show that at the flow rate of 0.2 L min^{-1}, 0.4 L min^{-1} and 1.5 L min^{-1} for CH_4, CO_2 and N_2 respectively, the carbon formation was not detectable at the input power of 700 W. This reaction condition offers an opportunity to study the effect of adding water to the feed on the syngas ratio H_2/CO. The test results show that a higher CH_4 conversion (82.74%), H_2 selectivity (98.79%) and yield (81.73%) were achieved compared with those of the dry reforming at the same operating conditions. With the steam addition, the desired H_2/CO ratio for the Fischer-Tropsch synthesis process can be reached.

1. Introduction

Nowadays, the increasing energy demand of the growing population has led to the rapid consumption of fossil fuels, inevitably releasing carbon dioxide (CO_2) which is a prime contributor to global warming and climate change. For this reason, significant efforts have been devoted to developing innovative and cost-effective technologies to produce synthesis gas (syngas) from CO_2 [1]. Syngas, a mixture of hydrogen (H_2) and carbon monoxide (CO), is a versatile intermediate to the synthesis of a variety of valuable chemical feedstock and liquid fuels such as ammonia, methanol, ethanol, acetic acid, methyl format, dimethyl ether, synthetic gasoline and diesel via Fischer-Tropsch process [2-9]. Syngas can be produced from a variety of primary feedstock such as coal, natural gas (NG) and biomass. Among them, NG is the cheapest and cleanest source [10]. Many reforming technologies can be used to produce syngas including steam reforming, dry reforming (CO_2 reforming) and partial oxidation [11-13]:

Steam Reforming of Methane (SRM)

$$CH_4 + H_2O \rightleftarrows CO + 3H_2 \tag{1}$$

$$\Delta H = +206 \, k \, /m$$

Dry Reforming of Methane (DRM)

Published paper

2. **"Syngas formation by dry and steam reforming of methane using microwave plasma technology.** IOP Conf. Series: Materials Science and Engineering 579 (2019) 012022".

Authors	Conception and design	Acquisition of data and method	Data conditioning and manipulation	Analysis & statistical method	Interpretation & discussion	Final Approval
Dr Gia Hung Pham						
I acknowledge that these represent my contribution to the above research output						
Singed.						
Associate Professor Ahmed Barifcani						
I acknowledge that these represent my contribution to the above research output						
Singed.						
PhD Student Minh Hoang Nguyen						
I acknowledge that these represent my contribution to the above research output						
Singed.						
Prof Shaomin Liu						
I acknowledge that these represent my contribution to the above research output						
Singed.						

Comparative study on the performance of microwave-assisted plasma DRM in nitrogen and argon atmospheres at a low microwave power

Nabil Majd Alawi[a,b], Jaka Sunarso[c,*], Gia Hung Pham[a], Ahmed Barifcani[a], Minh Hoang Nguyen[a,d], Shaomin Liu[a]

[a] Department of Chemical Engineering, Curtin University, Perth, Western Australia 6845, Australia
[b] Petroleum Technology Department, University of Technology, Baghdad, Iraq
[c] Research Centre for Sustainable Technologies, Faculty of Engineering, Computing and Science, Swinburne University of Technology, Jalan Simpang Tiga, 93350, Kuching, Sarawak, Malaysia
[d] The University of Da Nang - University of Science and Technology, Da Nang 550000, Vietnam

ABSTRACT

Dry reforming of methane (DRM) is an attractive route to convert CH_4 and CO_2 into syngas (a mixture of CO and H_2). In this work, the performance of microwave-assisted DRM at atmospheric pressure (in terms of CH_4 and CO_2 conversions, H_2 and CO selectivities, H_2 and CO yields, and H_2 to CO ratio) is studied as functions of additive gas flow rate, microwave power, CO_2 to CH_4 inlet supply ratio, and reaction time. Two additive gases were used, i.e., nitrogen and argon. Microwave-assisted DRM experiments in both gases show identical trend of conversions, selectivities, yields, and product ratio. DRM performances in both additive gases atmosphere were stable for up to 8 h. Under the same operating conditions, using Ar as an additive gas, however, led to higher H_2 and CO selectivities and yields and thus, higher H_2 to CO ratio relative to using N_2 as an additive gas. Maximum CH_4 and CO_2 conversions of 79.35% and 44.82%, H_2 and CO selectivities of 50.12% and 58.42%, H_2 and CO yields of 39.77% and 32.89%, and H_2 to CO ratio of 0.86 were obtained at 700 W and N_2, CO_2, and CH_4 flow rates of 1.5, 0.4, and 0.2 L min^{-1}, respectively.

© 2020 The Korean Society of Industrial and Engineering Chemistry. Published by Elsevier B.V. All rights reserved.

Introduction

Greenhouse gases such as methane (CH_4) and carbon dioxide (CO_2) are undesirable products of energy and chemicals production from fossil fuel-based resources, which can be used more productively in their concentrated forms as a feedstock for the production of syngas [1–5]. Syngas is a mixture of carbon monoxide (CO) and hydrogen (H_2) that can be utilised directly as a fuel for combustion with oxygen (O_2) or as a fuel in molten carbonate and solid oxide fuel cells as well as a raw material for the production of chemicals such as ammonia, ethanol, methanol, acetic acid, dimethyl ether, and methyl formate [6–10]. Three different chemical pathways have been established to convert CH_4 to syngas, i.e., (1) steam reforming of methane (SRM, Eq. (1)), (2) partial oxidation of methane (POM, Eq. (2)), and (3) dry reforming of methane (DRM, Eq. (3)).

$$CH_4 + H_2O \rightarrow CO + 3H_2 \qquad (1)$$

$$CH_4 + \frac{1}{2}O_2 \rightarrow CO + 2H_2 \qquad (2)$$

$$CH_4 + CO_2 \rightarrow 2CO + 2H_2 \qquad (3)$$

SRM is presently one of the most widely used pathways to obtain syngas (and H_2) from CH_4 since it generates syngas with the highest H_2 to CO ratio of 3 among the three pathways [11]. SRM however is a highly endothermic reaction (ΔH (298 K) = 206 kJ mol^{-1}) that requires temperature above 700 °C to activate and self-sustain [12], which translates to high capital and energy investments requirement. POM, on the other hand, is a mildly exothermic reaction (ΔH(298 K) = −36 kJ mol^{-1}) [13]. Although the H_2 to CO ratio of POM is approximately two, which is ideal for syngas conversion to liquid

* Corresponding author.
E-mail addresses: nabilmajd@yahoo.com, n.alawi@postgrad.curtin.edu.au (N.M. Alawi), barryjakasunarso@yahoo.com, jsunarso@swinburne.edu.my (J. Sunarso).

Published paper

3. "Comparative study on the performance of microwave-assisted plasma DRM in nitrogen and argon atmospheres at a low microwave power. Journal of Industrial and Engineering Chemistry. (Accepted)".

Authors	Conception and design	Acquisition of data and method	Data conditioning and manipulation	Analysis & statistical method	Interpretation & discussion	Final Approval
A. Dr Jaka Sunarso						
I acknowledge that these represent my contribution to the above research output Singed.						
B. Dr Gia Hung Pham						
I acknowledge that these represent my contribution to the above research output Singed.						
C. Associate Professor Ahmed Barifcani						
I acknowledge that these represent my contribution to the above research output Singed.						

Published paper

3. "Comparative study on the performance of microwave-assisted plasma DRM in nitrogen and argon atmospheres at a low microwave power. Journal of Industrial and Engineering Chemistry. (Accepted)".

Authors	Conception and design	Acquisition of data and method	Data conditioning and manipulation	Analysis & statistical method	Interpretation & discussion	Final Approval
D. Dr Minh Hoang Nguyen						
I acknowledge that these represent my contribution to the above research output						
Singed.						
E. Prof Shaomin Liu						
I acknowledge that these represent my contribution to the above research output						
Singed.						

Microwave Plasma Dry Reforming of Methane at High CO₂/CH₄ Feed Ratio

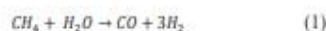Nabil Majd Alawi, Gia Hung Pham, Ahmed Barifcani

Abstract—Dry reforming of methane that converts two greenhouses gases (CH_4 and CO_2) to synthesis gas (a mixture of H_2 and CO) was studied in a commercial bench scale microwave (MW) plasma reactor system at atmospheric pressure. The CO_2, CH_4 and N_2 conversions; H_2, CO selectivities and yields, and syngas ratio (H_2/CO) were investigated in a wide range of total feed flow rate (0.45 – 2.1 L/min), MW power (700 – 1200 watt) and CO_2/CH_4 molar ratio (2 – 5). At the feed flow rates of CH_4, CO_2 and N_2 of 0.2, 0.4 and 1.5 L/min respectively, and the MWs input power of 700 W, the highest conversions of CH_4 and CO_2, selectivity and yield of H_2, CO and H_2/CO ratio of 79.35%, 44.82%, 50.12, 58.42, 39.77%, 32.89%, and 0.86, respectively, were achieved. The results of this work show that the product ratio increases slightly with the increasing total feed flow rate, but it decreases significantly with the increasing MW power and feeds CO_2/CH_4 ratio.

Keywords—Atmospheric pressure, methane dry reforming, microwave plasma, synthesis gas production.

I. INTRODUCTION

CURRENTLY, the demand for the development of alternative, clean energy and the reduction of greenhouse gas emissions (CO_2 and CH_4) are becoming urgent to reduce the risk of global warming and climate change. It is therefore necessary to find modern and cost-effective technologies to convert these undesirable gases to valuable products such as synthesis gas [1]. Synthesis gas (syngas) is an important intermediate for the production of synthetic fuels and value-added chemicals through Fischer-Tropsch Synthesis (FTS) [2]. There are different methane reforming processes used to produce syngas as summarised below [3]-[5]:
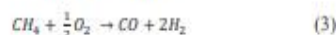
Steam Reforming of Methane (SRM):

$$CH_4 + H_2O \rightarrow CO + 3H_2 \qquad (1)$$

Dry Reforming of Methane (DRM):

$$CH_4 + CO_2 \rightarrow 2CO + 2H_2 \qquad (2)$$

Partial Oxidation of Methane (POM):

$$CH_4 + \tfrac{1}{2}O_2 \rightarrow CO + 2H_2 \qquad (3)$$

SRM produces a syngas with the high ratio of H_2/CO.

Nabil Majd Alawi is a PhD student at Department of Chemical Engineering, Curtin University, Perth, WA, Australia and he is with Petroleum Technology Department, University of Technology, Baghdad, Iraq (e-mail: n.alawi@postgrad.curtin.edu.au).

However, POM has attracted more interest than SRM, due to its mild exothermicity and a perfect H_2/CO ratio of 2, and a desirable ratio for Fischer-Tropsch (F–T) synthesis. DRM is environmentally favourable and promising way to produce syngas from CO_2 and CH_4 [6], [7]. Dry reforming of methane yields a lower syngas ratio ($H_2/CO=1$), which is suitable for the synthesis of oxygenated chemicals, hydrocarbons and liquid fuels from (F–T) process [7].

Plasma is considered to be the fourth state of matter, consisting of the highly reactive species such as electrons, ions, radicals and neutral particles [8]. Two main methods are used to convert chemical to plasma state and they are non-thermal (cold) such as dielectric barrier discharge (DBD), corona discharge (CD), atmospheric pressure glow discharge (APGD), gliding arc discharge (GAD), MW discharge (MWD) and thermal (hot) plasma discharge such as direct current heating [9]. The non-thermal plasma discharge processes offer some important advantages as they are cheap and easy to build at any scale for research and production [10].

In order to improve the product H_2/CO ratio in plasma DRM process, the reducing of feed ratio CO_2/CH_4 was studied [11]-[13]. Unfortunately, carbon formation during the reaction at the feed ratio ≤ 2 leads to an instability of the plasma. As a consequence, the study of the plasma DRM is very complicated and has some unavoidable errors.

In this paper, the effects of input parameters (the total feed gas flow rate, the microwave power, the ratio of CO_2/CH_4) on the performance of processes such as conversions of CH_4, CO_2 and N_2, the product selectivities and yields of H_2 and CO, and H_2/CO ratio, respectively were investigated under microwave plasma at atmospheric pressure. The results could be important information for closing the knowledge gap of plasma stability, plasma condition and side reactions in complex microwave plasma DRM reaction zone.

II. EXPERIMENTAL

The schematic diagram of the experimental set-up is shown in Fig. 1; MW plasma system fundamentally consists of gas cylinders, mass flow controllers, gas mixer, feed gas system, plasma reactor, MW generator, and gas chromatographic (GC-MSD and GC-TCD) analysis system. A commercial MW reactor system (Alter, SM 1150T, Canada) was used in this

Gia Hung Pham is with Department of Chemical Engineering, Curtin University, Perth, WA, Australia (corresponding author, e-mail: g.pham@exchange.curtin.edu.au).

Ahmed Barifcani is with Department of Chemical Engineering, Curtin University, Perth, WA, Australia (e-mail: a.barifcani@curtin.edu.au).

Optimization of microwave plasma dry reforming of methane using the response surface methodology

Nabil Majd Alawi[1,2,*], Ahmed Barifcani[2]

[1] *Petroleum Technology Department, University of Technology, Baghdad, Iraq*
[2] *Curtin University, Kent St, Bentley WA 6102, Australia*
*Corresponding author: n.alawi@postgrad.curtin.edu.au

Abstract: In this study, a microwave plasma reactor has been used for dry reforming of methane at atmospheric pressure. A set of 15 experiments have been carried out, and the test results have been utilised for the purpose of process optimisation. The Box-Behnken design, which is of three factors and three levels, is based on the response surface methodology (RSM). RSM has been applied to investigate the effects of CH_4, CO_2, and N_2 feed flow rates and their interactions on the process performance in term of H_2/CO ratio of production of syngas. The results show that the CO_2 feed flow rate affects the ratio of H_2/CO strongly. At the maximum desirable value of 0.92, the optimum H_2/CO ratio reached 0.7 at the feed flow rate of CH_4, CO_2, and N_2 equal to 0.16, 0.35, and 1.5 L min^{-1}, respectively. The results from the RSM analysis can be proven by experimental work. These results suggest that the RSM method is capable of optimising the microwave plasma dry reforming of methane.

Keywords: Methane dry reforming, Microwave Plasma, Syngas Production, Response surface methodology

1. INTRODUCTION

Nowadays, Nowadays, demand for the use of fossil fuels in various industries has been increased and leading to increased carbon dioxide emissions in the atmosphere air and which resulted in global warming and climate change (Ebrahimi-Najafabadi, Leardi et al. 2014). For this reason, For this reason, many researches have been focused on developing modern and economical technologies to reduce fossil fuels and also to use CO2 as raw materials (Mei, He et al. 2016). In general, synthesis gas (syngas), a mixture of carbon monoxide and hydrogen, is an important intermediate for various synthesising chemicals and environmentally clean chemicals such as ammonia, methanol, ethanol, acetic acid, methyl formate, dimethyl ether, synthetic gasoline and diesel via F-T process (Rostrup-Nielsen 2000) (Allah and Whitehead 2015). There are three main methods that are used to convert CH_4 to synthesis gas (H_2 and CO) such as dry reforming of methane (DRM), steam reforming of methane (SRM), and partial oxidation of methane (POX) (Pacheco, Soria et al. 2015) (Ramachandran, Balasubramanian et al. 2011) (Centi, Quadrelli et al. 2013).

The optimisation of the reaction parameters has been executed out by using multivariate statistic techniques (Kwak 2005). The studies on using the Design of experimental (DoE) have been increased in these days to find the optimum value for the process at fewer experiments (Montgomery 2017). Response surface methodology (RSM) is considered one of the most used methodology in DoE. This methodology, which is based on the Box-Behnken design (BBD), it takes the various input parameters and output responses, which could understand the impact of individual factors and their interactions on the responses by three-dimensional and contour interpretations (Rowshanzamir and Eikani 2009). However, to the best of authors knowledge, a limit report has been found so far using DoE method to optimise the plasma chemical reactions in the microwave technique such as H2/CO ratio. Therefore, the present work aims to investigate and optimise the effect of the feed gas flow rate upon the CO2 and CH4 conversions and yield of H2 and CO. The paper also explores the impact of different process parameters and their interaction on the reaction performance. Also, this work is a part of ongoing research in Curtin University (Alawi and Barifcani 2017).

2. EXPERIMENTAL
2.1. EXPERIMENTAL CONDITIONS

A commercial microwave reactor system (Alter, SM 1150T, Canada) was used in this study. The three gases are feeding system included CH_4 (99.99%), CO_2 (99.99%) and N_2 (99.99%) which were controlled by a mass flow controller and send into the gas mixer. All experiments were performed at atmospheric pressure. Then, the gas samples were collected and analysed by the GC/MSD. Each measurement was repeated three times to avoid possible variances. The calculation of H2/CO ratio are presented by the following equation:

$$\frac{H_2}{CO} \, Ratio = \frac{\text{moles of } H_2 \text{ produced}}{\text{moles of CO produced}} \tag{1}$$

107

A comparative study of the experimental investigation and response surface optimization of dry reforming of methane

Nabil Majd Alawi[1,2,*], Ahmed Barifcani[2]

[1]Department of Chemical Engineering, Curtin University, Kent St, Bentley WA 6102, Australia
[2]Petroleum Technology Department, University of Technology, Baghdad, Iraq
*Corresponding author: n.alawi@postgrad.curtin.edu.au *(Nabil Majd Alawi)*

Abstract: This paper reports, the syngas production by microwave plasma dry reforming of methane. The process variables used feed gas flow rates of CH_4, CO_2 and N_2 are syngas production, which were optimized using response surface methodology (RSM). The RSM was used to predict the syngas production from the experimental data. The results show that the CO_2 feed flow rate affects the yields of H_2 and CO. Good agreement was shown between the predicted outputs from the RSM model and the experimental data. At maximum desirability value of 0.92, optimum CH_4, CO_2 and N_2 of 0.19, 0.38 and 1.49 L min^{-1} were obtained at atmospheric pressure resulting in syngas yield of 37.52% and 29.50% for hydrogen (H_2) and carbon monoxide (CO), respectively.

Keywords: CO_2 reforming of methane optimization, Microwave plasma, Syngas, Response surface methodology

1. INTRODUCTION

The rapid increase in population and high energy consumption has been created environmental issues by the production of greenhouse gases (GHG). Methane and carbon dioxide constitutes a significant part of GHG and is a prime contributor to global warming and climate change (Tu and Whitehead 2014). Various technologies have been developed to produce synthesis gas (syngas) from CH_4 and CO_2 (Li, Nakagawa et al. 2011). Syngas plays an important role in chemical engineering since it is an intermediate for synthesising various chemicals and fuels, such as methanol, dimethyl and diesel fuel (Wang, Yao et al. 2018). Plasma technology offers a unique way to induce gas phase reaction. Several plasmas dry reforming of methane methods have been employed to convert methane and carbon dioxide into syngas, which include: non-thermal plasma discharge and thermal plasma (Hrycak, Czylkowski et al. 2015, Snoeckx, Zeng et al. 2015). Various research that methane based on syngas production technology have been reported including steam reforming of methane (($CH_4 + H_2O \rightarrow CO + 3H_2$) (Giaconia, & Lemonidou, 2014)), dry reforming of methane ($CH_4 + CO_2 \rightarrow 2CO + 2H_2$) (Centi, Quadrelli et al. 2013)), partial oxidation of methane ($2CH_4 + O_2 \rightarrow 2CO + 4H_2$) (Pacheco et al., 2015)).

Identifying the optimum performance of the plasma process using standard experiments is time-consuming and costly due to the need for multiple experiments under different test conditions (Ayodele, Khan et al. 2017). To reduce the difficulty in determining the optimum performance of the plasma process, previous studies have used the chemical model (Ramachandran, Balasubramanian et al. 2011, Wu, Yick et al. 2012, De Bie, van Dijk et al. 2015, Hafizi,

Rahimpour et al. 2016, Mei, He et al. 2016, Senseni, Fattahi et al. 2016, Sidik, Triwahyono et al. 2016, Abbasi, Niaei et al. 2017, Abedini, Hosseini et al. 2017, Challiwala, Ghouri et al. 2017, Montgomery 2017). It has been found that the chemical model is useful in determining the optimum value for output responses. This model requires a significantly lower number of experiments compared to using a traditional method (Mei, He et al. 2016). Design of experimental (DoE) is a powerful tool for process optimization since it allows multiple input factors to be manipulated, determining their individual and combined effects on the process performance in the form of one or more output responses, while significantly reducing the number of experiments compared to conventional experiments with one factor at a time (Montgomery 2017). Response surface methodology (RSM) is one of the most useful experimental designing methodologies for building the relationship between the multiple input parameters and output responses, which enable us to get a better understanding of the effect of individual factors and their interactions on the responses by three-dimensional and contour interpretations.

However, to the best of authors knowledge, a limit report has been found so far using DoE method to optimise the plasma chemical reactions in the microwave technique such as H_2 and CO yields. Therefore, the present work aims to investigate and optimise the effect of the feed gas flow rate upon the yield of H_2 and CO. The paper also explores the impact of different process variables and their interaction on the reaction performance.

Effect of steam addition on the syngas formation from microwave plasma dry reforming of methane

Nabil Majd Alawi[1,2], Gia Hung Pham[1], Ahmed Barifcani[1], Minh Hoang Nguyen[1] and Shaomin Liu[1]

[1]Petroleum Technology Department, University of Technology, Baghdad, Iraq
[2]Department of Chemical Engineering, Curtin University, Perth, Western Australia 6845, Australia

Corresponding author's e-mail address: n.alawi@postgrad.curtin.edu.au

Abstract. The combined dry and steam reforming of methane at atmospheric pressure was experimentally studied by using microwave plasma technology. The effect of the process parameters such as total feed gas flow rate, steam concentration and input microwave power on the synthesis gas H_2/CO ratio was investigated using a commercial microwave reactor system. In order to minimise the carbon formation and plasma instability, the concentration of methane and carbon dioxide in nitrogen plasma were kept at a low level in this study. The long-term test results show that at the flow rate of 0.2 L min^{-1}, 0.4 L min^{-1} and 1.5 L min^{-1} for CH_4, CO_2 and N_2 respectively, the carbon formation was not detectable at the input power of 700 W. This reaction condition offers an opportunity to study the effect of adding water to the feed on the syngas ratio H_2/CO. The test results show that a higher CH_4 conversion (82.74%), H_2 selectivity (98.79%) and yield (81.73%) were achieved compared with those of the dry reforming at the same operating conditions. With the steam addition, the desired H_2/CO ratio for the Fischer-Tropsch synthesis process can be reached.

1. Introduction

Nowadays, the increasing energy demand of the growing population has led to the rapid consumption of fossil fuels, inevitably releasing carbon dioxide (CO_2) which is a prime contributor to global warming and climate change. For this reason, significant efforts have been devoted to developing innovative and cost-effective technologies to produce synthesis gas (syngas) from CO_2 [1]. Syngas, a mixture of hydrogen (H_2) and carbon monoxide (CO), is a versatile intermediate to the synthesis of a variety of valuable chemical feedstock and liquid fuels such as ammonia, methanol, ethanol, acetic acid, methyl format, dimethyl ether, synthetic gasoline and diesel via Fischer-Tropsch process [2-9]. Syngas can be produced from a variety of primary feedstock such as coal, natural gas (NG) and biomass. Among them, NG is the cheapest and cleanest source [10]. Many reforming technologies can be used to produce syngas including steam reforming, dry reforming (CO_2 reforming) and partial oxidation [11-13]:

Steam Reforming of Methane (SRM)

$$CH_4 + H_2O \rightleftharpoons CO + 3H_2 \tag{1}$$

$$\Delta H = +206 \, kJ/mol$$

Dry Reforming of Methane (DRM)

$$CH_4 + CO_2 \rightleftharpoons 2CO + 2H_2 \tag{2}$$

$$\Delta H = +247 \, kJ/mol$$

Partial Oxidation of Methane (POM)

$$CH_4 + \tfrac{1}{2}O_2 \rightleftharpoons CO + 2H_2 \tag{3}$$

$$\Delta H = -36 \, kJ/mol$$